Hyaluronan Hydrogels, 3-Dimensional Scaffolds for *Ex Vivo* Maintenance of Human Hepatic Stem Cells and Hepatoblasts

William S. Turner

A dissertation submitted to the faculty of the University of North Carolina at Chapel Hill in partial fulfillment of the requirements for the degree of Doctor of Philosophy in the department of Biomedical Engineering.

Chapel Hill
2007

Approved by

Advisor: Professor Lola M Reid, Ph.D.

Reader: Professor Jeffrey M. Macdonald, Ph.D.

Reader: Professor John Sheehan, Ph.D.

Reader: Professor Edward Salmon, Ph.D

Reader: Professor Robert Dennis, Ph.D.

ABSTRACT

William S. Turner: Hyaluronan Hydrogels, 3-Dimensional Scaffolds for *Ex Vivo* Maintenance of Human Hepatic Stem Cells and Hepatoblasts
(Under the direction of Lola M. Reid, Ph.D.)

Sourcing of human liver cells has remained a challenge obviating *ex vivo* studies of human cells and clinical therapies such as cell transplantation and assist devices using bioartificial livers. The expansion potential of human hepatic progenitors under appropriate conditions can overcome this problem, and the potential medical applications include the treatment of liver disease by cell therapies such as cell transplantation and/or bioartificial livers.

Human hepatic stem cells (hHpSCs) *in vivo* are located in ductal plates in fetal livers and neonatal livers and in canals of Herring in pediatric and adult livers, are ~9 μm in diameter, can be isolated by immunoselection for epithelial cell adhesion molecule (EpCAM) or neural cell adhesion molecule (NCAM), and constitute ~ 0.5-1.5% of parenchymal cells in non-ischemic livers of all donor ages. They express cytokeratins 8, 18 and 19, CD133/1, CD44H, telomerase, NCAM, weakly express albumin, are negative for ICAM-1, for markers for adult liver cells (e.g. P450s), hemopoietic cells (e.g. CD45, CD34), endothelia (e.g. VEGFr, Van Willebrand Factor), and other mesenchymal cells (α-smooth muscle actin, desmin, CD146) and for α-fetoprotein (AFP). Self-replication (also called self-renewal) *ex vivo* occurs in hHpSCs cultured in a serum-free medium tailored for hepatic

progenitors, “Kubota’s Medium” (KM), yielding doubling times of ~35 hrs (plastic) or <24 hrs (type III collagen) and a stable phenotype for more than 150 population doublings. Colonies of hHpSCs are in close association with angioblasts and hepatic stellate cell precursors; elimination of them results in slowed growth and reduced viability.

Ex vivo expansion conditions comprise serum-free KM with varying soluble signal supplements in combination with monolayer substrata versus 3-dimensional (3-D) scaffolds of purified extracellular matrix components (used individually or in combinations). The best of the 3-D scaffolds for the hHpSCs and their progeny, hepatoblasts, and committed progenitors have thus far proven to be complexes of chemically modified hyaluronans combined with other matrix components. The precise mix of matrix molecules with the hyaluronans enables the cells to be in a 3-dimensional format and yet kept in an undifferentiated state (certain combinations) versus driven to differentiate (other combinations). The hydrogels offer stable support of the cells with *ex vivo* maintenance for longer than four weeks in culture. Human hepatic progenitors cultured in the hydrogels and in KM have been characterized by classic cell biological techniques including growth analyses, immunohistochemistry and RT-PCR. In parallel, nuclear magnetic resonance spectroscopy (NMR) has been used to monitor the cells without the use of techniques that destroy them. Metabolomic profiling of the cells within their 3-D microenvironment has allowed tracking of metabolites such as glucose, lactate, glutamine, alanine and others which allows for the elucidation of the cellular regulation of glycolysis, the Krebs cycle and other unique metabolic pathways.

Dedication

I dedicate this document to the people whom I love and have helped me through life, my family and friends. Thank you for your time, efforts and spirit. If not for your support I would never have attained the goals that I am now reaching. With great gratitude, I thank David Michael King, Gay Nell Turner, and Christopher Brent Turner for understanding and the willingness to sacrifice to achieve my dreams. I also thank my father for instilling the values and attitudes of a winner at an early age in life. You took your leave of the world too soon, and have been missed.

Acknowledgements

Often it is the situation that one can succeed when he puts his mind to it. However, success is bound to the good people by whom we work and live. For this reason I acknowledge the many people who have helped guide me along the academic path. Mentors such as Dr. Betty Baker at Belmont Abbey College and Dr. Lola Reid at the University of North Carolina are worth their weight in gold. I would like to thank those people from the Reid lab as well as the Macdonald lab at the UNC campus for their contributions to my tutelage.

Table of Contents

List of Tables

Chapter I: BACKGROUND

Chapter II:

Chapter III:

Chapter V:

List of Illustrations

List of Abbreviations and Symbols

AFP = α feto-protein

CS-PGs = Condroitin Sulfate - Proteoglycans

EpCAM = epithelial cell adhesion molecule

ES = Embryonic Stem

FACS = Fluorescence Activated Cell Sorting

GAG = Glycosaminoglycan

HA = Hyaluronic Acid

HAS = Hyaluronan Synthesis Protein

HDM = Hormonally Defined Media

hHpSCs = Human hepatic stem cells

HS-PGs = Heperan Sulfate - Proteoglycans

ICAM-1 = Intercellular Adhesion Molecule

KM = Kubota's Medium

LYVE = Lymphatic Vessel Endothelial Receptor

NCAM = neural cell adhesion molecule

NMR = Nuclear Magnetic Resonance Spectroscopy

PCA = Principle Component Analysis

PGs = Proteoglycans

RHAMM = Receptor for Hyaluronan-Mediated Motility

RPMI = Basal Medium

RT-PCR = Real Time Polymerase Chain Reaction

VEGFr = Vascular Endothelial

1 Chapter I: Background

1.1 Epithelial Mesenchymal Relationships

The liver is similar to all metazoan tissues in that the epithelial-mesenchymal relationship constitutes the organizational basis for the tissue[1-4]. Epithelia (hepatic, lung, pancreas, etc.) are wed to a specific type of mesenchymal cells (endothelia, stroma, stellate cells, smooth muscle cells), and dynamic interactions between the two are mediated by a set of soluble signals (both autocrine and paracrine) and a set of insoluble signals found on the lateral borders of homotypic cells (the lateral extracellular matrix) and on the basal borders (the basal extracellular matrix) between heterotypic cells.[5-13] Furthermore, endocrine (i.e. systemic) regulation and modulation is achieved, in part, by regulating some aspect of the epithelial-mesenchymal relationship.[14] Normal epithelial cells will not survive for long and will not function properly unless epithelial cells and appropriate mesenchymal cells are co-cultured.[3, 15-17] To escape from the need for co-cultures, one can place the cells of interest in contact with appropriate extracellular matrix components and in medium containing the soluble signals (either defined components or “conditioned medium”) produced by interactions between epithelia and mesenchymal cells.[5, 18-20]

In recent years, there has been recognition that the epithelial-mesenchymal relationship is lineage dependent.[5, 21-23] Epithelial stem cells are partnered with mesenchymal stem cells, and their differentiation is co-ordinate [1, 24-26]. In the liver, the lineages begin with the hepatic stem cells (hHpSCs) and with their mesenchymal partners, angioblasts [27] that interact with multiple forms of paracrine signals [28]. These two give rise to descendents in a step-wise, lineage-dependent fashion, and their descendents remain in a partnership throughout differentiation (**Table 1**). Tissue engineering involves the mimicking of the liver's epithelial-mesenchymal relationship with recognition of the lineage-dependent phenomena [20, 29].

Table 1. Epithelial-Mesenchymal Partners in Liver (known or assumed)

<table>
<tr><td colspan="2">Lineage Stage (#): Epithelia</td><td colspan="2">Mesenchymal Cells</td></tr>
<tr><td colspan="4">Stem Cell Niche: Ductal Plates (fetal/neonatal livers)/ Canals of Herring (pediatric/adult livers)</td></tr>
<tr><td colspan="2">(1) Hepatic Stem Cells
[pluripotent]</td><td colspan="2">Angioblasts</td></tr>
<tr><td colspan="2">(2) Hepatoblasts
[bipotent]</td><td colspan="2">Activated angioblasts and hepatic stellate cells</td></tr>
<tr><td colspan="4">Immediately outside the stem cell niche</td></tr>
<tr><td>(3A) Committed Hepatocytic Progenitors
[unipotent]</td><td>Endothelial cell precursors</td><td>(3B) Committed Biliary Progenitors
[unipotent]</td><td>Stromal cell precursors</td></tr>
<tr><td colspan="4">Zone 1 Parenchymal Cells of the Liver Acinus</td></tr>
</table>

(4A) "Small" hepatocytes [diploid]	Continuous Endothelia	(4B) Bile Duct Epithelium [diploid]	Stroma
Zone 2 Hepatocytes the Liver Acinus		"**Zone 2**" Bile duct* Not known: Hypothesized to be Immediately Outside of Liver	
(5A) **Zone 2** hepatocytes (ploidy profile depends on the species)	Continuous Endothelium	(5B) Bile Duct Epithelium (ploidy profile not known)	Stroma
Zone 3 Hepatocytes, Near Central Vein		"**Zone 3**" Bile duct* Not known. Hypothesized to be after gall bladder and connecting to gut	
(6A) **Zone 3** Hepatocytes (polyploid; ploidy profile depends on species)	Fenestrated Endothelia	(6B) Bile Duct Epithelium	Stroma
7A) Apoptotic hepatocytes (polyploid; DNA fragmentation)	Fenestrated Endothelia	Apoptotic Bile Duct Epithelium	Stroma

The lineage stages noted above are proven for the hepatocytes and their associated mesenchymal cells. *It is hypothesized that there are equivalent maturational lineage stages for the bile duct epithelia; yet these lineage stages have yet to be defined. There are recent studies supportive of this assumption [30-33]

1.2 Stem Cells and Maturational Lineage Biology

1.2.1 General Comments

Quiescent tissues (liver, brain), as well as rapidly renewing tissues (skin, intestine), are organized as precursor cell populations (i.e. stem cells and committed progenitors) that yield daughter cells undergoing a maturational process ending in apoptotic cells [23, 34-39]. The different maturational stages of cells within the maturational lineages are distinct phenotypically and in their requirements for *ex vivo* maintenance [40]. Therefore, it is ideal to purify specific subpopulations of cells at distinct maturational stages in order to have cells that behave uniformly under specified culture conditions. Purification of the cells involves enzymatic dissociation of the tissue followed by fractionation methods that can include immunoselection technologies [26, 41-44]. Most of the culture conditions required for the different maturational stages of liver cells have been defined and involve the use of entirely purified soluble signals and extracellular matrix components [27, 40, 45-47]. Certain conditions can be used to maintain the cells with reproducible growth properties and others used to put the cells into a state of growth arrest and with expression of particular tissue-specific genes.

Each cellular subpopulation at a specific maturational stage (e.g. stem cells, committed progenitors, diploid adult cells, polyploid adult cells) has a unique phenotype (antigenically, biochemically, morphologically) with its own distinct set of conditions for *ex vivo* growth versus differentiation. For example, hHpSCs must be co-cultured with their natural partners, angioblasts; hepatoblasts with hepatic

stellate cells (hHpSTCs) ; hepatocytes with endothelia; and biliary epithelia with stroma [25]. If the paracrine signals mediating the epithelial-mesenchymal relationship are known, they can be used to prepare completely defined culture conditions. If they are not known, then co-culturing of the epithelia and mesenchymal subpopulations is required for full extent of functioning.

1.2.2 Cellular Components of Stem Cell Niches

A survey of stem cell niches described to date indicates certain paradigms. As shown in Table 2, the cellular components in all stem cell niches include an epithelial stem cell, angioblasts (precursor for endothelia), and a "nurse" cell that is pigmented or steroidogenic. In the liver these include the hepatic stem cells (hHpSCs), the angioblasts, and hepatic stellate cells. In addition, there are hemopoietic progenitors in the stem cell niche, especially in fetal livers. We have been working towards being able to isolate and to purify each of these subpopulations, to have wholly defined culture conditions for them, and then to co-culture and/or utilize defined paracrine signals from the subpopulations to maintain the one(s) of interest.

Table 2. Known Cellular Components in Stem Cell Niches (with focus on endodermal tissues)					
Germ Layer	**Represen-tative Tissue Types**	**Cellular Components**			
		Epithelial Stem Cells*	**Mesenchymal Cells**		
			Blood Vessel Precursors	**Pigmented/ steroidogenic "Nurse" Cells****	**Other**
Ectoderm	Skin	Epidermal stem cells	Angioblasts	Melanocytes	---
	Brain	Neuronal stem cells	Angioblasts	Ependymal Cells	---
Endoderm	Gut	Intestinal stem cell	Angioblasts	Paneth Cells	---
	Pancreas	Pancreatic stem cells	Angioblasts	Pancreatic Stellate Cells	---
	Liver	Hepatic stem cells	Angioblasts	Hepatic Stellate Cells	Hemopoietic Stem Cells
	Lung	Lung stem cells (Clara cells)	Angioblasts	Pulmonary Neuroendocrine cells	---
Mesoderm	Bone Marrow	Hemopoietic Stem Cells	Angioblasts	Adipocytes	Osteoblasts
Mixed germ layer origins	Ovary	Oogonia	Angioblasts	Granulosa cells	----
	Testis	Spermatogonia	Angioblasts	Sertoli cells	----

*All of the stem cells are "label retaining cells" that retain label in pulse chase labeling studies indicating that they divide very slowly. They do not respond to mild or moderate injuries to the tissue but rather only to massive loss of mature cells in the tissue. The cells responding to mild or moderate injuries are "transit amplifying" cells that are the immediate descendents of the stem cells. In the liver these are the hepatoblasts with their signature feature of α-fetoprotein.

**It is unknown if the pigmented cells found in stem cell niches are themselves stem cells. Typically they produce steroidogenic signals, retinoids, a variety of growth factors and matrix molecules.

1.2.3 Strategies influenced by the knowledge of lineage biology

Whereas all forms of progenitors are found in embryonic tissues, most adult tissues contain only determined stem cells and/or committed progenitors [48]. The known properties of the different maturational lineage stages of cells help to define their potential in academic, clinical or industrial programs. Of the types of progenitors studied (e.g. mesenchymal, neuronal, muscle, epidermal, hepatic), all have been found to be readily cryopreserved [49-51] and expanded *ex vivo* [43, 52, 53]. However, the embryonic stem cells are especially notable for their ability to survive freezing and to expand without differentiating if maintained under precise culture conditions [49, 54-57]. By contrast, attempts to cryopreserve adult liver cells (predominantly the polyploid cells), have met with limited success, and even that limited success is achieved only by embedding the cells in alginate or a form of extracellular matrix [58-61]. Significant *ex vivo* expansion and the ability to subculture adult liver cells have been observed only with the so-called "small hepatocytes" [62-64], a diploid subpopulation of liver cells. Typically, the mature cells undergo one or two rounds of division and then survive for a matter of days in culture, or for a few weeks when supplied with the appropriate extracellular matrix and medium conditions [40, 65].

The ability of totipotent cells and embryonic stem cells to give rise to all, or almost all, possible adult fates makes them appealing as a possible "one serves all" approach for cell therapies and makes them the most exploitable of the classes of stem or progenitor cells [57, 66-68]. However, their use in cell transplantation for patients is precluded by their tumorigenic potential [69-72]. The tumorigenicity of

ES cells when injected at ectopic sites is being investigated extensively, especially by biotechnology companies [70, 72], in hopes that it can be controlled to enable ES cells to reach their full potential both industrially and clinically. Until this is solved, the ES cells will become an excellent choice for pharmaceutical/biotechnology companies and for bioartificial organs but cannot be used for cell therapies.

While determined stem cells are more restricted in their adult cell fates, they have not been found to be tumorigenic, making them the first choice for clinical programs in cell transplantation or for bioartificial organs.[23, 66, 73] Bone marrow and cord blood transplants, which represent the first forms of progenitor cell therapies, have been performed for years.[74, 75] More recently, other forms of progenitor cell therapies are being tested in clinical trials; these include mesenchymal progenitor cells,[52, 76, 77] neuronal progenitor cells,[53, 78] and fetal pancreatic islet cell transplants,[79, 80] and the early data from these trials are very encouraging for the future of progenitor cell therapies as a class.

The problems with determined stem cells include a) availability of tissues, a particular problem for organs that until now have derived only from brain-dead, but beating-heart donors; b) the need for the development of purification schemes for isolation of the cells; c) identification of optimal cryopreservation conditions; and d) defining the *ex vivo* expansion and differentiation conditions.

1.3 Human Liver Maturational Lineage

The development of a tissue begins with the zygote, a fertilized egg, It is, of course, a totipotent stem cell. In human embryogenesis, it undergoes 3 equal

divisions to give rise to 8 equal cells, all of which are "totipotent", meaning that they can give rise to all cell types within the embryo and also to the amnionic membrane and placenta.

Totipotent stem cells= zygote or cells of the morula (resulting from the first 3 cell divisions). These can produce all the extraembryonic and embryonic cell types.

Pluripotent embryonic stem (ES) cells=ES cells can give rise to any of the daughter cells of the 3 germ layers: ectoderm, mesoderm and endoderm but cannot give rise to extraembryonic tissue (e.g. amnion) [69, 81-83].

Determined Stem Cells in liver→hepatic stem cells (hHpSCs) are pluripotent cells that give rise to hepatoblasts and to committed biliary progenitors [27, 28, 45]. Their known antigenic profile is summarized in brief in Table 2 and is given in more detail elsewhere [46]. Unique defining markers include EpCAM+, NCAM+, Claudin 3+, and CK19+. They can be expanded *ex vivo* only when co-cultured with angioblasts or early stage endothelia [25] or with appropriate matrix and soluble signals mimicking the hHpSC-angioblast relationship.[45, 47] These conditions have been defined and include a serum-free medium, "Kubota's Medium" (KM), designed for hepatic progenitors,[43] that can be used in combination with matrix components and that include type III collagen [47] and hyaluronans.[45] The division rate under optimal conditions has been found to be a division every ~26 hours.

Hepatoblasts (bipotent) are derived from hHpSCs. They have a phenotype that overlaps extensively with that of the hHpSCs[46] with the qualifiers that they express ICAM-1 but not NCAM, fetal forms of P450s (e.g. human P450-3A7), high levels of AFP, elevated levels of albumin and have lost expression of claudin 3. The division rate for hepatoblasts is estimated to be a division every ~40-50 hours under the conditions tested to date.

Committed progenitors are unipotent precursors for a single cell type. They include biliary committed progenitors (CK19+, ALB-) and hepatocytic committed progenitors (CK19-, ALB+). The culture conditions for these cells overlap extensively with that of the hHpSCs and hepatoblasts. The division rate for these is not known.

Adult diploid cells All fetal and neonatal tissues contain only diploid cells, and these cells are able to undergo complete cell divisions both *in vivo* and *in vitro*. The number of divisions possible for adult diploid cells is estimated to be 5-8 divisions.[43, 62, 84, 85] The clonogenic expansion conditions that are successful with hHpSCs and hepatoblasts are permissive for colony formation of diploid hepatocytes though the cells divide much more slowly, a division every ~60 hours,[43] and show limited ability to be passaged.

Table 3. Ploidy Profiles of Parenchymal Cells	
Rodents	**Humans****
Fetal and neonatal: entirely diploid	Fetuses, neonates, and children up to teenage years: entirely diploid
Young adults: 4-5 weeks of age: 10% diploid; 80% tetraploid; 10% octaploid	Young adults: 20-40 years of age mostly diploid with perhaps up to 30% tetraploid
6 months and older: <5% diploid; >95% polyploid Polyploid cells are a mix of mononucleated and binucleated cells	Older adults: steady increase of polyploid cells with age; polyploid cells are mostly (entirely?) binucleated, tetraploid cells
**Estimates of ploidy profiles in human parenchyma vary due to the effects of ischemia: polyploid cells are lost selectively with ischemia, especially warm ischemia[86]	

Adult polyploid cells. Polyploid cells appear in liver tissue within a few weeks of postnatal life in mice or rats or by teenage years in humans.[87-91] The majority of the human liver's polyploid cells are tetraploid, whereas higher levels of ploidy have been observed in murine hepatocytes (up to 32 N) and rat hepatocytes (up to 8N) [92, 93]. The percentage of polyploid cells increases with age[42, 91, 94-96] and after partial hepatectomy [42] and is achieved by cells undergoing nuclear division without cytokinesis.[91] By approximately six weeks of age, adult rats have livers in which the extent of polyploidy is at least 90% comprising 80% tetraploid cells and 10% octaploid cells. Published data on ploidy in human liver varies greatly, and the interpretations to date are suspect due in some studies to the methods used for analyzing ploidy, in others to the sampling methods used, and in all of them to the sparse number of human liver samples analyzed. Prior to the 1970's, some investigators used the assumption that cells with multiple nuclei are polyploid and

those with a single nucleus are diploid and defined the extent of polyploidy using that as a guide in analyses of histological sections of tissue. Since it is now well known that polyploid cells can be mononucleated, the data from these older studies must be re-evaluated. In more recent studies using valid methods for analyzing ploidy, the authors have used a small piece of the liver or even a needle aspirate [89, 94, 97-99]. Considering the heterogeneous nature of liver cells [100-103], such small samples are unlikely to be representative of the tissue as a whole. All studies on human liver are made difficult by the extremely limited supply of reasonable quality samples and usually of only certain ages. Altogether these difficulties may explain the wide variations in findings on the extent of polyploidy in adult human livers. Some have claimed as few as 10%, others about 30%, and the highest numbers reported are up to 60% of the cells as polyploid. All agree that the percentage of polyploid liver cells increases with age, and that that percentage increases with special significance after 60 years of age.[87, 89, 94, 98, 99, 104] In summary, a rigorous analysis of polyploidy in human liver and the data correlated with age of donor has yet to be done.

The properties of the diploid versus polyploid cells are quite distinct. Whereas diploid cells have been found capable of colony formation [43, 62, 64, 84, 105], the tetraploid cells are able only to go through one or two complete cell divisions represented by the customary findings of studies on routine primary cultures of adult liver cells [106, 107]. Tetraploid cells are thought incapable of clonogenic growth, an assumption that has yet to be tested rigorously. Instead, they are ideal

for an analysis of highly differentiated functions, some of which are expressed only in the polyploid cells such as certain of the cytochrome P450's [108].

Table 4. Comparison of Maturational Lineages varying in Kinetics	
Rapidly Regenerating Tissues (rapid kinetics)	**Quiescent Tissues (slow kinetics)**
Turnover in days to weeks **% polyploid cells** low (e.g. 5-10%) **Representative tissues** • Hemopoietic Cells • Epidermis • Intestinal Epithelia • Hair	**Turnover** in months to years **% polyploid cells** intermediate (e.g. 30%) to high levels (e.g. 95%) **Representative tissues** • Lung, liver, pancreas, other internal organs • Blood vessels • Skeletal muscle • Nerve cells - including the brain • Heart muscle
Hypothesis: Kinetics of lineage inversely correlated with extent of polyploidy	
References: [94, 109-112]	

Table 5: Summary of Lineage Stages within Liver for Representative Species			
Maturational Lineage Stage	**Mouse**	**Rat**	**Human**
1. Hepatic Stem Cells	Class I MHC negative	Class 1 MHC negative	EpCAM+, NCAM+, claudin 3+, Class I MHC antigens negative, AFP-, Hedgehog proteins and their receptor, Patched, Telomerase

2. Hepatoblasts (probable transit amplifying cells) Parenchyma of fetal/neonatal livers; tethered to ends of canals of Herring in pediatric and adult livers. ~10-12 μm, diploid	Class 1 MHC negative, ICAM+, AFP++	Class 1 MHC negative, ICAM+, AFP++	EpCAM+, ICAM+, Class I MHC antigens negative, AFP++, Hedgehog proteins and Patched; Telomerase, P450 3A7
3.Unipotent Progenitors (rare except in fetal/neonatal livers), ~12-15 μm/ diploid	<u>Committed Biliary Progenitors:</u> CK19+, ALB- <u>Committed Hepatocytic Progenitors:</u> CK19-, ALB+		
4. Diploid Hepatocytes ("Small hepatocytes") ~18 μm	~5% of adult hepatocytes all in zone 1	~10% of adult parenchyma, all in zone 1	Zone 1 and 2 hepatocytes. Gluconeogenesis; Connexins 26, 32

5. Diploid Cholangiocytes Zone 1 of liver acinus	Aquaporins, DPPIV, various pumps associated with bile production (e.g. MDR3)		
6. Tetraploid Hepatocytes	Zone 2 parenchyma	Zone 2. The majority of the parenchyma (~80%)	Zone 3. 10% to 50% of adult parenchyma depending on donor age; express late genes such as P450 3A1
6B Polyploid biliary epithelia (?)	Unknown if they exist, or if they do then their location is unknown. We hypothesize that they do exist and are probably in the bile duct external to the liver		

7. Hepatocytes of higher ploidy (8N to 32 N)	Zone 2/3 ~ 10-20 % of adult parenchyma	Zone 3 (~10% of adult parenchyma;	Not present
8. Apoptotic Cells	Next to central vein. Markers for apoptosis evident.		

1.3.1 Key Markers for Hepatic Stem Cells and Hepatoblasts.

In Table 6 are summarized major markers used for hepatic stem cells and hepatoblasts. These markers are among those that were used to identify and isolate the stem cells and progenitors and/or to define the cells when under specified culture conditions.

Table 6. Markers for Hepatic Stem Cells and Other Hepatic Progenitors

Marker	Species	Comments/References
A. Hepatic Stem Cell/Progenitor Cell Markers that are cloned and sequenced		
Albumin	All species	Found weakly expressed in HpSCs; steady increase in level with hepatoblasts and with the differentiation of cells of the hepatocytic lineage [27, 113, 114]
Alpha-fetoprotein (AFP)	All species	AFP is **not** expressed by HpSCs[22, 27] but rather by hepatoblasts.[115] A variant form of α-fetoprotein is expressed by hemopoietic progenitors[116] and is identical to that in hepatic cells except for exon-1 encoded sequences
Cytokeratin (CK) 7/19	All species	CK 7/19 are found in the hepatic stem cells, the

		hepatoblasts and in some mature biliary epithelia but not the mature hepatocytic parenchyma.[27, 117-121]
Claudin 3	Humans	Present in hHpSCs but not in hepatoblasts or later hepatocytic stages.[46] Expression in biliary lineage
CD133/1 (prominin)	Humans	A transmembrane protein found on hepatic, endothelial, and hemopoietic stem cells [27, 122-124]
Epithelial cell adhesion molecule (EpCAM)	Humans	Present on hHpSCs, hHepatoblasts and some committed progenitors but not on mature hepatocytes[27, 28, 44, 125]

Table 6 Continued

CD44H (hyaluronan receptor)	Rats and humans	Present on hepatoblasts and on hHpSCs and hHepatoblasts [43, 45].
MDR1 (multidrug resistance gene)	Rats, mice	Present on murine and rodent hepatoblasts [126, 127]. [not yet tested in humans but hypothesized to be present in hHpSCs and hHepatoblasts]
ICAM1 (intercellular cell adhesion molecule)	Rats and humans	Present on hepatoblasts, committed progenitors and mature parenchymal cells; not expressed by hHpSCs.[27, 43]
NCAM (neuronal cell adhesion molecule)	Humans	Present on hHpSCs but not hHepatoblasts[27, 32, 128]. NCAM was first identified in neuronal cells; its functions in neurons include interactions with the fibroblast growth factor receptor (FGFR) through the p59Fyn signaling pathway. Its functions in HpSCs are unknown.
Delta-like/Preadipocyte factor-1 (DLK-Pref-1)	Mice	Transmembrane protein that contains epidermal growth factor-like repeats related to notch/delta/serrate family of proteins.[117, 129, 130]

1.3.2 Sourcing of Human Livers

1.3.2.1 Fetal Livers

Human fetal livers can be obtained from organizations affiliated with abortion clinics. Once the application process is completed, then the agencies procure the tissue and ship them to investigators. Most of the studies done for this thesis involved use of fetal liver samples. However, sufficient studies were done with postnatal livers to warrant some background on their sourcing.

1.3.2.2 Pediatric and Adult Human Livers

Pediatric and adult human livers are from brain-dead-but-beating-heart donors, since the donor organ is procured for organ transplantation, and the liver's exquisite sensitivity to ischemia necessitates that the procurement process occurs at the moment of death. The organ is removed from the donor and placed into transport buffer (typically University of Wisconsin solution, "UW" solution; also called Viaspan available commercially from UpJohn). In the U.S., only 1-2% of the deaths are those who have undergone brain death prior to heart arrest. Thus, the number of donor organs/year is very small, on average ~5000 per year. Over 95% of these are used successfully for organ transplantation. The remaining 5% of the donor organs, or up to ~ 250 livers/year, are livers rejected for organ transplantation for a variety of reasons including infections that result in the liver going to investigators studying that type of infection or ischemia, high percentage of fat or other

conditions resulting in the liver going to diverse academic or industrial investigators. The rejected livers are shunted to federal agencies that handle the distribution process to researchers. These livers, ranging in weight from 1500 to 2500 grams, can be shipped as intact organ to groups that can afford them or, more commonly due to the costs, shipped as sections of liver, partitioned by federal agency staff members to maximize the number of researchers receiving samples. The sample is shipped to the investigators within ~10-20 hours from the time of removal from the donor or the "clamp time". The samples arrive flushed with the transport buffer, bagged and on ice. If one receives a portion of a partitioned liver, one receives a piece that is usually about 100-200 grams and that must be perfused through cut blood vessels exposed on the surface of the sample. The conditions prior to death and the cold ischemia associated with the transport conditions of the liver or portion of a liver can result in the deterioration of the sample. Thus, the quality of the starting material is extremely variable.

For donor organs, the overall organ integrity and functions begin to deteriorate after 18 hours post-clamp; such organs will not be used for transplant after this time. This cut-off timing for transplantation is under extensive investigation by groups trying to prolong the time, and, therefore, increase the numbers of organs that might be transplanted. In our experience, the quality of the cells prepared from donor organs that have been procured >18-20 hours reflect this general phenomenon of deterioration, and lower yields and viability of the polyploid cell populations are observed compared with fresher organs or tissue. In general, organs received more than 24 hours after clamp time often do not yield cells of

adequate quality; nor are the cells able to attach efficiently to culture substrata. However, the time threshold after which a particular organ cannot produce cells of adequate quality is affected by multiple factors including age of the donor, proficiency of organ preservation, the quality of the tissue perfusion, and disease state of the organ (e.g., extent of cirrhosis and steatosis).

Mature parenchymal cells in pediatric and adult livers are very sensitive to ischemia, even cold ischemia, and begin dying soon after cardiac arrest. With every hour after death, more mature liver parenchymal cells die such that by the latest time points tested, the only cells left are the stem cells and other early progenitors, the subpopulations most tolerant of ischemia [86]. Although the stem cells can survive many hours, the dying mature cells release lytic enzymes that can damage the stem cells. Empirically, one can find stem cells and other early progenitors from livers of asystolic donors for up to ~4-5 hours. They are recognizable by their expression of stem cell markers such as epithelial cell adhesion molecule, EpCAM.[27, 44] The EpCAM+ cells obtained from such livers are viable and will attach and grow in culture if the correct culture conditions are used for them and that include substrata of embryonic matrix components (type III collagen, type IV collagen, laminin, hyaluronans). However, the studies on them to date have been very limited. So, it is unknown if they have the potential to differentiate to fully mature parenchymal cells. Needed are studies defining the extent of ischemia (cold or warm) to which they can be subjected and still leave the stem cells with full differentiation potential

1.3.2.3 Neonatal Livers

Neonatal livers are from infants who die within the first year of life. It is not possible to define brain death in a neonate, since the posterior skull of a neonate does not close until 8 weeks and the anterior for up to 18 months after birth. Consequently, neonates can suffer significant brain damage resulting in swelling of the brain and yet recover. For them, death is defined always as cardiac arrest resulting in the fact that neonatal tissues are always from asystolic donors. Since neonatal organs and tissues are comprised predominantly of stem cells and progenitors, the entire organ as an organ survives for hours (up to ~8 hours!). Therefore, the stem/progenitors can survive even longer than those in adult livers given that the extent of mature cells dying is minimal (so, low levels of enzymes released).

TABLE 7. SOURCING OF HUMAN LIVERS

- **Fetal Livers (14-20 weeks gestation)**
  - High percentage of stem cells, hepatoblasts and committed progenitors
  - Ease in isolation
  - Ability to obtain and use them depends on political and cultural attitudes
- **Liver Resections**
  - Neonatal, pediatric and adult livers
  - Difficult to obtain; highly variable quality of tissue; small amounts
- **Organ donors ("Brain-dead but beating heart donors") : cold ischemia**
  - ~ 1-2% of deaths; ~ 5000/year in United States
  - Pediatric and adult livers
  - Most used for transplantation; must compete for the small numbers of rejected livers ~100-200/year
  - Highly variable quality of tissue
- **Cadaveric Livers (asystolic donors): warm and cold ischemia**
  - All neonatal deaths and 98-99% of pediatric and adult deaths
  - Neonatal, pediatric and adult livers
  - Cannot be used for transplantation, so all available for research and cell therapy programs
  - Pediatric and Adult Livers--mature liver cells die within ~1 hour of death; stem cells (EpCAM+ cells) survive for 6-8 hours but with increasing damage to the stem cells due to enzymes released by dying cells
  - Neonatal livers are ideal since so rich in stem cells and progenitors. Can isolate viable cells from neonatal livers for up to 7-8 hours after death.

Consequently, neonatal livers are an ideal source of highly viable parenchymal cells for some hours after death [27, 86]. Procurement of neonatal livers by organ procurement organizations (OPOs) began in 2001 after years of efforts of LM Reid and two transplant surgeons, Jeff Fair and David Gerber. The program for procurement of neonatal organs was transferred from UNC to a biotechnology company, Vesta Therapeutics (Research Triangle Park, NC), that now works with OPOs to obtain the neonatal tissues. At present it is the only company procuring and processing neonatal livers, though surely this will change in the coming years. There are rough estimates that at least one neonate dies on a medical center's neonatal

intensive care unit (NICU) every week, and there are many such NICU units within the United States. Even conservative estimates suggest several thousand neonatal deaths/year in the United States, and, at present, only a handful of these neonates have been donors for tissue/organs procured by OPOs. Thus, there is considerable potential for tissue and organs from neonates who have died to become a major new source of high quality tissue for use for both research and clinical programs.

1.3.3 Processing Human Liver Tissue and Liver Cell Isolation

The quality of the liver cell preparation is a reflection of the quality of the starting tissue. As such, the best sources of tissue for the isolation of liver cells are freshly resected biopsy samples, freshly preserved donor organs (<12 hours from clamp time), and neonatal livers. Of course, these sources of tissue are rarely available to the average academic or industrial investigator. There are a number of methods described in the literature for the isolation of human liver cells from partial biopsy segments and from whole lobes [131-133]. These approaches are essentially modified versions of the original two-step perfusion methods developed by Seglen and others[134] for the isolation of liver cells from rat livers. In addition, we have established a novel method for fractionating liver cell suspensions from liver sections or whole livers and that involves fractionation with Optiprep (60% solution of Iodixanol, Accurate Chemicals, Westbury, NY) used for live-dead fractionation in combination with a Cobe cell washer[135]. The Optiprep fractionation results in preservation of the hepatic progenitors within the live fraction. The progenitors can be immunoselected from the cell suspensions.

1.3.4 *Ex Vivo* Maintenance of Cells

For detailed descriptions and discussions of classical cell culture methods, see recently published book on cell culture [136]. All methods of preparing cells for culture start with the disruption of the tissue and its dispersal into chunks or single-cell suspensions. In classical cell culture, the dispersed tissue or cells are plated onto an inflexible plastic substratum that has been exposed to a cationic ionizing gas making the polystyrene in the dishes polarized to reveal a negatively charged layer. Cells attach to the dishes via that negatively charged surface and subsequently form a more complicated adhesion surface with secreted forms of extracellular matrix complemented by matrix components from serum. The cells are suspended in or covered with a liquid medium consisting of a basal medium of salts and nutrients supplemented with a biological fluid such as serum We have prepared a serum-free, hormonally defined medium (HDM) for liver cells and have found that some requirements are generic for all the maturational lineage stages and others are lineage-stage specific. Below is provided general information about the media requirements and then are given tables of serum-free conditions for *ex vivo* maintenance of liver cells.

Basal Medium. The basal media that are commonly used (e.g., RPMI, DME, BME, Waymouth's) were developed originally for cultures of fibroblasts [136]. Although most of the constituents in these basal media are requirements for both epithelial cells and fibroblasts, some aspects of the basal media have had to be been

redefined for the needs of epithelia [136]. Two examples are trace elements and calcium levels. Highly differentiated epithelia require various trace elements or other factors that act as cofactors for the enzymes associated with their tissue-specific functions [137-139]. With respect to the calcium, its level in many of the commercially available media is above 1 mM, concentrations permissive for growth of fibroblasts, but that have been shown to be inhibitory to most epithelial cell types [140]. This problem is exacerbated by culturing the cells in serum-supplemented media, since serum also contributes significantly to the calcium level. Most normal epithelial cells can grow in calcium concentration of approximately 0.4 mM.[140, 141]

Serum. Since the 1950s, the primary form of biological fluid used for supplementation of the basal media has been serum obtained from animals taken to commercial slaughterhouses. Some investigators utilize serum autologous to the cell types to be cultured. However, it is more common that the serum derives from animals that are routinely slaughtered for commercial usage, such as cows, horses, sheep, or pigs.[136] Fibroblasts (stroma and other mesenchymal cell types) do well in serum-supplemented media (SSM). By contrast, epithelial cell types such as liver parenchymal cells dedifferentiate rapidly, within hours to a few days, in SSM and then die, usually within 5-7 days when on culture plastic or within 7-14 days when on various matrix substrata[18]. Over the last about 20 years, the need for serum supplementation has been reduced or eliminated through numerous efforts by many investigators. The serum supplementation has been replaced with mixtures of

defined and purified hormones and growth factors as proposed by the pioneering strategies of Gordon Sato [137-139].

Lipids. All cells require lipids, but mature hepatocytes are capable of converting linoleic acid into most lipid derivatives. This is not true for progenitors. They must be provided with a mixture of free fatty acids, bound to an appropriate carrier molecule (e.g. albumin) and supplied also with high density lipoprotein (10 μg/ml) for long-term management of uptake and release of lipids by the cells. The preparation of a mixture of free fatty acids is described originally by Chessebeuf and associates [142]. The mixture can be combined with albumin (bovine, human, etc.) to prevent the free fatty acids from being toxic. The fatty acids are a strict requirement for the progenitor subpopulations.

Soluble Signals: Autocrine, Paracrine, and Endocrine Factors (Hormonally defined Media, HDM) An approach to defining the soluble signals from cell-cell interactions has been to replace the serum supplements in medium with known and purified hormones and growth factors to yield a serum-free, hormonally defined medium or "HDM" as summarized in recent reviews[20, 40]. Such media have been developed for many cell types enabling investigators to have greater control over cells being maintained ex vivo. Use of HDM results in selection of the epithelial cell type of interest from primary cultures containing multiple cell types. Almost all of the published HDM are optimized for cell growth. To observe optimal expression of differentiated functions, the HDM must be

retailored [37, 143]. Each tissue-specific function requires a discrete set of hormones and growth factors, often at concentrations that differ from those required for cell growth. For example, insulin levels required for growth are typically about 1-5 μg/ml, whereas those needed for optimal expression of connexins are 50-100 ng/ml [144-146]. Thus, some of the hormones conducive to growth can markedly inhibit tissue-specific functions. A rule of thumb is to develop an HDM for growth of cells and then use it as a starting point for identifying the conditions needed for differentiation of those cells. Detailed protocols for the development of an HDM for a cell type at a given lineage stage have been described elsewhere and will not be presented here.[40]

Purified hormones and growth factors are prepared individually and aliquoted as 1000 x stocks. They are added to the basal medium and then filtered through a sterilization filtration unit that is low protein binding. In the tables below are the serum-free conditions (media used in combination with feeders or with matrix substrata) found useful for hepatic progenitors and their associated mesenchymal companion cells.

The basal media given in the tables below is RPMI 1640. It can be replaced with any of a number of basal media (DME/F12, William's, etc.) with the qualifier that the medium must be chosen to be rich in amino acids, with a calcium concentration below 0.5 mM for growth versus greater than 0.5 mM for differentiation, and with copper avoided for stem cell cultures that are being kept in self-replicative mode.

Table 8	**Serum-free Conditions for Expansion of hHpSCs and Hepatoblasts**
Basal Media	RPMI 1640 + nicotinamide (4.4 mM) + L-glutamine (2 mM)
Lipids	High density lipoprotein, HDL (10 μg/ml) + Free fatty acids bound to purified human albumin (0.2% w/v) and at 7.6 μEq of a mixture of free fatty acids
	Free fatty acids Mixture: see Materials and Methods
Hormone requirements	Insulin (5 μg/ml), transferrin/fe (5 μg/ml)
Trace elements*	selenium: 3 x 10^{-10} M; zinc sulfate: 5 X 10^{-11} M
Calcium	~0.3 mM
Feeders (these can be replaced, in part, by the matrix substrata given below)	Angioblasts/endothelia for self-replication Activated hepatic stellate cells for expansion with lineage restriction to hepatoblasts STO cells for expansion of rodent hepatoblasts and for differentiation of human hHpSCs and hepatoblasts[25]
Matrix Substrata	Type III collagen or hyaluronans for self-replication[45, 47]; type IV collagen and/or laminin for lineage restriction to hepatoblasts[25]
Representative Known Soluble Signals from feeders	Angioblasts: LIF[147] Activated hepatic stellate cells: HGF[26]

Table 9	**Serum-free conditions for Differentiation of hHpSCs (or of hepatoblasts)**
Basal Media	RPM 1640 + nicotinamide (4.4 mM) + L-glutamine (2 mM)
Lipids	High density lipoprotein, HDL (10 μg/ml) + free fatty acids bound to purified human albumin (0.2% w/v) and at 7.6 μEq of a free fatty acid mixture
	Free Fatty Acid Mixture: see Materials and Methods
Shared Hormone requirements	Insulin (5 μg/ml), transferrin/fe (5 μg/ml)
Trace elements*	Selenium: 3 x 10^{-10} M; zinc sulfate: 5 X 10^{-11} M; copper sulfate: 10^{-10} M
Calcium	~0.6 mM

Hormones/Growth Factors	EGF (50 ng/ml), T3 (10^{-9}M), hydrocortisone (10^{-8} M)
Heparins or Heparin proteoglycans	10 μg/ml (heparins) or 1-5 ng/ml (Heparin PGs)
Feeders	For hHpSCs, one can use STO feeders; unknown for rodent or murine hHpSCs or hepatoblasts
Matrix Substrata	Plating on or embedding in type I collagen gels[25, 47]

Table 10. Serum-free Conditions for Mature Parenchymal Cells [6, 20, 40]	
Components	**Concentrations**
Basal Media	RPMI 1640`+ Nicotinomide (4.4 mM) + L-glutamine (2 mM)
Trace Elements	Selenium: 3 x 10^{-10} M; zinc sulfate: 5 X 10^{-11} M; copper sulfate: 10^{-10} M
Lipids	High Density Lipoprotein (10 μg/ml)
Free Fatty Acids	Linoleic acid, 2.7 x 10^{-6} M; [Mature parenchyma can survive on linoleic acid alone; however, the cells do better if given the entire mixture of free fatty acids as described in Materials and Methods]
Calcium	0.6 mM
Hormones/growth factors	Insulin (5 μg/ml), epidermal growth factor (50 ng/ml), Tri-iodothyronine or T3 (10^{-9}M), hydrocortisone (10^{-8} M)
Matrix substrata	Ideal is to let the cells be 3-dimensional (spheroids). Partial effects are observed with cells embedded in type I collagen especially if combined with heparin proteoglycan

3. Influence of Serum-free Hormonally Defined Media on Epithelial Cells in Culture

Serum-free, hormonally defined media have been found to select for parenchymal cells even when the cells are on tissue culture plastic [20, 43, 139] This results, within a few days, in cultures that are predominantly the cell type for which the HDM was developed. However, if the cultures are plated onto tissue culture plastic and in HDM, the life span of the primary cultures has been found to be approximately 1 week, at which time, the cells peel off the plates in sheets. Achievement of longer culture life spans under serum-free conditions has been found to be dependent upon using substrata of matrix components or extracts enriched in extracellular matrix in combination with the serum-free, hormonally defined medium[20].

Table 11	**Serum-free conditions used for rodent hepatic stellate cells, rHpSTCs[26]**
Basal medium	RPMI 1640 (GIBCO) + L-glutamine (1 mM, GIBCO)
Lipids	High density lipoprotein (10 μg/ml) + mixture of free fatty acids bound to albumin
Free Fatty Acids	See preparation of these in Materials and Methods
Trace Elements	Selenium: 3 x 10^{-10} M; zinc sulfate: 5 X 10^{-11} M; copper sulfate: 10^{-10} M
Hormones and Growth Factors	Insulin (5 μg/ml), transferrin/fe (5 μg/ml); EGF (10ng/ml; Pepro Tech, Inc.); LIF (10 ng/ml; StemCell Technologies, Inc.),
Antimicrobials	Antibiotics from GIBCO 91%)
Feeders	STO Feeders (Mitomycin C-treated)

Tissue-specific gene expression is dramatically improved in cultures under serum-free conditions and especially with serum-free medium supplemented with only the specific hormones needed to drive expression of a given tissue-specific gene[148, 149]. However, mRNA synthesis of tissue-specific genes is not restored by serum-free medium or by any known combination of hormones and growth factors; rather, the improved tissue-specific gene expression in serum-free media or in hormonally defined media is due to posttranscriptional regulatory mechanisms, often an increase in stability of specific mRNA species[18]. Restoration of mRNA synthesis occurs only with serum-free media or with a serum-free, hormonally defined media containing the specific hormones or factors found to influence a given gene and presented in combination with tissue-specific forms of heparin proteoglycans or

Table 12	**Partially Defined Medium used for human angioblasts and endothelia[25]**
Basal medium	RPMI 1640 (GIBCO) + L-glutamine (1 mM, GIBCO)
Lipids	High density lipoprotein (10 μg/ml) + mixture of free fatty acids bound to albumin
Free Fatty Acids	See Materials and Methods
Trace Elements	Selenium: 3 x 10^{-10} M; zinc sulfate: 5 X 10^{-11} M; copper sulfate: 10^{-10} M
Hormones and Growth Factors	Insulin (5 μg/ml), transferrin/fe (5 μg/ml); EGF (10 ng/ml; Pepro Tech, Inc.); LIF (10 ng/ml; StemCell Technologies, Inc.), VEGF (10 ng/ml; Sigma) ; basic FGF (10 ng/ml; Sigma)
Antimicrobials	Antibiotics from GIBCO
Substratum	Type III collagen
Other	2-mercaptoethanol (0.1 mM), knockout serum (I15%, In Vitrogen)

their glycosaminoglycan chains, heparins[146, 150, 151]. Heparins are often bleached in commercial processes to eliminate the brown coloration that is due to iron deposits; the bleaching process is destructive to heparin's biological activity on gene expression, so use unbleached fractions. At present one cannot obtain the most potent matrix components regulating tissue-specific gene expression: the tissue-specific forms of proteoglycans. Efforts are ongoing in a number of laboratories to isolate and characterize them. It is hoped that they will become available commercially in the near future.

Table 13. *Ex Vivo* Growth Potential for the Known Lineage Stages	
Hepatic Stem Cells	Division rates of ~1/26 hours under optimal conditions; can be subcultured repeatedly [27, 47]. One cell can generate >40,000 daughter cells in ~15 days [28]
Hepatoblasts and committed progenitors	Division rates of ~1/40-50 hours; rodent hepatoblasts have been found to undergo ~12 divisions in 3 weeks and with one hepatoblast generating 4,000 - 5,000 daughter cells in 3 weeks [43]. The division rates possible for human hepatoblasts are not known though estimated to be similar probably to that of the rodent hepatoblasts. Addition of various mitogens (e.g. HGF) can dramatically affect their division potential.
Diploid adult cells ["small hepatocytes"]	One cell yields ~130 daughter cell in 3 weeks (~ 5-7 divisions total); limited ability to be subcultured[43]
Polyploid adult cells	Attach, survive; DNA synthesis but limited or no cytokinesis[91]

Table 14. Requirements for Tissue-specific Gene Expression (both transcriptional and post-transcriptional)		
Requirements for all genes	Basal Media: nutrient rich. One option= RPMI 1640 (GIBCO) + L-glutamine (1 mM, GIBCO)	
	Calcium	~0.6 mM
	Trace Elements:	Selenium: 3 x 10^{-10} M; zinc sulfate: 5 X 10^{-11} M; copper sulfate: 10^{-10} M
	Lipids	High density lipoprotein (10 μg/ml) + mixture of free fatty acids bound to albumin
	Free Fatty Acids	See details for preparation of these in Appendix 2
	Hormones	Insulin (5 μg/ml), tri-iodothyronine or T3 (10^{-9}M), hydrocortisone (10^{-8} M)
	Proteoglycan/ GAGs	Heparin proteoglycan (ideally liver-specific) (1-5 ng/ml) or can see partial effects with bovine lung heparin (5-10 μg/ml); intestinal heparin is weaker (15-20 μg/ml)
Additional Requirements for Representative Genes	Albumin	Epidermal growth factor (50 ng/ml)
	Connexins	Epidermal growth factor (50 ng/ml); glucagon (10 μg/ml)
	IGF II	Prolactin (2 mU/ml), growth hormone (10 μU/ml)
References	[146, 150, 151]	

Table 15. Feedback Loop: Relevance to Studies Tissue Engineering of Liver whether *ex vivo* or *in vivo***		
Findings	**Hypothesis**	**Predictions**
Stem cells or progenitors do not grow *ex vivo* when co-cultured with mature parenchymal cells	Mature parenchymal cells (e.g. polyploid cells) produce soluble signals constituting feedback loop that regulates stem cell compartment	• The signals do not exist in peritoneum; site is permissive for expansion and maturation of human liver cells • Other hosts (e.g. sheep, pig) that have higher proportion of diploid cells will be better models for studies of human hepatic progenitors. • Strategies for clinical programs must

or with conditioned medium from the mature cells		take feedback loops into account • Transplant purified human hepatic stem cells or progenitors (therefore avoiding feedback loop from mature human cells) • Hosts with high polyploidy will require liver injury to mature cells (zones 2/3)

1.3.5 Extracellular Matrix

Extracellular matrix is essential, especially for normal cells to survive and function.[6, 7, 152] The chemistry and physical features of extracellular matrix are known to regulate gene expression and influence cell morphology in all tissues including liver[5, 6, 145, 150, 153-155]. The extracellular matrix is a complex mixture of molecules between and around cells made insoluble by crosslinking. There are many types of matrices, each with distinct chemical composition, contributed to by all of the cells within the tissue, and changing quantitatively and qualitatively with changes in physiological states or pathological condition. Excellent reviews are available on its chemistry and functions.[8, 10, 65, 153, 156-159]

In the past, the extracellular matrix was thought to play an entirely mechanical role binding together cells in specific arrays. Now it is realized that it is a dynamic chemical scaffold that confers persistent signaling in combination with mechanical effects. The matrices mechanical effects influence genetic expression within the cell via attachment through specific integrin complexes and through them to cells'

cytoskeleton and associated networks. Another role for the matrix is as a storage depot for soluble signals both in that some of its components have amino acid sequences encoding soluble signals and in the ability of matrix to bind soluble signals, thereby sequestering them in the matrix. Extracellular matrix components and their synergistic effects with soluble paracrine signals mediate the regulation of the cell's morphology, growth and gene expression.[6, 10, 37, 145, 156, 157, 160-165]

1.3.5.1 Overview of Paradigms in Extracellular Matrix in Tissues

In order for the cell type of interest to mimic its *in vivo* counterpart in a specific physiological or pathological state, the associated matrix chemistry must be identified. One is helped by the understanding that there is a paradigm to how all types of extracellular matrix are made, and by the numerous studies identifying the matrix chemistry in various tissues.

All cells produce an extracellular matrix, and the extracellular matrix in between any given set of cells contains components derived from all the cell types in contact with the matrix. The matrix components present on the lateral borders between homotypic cells includes cell adhesion molecules or "CAMs"[11, 12, 166] and proteoglycans[14, 167-169] and will be referred to as the "lateral matrix". That between the epithelium and a mesenchymal cell partner will be referred to as the basal matrix. It consists of basal adhesion molecules (laminins, fibronectins) that bind the cells to collagen scaffolding; in addition there are other matrix molecules such as proteoglycans that are attached in many ways to the plasma membrane surface, to the basal adhesion molecules and/or to the collagens.

The matrix chemistry in all tissues changes during development. Thus, embryonic or fetal tissues are comprised of a mixture of matrix components that differ qualitatively and/or quantitatively with that found in the adult tissues. They have the common feature that those found in fetal tissues are less stable and turnover more readily than those in mature tissues. Below are provided brief summaries about each of the categories of matrix components found in tissues, including liver, and have been molecules of interest for the research studies completed.

1.3.5.2 Collagens

Collagens are a centerpiece of metazoan development. There are more than 25 families of collagens, all of them having molecules with the features of 1) numerous repeats of glycine-proline-X, where X is an amino acid defining a specific collagen type; 2) each molecule being 3 amino acid chains braided together and deriving from one to three separate genes; 3) aggregation of molecules into fibrils depending on the exact amino acid sequence of the molecules.[8, 170-173] They contribute to the major scaffolding sources for the basal matrix. Although almost all culture studies using collagens have only made use of type I collagen, a type found in vivo in tendons, bones, and in the most mature portions of tissues, there have been increasing efforts to give recognition to the diverse collagen types that are present in tissues and that confer critical facets of the cells' functions. We have found that specific collagens are requisite for the cells to expand versus differentiate. Model systems such as the lineage state and disease state systems inherently focus on the changes of matrix in time with a change in capacity for the cells. Such is the case of certain liver diseases in which collagens as well as non-collagenous extracellular

matrix components change in their ratios or in facets of posttranslational modifications.[174]

The forms produced by cells are distinct in embryos versus mature tissues. Those in embryos and fetal tissues have a chemistry that makes them less stable and/or they turn over more frequently, whereas those in adult tissues are very stable, and some of them have large numbers of molecules/fibril (e.g. type I), a factor in their stability.

1.3.5.2.1 Type III collagen:

Type III collagen is a fibrillar forming collagen comprising three α1(III) chains and is expressed in early embryos and throughout embryogenesis; it is critical for formation of blood vessels and works in conjunction with type I collagen in adult tissues in the formation of the cardiovascular system. In adult mammals, type III collagen is a major component of the extracellular matrix in a variety of internal organs and skin. Mutations in the COL3A1 gene are associated with aortic rupture in early adult life.*[174]* Type III collagen has been shown to be the substratum of choice for hepatic stem cells to elicit self-replication.*[47]*

1.3.5.2.2 Type IV collagen .

Type IV collagen is the only collagen molecule in which aggregation of molecules results in end-on-end aggregation to make a network or chicken-wire-like structure that is a single molecular thick.[175-178] Cells are bound to type IV

collagen via laminin bridges. It is present in early embryos or in epithelial-endothelial relationships (eg. liver, kidney, endocrine organs).

1.3.5.2.3 Type VI collagen

Type VI collagen filaments are found associated with interstitial collagen fibers, cells in contact with endothelial cells' matrix and with co-distribution of type VI and type IV collagen.[179, 180]

1.3.5.3 Basal Adhesion Molecules

1.3.5.3.1 Laminins

Laminin, composed of 3 polypeptide chains is a major component of the basement membrane helping assembly creating tissue architecture and is uniquely shaped like a cross. Physically, it creates a somewhat regular lattice much like, but distinguishable from type IV collagen, although it can associate with it via entactin and perlecan. Domain affinities also exist for heparan sulfates and nidogen [181-188]. Each trimer is assembled from alpha, beta, and gamma chain subunits of which in mammalian systems there have been five alpha, three beta, and three gamma subchains identified. In addition there are suspected variants to these in alternatively spliced forms.[189-192]

In non-diseased liver, laminin is present in the basement membrane of blood vessels and ducts and spottedly in the Space of Disse [153, 158, 176, 186, 193-195]. Laminin is produced by epithelial cells, both vascular and biliary, lipocytes and hepatocytes in *ex vivo* cultured conditions[153, 158, 186, 196-198] posses the ability

to self assemble like many other known matrix components. They bi-functionally bind to scaffold components, like heparan sulfates, and cells, interacting by integrins and specific receptors such as beta-1/beta-4 integrins and tyrosine phosphatase receptor.[192, 199, 200] The forms of the laminin as composed by the 3 trimers change in expression over embryogenesis, and there are noted changes within the specific tissues such as the liver where niche components are located at higher levels. For example, Laminin 1, composed of alpha 1, beta 1, and gamma 1 is present during embryogenesis as early as the blastocyst, but is absent in the majority of most adult tissues;[192, 201-207] It has been noted that hypatocytes have a high affinity for the attachment of laminin and their fragments.[186, 193, 208]

1.3.5.3.2 Fibronectins

Fibronectins are large glycoproteins composed of two chains connected by a disulfide bridge, which helps to maintain the stability of the extracellular matrix by acting as an attachment site for both cells and other matrix components. Functionally it is interactive with itself, and a site for binding of other matrix components such as heparan sulfates and heparins.[209] Small functional domains have been identified by denaturing of the fibronectin. It has been identified in a regulatory role in cell migration and cellular cytoskeleton organization[210].

1.3.5.3.3 Proteoglycans

(PGs) are among the most complicated of the matrix components having effects through their core proteins as well as their carbohydrate side chains.

Examples of biologically active core proteins are the transferrin receptor (Tf-R) and colony stimulating factor receptor (CSF-R). The forms in the liver include glypicans bound to the cell surface via linkage with phosphotidyl inositol (PI) and syndecans, heparan sulfate-PGs with transmembrane core proteins connected intracellularly to cytoskeletal elements and extracellularly having glycosaminoglycan (GAG) chains, heparan sulfates or heparins, that bind and stabilize soluble signals. The GAG chains can influence receptor binding of the signal and receptor and ligand turnover rates. The mechanisms are not fully understood, but empirically it has been found that the signals bound to poorly sulfated GAGs (e.g. heparan sulfates and chondroitin sulfates) behave as mitogens, whereas the same signals when bound to the highly sulfated GAGs (e.g. dermatan sulfate-PGs, heparin-PGs) behave as differentiation mediators.

1.3.6 Impact of Matrix chemistry to Growth and Differentiation

Achieving liver histological structure and possibly organotypic functions is important for expression of tissue-specific functions of cells cultured under ex vivo conditions and requires substrata of appropriate forms of extracellular matrix [211-213].

Different modifications of substrata for culturing hepatic cells have been tried, including collagens, laminins, and fibronectins.[214] Coating of these matrix molecules on tissue culture plastic results in discrete behavioral and phenotypic responses of hepatocytes [159, 162, 193, 214-217]. The matrix substrata have been characterized under monolayer culture conditions and are now being evalulated in 3-

D culture systems. Interestingly, cells such as parenchymal cell lineages are relatively static ex vivo, whereas they are much less static *in vivo*. As pointed out by Allen and others, there is limited information on the matrix regulation of hepatocyte-specific functions *in vivo*. To further complicate matters, a comparison between 3-D cultures and hepatocytes *in vivo* is difficult in attempts to recapitulate the extracellular system where microenvironment causes specific effects such as secretion of albumin, urea synthesis and P450 activity.[218] Furthermore, how these events influence lineage state of parenchymal cells is not known and comprises studies in their infancy. Recent findings suggest that proteoglycans are imperative to fate commitments by stem cells.

Some matrix components (e.g. laminin) influence specific biological functions such as adhesion to endothelial cells through functional peptide sequences found on the individual chain trimers.[192] Laminin has been shown to be a central component to cellular differentiation, regulation of growth, movement, morphology, and survival.[186, 219] As it is deposited intermittently along the Space of Disse but only in the periportal region[186, 193, 195, 220] it potentially plays key roles in the regulation of stem cells, progenitors and the early lineage stages of adult parenchymal cells offering a microenvironment paralleling embryonic conditions.

Laminin-1 has been shown through culture to be involved in organ development and cell migration[192, 203, 221-224] Effects of the components of the ECM can be regulated by the proteoglycan components as seen as heparin concentrations that influences laminin polymerization through binding and bridging the G domain, a functional domain of the laminin structure.[192, 225] Furthermore,

as the chemistry of matrix molecule interactions are further studied, functional domains of these varied molecules are able to replace whole segments in end specified goals. Improvement of understanding and application of defined culture conditions of hepatic cells enhances the ability to steer the cells through growth,[214] and through differentiation.[27]

Biological activities of hyaluronans (more described below) has been linked to cell differentiation, development, and proliferation, in addition to cell homing, locomotion and immune response.[226] It is recognized, especially for hyaluronans, that oligomer length is implicated in physiological results. In vivo cells maintain the ability to modify the extracellular matrix, and there are known hyaluronidases which degrade HA, and thus create a cascade of physiological responses.

1.3.7 The Matrix Chemistry in Liver and Changes with Development

The chemistry of the extracellular matrix in the liver changes during development with various types of matrix molecules dominant in fetal tissues and others dominant in adult tissues. The stem cell niche for human livers is the ductal plate (also called limiting plate) in fetal and neonatal livers that is the antecedent to the Canals of Herring in pediatric and adult livers [128]. The known matrix chemistry in the liver's stem cell niche is comprised of type III and IV collagen, laminin, hyaluronans and specific forms of chondroitin sulfate proteoglycan[11, 227, 228] [227](Dr. Bruce Caterson, Cardiff, England, personal communication). Two forms of hyaluronan receptors have been found: CD44 found on the hepatic stem cells[45] and LYVE-1 found on the angioblasts.[229] The integrins found in ductal

plate and associated with the hepatic stem cells, the multipotent progenitors in the liver, include: α2, α3, α6, and β4, but no α1 or β1; those associated with hepatoblasts, the liver's bipotent progenitors, are α1, α5, α6, α9, and β1 but no β4; with maturation towards hepatocytes, there is a disappearance of integrin receptors that bind to laminin, whereas maturation towards biliary is associated with a maintenance of laminin-binding integrin receptors.[228]

Outside the liver's stem cell niche, the basal matrix components are found in the Space of Disse, the layer between the parenchymal cells and their mesenchymal partners: the endothelium for the hepatocytes and the stroma for the biliary cells [153, 157] The chemistry within the Space of Disse transitions in gradient fashion from that in zone 1 (periportal zone next to the portal triads) to that in zone 3 in contact with the most mature parenchymal cells in zone 3 (next to the central vein). That within zone 1 (periportal zone) and associated with periportal hepatocytes consists of laminin, type IV collagens, hyaluronans, chondroitin sulfate (CS)-PGs and weakly sulfated heparan sulfate (HS)-PGs.[10, 156, 157, 230-232] This transitions to that found in Zone 3 (pericentral zone): collagen I, small amounts of type III collagen, fibronectin, and highly sulfated proteoglycans such as heparin (HP)-PGs and a complete absence of type IV, laminin and hyaluronans.[91, 233] In addition, there are components of undulin, elastin, forms of dermatan sulfate-PGs. *[5, 10, 156, 157, 167, 234]*[5, 235-238].

Table 16. Lineage-dependent Matrix Chemistry within the Liver Acinus**				
Category of Matrix Molecules	**Stem Cell Niche**	**Zone 1 parenchyma (Periportal)**	**Zone 2 hepatocytes (mid-acinar)**	**Zone 3 hepatocytes (Pericentral)**
Collagens	Type III, IV, (some type VI)	Type III, IV	Type III	Type I, small amounts of III
Laminins	Laminin	Small amounts	none	None
Fibronectin	None	Mesenchymal cells	Mesenchymal cells	Mesenchymal cells Plasma fibronectin
Proteoglycans/ GAGs	Hyaluronans; Poorly sulfated CS-PGs	HS-PGs (glypicans, syndecans) More highly sulfated CS-PGs	HS-PGs CS-PGs	HP-PG DS-PG
Hyaluronans	Present	Present	None	None
Hyaluronan receptors	CD44 RHAMM LYVE1	+ Appears with HA +	None ++	None +++
Integrins**	α6β4, α2, α3	α1,α5, α9, α6, β1	α1, α5, α9, β1	
References	[228, 239-241]	**[153, 156, 178, 193, 235-237, 241-244],[245, 246]**		

*Stem Cell Niche= ductal plate in fetal and neonatal livers; Canals of Hering in pediatric and adult livers. HS-PGs=forms of heparan sulfate proteoglycan (PG); CS-PGs= chondroitin sulfate-PGs; DS-PG=dermatan sulfate proteoglycan

**The biliary lineage comprises two stages of cells that are intrahepatic, small and large cholangiocytes, and then multiple stages that are extrahepatic and connecting the liver to the gut. Very little is known about them with respect to matrix molecules or receptors. What has been reported is that definitive bile ducts express β1, β4, α2, α3, α5, α6, α9, and αV.

1.3.8 Availability of Extracellular Matrix Components

Many of the extracellular matrix components can now be purchased commercially including many of the collagens (e.g. types I, III, IV), basal adhesion proteins (laminins, fibronectins), a few proteoglycans (heparan sulfate proteoglycans or HS-PGs and chondroitin sulfate proteoglycans or CS-PGs) and various

glycosaminoglycans (chondroitin sulfates, heparan sulfates, dermatan sulfates, heparins). Commercially available matrix substrata also include tissue extracts enriched in matrix (e.g. Matrigel). Tissue extracts enriched in extracellular matrix ("ECM", biomatrix, Matrigel, amniotic matrix) can also be prepared with protocols that take advantage of the relative insolubility of extracellular matrix components[20, 40, 152].

1.4 Hyaluronan Chemistry and Biology

HAs are one of the families of glycosaminoglycans (GAGs), all being polymers of uronic acid and an amino sugar. Other GAG families include chondroitin sulfates, keratin sulfates, heparan sulfates, and heparins, all following the same "equatorial bonding scheme."[247] A possible similar genetic lineage for the family of proteins has been discussed with the origin of chondroitins and keratins derived from polylactose, heparan sulfates from polymaltose, and hyaluronans from cellobiose [247]. The chemistry of hyaluronans (HAs) is described most simply as "Hyaluronic acid is a glycosaminoglycan characterized by a disaccharide unit linked with a Beta 1-4,Beta 1-3 bonds between glucosamine and glucuronic acid moieties respectively." However, as biologists, chemists and engineers are exploring the nature and potential uses of the molecules, it is becoming evident that hyaluronans are more complex than has been realized heretofore. Biologically, the polymeric glycan is composed of linear repeats of a few hundreds to as many as 20,000 or more disaccharides units.[226] It is found in extracellular matrix, on the cell surface and inside the cell.[248] Hyaluronic acid may prove to be a key element in defining the

extracellular matrix (ECM) for clonal growth of soft tissue adherent type cells. Attention is focused on this particular molecule over others of the ECM, because HAs are present in greater quantities at times of cellular expansion/proliferation[249, 250] such as embryogenesis,[251] wound repair[252, 253], and organ regeneration.[253] There is a change over in matrix chemistry as liver parenchymal cells differentiate through their maturational lineage stages.HA performs a host of noted tasks within the ECM other than those already stated: matrix structure stabilization and integrity, water and protein homeostasis, tissue protection, separation and lubrication, facilitation of cell movement/migration and cancer metastasis, transport regulation including steric exclusion, anchoring of hormones as a reservoir and integration of the immune inflammation response.[249, 251, 252, 254, 255] Endothelial cells within the lymphatic system posses a large quantity of LYVE-1 to that of CD44, creating a basis for lymphatic recognition and motility of cells within the system.[256, 257]. Some have shown that HA is prominent in early liver injury models. Hepatic stellate cells produce it in primary cultures and in liver injury. Their production of HA increases in parallel with expression of CD44.[258] Some of these characteristics have been implied to change along with exon variants of the major receptor CD44 [258]. In addition there is evidence of inhibitory effects of HA including the inhibition of cellular differentiation.[253] Shepard et al 1996, in a series of experiments have shown that cellular expansion can be facilitated by HA without scarring in wound healing responses.

Hyaluronic acid was first discovered by Meyer and Palmer in 1934. They named the polysaccharide with a Greek-based derivative “hyalos” meaning glassy

since they first extracted it from the vitreous of bovine eyes.[259] Over the century, new methods for acquiring HAs have been developed including extraction from cock's combs and bacteria. Endre Balaz, who has studied the polysaccharide, coined the term hyaluronan to include the different forms of the molecule such as the salt forms that are present at physiological pH [260]. HAs are high-molecular weight polysaccharides estimated to be in amounts found in the average human body of anywhere from 11 to 17 grams [257, 261] HA turnover rate is much greater than that of other extracellular matrix components [257]. As a part of the ECM [262], HAs exist as a nonsulfated glycosaminoglycan (GAG) [254], [255], [263] [251] unlike most other members of GAG families. *In vivo*, synthesized HA is linear [264] unbranched [265] and has a mass between 100 thousand (1E5) to 10 billion (1E10) Daltons depending on the species[250] [Laurent, et al quote naturally occurring numbers to be from 1000 to 10,000,000 Daltons[251], with the size of the polysaccharide being 200 to 10,000 repeating units[266]] Tammi, et al, report the size of hyaluronans generally in the mass range of about 10^5 to 10^7 Daltons, depending upon the tissue type. Depending on the physiology and pathological conditions, the HA oligomer can be fractioned into much smaller fragments[248]. It does not undergo post-polymerization modification, as it is produced at the site of the outer cell wall and pushed into the extracellular space[267].

HAs are central to many functions in development and homeostasis and activated by regulation of their production, turnover and size within a given tissue [248] Interestingly, deletion of either CD44 or RHAMM1 receptors in mice is not

lethal.[248] So, either there is redundancy with another entity handling the role(s) of these receptors or their relevance comes into question.

Biological functions of hyaluronan have been investigated greatly, and the nature of the highly conserved molecule in relation to function has been central to many studies and subsequent papers, including process of morphogenesis of the heart, ovulation and fertilization [248]. Published reviews show how the prevalence of HA in protein interactions, signaling pathways, and pathologies [248] [268-270]The primary biological function assigned to the GAG is one of mediating hydration in vertebrate tissues [253]. HA is found in all tissues and body fluids, and most abundant in soft connective tissue [271, 272]That natural water carrying capacity lends itself to speculation to other roles to be discussed subsequently including influences of tissue form and function.. As stated before, HA is anionic and bears a negative charge [250] This in turn becomes basic chemistry as it attracts the positive charged hydrogen of water molecules. There is overwhelming evidence hyaluronic acid HA is particularly conducive to migration.[269]

The bifunctionality of the HA within the body maintains that removal and synthesis can be equally important in both morphogenesis and tissue homeostasis. Although most cells are capable of synthesizing HA, the highest concentrations are found in the mesenchymal tissues.[273] The relationship between liver and hyaluronan is not clear. However, levels of HA in the blood have been correlated to hepatic regeneration.[274] This seems reasonable since the liver is a major site for removal of HA as is the lymphatic system. Catabolic clearance of HA seems to be the preferred method for eliminating it from the body.[257] The estimated amount of

HA carried to the blood from the lymphatic system in a healthy adult is between 20 and 40 milligrams per day.[265] In humans, about 5 grams or one third of the total body weight is replaced daily. This in fact facilitates many known properties, such as cell differentiation and development, cell proliferation, recognition, locomotion and the immunological responses.[226, 248] In the liver, HA is cleared by a receptor-mediated uptake by endothelial cells via a HA receptor, LYVE-1. As indicated by McCourt et al, the likelihood that disposal of HA without receptor mediated specificity is highly unlikely due to high levels of fluid transfer needed to move the macromolecules across the cell membrane against electrolyte gradients.[257] Radiolabeled HA was found to pool in the non-parenchymal cells.[265] Removal of HA is achieved by endocytic uptake.[248] Hyaluronan concentrations correlate with extent of cellular proliferation and migration. The derived metabolites of endothelial cells are acetate and lactate, which can be degraded by other resident cells of the liver into simple carbon dioxide and water.[265] The pathways as described by Laurent et al[265] describes HA as being transported to the lysosomal bodies after receptor-mediated uptake. There it is broken into metabolites and excreted into the cytoplasm. The glucuronic acid is degraded via the gulonic acid pathway and a deacetylase degradation occurs to the N-acetylglucosamine. [257] [275]"Both acetate and lactate have been detected in liver after degradation of HA." They are transported out of the lysosomes for further degradation in the cytoplasm. Glucuronic acid is degraded via the gulonic acid pathway. N-acetylglucosamine 6-phosphate deacetylase degrades the N-acetylglucosamine. This enzyme is present in large amounts in the mature liver endothelial cells and Kuppfer cells, but not in the

hepatocytes. [265] Information and speculation of the role(s) of HA in normal developmental processes implicates important facets of embryogenesis. Obviously implications are made about the regulation of cell adhesion and motility to its effects.[266]

Karvinen, et al have linked increased HA gene expression in karytinocytes to cell motility in wound healing.[276] A plausible hypothesis is that an abundance of HA within a tissue allows for the creation of highly hydrated areas. These areas, lacking sufficient ECM for cells to attach become a region of low cell density. Low cell density is correlated with cellular proliferation through several mechanisms including decreased paracrine signaling, negation of feedback loops, and cell adhesion and structural changes leading to phenotypic regulation. Soluble signals within the intracellular space help organize a variety of cellular events including "proliferation, communication, and transformation" [264]. The detachment of adherent type cells may be directly linked to the use of hyaluronan as a substrate before divisions.[259] The concentration of HA in amniotic fluid at approximately 16 weeks gestation time in humans averages to 20 milligrams per liter. By birth it is 1 milligram per liter.[273]

1.4.1 Receptor Binding and Cell Mediated Attachment

A key to figuring out the mode in which the HA polysaccharide influences a tissue is to define the method of attachment to cells and to the ECM. HA binds proteins in the ECM, on the cell surface and in the cytosol [251]. Fibroblasts have been shown to proliferate at a faster rate when exposed to higher concentrations of

hyaluronans[253]. Two cell-surface hyaluronan receptors, CD44 and RHAMM, have a direct role for hyaluronans in regulating cell motility, invasion and proliferation.[248] CD44, a cell surface protein mediates cellular attachment of the parenchymal progenitors to HA components of the ECM. It has also been known as Prp-1, ECMR III, and Hermes antigen [277]. CD44 is well characterized as a major receptor for HA. It is a single, 50 kilobases gene. However, there are a large number of variants formed by alternative splicing of a 10 exon region.[258] Although the expression of CD44 is prevalent in almost all tissues, not all forms of CD44 bind HA.[257, 278] It is for this reason that the elucidation of the CD44 regulatory process remains poorly defined as do the roles of ligand and growth factor signaling[248]. In addition physiological responses have been reported through the hyaluronan mediated motility (RHAMM) receptor, ICAM-1, and LEVY-1[266, 279]. ICAM-1 was later shown not to be a binding receptor for HA, and nomenclature has changed for the other receptor to LYVE-1. It is thought that LYVE-1 acts as an anchor for HA, upon which lymphocytes with activated CD44 can move.[280] Hyaluronan receptors related to the link protein family, but unrelated to CD44 or RHAMM, have been described but their function is not yet known.[248] Along with CD44, the (RHAMM) receptor are the two most studied and characterized for HA attachment.[250] Like most integral protein receptors, CD44 spans the outer membrane of a cell[250, 277] and aligns a hexasaccharide element in order to bind HA.[277] On the interior side of the membrane, CD44 can link directly to cytoskeletal elements, thus mechanically triggering signal transduction. This unique position has been studied for effects on cellular adhesion and motility.[250]

Hyaluronate is principally recognized by the CD44 receptor, but there is nonspecific binding of sulfated and non-sulfated forms of chondroitin,[277] which have a similar chain structure to HA.[265] In addition to attachment to surface receptors of some cells, it has specific affinities for binding to proteins in the ECM. CD44 receptor uptake can be inhibited with certain sulphated glycosamino-glycans such as chondroitin sulphate [281] [257]. Attachment acts as a stabilizing force creating a loose fabric of connection [255]). The composition of matrices vary with amount of HA on a tissue-specific basis, but generally the ECM contain HA binding proteoglycans [versican, aggrecan, and link proteins] [250]. Binding of HA by specific cell types has been reported, and particularly in the liver, endothelial cells bind the HA as it passes in the plasma. Elimination in the liver by these cells is regulated primarily through receptor-mediated uptake (via LYVE-1), and the rate of elimination is due to a characteristic affinity. The affinity for the molecule is proportional to the molecular weight of the HA polysaccharide.[265] The underlying reason for this is that larger polysaccharides provide a greater number of attachment sites to interact with the receptors. As another bi-modality of the relationship of molecular weight/size of HA and cellular attachment, large concentrations of HA in the extracellular space decrease the number of cell surface receptors for multiple interactions.

1.4.2 Hyaluronans and Embryonic Development

Defining the relationship between clonal expansion, differentiation, and HA depends largely on the work done with the effects of HA in embryonic development. Concentrations of resident HA increase with rapid repair and

regeneration [266]. Reasoned to be crucial in this role by provision of highly hydrated locals allowing uninhibited cellular migration, and decreased density, HA is a key regulator of embryogenesis [277]. Studies have indicated upregulation in specific variants of HA synthesis. HAS2 is thought to stimulate motility in embryonic development. Further studies indicate that the production of each HAS is differentially scheduled during the embryonic development. Furthermore, their expression is tissue and cell specific. Mouse models in which the HAS synthesis genes have been deleted show that only the HAS2 is vital in development. Without it, the mice never develop hearts [248]. In fact, HA is a major component of the extracellular matrix during embryogenesis. [257] The turn over rate of endogenous HA is equal to at least a 12-fold difference between fetus and adults depending on species.[265] As a scaffolding component, HA has been linked to neural crest cell migration, cardiac development and prostate duct formation [250]. Rapidly dividing epithelial cells show increased binding activity towards HA, and it is plausible that transformation from epithelial to mesenchymal phenotypes take place via interactions mediated by HA binding [250, 277]. Under such conditions, delamination of cells in the embryo go from a tightly bound sheet into an unconnected operational cell unit. Lannace et al, report HA-CD44 interactions enhance matrix dependent locomotion by establishing phosphoinositide 3-kinase, (PI3-kinase) activity [264]. In addition to the transition from a tight to loose tissue connective type, digestion of HA can drive cells to change phenotype. As HA within the extracellular matrix disappears, cells become more tightly bound in a smaller area triggering differentiation.[282]

Recreating a similar environment for stem cells/progenitors to proliferate within a HA matrix is feasible. As concentrations of HA decrease towards the end of embryogenesis by hyaluronidase activity, cells produce a differentiated type matrix containing more stable forms of collagens and more highly sulfated GAGs and proteoglycans [259].

1.4.3 Prevalence in the Body, General Forms, and Structure of HA

HA is produced continuously in the peripheral tissues of vertebrate animals, and every tissue analyzed shows traces of the GAG.[265] There are several different isoforms of the polysaccharide-producing proteins defined by coding of the hyaluronic synthases. They are classified by numeric nomenclature as HAS1, HAS2, and HAS3; are transcribed from 3 different chromosomes; and share a 50 to 70 percent homology.[283] Eukaryotic HA-synthase is located in the extracellular membrane, and has activity correlated with a number of cellular actions (growth, transformation, differentiation, metastasis, and mitosis).[284] Elevation of HA synthase activity and matrix deposition correlates with cellular proliferation and migration.[264] Once produced and exuded into the extracellular space, hyaluronans can still maintain associations with specific ions such as sodium.[285]

HA is produced continuously in the peripheral tissues of vertebrate animals, and every tissue analyzed shows traces of the GAG.[265] Mammals however produce relatively longer chains of HA and also express the ability to degrade the oligosaccharide with hyaluronidases [226]. The extracellular polysaccharide is found throughout the ECM and especially in connective tissues [257]. There are several different isoforms of the polysaccharide-producing proteins defined by

coding of the hyaluronic synthases and resulting in variants within the HA oligomers.

In addition, there are splice variants within HA receptors. Kikuchi and associates described such variants in their studies of CD44 expression by hepatic stellate cells in normal and injured rat liver.[258] The polysaccharide-producing proteins are classified by numeric nomenclature as HAS1, HAS2, and HAS3; are transcribed from 3 different chromosomes; and share a 50 to 70 percent homology [250] The isoenzymes, all homologous to the original streptococcal enzyme isolated and to invertebrate chitin synthases, have been identified in xenopus, chicken, mice, and humans [248]. Eukaryotic HA-synthase is located in the extracellular membrane, and has activity correlated with a number of cellular actions including growth, transformation, differentiation, metastasis, and mitosis.[284, 286] Elevation of HA synthase activity and matrix deposition correlates with cellular proliferation and migration [264]. Once produced and exuded into the extracellular space, physiological associations can persist such as a close relationship between sodium and the hyaluronan GAG [285].

1.4.4 Clinical and Investigational Uses of HA

HAs have been a economically valuable and powerful reagent used clinically. they are readily available and FDA approved. No matter what the source, the polysaccharide is conserved across all species and is biocompatible, eliciting no pyrogenic, inflammatory, immunologic or toxic response [254]. Immuno-neutrality and high water saturation make it a great building block for biomaterials [262]. In

the interest of looking at possible expansion apparatus, it is obtainable, and allowing for advances in chemistry more cost effective to modify as compared to other ECM components like collagen III. Recent research has been furthered because five hyaluronidase genes, and 1 pseudo gene have been recently cloned [248]. Independent of creating the HA oligomer for synthesis, the field of study is using it's important remnants to further Tissue Engineering. Most research and medical forms of HA, both cheap and relatively pure, are obtained from bacteria (Streptococcus Equi) [287]. Improved methods of production along with chemical advances in modification increased general use of HA in fields from cosmetics to surgery. In clinical settings, HA has been used for drug delivery [255], hydrophilic coatings of catheters, sensors and guide wires [260, 266] surgical adhesion reducing agents [287], lubrication agents [251], treatment for arthritis [287],cataract, ophthalmic surgery [251, 260, 285] and have been suggested as a sensitive biomarker for tracking liver cirrhosis.[265] Each of these uses proclaims various benefits of the GAG. Lubrication depends on HAs water homeostasis ability, whereas reduction of surgical adhesions can make use of its steric exclusion phenomena.[251] Surfaces coated with HA show reduction of cellular attachment, fouling and bacterial growth.[266]

1.4.5 Cancer

Developmental mechanisms tend to occur both in simple and more complex systems with evidence of the conservativeness of evolution in these processes. In fact, conservation of essential gene sequences is shown in the

homologies of the molecules between many species within and outside of a specific phyla. The role of HA to cancers is implicated by the long-known phenomena that cancers are somehow related to stem cells and early progenitors. In the 1960s, Van Potter proposed that cancers are cells blocked in ontogeny [288] Later, Stewart Sell and Barry Pierce also focused on cancers as transformants of stem cells and early progenitors [289, 290] they hypothesized that known oncogenic insults somehow targeted the stem cells. More recently, it has been realized that tissues are organized as maturational lineages with the most mature cells producing signals that inhibit the growth of the stem cells, constituting a feedback loop of regulation.[23, 37, 38, 152] Oncogenic insults actually kill the most mature cells in the lineage(s) eliminating the feedback loop and resulting in expansion of stem cells and early progenitors. If the insults are chronic, then there is an increased risk of one or more mutational events in the expanding stem cells and leading to loss of ability to undergo apoptosis and then to malignant transformation.[23, 38] Thus, tumors are enriched in transformed stem cells and/or progenitors with phenotypes overlapping extensively with that of normal stem cells and/or progenitors[23, 291] This background provides an explanation for some of the findings of HA's roles in regulating tumor cells. Several studies have shown that there is a marked increase in HA accumulation in growth, survival and invasion of carcinomas.[250] Up-regulation of HA in embryos leads to cell migration, and it is assumed that some cancers may mobilize in a similar fashion.[264] One postulated role of the CD44 integral glycoprotein receptor is lymphatic homing used by HA-binding cells.[277] Tumors and proliferating cells are often surrounded by heavily enriched

environment of HA, and that can "enhance anchorage-independent growth."[264, 277] In addition to cellular metastasis, cancers that spread through HA-regulated pathways may also be affected by HA's known roles in angiogenesis. This pathway isn't exactly clear but there is an association between HA rich matrices and newly forming blood vessels in tumors.[250]

1.4.6 Inhibitory Characteristics

The presence of high levels of HA is assumed to be associated with known functions of HA such as cell attachment, migration, and creating water tunnels. However, there is a bi-modality to HAs, and it can truly be thought of as a matrix component that is biphasic functionally. In addition to the achievements allowed through interactions, HA can be inhibitory. High concentrations of HA around cells can inhibit migration (e.g. peritoneal macrophages)[277] by filling pathways. High concentrations can limit phagocytosis and immune response[282, 292] including mitogen-induced proliferation of cultured lymphocytes[277]. Responses of the cell types are dependent on intercellular communications. Migration of the cells dropped by 50% when cells were contact with specific splice variants of the HAs.[293]

1.4.7 Characteristics Defined by the Molecule

Interactions between HAs and other biological components are controlled by the chemical structure of the GAG. Many of the polar groups of HAs form interactions within the protein leaving limited availability for reactions outside the

individual structure[267]. As a result, fewer reactive groups offer fewer points of attachment for multipoint functional adhesions. The twist is that the molecule experiences lower non-specific interactions with the environment. The adage of form follows function is easily applied to HA. The biophysical [mechanical strength and flexibility], and biochemical [polar group interactions] characteristics of the GAG underlie its functional properties as a matrix component. Many of the clinical applications, discussed later, are not possible without modifications. Naturally occurring HA has a quick turn over rate *in vivo* and has poor biomechanical properties[255]. When in its natural molecular form, unbranched[294] and unmodified, HA is hydrophilic[250] and water soluble at room temperature.[295] Mo, et al reported that the hydration of HA is 0.77 cm^3/g."[296] This hydration is due to the large negative charge carried by the molecule and the positioning of acidic groups, generating great water binding capacity.[254] NMR studies show that five hydrogen bonds can exist over as little space as four sugar units.[247] As a result of its water binding capacity, HA tends to become less flexible. The positive attribute of having a greater stiffness is the ability to resist compressive forces [253]. The pitfall of giving up flexibility in turn generates a stiff matrix component which is susceptible to shear forces in any fluidic or motion system. As applicable to tissue, it is highly likely that a stiff spring like component of HA can function to keep other matrix components separated and thus form fairly large water tunnels through which soluble molecules can diffuse.[267]

Although linear in molecular form as shown by electron microscopy,[259] HA exists as a collapsed coil in secondary structure.[273] The coiled structure can be

linked to viscosity through charge related changes in the physical dynamics demonstrated by expansions in low ionic strength buffers and high pH[294]. This viscosity effect is primarily dependent on the degree of ionization of the carboxyl groups. HA expands at low ionic strength due to repulsion effects of the molecular charges whereas at physiological pH, the carboxyl group on each disaccharide unit is dissociated negating this effect.[254, 259] Changes in the concentration of HA present in solution can greatly change the values for viscosity and shear due to entanglement of the coiled chains.[294]

HA has rheological properties based on the tendency towards self association. Individual chains become entangled at low concentrations.[273] The entanglement is comparable to placing a number of "slinky – toys" in a box and jostling it around. A few individual chains can form a contiguous network. Mo, etal[296] have found the critical concentration of coil-induced entanglement to be 1 milligram/cm for extracted HA with an average molecular weight of 3.9E5. The characteristic structure of the GAG that allows for nonpolar interactions is a number of hydrophobic patches repeated in intervals on alternating sides by CH groups. Although broad in coverage [over eight or nine units] and relatively weak, they allow for self-association as well as interactions with membranes and hydrophobic proteins.[247, 267] As expressed by Tammi et al "Hyaluronan exhibits unusual physicochemical properties in concentrated solutions due to a combination of its random-coil structure, its large size, which results in molecular entanglement, and its capacity to interact with water molecules. A molecule of hyaluronan, therefore,

has a large hydrodynamic volume and forms solutions with high viscosity and elasticity that provide space filling, lubricating, and filtering functions."[248]

1.5 Nuclear Magnetic Resonance Spectroscopy (NMR)

Nuclear magnetic resonance is based on the same technologies used for magnetic resonance imaging. The key feature presented by the technologies is based around the known fact that when materials are placed within a magnetic field, they align their magnetic angular axis in parallel with the field, and spins of nuclei are able to be identified according to their resonance frequencies. Within the system, an atom is surrounded by a magnetic field. Then a radio frequency pulse is used to knock the alignment of that molecule out of the field of which it is parallel. Subsequently, the electrons precess around an axis to realign to the field and resonate the frequency at which they move, where the spin is the angular momentum created by the precession of the unpaired nuclear particles.

The best commonly found biological elements for NMR detection are ones with non-zero spins such as 1H, 13C, 15N, and 32P.[297] A transceiver to the radio frequencies can then detect the free induction decay described as the relaxation signal. These decays are recorded and are available for mathematical manipulation to facilitate analyses of characteristics of the molecules of interest.

NMR is used in chemistry, biology, medicine, materials science and geology.[298] Biological investigators find that it is useful given that it is non-invasive, and it does not destroy the sample as other methods do, in a trade for sensitivity. Probably even more important is the fact that the complex mixtures

offered by biological samples do not have to be pure to discern molecular structures of interest, and NMR is a perfect mining tool advantageous to creating usable data.[299] As technology proceeds with engineering stronger magnetic fields, NMR resolution becomes better.

1.5.1 Use of NMR for Phenotyping and Metabolomics

1.5.1.1 Metabolomics Historical Perspective

Taking a step upward from clinical chemistry metabolomics does not look to define one metabolite or even just two for that manner. It's power comes in the resolution of literally hundreds of metabolites simultaneously [300], making it "ultrahigh-throughput."[301] Furthermore, historically, one perceives the cell as a unit, but the observation of metabolites can be subdivided into extracellular and intracellular aspects both following nomenclature that is developing as techniques and methods develop around phenotyping methodologies. Each type of cell can have an appreciated phenotype based on the capacity to metabolize given compounds. In fact, the hundreds of specialized human cell types interact differently with environmental factors to influence day to day functions, and furthermore play a role in development, pathophysiological processes, and certainly homeostatic maintenance through daily metabolic processes [302]

Metabolites by definition are the end products as effect by cellular process on present compounds. Metabolites fall into defined classes of compounds such as polar lipids and carbohydrates [303]. Endogenous metabolism follows all energy

generating and biosynthetic pathways by which host cells modify their environment from a proteomics and genetic point of view [302]. It is well known that every organism from microorganisms to humans excretes metabolites into their external environment. An analysis of distribution of the metabolome of several species suggests that the molecular weights of interest by any detection method pursued generally falls with a capped range of under 300 Daltons [304]. As a discrete method of discriminating the difference between what occurs within the cell (internally detectable metabolites) and outside of the cell (extracellular metabolites excreted by the cell) Kell and others proposed the nomenclature of "footprinting and fingerprinting," where footprinting specifically monitors metabolites consumed and secreted into the extracellular compartment. Furthermore, environmental provocations of the metabolic pathways of any system can be analyzed by the excretion of metabolites into the extracellular space. These profiles are highly specific to species and genetic backgrounds [305]. This method was and is particularly useful in describing microorganisms at the metabolic level based on its genome, and was forwarded as a technology for high throughput analysis even without identification of particular metabolites. Remarkably, single gene knockouts were distinguished from wild type organisms in subsequent studies [305]. Furthermore, the discrimination between seemingly similar phenotypes has been applied to transgenic yeast, plants and mice [300] Fingerprinting looks at both inside and outside the cells/tissues of interest. In respect, only looking at the footprint offers advantages over total metabolic analysis (looking at both intracellular and extracellular). It potentially pares down the number of pathways of

the system and thus the complexity added by the intracellular metabolites. Those metabolites excreted into the environment are usually long lived as compared to that of turnover rates of intracellular metabolites, which doesn't require a stabilization and fast quenching method for isolation, which most of the time are time consuming and impede reproducibility because of added complexity [305].

As to what can be learned by looking at the metabolites of a closed system, it starts with a mass balance and a careful look at fluxomics, where metabolites are used to report the end response of the given biological system to environment and genetic changes. In this way, a scientist can trace the perturbations of a system and the concurrent changes within the cells (ie stem cell differentiation). Prediction of cellular order and control is strongly stressed by the methodologies of metabolytic pathways, which when diagrammed represent cell capacity and interchange within the environment. In such a manner, mapping of metabolites can be used as an insight into the cells biotransformation capabilities [302]. Reflections of the metabolome response are caught in the rippled effects of system perturbations throughout the transcriptome, proteome and metabolome. Often the result of small changes in each upstream event cause greater changes in the downstream event. Consequently, the metabolome exemplifies conditions where perturbations become more responsive extending through mechanisms of both the transcriptome and the proteome. [304] These events, are helpful in inferring genetic functionality by metabolome inspection, where changes in the levels of enzymatic activity have occurred. Much of the early work revolved around finding a single metabolite and then correlating it to other known expressions of cell activity [306] As with the other

"omics" the study of the metabolites lend to the accomplishment of understanding systems biology better.[307, 308]

Conditionally, many different devices have been used to look at the metabolome of various cell types and organs, producing signatures of the biomaterial. Listed as various methods inclusive of NMR, are infrared spectroscopy, thin layer chromatography, high performance liquid chromatography with ultraviolet and photodiode array detection, capillary electrophoresis coupled to ultraviolet absorbance detection, capillary electrophoresis coupled to laser induced fluorescence detection, capillary electrophoresis coupled to mass spectrometry, gas chromatography-mass spectrometry, liquid chromatography-mass spectrometry, liquid chromatography tandem mass spectrometry, Fourier transform ion cyclotron mass spectrometry, high performance liquid chromatography coupled with both mass spectrometry and nuclear magnetic resonance detection [299, 306]. No matter what the technique, the method chosen must maintain sensitivity, selectivity, and universal applicability. Early metabolic profiling is often credited to Devaux, Horning and Horning of the Baylor College of Medicine [306]. The metabolome is described as the full set of metabolites within or secreted by a specific cell type or [302]. Applications of various methodologies have led to the systematic methods of identifying and quantifying those recognized metabolites within a given system.[303, 308] Robertson describes metabolomics as being "the quantitative measurement of the time related multi-parametric metabolic response of living systems to pathophysiological stimuli or genetic modification."[308] Jeremy Nicholson further demarks the difference between metabolomics and metabonomics, where

"Metabolomics is the measurement of metabolite concentrations, fluxes and secretions in cells and tissues in which there is a direct connection between the gene expression, protein activity and the metabolic activity itself and metabonomics is the quantitative measurement of the multivariate metabolic responses of multicellular systems to pathophysiological stimuli or genetic modification, [302]" and that continues to be on ongoing debate. Terminally the debate ends where one is the study of and the second is the application of the technology of phenotyping to specific physiological process. And as follows the metabolome is the set of metabolites that an organism can synthesize[303, 309] and generally falls within a low molecular weight.[304]

1.5.1.2 Metabolite Profiling

As with the proteome, metabolites can be tagged as belonging to the simplest systems of cellular compartments or all the way to tissue and even to organismal level.[303] As mentioned before, Devaux et al, and Horning and Horning in the early 1970s are credited with metabolite profiling of steroids and acid urinary metabolites by gas chromatography and mass spectroscopy methodologies [306]. In the last 30 years, metabolomics has been become a growing field. With the use of computer-aided analyses, scientists are able to handle copious amounts of data that are produced. In this regard, metabolomics parallels proteomics and genomics.[310] The potential of studying the metabolic biomarkers is underscored by methodologies introduced into various facets of study including toxicology. To this effect, it has

evolved as a critical process to measure timed responses in toxic processes, drug efficacy and safety when dealing with metabolic studies [300, 311] Applications to toxicology are an ideal use because of the need to identify time dependent changes in metabolites as they change, furthermore exhaustive characterization of activity is pursued along with drug metabolic stability, profiles, and enzymatic inhibition and induction.[312]

Using the metabolome as a study tool is prevalent from plant to animal. Functional genomics and systems biology based on phytochemical reactions in plants are analyzed using metabolomics [306]. Allen et al. has used metabolic footprinting, the original paper discussing the methodology, to classify yeast mutants.[313] Metabolic profiling has been used to identifying biomarkers in renal and hepatic toxicity [308]. Pharmaceutical companies have adopted metabonomics techniques for evaluation of drug-candidates [299]. Others have used it as an organ monitoring tool after transplantation. However the evaluation is done ex vivo on biofluids, and those that are in vivo often only model a few metabolites based on inorganic phosphates.[301]

Furthermore, functional genomics can make use of metabonomics to classify variant species or variants within the same species. Examples of this have been done with mice and rats, simply based on metabolite patterns. As a means of diagnosis, metabolitic profiles in biomedical applications other than toxicology have been used to differentiate tumor progression and development.[300, 308]

1.5.1.3 Metabolomics in NMR

Use of NMR to study biofluids (urine, blood plasma, and cerebrospinal fluid) has been around for about as long as the instrumentation [308]. Its speed and selective uses have been successful in investigation of disease and toxic processes, despite it's low sensitivity[299, 306]. However, it was not until the early 1980s that the application of NMR metabolite profiling started to be published.[306, 314, 315] Each biofluid yields a characteristic 1H-NMR spectra dependant upon the distribution and concentration of metabolites within the sample. As the frequency of the NMR climbs higher, resolution of metabolite peaks increases and potentially hundreds to thousands of individual peaks can be isolated from a 1H-NMR spectra [299]. Specific metabolites can be masked by co-resolution around the same peak or by specific interactions with other metabolites present within the system, and as the power of the spectroscopy is decreased the resolution of fine peaks becomes spread and interpretable. Unfortunately, the strongest peak within samples containing mostly water is that of the water itself, which denies the ability to correctly identify metabolites with spectral peaks within that region without refined methods of water suppression. The large interfering peak is eliminated from many samples in this manner.[299]

1.5.1.4 Advantages of Metabolomics

The noninvasive techniques of proton NMR give a large chunk of information about the processes of the subject with no harm.[300, 316] In fact the technique

produces large amounts of data, with little sample preparation, about multiple metabolic pathways without destroying the sample as other methods do.[317] Those metabolites are associated with generic cellular process present in every cell. Insight into glycolysis, gluconogenesis, lipid metabolism is all reflected and indicative of cell viability, apoptosis, anoxia, local pH, and homeostatsis maintained within the system of interest [301]. Quantification of the substances can be performed in a straightforward manner.[318, 319] For this reason, it is a preeminent tool for biofluid and tissue extraction analysis,[320-322] with high reproducibility [300]

1.5.1.5 Applications of NMR to Metabolite Profiling

Applications of NMR to metabolite profiling is far reaching, from differentiating cell lines to tumor types [300] Groups have made quantitative and qualitative analyses applied to disease state and genetic modifications of model systems [323]. In addition, varied methods of NMR (one and two dimensional, gradient-selected heteronuclear NMR techniques) lends itself to more in depth investigations of the metabolome.[324, 325] Hundreds of low molecular weight metabolites result in the generation of an endogenous profile responsive to physiological states.[326] NMR spectroscopy is useful in the analysis biological mixtures of mammalian biofuids, cell cultures, and microbial cultures.[324, 327-332] Toxicology is a large component of current NMR application which has been used to show time related changes of urine exposed to various mouse and rat models of liver and kidney toxic injury, including exposure to hydrazine and HgCl2.[317,

326] Warne and others investigated the metabolic effects of toxins in earthworms.[303] The majority of research with metabolic profiling is done on biofluids and not tissues [301], and certainly not organisms.

Dealing with organismal work, E Holmes and others demonstrated the biochemical differences between Han Wistar and Sprague-Dawley rats using NMR, which was supplemental to work showing that even similar strains of mice could be differentiated by coat color by acquisition and analysis of its metabolic profile.[317] This is functional genomics by means of metabolic assays. Although the animals are phenotypically the same, silent genes function to influence metabolic pathways.[299] The NMR analysis was used to differentiate biomarkers of phenotypical normal mice.[303, 308, 333] The metabolic fingerprints of mutated yeast strains were investigated by Raamsdonk et al. [303] Supernatants from cryptococcal cultures indentified more than 30 individual metabolites, including many amino acids, alditols, nucleosides, acetate, and ethanol.[325] Metabolites from both supernatants and cell containing solutions have been characterized including investigations on microbial cultures.[324]

On a cellular level 1H-NMR is used to provide information of cultured primary cells, [318] including differentiating cancer cell types and monitoring cellular events such as apoptosis [300] It has been used to profile neuronal cell,[316] and the current underlying suggestion is that each individual cell type has its own unique metabolic pattern which can be discerned by NMR patterning. Spectroscopy, can potentially identify these markers and allow examination of systems differentiation in the cellular metabolism pathways, as is projected Nesti

etal in looking at the metabolic properties of mitochondrial specific metabolic pathways as a sign of "stemness."[334, 335] In fact, Grayson et al. recently released a publication on the effects of low physiological oxygen conditions on the human mesenchymal stem cell population, drawing implications that tissue development can be effected by the oxygen level and significantly characterized using metabolomics.[336] Other metabolic stem cell studies have been performed including distinguishing neural cell types inclusive of adult differentiated cells and progenitors[337] classification of murine embryonic stem cells and neural stem cell derivatives based on metabolic profiles.[335]

Generating data that applies to specific pathways of metabolism is key in identifying metabolic disfunction in disease state[317]. As forwarded in the methodologies, 1H NMR can be used to access many known pathways of metabolism. Systems pathways able to be investigated by NMR include glycolysis, the Krebs cycle, acetate production, urea synthesis, transamination events.[318] The disadvantage of the NMR identification system is substances identification depends on spectral comparisons to like identified samples. Thus there is a need for a database for the computational evaluation of peaks under various conditions. Samples undergo chemical shifts and couplings due to their environment which can often obscure those patterns which readily identify the metabolite.[325, 338, 339]

1.5.1.6 Applications of Mathematics to NMR spectroscopy

Robust studies can produce thousands of samples, and even the simplest studies can produce hundreds, compounded by exponential data derivation by NMR, biofluids offer a niche in which individual characterization of one spectra at a time is nearly impossible to deal with mass metabolite comparisons across a data set [308] Application of statistical analysis methods allow for reduction of the mass data set and in fact reduces the complexity hidden within the dynamic range of the metabolic profile allowing for classification methods based on a few simple rules or observations. The value of the methodology allows data mining and in fact is useful for bioinformatics.[326, 340-342] Methods in which mathematics allows quantitative modeling of constrained systems prove to be informative, and leads to analysis and qualitative predictions and assessments of the systems of interest.[310]

NMR spectroscopy data used in metabolomics is dependent on the use of multivariant statistics. Application of Fourier transformations to data analysis to produce the spectra have greatly facilitated data analyses.[343] Techniques have been derived mathematically and instrumentally to simplify spectra and to identify the components of mixtures including the biofluids.[325] Many different mathematical tools are used in the analysis of current spectra. Principle component analysis (PCA) is a popular method to investigate the individual components of a system to observe which gives the most variance within the system based on combinatorial linear relations. It is unsupervised method,[300] meaning that the data points are able to organize themselves without any predetermined classifications. It is one of the oldest and most widely used methods [344] for dealing with multivariate systems. PCA reduces the variables into a system of

uncorrelated components. As the data is scored upon a plot in which each variable is represented as a different dimension of the plot, the relationships are indicated, and related by their variability.[308] Sumner et al [306] summarize the method as:

> "The concept behind PCA is to describe the variance in a set of multivariate data in terms of a set of underlying orthogonal variables (principal components). The original variables (metabolite concentrations) can be expressed as a particular linear combination of the principal components. PCA is a linear additive model, in the sense that each principal component (PC) accounts for a portion of the total variance of the data set. Often, a small set of principal components (2 or 3) account for over 90% of the total variance, and in such circumstances, one can resynthesize the data from those few PCs and thus reduce the dimension of the data set. Plotting the data in the space defined by the two or three largest PCs provides a rapid means of visualizing similarities or differences in the data set, perhaps allowing for improved discrimination of samples."

Other techniques in addition, applied to data sets are pattern recognition hierarchies and cluster analysis, as applied in studies differentiating hydrazine treated rats from control.[300, 326] Groups have used discriminate partial least squares as part of algorithms to distinguish coronary heart disease, and to observe changes in the normal human serum due to dietary changes. Yet others have combined NMR spectra with neural networks in success.[310] Many applications, such as studying drug effects on whole organisms can not be accomplished without multiparametric measurement and analysis.[299]

1.5.1.7 NMR Analyses of Liver Tissue and Cells

The field of characterization of the metabolic profiles of liver and nonparenchymal hepatic cells is in its infancy. As the largest internal organ, the

liver is approximately 2 percent of the body's mass, of which only 65 percent of the adult liver cells are hepatocytes, but these displace 80 percent of the volume of the liver.[345] As reported previously, toxicology is a major focus for the use of NMR. Isolated hepatocytes are a key model system for drug metabolism interactions[312] Measured effects of hepatic metabolism is important in order to access the full complement of enzymes in primary cultures. Drug testing in liver, the major cite for xenobiotic metabolism, is assessed at this first pass encounters, but the down side is recognized that monolayered cultures of hepatocytes tend to quickly lose gene expression and thus utility as a model system.[346]

However, there are many studies that show the uses of NMR as a tool including the investigations of cryopreservations of primary hepatocytes derived from pig livers, most similar to human in many cases.[318] Dabose and all, used simple 1H NMR to evaluate the metabolic function of hepatocytes frozen under various protocols and compared to freshly isolated cells.

Zonation of the metabolomic profiles with respect to the zones of the liver acinus has been shown.[347] Oxidative energy, carbohydrate, lipid, nitrogen, bile conjugation, and xenobiotic metabolisms have been identified as compartmentalized within zones of the liver acinus.[346] ^{1}H NMR can be effective in identifying small concentration of metabolite changes in conditioned media supernates taken from cultures. As applied to cultures of hepatocytes and nonparenchymal cells in order to understand metabolism, cycles such as glycolysis, the Krebs cycle, acetate production, glucose metabolism, transamination, glutamine synthesis and succinate synthesis, urea and albumin production have been examined.[318] The various

methods work in combinations of known pathways where the observation of one metabolite decreasing leads to the generation of other metabolites as seen in glycolysis, based on anaerobic respiration and production of lactate. Liver metabolic pathways of cultures subjected to various treatments show differences in the manner of respiration. Wishart etal [301] describes the injury response for metabolites in the liver in terms of net increase and decrease of normal levels, where lactate, pyruvate, glycerol, alanine, glutamate, GABA, taurine, and arininine all increase after 19 hours post injury and only arginine was reported as decreasing prior to that time However under other conditions, ischemia, grafting, and post transplantation, a different set of biomarkers can be observed as key metabolites including methylated arginine, glutamine, urea, and phosphatidylcholine.[301]

There have been few studies regarding mammalian primary hepatic cells and monitoring perturbations of identified metabolites such as those found in mitochondrial pathways or glucose production and metabolism, but it is feasible to do this with NMR spectroscopy.[318] One such study characterized the specific metabolite pathway (induced by hypoxia-inducible factor 1) as applied to tumor growth and angiogenesis in hepatomas, of glucose metabolism, [300] Applications derived from metabolic characterization can easily be applied towards the ongoing bioartificial organ programs for cell culture and production of cell therapy methods.

1.5.2 Technical Issues.

Metabolic profiling surpasses proteomics and transcriptomics, in the ability to be high through-put, cheap, reliable and precise [300, 303, 304]However, it is not

without its faults. A major liability is the identification of metabolites without the use of a standard library. The daunting task of creating a library for such biomarkers has already begun with groups in North America and world wide (http://www.hmdb.ca)[301] and there are general, non-species specific databases already in existence like the Kyoto encyclopedia of genes and genomes (KEGG, http://www.genome.ad.jp/kegg). Those spectra which teeter towards being ambiguous often lead to a challenge in the identification of the characteristic peaks, and in complicate predicting/modeling the complex behaviors of even the most basic cellular systems.

NMR has rapid time analysis, but this advantage is paralleled by less sensitivity. Other methods like mass spectroscopy are more sensitive but that becomes part of weighing out what is needed as compared to costs [299] This can be modulated to increase sensitivity by letting samples resolve for longer periods of time within the magnet. Recent publications show value to the claim that high-resolution 1H NMR spectra can identify metabolites at far lower concentrations than standard clinical systems of different natures.[337] Griffin et al in 2004 reported current detection levels for proton NMR on the order of 100 uM in biofluids and tissue extracts, with acquisition times of 10 minutes or longer [300] Low sensitivity only allows interpretable spectra from more concentrated metabolites, which show as higher peaks [306]. Compounding the situation is the problem of co-resonation. In the end, the complexity of signals given off by the compounds range through such an array of substances that no single analytical technique can provide all the information about them in one single sweep. Being able to do that would give a

perspective on the overall physiology of the cell and tissues for comprehension [301] Different facets of NMR have been developed such as magic angle spinning to address how to identify variable moieties. However, as any spectroscopist will point out, being able to quantitate and qualitate a system of metabolites for the very simplest of cells is not a reality for various reasons, but it doesn't mean that we can't identify key metabolites which show us a picture of what is going on within the metabolic and genetic world. The technical challenges make a thourough analysis of a complete system a dream at this juncture in time and not a reality [300]

For use in endogenous detections it has been shown that simple variations in diet can change the metabolic signature of a system.[311] This in turn can have the value of giving a very strong control as to where cultured cells can be given the exact same external stimuli with the variation of one component for computational interpretation. The data that is produced from the metabolic profile is very different in terms of other -omics in that it is modified by outside sources and by self, and that by chance alone makes the data complex and hard to integrate with other functional genomic data.[305] Even though the generated data is highly reproducible, the number of metabolites is deemed to be smaller than the number of transcripts that gives rise to them, and thus in a response situation, a given metabolic pattern may reflect multiple changes in the genome transcription and translation process.[300]

1.5.3 Summary

As Sumner, et al noted "The comprehensive quantitative and qualitative analysis of all metabolites within a cell, tissue or organism is a very ambitious goal and is still far from a reality for any system, although substantial progress is being made."[306] By using defined metabolic phenotypes of cells, tissues and organisms we can still assess various natures indicative of disease, stem-ness, and physiological state. Limited headway has been made in each of these categories, Jansen et al.[335] has established that classifying ES and adult stem cells along with their progeny is limited, and as a direct abuttal to conflicting gene array results, NMR metabolite analysis should be seriously considered as a path to pursue. Wishart, et al.[301] notes that metabolomics will not be the miracle answer for solid organ transplant monitoring, but it has its usefulness already showing itself in clinical applications. The ease of metabolomics may make it an ideal screening technique for common metabolic disorders. It's systematic approach is informative in drug assessment, disease process and diagnosis, genetic functioning, and developmental discovery.[299] Metabolomics ties genomics and transcriptomics together by analytical computations.

2 Chapter II. Identification, Isolation and Characterization of Human Hepatic Stem Cells and Hepatoblasts

Hepatic stem cells and maturational lineage biology of the liver are central themes in my studies. The pluripotent hepatic populations in human livers were found by us to be two: hepatic stem cells (hHpSCs), multipotent stem cells (that are possibly endodermal stem cells), and hepatoblasts (hHBs), bipotent progenitors, the probable transit amplifying cell of the liver. These give rise to unipotent, committed biliary and hepatocytic progenitors. The antigenic, biochemical and morphological characteristics of hHpSCs and hHBs were defined enabling the cells to be identified in vivo and by flow cytometry and isolated by immunoselection technologies. Methods for their *ex vivo* culture were also established. The paper is in press in the Journal of Experimental Medicine (due to come out this summer). The findings of the paper undermine a number of dearly held dogmas: 1) that hepatic stem cells must express α-fetoprotein (AFP)---they do not; 2) that there are no hHpSCs in adult tissues---there are but they have an antigenic/biochemical profile distinct from the one used in the past to identify hHpSCs; 3) that the liver's stem cell niche is the bulk of the parenchyma in fetal liver---it is, in fact, the ductal plates (also called limiting

plates) in fetal and neonatal livers and the canals of Hering in pediatric and adult livers.

IDENTIFICATION, ISOLATION AND CHARACTERIZTION OF HHPSCS AND HEPATOBLASTS FROM FETAL AND POSTNATAL DONORS

A paper in press in Journal of Experimental Medicine, 2007

Eva Schmelzer[1,5], Lili Zhang[1,5], Andrew Bruce[2,5], Eliane Wauthier[1,6], John Ludlow[2,6], Hsin-lei Yao[1,3,6], Nicholas Moss[1,6], Alaa Melhem[1], Randall McClelland[1], William Turner[1,3], Michael Kulik[2], Sonya Sherwood[2], Tommi Tallheden[1], Nancy Cheng[1], Mark E. Furth [7,8], and Lola M. Reid[1,3,4,8]

[1]Departments of Cell and Molecular Physiology and [3]Biomedical Engineering

[4]Program in Molecular Biology and Biotechnology

UNC School of Medicine

Chapel Hill, NC 27599 USA 27599

and

[2]Vesta Therapeutics

801-8 Capitola Drive

Durham, NC 27713

And

[7]Institute for Regenerative Medicine

Wake Forest Baptist Medical Center

Winston Salem, North Carolina 27157

Running Title: HhHpSCs

[5]Co-equal first authors; [6]co-equal second authors; [8]co-equal senior authors

2.1 Abstract

Human hepatic stem cells (hHpSCs), pluripotent precursors of hepatoblasts and thence of hepatocytic and biliary epithelia, are located in ductal plates in fetal livers and in Canals of Hering in adult livers. They can be isolated by immunoselection for EpCAM+ cells and constitute ~ 0.5-2.5% of liver parenchyma of all donor ages. Self-renewal capacity of hHpSCs is indicated by phenotypic stability after expansion for more than 150 population doublings in a serum-free, defined medium and with a doubling time of ~36 hours. Survival and proliferation of hHpSCs require paracrine signaling by hepatic stellate cells and/or angioblasts that co-isolate with them. The hHpSCs are ~9 μm in diameter, express cytokeratins 8, 18 and 19, CD133/1, telomerase, CD44H, claudin 3, and albumin (weakly). They are negative for α-fetoprotein, ICAM1, and for markers of adult liver cells (e.g. cytochrome P450s), hemopoietic cells (e.g. CD45), and mesenchymal cells (e.g. VEGFr, desmin). If transferred to STO feeders, hHpSCs give rise to hepatoblasts, recognizable by cord-like colony morphology and up-regulation of α-fetoprotein, P450A7 and ICAM1. Transplantation of freshly isolated EpCAM+ cells or of hHpSCs expanded in culture into NOD/SCID mice results in mature liver tissue expressing human-specific proteins. The hHpSCs are candidates for liver cell therapies.

2.2 Introduction

The role of hepatic stem cells (hHpSCs), particularly in the maintenance and regeneration of the adult liver, has been a subject of debate without clear consensus

[22, 348-351]. During embryonic development, endodermal cells in the mid-region of the embryo bulge into the cardiac mesenchyme, are affected by critical signaling from endothelia forming vasculature, and form the liver bud [1, 352]. The cells within the liver bud are recognized as hepatoblasts due to expression of a signature marker, α-fetoprotein (AFP) and are bipotent giving rise to hepatocytes and bile duct epithelial cells, cholangiocytes (11). We and others have described the isolation and expansion in culture of AFP+ cells from fetal and adult livers of several species [43, 117, 353]. Clonogenic expansion assays of rodent hepatoblasts under wholly defined conditions have demonstrated that hepatoblasts are capable of extensive expansion *ex vivo* as well as differentiation to both hepatocytic and biliary lineages [43]. The findings from investigations of liver organogenesis as well as the *ex vivo* studies of hepatoblasts have led to a long-standing assumption that hHpSCs correspond to hepatoblasts, and that hHpSCs would express AFP. However, AFP+ cells are rare in normal adult livers (<0.01%) except in livers with severe injury or disease [116, 354, 355]. In addition, the renowned replicative capacity of hepatocytes *in vivo* [107] has led to the opinion that adult livers do not have hHpScs and that all regenerative responses are from mature parenchymal cells except in certain disease states [348].

Here we define a novel class of AFP-negative cells in fetal and adult human livers, that are precursors to hepatoblasts, and have properties consistent with hHpSCs. The hHpSCs are negative for AFP but positive for epithelial cell adhesion molecule, EpCAM (CD326, C017-1A antigen, GA733-2). This protein, encoded by the tumor –associated calcium signal transducer 1 gene, is expressed by many

carcinomas and serves a regulatory function in certain normal epithelia, including all of those derived from endoderm (e.g. liver, lung, pancreas, intestine) [356, 357]. By immunohistochemistry, deBoer and colleagues observed that hepatoblasts in embryonic human liver are EpCAM+, whereas mature hepatocytes are EpCAM- [356] In adult livers, most (but not all) bile duct epithelia are EpCAM+. Also, expanded ductular structures, seen in cases of focal nodular hyperplasia or biliary cirrhosis, contain numerous EpCAM+ cells [356].

We have reported previously that EpCAM+ , AFP-negative cells from human livers are hHpSCs and have compared their pattern of gene expression with that of hepatoblasts and mature liver parenchyma [46]. We now show that the hHpSCs are located in ductal plates in fetal and neonatal livers and in the proximal branches of the intrahepatic biliary tree, the Canals of Hering, in pediatric and adult livers of all donor ages, with the frequency of hHpSCs remaining relatively constant throughout life. We further document the immunoselection of these cells using monoclonal antibodies to EpCAM and test whether they meet the defining criteria for stem cells, namely, self-renewal and pluripotency.

2.3 Results

2.3.1 *In Vivo* Localization of EpCAM+ Hepatic Stem Cells

Sections of fetal and adult livers were stained for EpCAM and for liver-specific markers (albumin, AFP, and CK19) **(Fig. 1).** We found that ductal plates, a band of tissue encircling each of the portal triads in fetal and neonatal livers, have small cells (7-10 μm) with a paucity of cytoplasm, and stained intensely both

cytoplasmically and at the surface for CK19, EpCAM, and weakly for albumin but are negative for AFP. In non-diseased, postnatal (pediatric and adult) livers, cells staining positively for EpCAM by immunohistochemistry appear exclusively in the Canals of Hering in the vicinity of the portal triads of acini. Theise and colleagues [358] reported that cells lining these ductules express cytokeratin (CK) 19, present in biliary epithelia but not hepatocytes. Our data confirm their report and demonstrate that the CK19+ cells within the Canals of Hering express EpCAM and that subpopulations of them also express albumin (**Fig. 1;** yellow color is due to overlap of CK19 and albumin expression). The co-expression of CK19 and albumin is consistent with hHpSCs and corroborates the hypothesis of others that the Canals of Hering comprise a niche for hHpSCs [359]. Below are data from *ex vivo* studies of EpCAM+ cells supportive of the interpretation that they include hHpSCs.

Most parenchymal cells of fetal and neonatal livers consisted of hepatoblasts, slightly larger cells (10-12 μm in diameter) that stained positively for albumin, AFP, and CK19. In hepatoblasts the distribution of CK19 is more particulate and less intense than that in ductal plate cells. EpCAM expression in AFP+ cells, both in fetal and postnatal livers, occurred at the membrane only. In pediatric and adult livers, hepatoblasts were found as individual cells or small clusters of cells tethered to the ends of the Canals of Hering (**Fig. 1**). The hepatoblasts in non-diseased, postnatal livers constitute fewer than 0.01% of cells and express AFP weakly.

Antigenic Profile of hHpSCs vs Hepatoblasts (*in vivo*)		
Marker	**hHpSCs**	**Hepatoblasts**
AFP	Negative	+++
Albumin	Negative or ±	++
CK19	+++	++
EpCAM	+++	++
NCAM	Fetal/Neonatal: ++ Pediatric/Adult: ~40% ++	Negative
CD133/1	++	++
ICAM1	Fetal/Neonatal: Negative Pediatric/Adult: - or ±	++
CD45	Negative	Negative

Figure 1

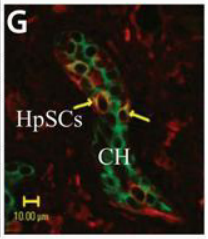

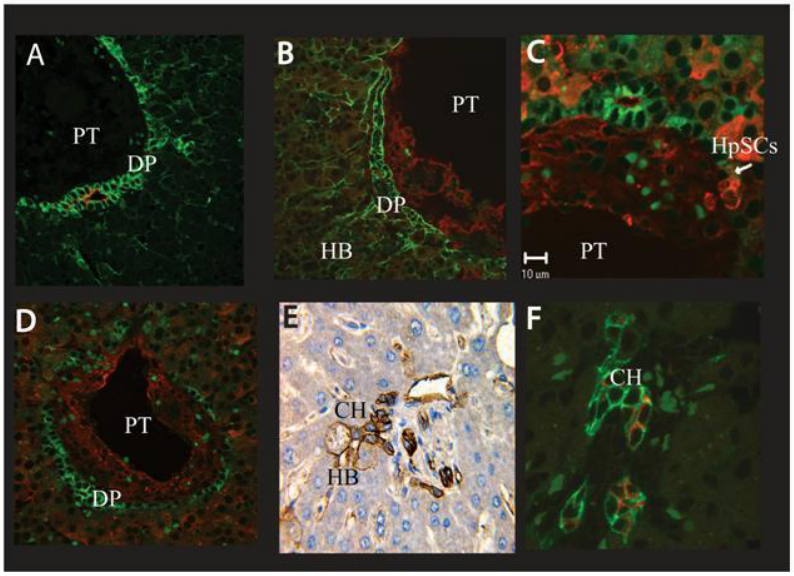

Figure 2-1 Immunohistochemical Studies on Human Fetal and Adult Livers

2.3.2 Flow Cytometry of EpCAM+ Cells

By flow cytometry we observed EpCAM+ cells in human liver cell suspensions of all donor ages (**Fig. 2A**). Suspensions from fetal livers from which hemopoietic cells had been purged contained, on average, 12% EpCAM+ cells. However, the percentage could be as high as 20% depending on the gestational age of the fetus. Most of the EpCAM- cells in fetal livers were of non-hepatic lineage and were predominantly hemopoietic. The vast majority (>90%) of the EpCAM+ cells in fetal livers co-express AFP, albumin (ALB), and CK19 (**Fig. 2**). They could be subdivided into two subpopulations: 1) Hepatoblasts showed expression of ICAM1,

AFP, ALB, CK19, CD133/1, P450A7 and CD44H (hyaluronan receptor); 2) hHpSCs, constituting ~5% of EpCAM+ cells from fetal livers, had an overlapping but distinct profile: they were positive for ALB (weak), CK19, CD44H, CD133/1+, NCAM+, and claudin 3, but negative for AFP and for P450A7.

Figure 2

A. Percentage of EpCAM+ Cells in Livers from Donors of Varying Age

Age Group	# samples	% EpCAM+ Cells	% EpCAM+ Cells that are	
			hHpSCs	Hepatoblasts
Fetuses (16-20 wks)	10	12.1 ± 2.3	~5%	~95%
Neonates (0-1 yr)	7	2.7 ± 2.4	~50%	~50%
Pediatric (2-13 yrs)	17	2.1 ± 1.6	>99%	<0.01%
Adult (19-81 yrs)	38	1.3 ± 1.0	>99%	<0.01%

hHpSCs =positive for EpCAM, NCAM and/or claudin 3 but not AFP
Hepatoblasts=positive for EpCAM, ICAM, AFP but not NCAM or claudin 3

B

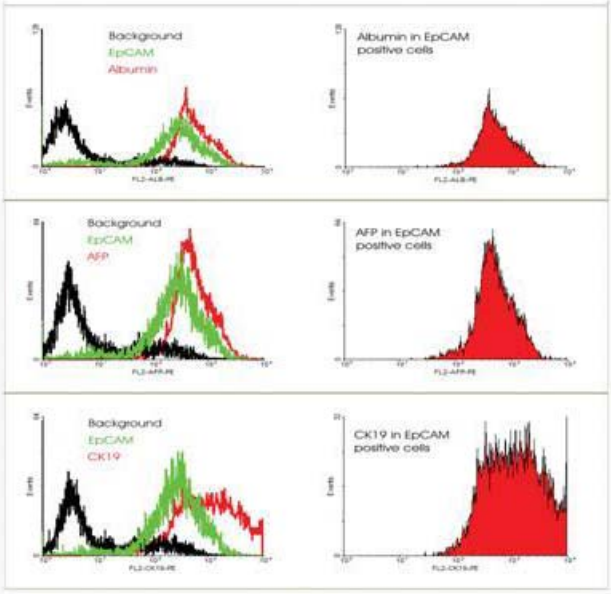

C. Gene Expression in EpCAM+ versus EpCAM- Cells in fetal vs Postnatal Livers

Gene	Fetal Livers	Postnatal Livers	hHpSC Colonies
	Ratio of # of Transcripts in EpCAM+ Cells/EpCAM- Cells		# Transcripts
AFP	2.0	0/0	0.0 ± 0.0
Albumin	2.9	0.14	4.0±1.6
CK19	1.7	433.3	97.2± 18.0
CD117 (ckit)	0.01/0.0	23.3	0.1±0.03
P450 3A4	0/0	0.045	0.0±0.0

Figure 2-2 Flow Cytometric Characterization of EpCAM+ Cells

Cell suspensions from adult human livers averaged 1.3% EpCAM+ cells, and those from neonatal and pediatric donors two to three-fold higher. Preparations

having EpCAM+ cell populations at levels above 1.5% were obtained typically from livers subjected to ischemia (cold or warm) prior to organ procurement and/or during transportation. This suggests that the EpCAM+ liver cells are more resistant to ischemia than mature liver cells. The postnatal EpCAM+ liver cells also co-express CK19 and ALB (data not shown) but have no detectable AFP+ cells (by flow cytometry), except in rare cases of overt hepatic disease (e.g. cirrhosis; data not shown). Neonatal livers, including some from premature births, showed rapidly decreasing levels of AFP+ cells as a function of age, falling below detection level by a few months after birth. Based on considerations detailed below and from our previously published work [46], we identify the EpCAM+ cells from pediatric and adult livers as almost exclusively hHpSCs, not hepatoblasts.

2.3.3 Culture Selection on Plastic and in Serum-free KM

Suspensions of liver cells plated in Kubota's Medium (KM), a serum-free medium optimized for *ex vivo* expansion of hepatic progenitors [43], either on tissue culture plastic or on embryonic stromal cell feeders, yielded parenchymal cell colonies with two distinct morphologies. Type I colonies consisted of cells forming a cord-like morphology interspersed with clear channels and expressing EpCAM, albumin, CK19, ICAM, and AFP but not NCAM (Supplement Figs. 1-4). Type 2 colonies consisted of densely packed, morphologically uniform cells, strongly expressing EpCAM, NCAM, CD44H, claudin 3, weakly expressing or negative for ALB, and negative for AFP and ICAM-1 (Fig. 3 and Supplement Fig. 3). We interpret

the type I colonies as corresponding to hepatoblasts and the type 2 colonies as corresponding to hHpSCs (Table 1).

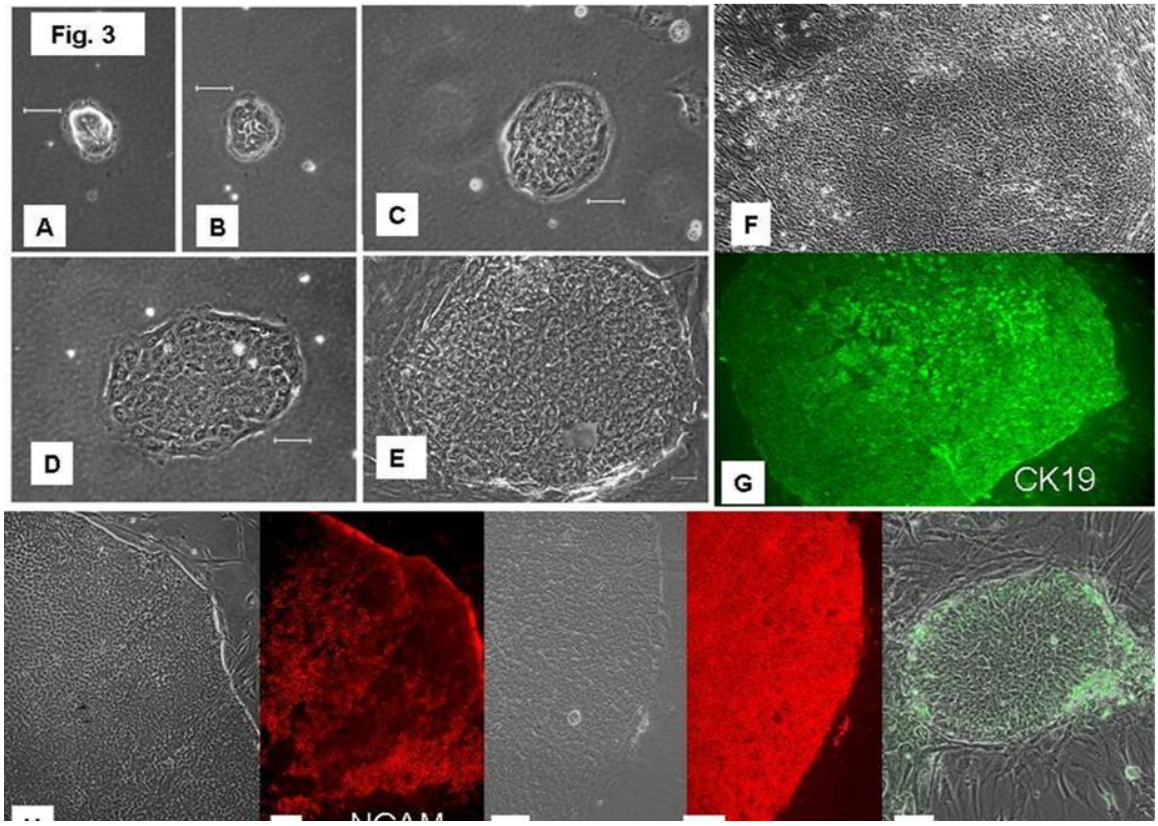

Figure 2-3 hhHpSCs in culture

In cultures on plastic, by 5-7 days (mean 5.2 ± 1.6; maximum of days), the hepatoblast colonies disappeared. However, if cultured on STO feeders, hepatoblasts survived for up to two months, continuing to show co-expression of ALB, AFP and CK19 (Supplement Figs. 1, 2). The hepatoblast colonies typically contained fewer than ~100 cells.

By contrast to hepatoblasts, hhHpSC colonies on plastic continued to expand. A time lapse sequence of a growing hhHpSC colony is shown in Fig 3A-E and in movies, given in the Supplement, in which the expansion of hHpScs seeded at

very low density is shown on day 1, day 3 and day 8. The hHpSCs can be subcultured after mechanical disaggregation and continue to multiply extensively. Their doubling time on plastic is ~36 hours. That doubling time decreased to less than 24 hours if they are plated on specific extracellular matrix substrata (R McClelland et al., submitted). By 2-3 weeks, hhHpSC colonies typically contained many thousands of cells.

The hhHpSC Colonies were assessed for expression of lineage markers by immunofluorescent staining. The expression pattern closely resembled that of ductal plate cells *in vivo*. They were positive for CK19, NCAM, EpCAM, and CD44H (Figs. 3F-L). In addition, they were positive for ALB (weak), E-Cadherin, N-Cadherin, CK8 and 18, CD133/1, integrin β-1 (CD29), claudin 3, and telomerase (data not shown). They were negative for AFP, any form of cytochrome P450, hemopoietic markers (CD34, CD45, CD38, CD14, CD90, and glycophorin A), endothelial cell markers (VEGFr, Von Willebrand Factor, and PECAM or CD31), and mesenchymal markers such as those for hepatic stellate cells (CD146, desmin, and α-smooth muscle actin). The expression of NCAM by the hHpSCs is significant, since previous studies have shown that this marker is present on the ductal plate in fetal livers and evident on liver cell populations proliferating under various disease states [166, 360-362].

2.3.4 Immunoselection using EpCAM Isolates Hepatoblasts from Fetal and Neonatal Livers; Immunoselection Using EpCAM or NCAM Isolates hHpSCs from Livers of All Donor Ages

To enrich for hepatic progenitors from liver cell suspensions, we explored a number of fractionation strategies, including separation by buoyant density on Ficoll gradients (see Supplement Table 1) and by immunoselection. The most satisfactory results were obtained using magnetic immunoselection. While fluorescence activated cell sorting (FACS) was able to yield highly purified cellular subpopulations, the shear forces and the use of buffers (e.g. phosphate buffered saline) that are not optimal resulted in low yields of viable cells. We used magnetic microspheres conjugated with monoclonal antibody to EpCAM (Miltenyi Biotec, Auburn, CA) to immunoselect EpCAM+ cells from liver cell suspensions and obtained robust, highly viable sorted cells that survived and expanded well when cultured (**Fig. 4 and Supplement**). From postnatal livers up to 10 billion viable cells were processed in a single pass using the CliniMACS apparatus (Miltenyi Biotec) and yielded over 100 million EpCAM+ cells. Purity of the enriched EpCAM+ cells was typically 75 to 90% and recovery usually exceeded 90%. Representative fractionation of a fetal liver and of a postnatal liver are depicted in **Fig. 4**. A cell suspension from the liver of a two year-old donor was found to contain 0.7% EpCAM+ cells. The immunoselected population contained 81% EpCAM+ cells, while the flow-through fraction was almost entirely depleted of EpCAM+ cells. The majority of hepatic EpCAM+ cells were of 8-10 μm diameter, as judged by Coulter Counter analysis, in contrast to 18-20 μm for diploid hepatocytes, the predominant

population in the initial liver cell suspension. A small peak of presumptive tetraploid cells also is evident, measuring ~25 μm in diameter. Light scatter ("Side Scatter") profiles indicate that the EpCAM+ liver cells are considerably smaller and less granular than the bulk of the parenchymal cell population.

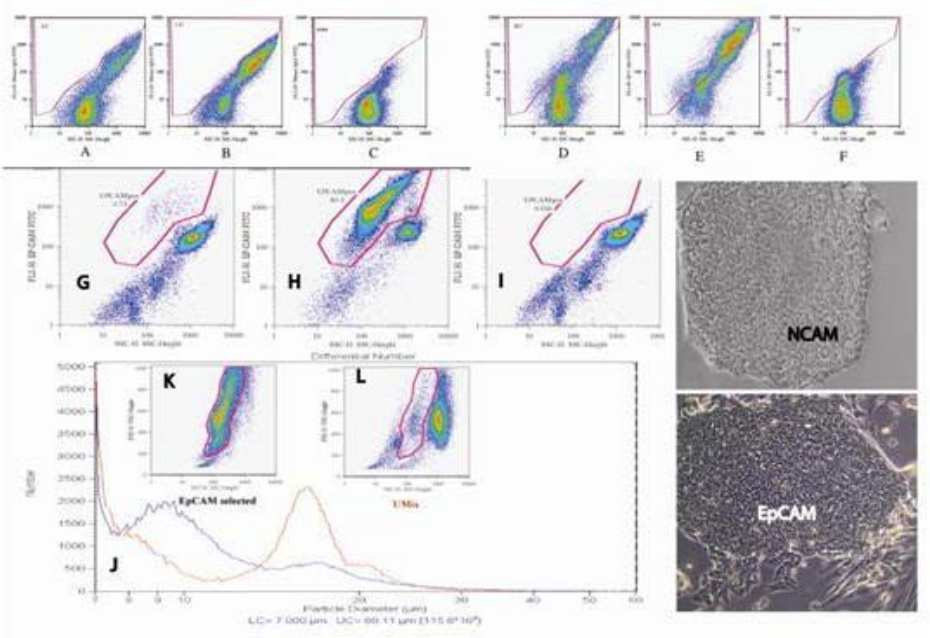

M. Antigenic Profiles of Immunoselected Cells

Markers	Cells Immunoselected for:			
	EpCAM+	NCAM +	VEGFr (KDR)+	EpCAM-/KDR-
AFP	+++ (fetal/neonatal) Neg (pediatric/adult)	Neg	Neg	Neg
Albumin	++	Weak	Neg	Neg
CK19	+++	+++	Neg	Neg
EpCAM	+++	+++	Neg	Neg
Claudin 3	Mixed + and Neg (fetal/neonatal) +++ (pediatric/adult)	+++	Neg	Neg
CD133/1	+++	+++	+++	Neg
Epithelial	+++	+++	Neg	Neg
Endothelial	Neg	Neg	+++	Neg
Hemopoietic	Neg	Neg	Neg*	Mixed + and Neg
Stellate Cell	Neg	Neg	Neg	+++

Epithelial markers: CK 8 and 18, CD29, CAM 5.2
Endothelial Markers:CD133/1, VEGFr, CD31, Von Willebrand Factor; *some with CD34
Hemopoietic Markers: CD45, CD34, CD38, CD14, CD90, Glycophorin A
Hepatic Stellate Cell Markers: Desmin, CD146, α-smooth muscle actin

Figure 4

Figure 2-4 Magnetic immunoselection

Magnetic immunoselection for NCAM+ cells from fetal livers enriched for cells capable of forming only hhHpSC colonies (**Fig. 4**). The majority of EpCAM+ cells from fetal liver co-expressed NCAM, whereas only ~40% of those from adult liver were also NCAM+. Therefore, sorting for NCAM+ cells proved useful for isolation of hHpSCs from fetal livers but less so from adult livers. It is unknown at this time whether NCAM and EpCAM co-expression is a definitive property of hHpSCs. An alternative hypothesis, now being tested, is that NCAM is present on angioblasts or other mesenchymal companion cells tightly bound to the hHpSCs such that immunoselection for it results in co-selection of the two cell types (see below for more on this theme). Sorts for KDR (VEGFr) resulted mostly in angioblasts (**Fig. 4**). However, these sorts also yielded an increase in hhHpSC colonies due, we assume, to co-selection of hHpSCs and angioblasts.

2.3.5 Proteins and Genes Expressed by EpCAM+ Cells

Immunoselected EpCAM+ cells from fetal and postnatal livers were examined by flow cytometry for expression of lineage markers characteristic of various cell types that reside in the liver (**Figs 2, 4 and Supplement**). As judged by double label flow cytometry, about 95% of the immunoselected EpCAM+ cells expressed CK19, and comparable percentages expressed ALB and CD133. Evaluations of many preparations indicated that over 90% of the EpCAM+ cells are positive for CD133, detected with monoclonal antibodies to two distinct epitopes (CD133-1 with monoclonal antibody AC133; CD133-2 with monoclonal antibody AC141). Virtually all CD133-1+ cells in adult liver cell suspensions were found in the

EpCAM+ selected fraction, and mature hepatocytes were clearly negative. However, it appeared that ~40% of liver cells with light scatter profiles consistent with mature hepatocytes were positive for CD133-2. Examination by immunofluorescent microscopy showed that staining for CD133-1 clearly outlines cell membranes, whereas that for CD133-2 shows a more diffuse pattern (data not shown). It is likely that the staining of many more liver cells by CD133-2 results from a known cross-reactivity with CK18 [363] which is expressed by hepatocytes and reportedly can be found on the cell surface [364]. Based on the more specific CD133-1 antibody, we conclude that EpCAM and CD133 (prominin) are co-expressed by the vast majority of hHpSCs.

Neural cell adhesion molecule, NCAM (CD56), shown previously to be expressed by glia, muscle cells and by neurons [365], was found on the majority of hHpSCs derived from fetal and neonatal livers, but only ~40% of the EpCAM+ cells from adult livers. In our prior studies NCAM mRNA was enriched strongly in EpCAM+ cells from both fetal and postnatal livers, but expression at the protein level was variable [46]. NCAM staining was most evident at the borders of the hhHpSC colonies (**Fig 3**).

Less than 1% of the enriched EpCAM+ cells stained for the hemopoietic marker CD45 (leucocyte common antigen), which is found on Kupffer cells (tissue macrophages) and lymphocytes in the liver**.** The EpCAM+ cells were negative for expression of other hemopoietic markers assayed (CD34, CD14, CD38, CD4, CD90, and glycophorin A), for endothelial cell markers (CD34, VEGFr or KDR, Von Willebrand factor, and CD31), and for mesenchymal markers, especially those

associated with hepatic stellate cells (CD146, also called Mel-CAM, desmin, α-smooth muscle actin) (data not shown). Finally, we found AFP expression at RNA and protein levels in EpCAM+ cells from fetal and neonatal livers, but not from pediatric or adult livers. As noted above, small numbers of cells weakly positive for AFP, as judged by immunohistochemistry, were observed tethered to the ends of the Canals of Hering in sections from pediatric and adult livers (Fig 1E). From our experience, these cells are too few and express AFP too weakly to permit recognition as a defined subpopulation by flow cytometry.

Assessment by RT-PCR of RNA expression in the EpCAM+ liver cells (**Fig 2**) gave results consistent with the flow cytometry data. Further details of these findings are reported elsewhere [46]. In brief, EpCAM+ selection from fetal livers more than doubled the expression levels of albumin, AFP and CK19. Immunoselection for EpCAM+ cells from postnatal livers strongly enriched for transcripts encoding EpCAM, CK19, CD133 and CD117 (c-Kit); these transcripts were barely detectable in the EpCAM-negative cells. AFP transcripts were not detectable in EpCAM+ or EpCAM-negative cells from postnatal livers.

Although immunoselected cells are enriched for relative expression of CD117 mRNA, we have not observed the corresponding protein by immunostaining of freshly isolated cells from fetal or postnatal livers nor on cultured cells from postnatal livers. However, we occasionally have observed low levels of CD117 staining on cells at the periphery of hhHpSC colonies from fetal livers, located in regions where hHpSCs overlap with mesenchymal companion cells.

Cytochrome P450 3A4 (CYP3A4), a protein expressed by mature hepatocytes, was not found at all in parenchymal cells, either EpCAM+ or EpCAM-, from fetal livers in terms of both mRNA and protein level of it. The level of mRNA for cytochrome P450 in EpCAM+ cells was twenty-fold lower relative to EpCAM-negative cells from postnatal livers. The small amount of CYP3A4 RNA in the EpCAM+ cell fraction from postnatal livers could be accounted for by residual hepatocyte contaminants. By contrast, the hepatoblasts, but not the hHpSCs, were found to express P450A7, a protein found in fetal livers (data not shown). EpCAM+ cells from postnatal livers also showed eight-fold lower relative expression of albumin RNA than the flow-through (EpCAM-negative) population. Again, some transcripts can be attributed to incomplete removal of hepatocytes. However, the detection of albumin protein in EpCAM+ cells by flow cytometry, taken together with the transcript data, demonstrates that these progenitor cells express the albumin gene, albeit at a significantly lower level than differentiated hepatocytes.

Assays for telomerase activity indicate significant levels in freshly isolated EpCAM+ cells from livers of all donor ages and in cultures of colonies of both hHpSCs and hepatoblasts. Full characterization of telomerase activity and its regulation in various fractions of human liver cells from fetal and postnatal donors is presented elsewhere (Schmelzer E and Reid L, submitted) as are studies on the effects of purified matrix substrata on telomerase activity in cultures of hHpSCs (McClelland et al, submitted).

2.3.6 *Ex Vivo* Clonogenic Expansion—Evidence for Self Renewal

Colony formation by committed hepatic progenitors or diploid adult parenchyma involves a limited number of divisions (typically 5-7 divisions) over a relatively short period of time (e.g. 2 to 3 weeks)[43]. By contrast, self-renewal involves clonogenic expansion that can go on for more than 100 population doublings with phenotypic stability, properties associated with stem cells. We found previously that rat hepatoblasts multiply far more extensively in KM with STO feeder cells than on tissue culture plastic [43]. However, STO feeders and KM were not permissive for clonogenic expansion of human hepatoblasts. Under these conditions the hepatoblasts survived for a few months but demonstrated limited growth. By contrast, hHpSCs from livers of all donor ages could undergo clonogenic expansion for more than 6 months (>150 population doublings) in culture on tissue culture plastic and in KM with only the native feeders (the companion cells) (**Table 2).** The cells maintained phenotypic stability as assessed by morphology and by antigenic and biochemical profiles (**Tables 1 and 2**). hhHpSC colonies starting from 1-3 cells (visual observation -**Supplement-Movies**) grew to cover 4.9+0.3 mm^2 in area and contained an average of 1400 + 520 cells (three independent counts of total cells from 50 dispersed colonies). Thus, the cells in this representative experiment had gone through 10-11 population doublings in 2 weeks corresponding to an average doubling time of 31-34 hours (**Supplement; Table 2**).

2.3.7 Mesenchymal Companion Cells Provide Critical Paracrine Signaling for hHpSCs

The tightly packed colonies of hHpSCs have a prominent ridge at the perimeter (see **Figs 3, 4 and 6**) at which we have identified mesenchymal companion cells (**Fig 5**). As the colonies grow, the companion cells penetrate the colonies and become found throughout them. Time lapse movies (**Supplement: Movies**) reveal a boundary zone between the companion cells and the hhHpSCS in which the companion cells fluctuate back and forth, touching the edge of the hhHpSC colony, or traversing it and moving below the colony. When removed from a culture dish, the attachment to the plastic surface is evident only at the edge of the colonies, not in the center. This suggests that attachment to the plastic is mediated either by mesenchymal cells or by cooperative interactions between the hHpSCs and the mesenchymal cells.

Fig. 5 Antigenic Profiles of Mesenchymal "Companion" Cells to hHpSCs

Markers	Angioblasts	Hepatic Stellate Cell Precursors
Parenchymal cell markers*	Neg	Neg
CD133/1, CD31 (PECAM), VEGFr (KDR)	+++	Neg
CD146	Not tested	+++
CD45, CD38, CD14, Glycophorin A	Neg	Neg
CD34	Variable (some positive)	Neg
CD117	+++	Variable
Desmin, α-smooth muscle actin (ASMA)	Neg	+++

*Parenchymal cell markers: albumin, AFP, EpCAM, CK19, CK8 and 18

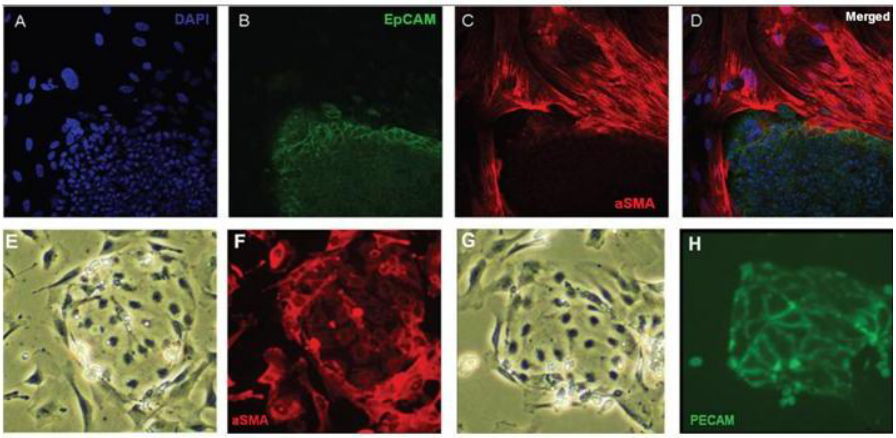

Figure 2-5 Companion cells to the hHpSC Colonies comprise Hepatic Stellate cells and Angioblasts

Phenotypic analyses of the companion cells indicates at least two distinct populations: angioblasts (VEGFr+ or KDR, CD133/1+, CD117+, Von Willebrand factor, $CD31^{weak}$); and hepatic stellate cells (desmin+, α-smooth muscle actin+, CD146+) (**Fig 5**). A comparison of their morphological and antigenic phenotypes is given in **Fig 5**. Cells rigorously purified away from the companion cells (e.g. by repeated immunoselection for EpCAM+ cells) did not survive on culture plastic but only on STO feeders (data not shown). Immunoselection of CD117+ cells yielded angioblasts but neither hepatic stellate cells nor hHpSCs (data not shown).

Immunoselection for other markers found on the companion cells (e.g. VEGFr) resulted mostly in selection of the companion cells alone, though we did find co-selection for hHpSCs to occur at low and variable frequency (**Fig. 4**). We still cannot rule out that the consistent enrichment of hHpSCs from fetal liver by immunoselection for NCAM could actually result from co-selection of the stem cells via tight association with NCAM+ companion cells.

2.3.8 Proof of Pluripotency of hHpSCs

Passaging (transfer) of colonies of hHpSCs (whether derived from fetal or adult livers) from culture plastic onto feeder layers of STO cells resulted within hours in eruption of hepatoblasts from the periphery of hhHpSC colonies (**Figs. 6 and 7; Table 1**). After the transfer, the morphology and antigenic profile of the cells within the hhHpSC colonies proper did not change in most of the cells, though there were occasional cells with distinct gene expression within the colony (**Fig. 7**). Rather the colonies of hHpSCs gave rise to cord-like eruptions from their edges, yielding cells with morphology, antigenic and biochemical profiles identical to that of hepatoblasts. The cells in these erupted areas strongly expressed AFP, ICAM-1, ALB, and were positive for cytochrome P450-A7 (data not shown), but were negative for NCAM (**Fig 7**). In addition, committed progenitors biliary progenitors were sometimes observed erupting from a colony of hHpSCs, as shown by staining for CK19 but not albumin (**Fig. 7**).

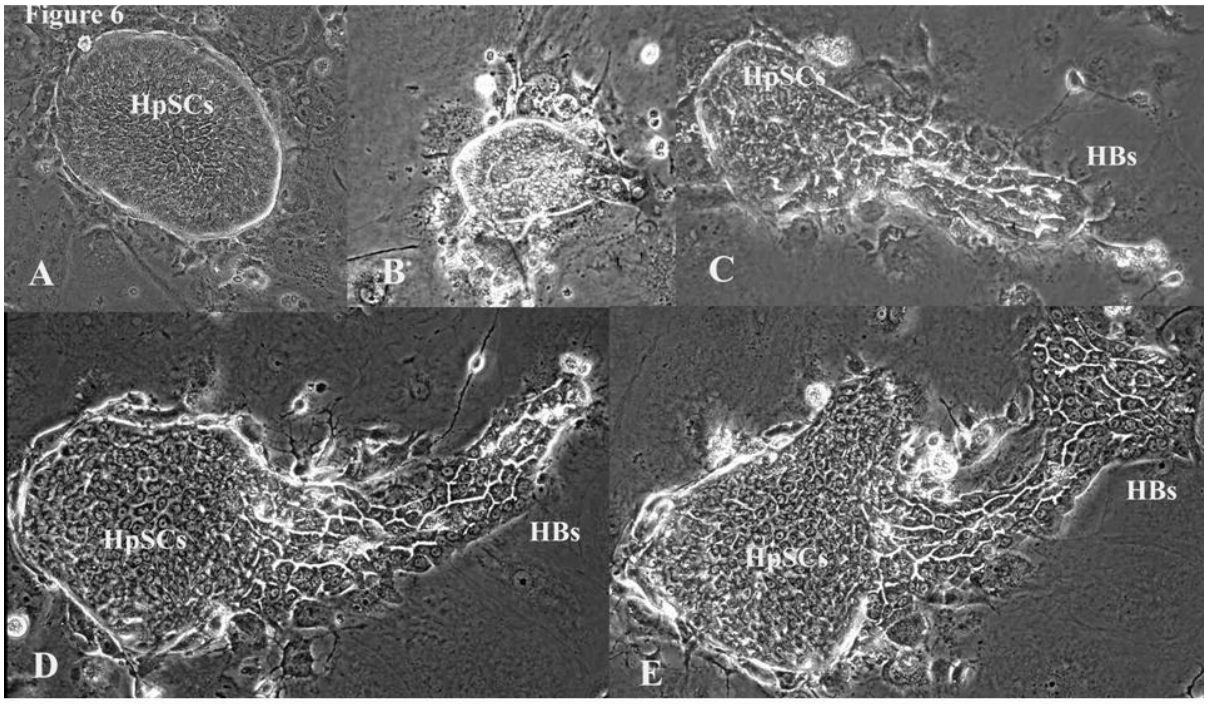

Figure 2-6 hhHpSCs shifted to STO Feeders Erupt Hepatoblasts

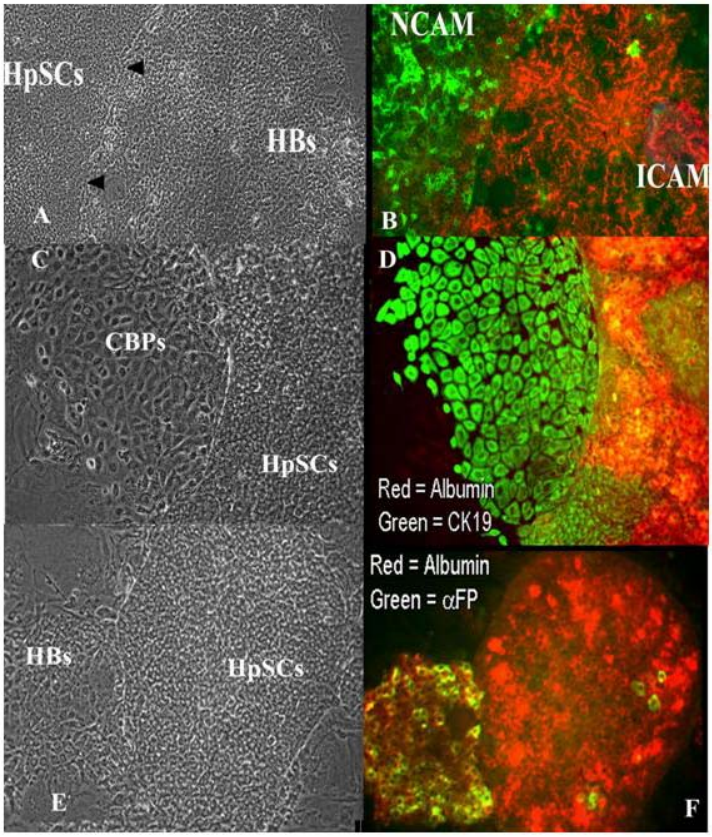

Figure 2-7 Shift in Antigenic Profile from hhHpSCs to Hepatoblasts when on STO Feeders

In cultures of cells from postnatal livers, in colonies stained by double label immunofluorescence for CK19 and ALB, we have observed distinct sectors positive for one or the other marker but not both (**Supplement Fig 4**). This was found most frequently in colonies of hepatoblast morphology. We interpret such sectors as deriving from unipotent cells, corresponding to committed progenitors for biliary and hepatocytic lineages, respectively. The sectoring could occur if at division a bipotent cell gives rise to a daughter cell restricted to the biliary or to the hepatocytic lineage. Occasional small colonies showed expression of only one of the lineage

markers (CK19 or ALB) and are assumed to have arisen from committed progenitors for the corresponding cell type.

2.3.9 EpCAM+ Cells and Colonies of hHpSCs Give Rise to Human Liver Tissue *in vivo*

Transplantation of freshly isolated EpCAM+ cells or of hhHpSC colonies, from either fetal or postnatal livers, into livers of NOD/SCID mice resulted in engraftment and the formation of human liver tissue (**Fig 8**). Islands of cells staining positive for human ALB, CK19 and AFP were found within 2 days of transplantation (**Fig. 8A, C, and E**) and persisted within the livers for weeks (**Fig. 8F**). The extent of engraftment and expansion of human liver cells *in vivo* was enhanced by treatment of the mice with carbon tetrachloride, CCL4, a poison for the pericentral zone of the liver acinus, often used to create a cellular vacuum in transplanted hosts (8B, D, G). Human-specific DNA sequences were found in the liver of animals that received the human cell transplants, but not in other tissues, nor in control animals that did not receive human cells (data not shown). Prior to transplantation, as expected, the cells were shown to express EpCAM and CK19 strongly and ALB weakly, but were negative for AFP at both RNA and protein levels. The liver sections from mice transplanted with hHpSCs contained cells strongly expressing human-specific forms of ALB, CK19, and AFP but were negative for EpCAM. However, human cytochrome P450 3A was not detectable. Therefore, it appears that after transplantation and expansion in recipient livers, the human cells lost expression of a marker (EpCAM) found only on stem and progenitor cells, and,

acquired some, but not yet all, of the functions specific to mature hepatocytes. We think it logical that transferrin is expressed by not yet P450 3A in transplanted cells given that in mature liver, transferrin is expressed by zone 2 parenchymal cells, whereas P450 3A by zone 3 parenchymal cells within the acinus. Thus, P450 3A is a late gene produced by cells at the end of the liver's maturational lineage.

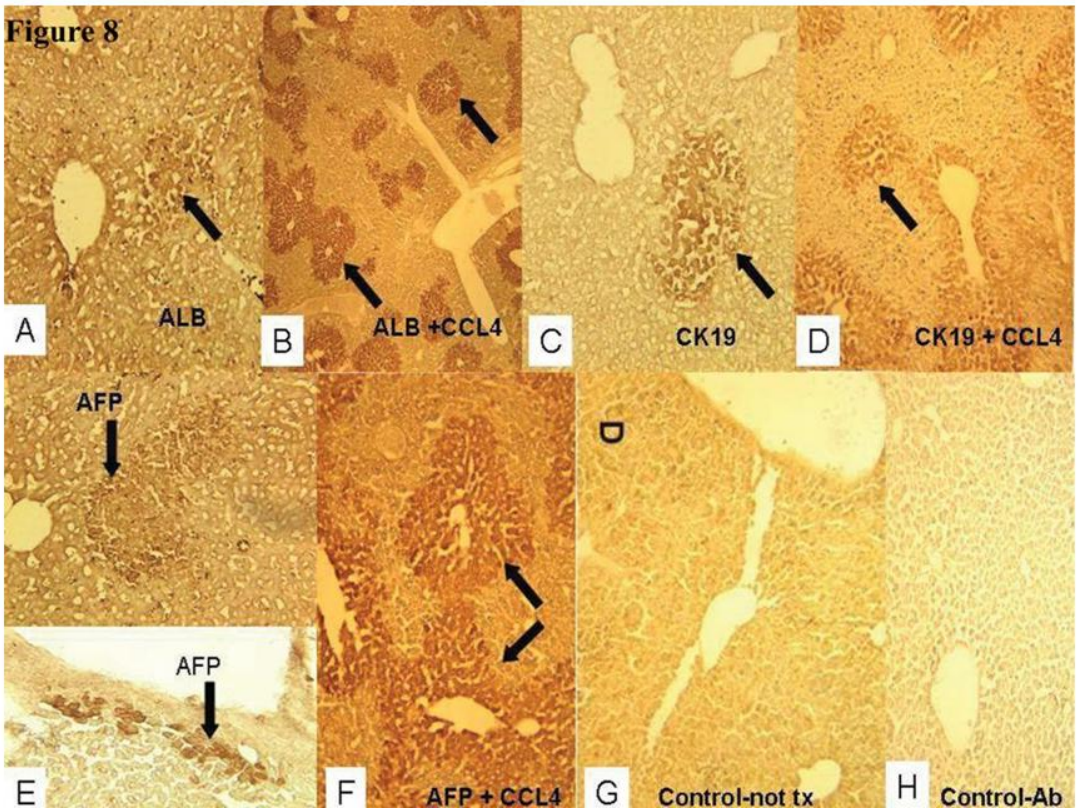

Figure 2-8 Transplantation of EpCAM+ Cells (or Colonies of Stem Cells in culture) results in Engrafted Liver Tissue in NOD/scid mice

As an independent test of engraftment, we assessed expression of the human transferrin gene, encoding a protein characteristic of mature hepatocytes. We found by quantitative RT-PCR analysis with human-specific primers that the livers of mice sampled one week after injection of the EpCAM+ cells derived from postnatal human

livers contained significant levels (2100 ± 1140 strands per 100 ng) of human transferrin RNA. Such sequences were undetectable in RNA from livers of control mice (<100 strands per 100 ng RNA). Although prior to transplantation over 80% of cells in the test cell population expressed EpCAM and CK19, cells in recipient animals were positive for human ALB and were negative for both of the progenitor cell markers. Taken together, the data suggest that within seven days *in vivo*, the engrafted hHpSCs gave rise to mature human liver cells.

2.4 Discussion

Cells in the ductal plates in fetal and neonatal livers and in the Canals of Hering in pediatric and adult livers are hHpSCs. They can be isolated efficiently by selective culture conditions and by immunoselection for EpCAM (CD326) and/or NCAM (CD56). The hHpSCs have features typical of stem cells including Sonic and Indian Hedgehog signaling [28] and high telomerase activity (Schmelzer E and Reid L, submitted).. They are capable of self-renewal, as shown by clonogenic expansion for over 150 population doublings, and are pluripotent, with the ability to give rise directly to committed biliary progenitors and to hepatoblasts and thence to hepatocytic and biliary lineages, as well as to other endodermal cell types (our unpublished data). The hHpSCs express certain markers of both hepatocytic and the biliary lineages but lack expression of mature liver functions [46]. They yield human liver tissue when transplanted intrahepatically in immune deficient mice. Hepatoblasts, expressing AFP, ALB and CK19, and emerging in newly forming liver tissue, have long been considered hepatic stem cells [366]. However, AFP-negative hHpSCs are actually precursors to hepatoblasts.

Recognition of the ductal plate as the liver's stem cell niche provides a new insight into organogenesis, The specification of foregut cells to an hepatic fate is associated with expansion of endoderm into the surrounding cardiac mesenchyme, a process leading to ductal plate formation [28]. Our data suggests that ductal plates are directly antecedent to the Canals of Hering, which have been identified as the reservoir of stem cells in postnatal livers.[358, 367]

The liver at all ages displays a remarkable capacity to regenerate after physical or toxic injury [348]. Two forms of regenerative response are known. The first is a hypertrophic cellular response by mature hepatocytes that undergo DNA synthesis with minimal cytokinesis, the predominant mechanism of regeneration after partial hepatectomy in postnatal livers [42, 368]. The other is a hyperplastic response by both progenitor cells and diploid hepatocytes following significant loss of liver cells in zones 2 and 3, as detailed in a number of review articles [349, 369, 370]. Contributions of progenitors to regeneration after partial hepatectomy have been presumed negligible based on assumptions that they should be AFP+ [348] Since hHpSCs are AFP-, their role in liver regeneration in adults requires re-evaluation by tracking the involvement of EpCAM+ and NCAM+ cells. The frequency of EpCAM+ cells in suspensions prepared from postnatal human livers is consistent at all ages beyond a few months, in the range of 0.5 to 2.5%. We infer that a substantial pool of hHpSCs is maintained throughout life. The number of hHpSCs is much higher than estimates based on the frequency of AFP+ cells (<0.01%). Some authors have argued that the mature liver contains only "facultative" stem cells, activated in response to pathological states and injuries that invoke a hyperplastic response [350,

358, 370, 371]. We have previously raised the alternative hypothesis that hHpSCs function routinely to replenish the liver as mature cells are lost slowly through terminal differentiation [38, 42, 46]. The presence of a much larger pool of hHpSCs than previously suspected in normal adult livers provides a further rationale to examine this possibility more carefully.

During development a limited number of hHpSCs are associated with developing portal tracts and steadily give rise to hepatoblasts that we hypothesize are the liver's transit amplifying cells. The hepatoblasts, in turn, are precursors to committed hepatocytic and biliary progenitors. Further evidence for hepatoblasts in normal adult livers is given elsewhere.[128] In the findings reported here, we show the generation of hepatoblasts and unipotent progenitors from hhHpSC colonies in culture. This occurs spontaneously from discrete regions at the periphery of hhHpSC colonies and may correspond to a localized signal that triggers a rapid burst of expansion from one or more cells. As noted below, cell-cell interactions are key to both maintenance and differentiation of hHpSCs. STO feeder cells promote differentiation of hHpSCs, whereas they contribute primarily to survival and expansion of rodent hepatoblasts, and may offer a tool to identify some of the differentiation-promoting signals for hHsPCs.

2.4.1 Functions of Cell Surface Markers of hHpSCs

Characteristic cell surface antigens of hHpSCs and hepatoblasts overlap extensively, with both populations expressing EpCAM, E-Cadherin, integrin β-1 (CD29), and CD133. The hHpSCs and hepatoblasts are negative for markers of

hematopoietic (CD34, CD45, CD38, CD14, CD90, glycophorin A), endothelial (VEGFr, Von Willebrand's factor, CD31) and mesenchymal (CD146, desmin, and α-smooth muscle actin) cell lineages.

EpCAM is present on proliferating epithelial cells in most, if not all, organs derived from endoderm (e.g. liver, lung, pancreas, intestine). The extracellular domain of EpCAM is thought to generate a relatively weak homotypic bond between adjacent cells [356]. Conversely, the cytosolic domain of EpCAM is believed to diminish the effectiveness of E-cadherin binding through impairment of the interaction between beta-catenin and the actin cytoskeleton [357]. This role may be physiologically relevant for hHpSCs and hepatoblasts, as E-cadherin was expressed with the same distribution as EpCAM.

The role of NCAM in the biology of hHpSCs requires further elucidation. We found that the hHpSCs from fetal and neonatal liver consistently show strong NCAM expression and that immunoselection for NCAM enriches for hHpSCs. However, only ~40% of hHpSCs from adult livers are positive for this antigen. In cultures of hHpSCs, NCAM expression is observed in a characteristic scalloped pattern located most prominently at the borders of the colonies. Thus far we have not been able to ascertain unequivocally whether NCAM is expressed by hHpSCs, by tightly associated mesenchymal companion cells, or both. Ultrastructural studies by electron microscopy are needed to resolve this point. NCAM is a member of the Ig superfamily, with more than 20 alternatively spliced mRNAs encoding multiple protein isoforms [166, 372]. It is the only sialated cell adhesion molecule and forms homotypic cell/cell attachments that are inversely proportional to the degree of

sialation; an increase in sialation results in muted cell-cell adhesion and consequent increase in migration and invasion [166]. Several groups have reported that NCAM is expressed by ductal plate cells within the fetal liver and, interestingly, also by proliferative ductular cells that characterize pathologies collectively termed ductal plate malformations, such as primary biliary atresia [94, 360, 362, 373, 374]. Thus, positive staining for NCAM, in addition to ALB, CK19 and CK8/18, supports the interpretation of these cells as ones derived from the ductal plate.

We found consistent expression of CD133 (prominin-1) by hHpSCs cultured on both plastic and on STO substrata, and by >90% of EpCAM+ cells immunoselected from adult livers. Although angioblasts also are CD133+, the staining in hhHpSC colonies was associated with most or all cells, indicating that CD133 is expressed by the hHpSCs and not only by companion cells. This pentaspan transmembrane glycoprotein was first identified on hematopoietic stem cells, and its expression also has been observed on stem/progenitor cells of a variety of lineages, including endothelia, muscle, neural, prostatic, epidermal, and others [375, 376]. The role, if any, of CD133 in the self-renewal and differentiative capacity of hHpSCs is not yet understood. However, it may be significant that an isoform of CD133 specifically associated with stem cells was found in cells of the basal layer of human neonatal epidermis, and co-expressed there with integrin β-1, which also is expressed by hHpSCs and hepatoblasts. Furthermore, CD133 expression was lost as the epidermal cells stopped proliferating and acquired a differentiated phenotype in culture [377].

2.4.2 Association of Mesenchymal "Companion" Cells with hHpSCs

The specific association of multiple adhesion molecules with hHpSCs and hepatoblasts suggests that they play important regulatory functions in modulating interactions with cells that comprise local inductive environments and/or stem cell niches. A critical, enabling event, required for formation of the liver, is that angioblasts from the septum transversum induce the hepatic bud to form.[352] Such key interactions are now amenable to study *in vitro* using hHpSCs. We observed that colony expansion and cell outgrowth of hHpSCs depends on mesenchymal companion cells prominent at the periphery of hhHpSC colonies and identified by antigenic profiles as angioblasts (positive for VEGFr , CD31 or PECAM, CD117, CD 133) or hepatic stellate cell precursors (positive for CD146 (MEL-CAM, MCAM), desmin and α-smooth muscle actin). These findings parallel our prior work defining hepatic stellate cell precursors supportive of rodent hepatic progenitors and in which we find that they express vitamin A, desmin, and alpha-smooth muscle actin but also various markers associated with endothelia such as VCAM.[26]

CD146 forms homotypic cell-cell connections that were first localized on melanoma cells and subsequently at cell junctions within endothelial cell layers [378]. CD146 has now been identified on many different cell types including keratinocytes and hair follicle epithelia, stromal cells in adipose tissue and bone marrow, and most cell types in the thymus [379, 380]. The expression of CD146 on cells at the periphery of colonies of hHpSCs, and extending to the innermost cells of aging colonies on plastic, is consistent with the known anti-cohesive activity of CD146. In this capacity CD146 functions as an outside-in transducer that suppresses

gap junction connections, inhibits β-1-mediated integrin binding, and disturbs E-cadherin-based adherens junctions [378, 381]. Furthermore, the strong expression of ICAM-1 by more differentiated cells emerging from hhHpSC colonies may also reflect modulation of cell-cell interactions. ICAM has been shown to act in conjunction with CD146 to disturb E-cadherin-based cell junctions [382]. The dramatic increase in expression of CD146 in association with differentiation of the hHpSCs into hepatoblasts is assumed to model angiogenesis in the forming liver, an interpretation supported by the findings of Sonic and Indian Hedgehog signaling and the Patched receptor in the ridge formed by the angioblasts and the hepatic stellate cells [28].

The possibility of co-isolation of hHpSCs with mesenchymal cells may account for some apparent differences between the hHpSCs described here and candidate hHpSCs reported by others.[383] For example, liver-derived, stem-like cells have been reported to express markers shared with hematopoietic progenitors, including CD45 (leucocyte common antigen), CD34, and CD117 , and/or to be capable of giving rise to both hepatic and endothelial cells [384]. Another report describes candidate hepatic stem cells found in regeneration after massive hepatic necrosis as “lymphoid blastlike” cells that express CD133 and CD117 but not CD45.[385] We suspect that the multipotent stem cells found in fetal liver and reported to give rise to liver and also mesenchymal lineages (e.g. cartilage) and that co-express EpCAM and various mesenchymal cell markers are also an example of co-selection (51).

The hhHpSC populations from both fetal and adult livers appear essentially negative for CD45, CD34 and CD117. However, CD34 and CD117 are expressed by angioblasts, which we have found in companion cells associated with hHpSCs. Based on immunofluorescent staining CD117 was variably present in the border zone between the companion cells and some (but not all) hhHpSC colonies cultured on plastic. Also, transcript analysis revealed a slight enrichment in CD117 mRNA in EpCAM+ cell populations from fetal livers and a significantly greater enrichment in EpCAM+ cells from postnatal liver.[46] Nonetheless, immunoselection for CD117 or CD34 yielded angioblasts, not hHpSCs. In summary, our data remain inconclusive; we cannot rule out that a minor subpopulation of hHpSCs cells express CD117.

It is conceivable that phenotypic differences between hHpSCs obtained by different isolation procedures reflect varying stages within a common lineage and/or subtle effects of *in vitro* selection protocols. However, it is clearly important to be aware of the physical and functional interaction of hepatic (endodermal lineage) and mesenchymal lineage cells both in the developing liver and the adult organ, and the possibility of ascribing properties to a single cell type that actually correspond to a mixed population. In any case we argue that the relative frequency and anatomical location of EpCAM+, CD133+. CD34-negative cells, and the growth and differentiation capacity of these cells, provide strong evidence that the hHpSCs described here are authentic stem cells in fetal and postnatal livers.

Purified EpCAM+ cells, from fetal or postnatal livers, are able to engraft the livers of immunodeficient adult mice, with or without prior injury, yielding mature human liver tissue. The engrafted cells lose expression of stem cell markers (e.g.,

EpCAM, CD133, and CK19) and show enhanced expression of mature human proteins and mRNAs characteristic of hepatocytes (e.g. ALB and transferrin). The use of human-specific antibodies and sequence probes confirmed that these were made by donor-origin cells. The extent of humanization of the murine livers was greatly enhanced by treatment of mice with CCl_4, known to selectively kill mature parenchymal cells and, thereby, to create a cellular vacuum in the host.

The efficiency with which EpCAM+ cells can be isolated from human livers, their ability to clonogenically expand *ex vivo*, their pluripotency, and the evidence that they yield mature liver tissue after transplantation encourage consideration of their clinical utility. Potential applications include cell-based therapies of liver disease and generation of cells for bioartificial livers.

2.5 Materials and Methods

(Details are provided in the supplement available online)

Human Liver Sourcing.

Fetal Livers. Liver tissue was provided by an accredited agency (Advanced Biological Resources, San Francisco, CA) from fetuses between 18-22 weeks gestational age obtained by elective terminations of pregnancy. The research protocol was reviewed and approved by the IRB for Human Research Studies at the UNC.

Postnatal Livers. Intact livers from cadaveric neonatal, pediatric and adult donors were obtained through organ donation programs via UNOS. Those used for these studies were considered normal with no evidence of disease processes. Informed consent was obtained from next of kin for use of the livers for research

purposes, protocols received Institutional Review Board approval, and processing was compliant with Good Manufacturing Practice.

Liver Processing.

Fetal livers. All processing and cell enrichment procedures were conducted in a cell wash buffer composed of a basal medium (RPMI 1640) supplemented with 0.1% bovine serum albumin (BSA Fraction V, 0.1%, Sigma, St. Louis, Mo.), insulin and iron saturated transferrin both at 5 ug/ml (Sigma St Louis MO) trace elements (selenious acid ,300 pM and $ZnSO_4$, 50 pM), and antibiotics (AAS, Gibco BRL/Invitrogen Corporation, Carlsbad, California). Liver tissue was subdivided into 3 mL fragments (total volume ranged from 2-12 mL) for digestion in 25 mL of cell wash buffer containing type IV collagenase and deoxyribonuclease (Sigma Chemical Co. St Louis, both at 6 mg per mL) at 32 EC with frequent agitation for 15 – 20 minutes. This resulted in a homogeneous suspension of cell aggregates that were passed through a 40 gauge mesh and spun at 1200 RPM for five minutes before resuspension in cell wash solution. Erythrocytes were eliminated by either slow speed centrifugation [386, 387] or by treating suspensions with anti-human red blood cell (RBC) antibodies (Rockland, #109-4139) (1:5000 dilution) for 15 min followed by LowTox Guinea Pig complement (Cedarlane Labs, # CL4051) (1:3000 dilution) for 10 min both at 37°C. Estimated cell viability by trypan blue exclusion was routinely higher than 95%. See supplemental data for further details.

Postnatal livers. The livers were perfused through the portal vein and hepatic artery for 15 min with EGTA-containing buffer and then with 600 mg/L collagenase (Sigma) for 30 min at 34°C. The organ was then mechanical dissociated in either collection buffer; the cell suspension passed through filters of pore size 1,000, 500, and 150 microns; the single cells collected and then live cells fractionated from dead cells and debris using density gradient centrifugation (500 x g for 15 min at room temperature) in Optiprep-supplemented buffer in a Cobe 2991 cell washer. The resulting hepatic cell band residing at the interface between the OptiPrep/cell solution and the RPMI-1640 without phenol red was collected.

Magnetic Immunoselection. Isolation of cells expressing EpCAM from human liver cell suspensions was carried out using monoclonal antibody HEA-125 coupled to magnetic microbeads, and separated using a miniMACS™ , a midiMACS ™, an autoMACS™ or CliniMACS® magnetic column separation system from Miltenyi Biotec (Bergisch Gladbach, Germany), following the manufacturer's recommended procedures. Similar protocols were used for sorts for NCAM+, CD117+, VEGFr (KDR)+, CD34+. and CD146+ cells.

Colony Formation. Cells were plated in serum-free, hormonally defined medium, "Kubota's Medium (KM), in 6-well tissue culture dishes seeded with monolayers of Mitomycin-treated STO feeder cells, as described by Kubota and Reid [43, 212]. Medium was changed every 2 to 4 days. Colonies were observed within a 7-10 days and were followed for up to six months using an inverted microscope.

Additional results (tables and figures) are given in the supplement available online.

Abbreviations: EpCAM: Epithelial Cell Adhesion Molecule; hHpSCs: HhHpSCs; AFP:α-Fetoprotein; ALB: albumin; CK: cytokeratin; NCAM: Neuronal Cell Adhesion Molecule; ICAM: Intercellular Adhesion Molecule; CD: common determinant; KM: Kubota's Medium; PBS: phosphate buffered saline; CCL4= carbon tetrachloride

Acknowledgements: We thank Thomas Asfeldt, Lucindea English, and especially Dr. Robert Susick for support and assistance. Funding was from a sponsored research grant (Vesta Therapeutics), by NIH grants (RO1 DK52851, RO1 AA014243 , RO1 IP30-DK065933), by a U.S. Department of Energy grant (DE-FG02-02ER-63477). LZ received partial salary support from the Chinese government. Patents have been filed on the intellectual property, are owned by UNC and licensed to Vesta Therapeutics. The authors have no conflicts of interest.

Figure Legends

Fig 1. Immunohistochemical Studies on Human Fetal Livers. Confocal microscopic images on 5 μm liver sections. The antigenic profiles are given in the Table. Sections were stained for:

Human Fetal Livers: A. EpCAM (green) and CK19 (red); B. EpCAM (green) and AFP (red); C. CK19 (green) and albumin (red); D. CK19 (green) and AFP (red)

Adult Livers: E. EpCAM. Black arrows denote probable hepatoblasts at the end of a canal of Hering; F. Canals of Hering around portal triad with EpCAM (green) and CK19 (red); G. A Canal of Hering showing EpCAM+ cells (green) some of which also express albumin (red).

Fig 2. Flow Cytometric Characterization of EpCAM+ Cells. A. The % of EpCAM+ cells in livers of varying donor ages. *The numbers for fetal livers have been reported previously (28) but are presented here for comparison to findings in livers from older donors. B. Analyses of EpCAM+ cells from fetal livers (similar findings occur with EpCAM+ cells from adult livers except that few cells express AFP). C. Quantitative RT-PCR Assays on freshly isolated EpCAM+ versus EpCAM- cells from fetal versus postnatal livers. These data are compared to the findings from colonies of hhHpSC grown on plastic and in serum-free KM for 30-60 days.

Fig 3. hHpSCs in culture. A-E show a stem cell colony forming at 2 days (A), 4 days (B), 7 days (C), 10 days (D), and 14 days (14) in culture on plastic and in KM. Scale bar: 20 um. Phase contrast coupled with image of cells with staining for NCAM (E and F), CK19 (G and H), EpCAM (I and J), and CD44H (L).

Fig 4. Magnetic immunoselection. A-F. Flow cytometry on human fetal liver cells stained for EpCAM (Panel D; Panel A is the isotype control for D used for setting the gate shown in pink) indicated 20.7 % of the cell suspension were positive for EpCAM. The cells were subjected to magnetic bead sorting and yielded a suspension enriched for EpCAM to 54.6% of the cells (Panel B is the isotype control used for the data in panel E). The flow-through cells (Panel F; Panel C is the isotype control for Panel F) were depleted in EpCAM yielding 7.15% of the cells. G-I. Flow cytometry on cells from adult livers. EpCAM expression (Y axis) vs side scatter (X axis) . In the original, unfractionated cell suspension were found 0.73% EpCAM+ cells. H. a single pass through Miltenyi microbead sorting resulted in enrichment for EpCAM+ cells to 80.9%. I. In the flow through were found only 0.06% EpCAM+ cells. J. The EpCAM+ cells were ~9-10 μm in diameter vs 18-22 μm for mature parenchyma and had low side scatter (K) relative to that found for mature cells in the unfractionated mixture (UMIX) of liver cells (L). **Table:** summary of profiles of cells immunoselected for EpCAM, NCAM, KDR (VEGFr) or for KDR-/EpCAM- cells. **Phase micrograph images** are of an hhHpSC colony from an EpCAM+ sort and one from an NCAM+ sort.

Fig 5. Companion cells to the hHpSC Colonies comprise Hepatic Stellate cells and Angioblasts. hHpSCs are associated with mesenchymal companion cells with distinct antigenic profiles. See movies in the Supplement. Two types of companion cells are evident: angioblasts (positive for VEGF-R, CD133/1,

CD117, weakly positive for CD31 and von Willebrand's factor) and hepatic stellate cells (positive for desmin and α-smooth muscle actin—ASMA).

Fig 6. hHpSCs shifted to STO Feeders Erupt Hepatoblasts. Passage of hHpSCs from plastic to STO feeders results in cord-like eruptions that morphologically and antigenically are identical to hepatoblasts. A. An hhHpSC colony shortly after passaging. B-E. A small group of passaged stem cells appears as a tightly compacted group of cells that erupts cords of hepatoblasts at the periphery of the colonies. Shown is a colony and the steady eruption of hepatoblasts by the end of day 1 (B), day 3 (C), day 5 (D) and day 7 (E) after passaging.

Fig 7. Shift in Antigenic Profile from hHpSCs to Hepatoblasts when on STO Feeders

The border between the hhHpSC colony and hepatoblast outgrowths is marked by arrowheads. A and B. The antigenic profile of the cords of cells erupting from the parent colony is identical to that of hepatoblasts and includes a shift from expression of NCAM (green) to ICAM (red)

C and D. Lineage restriction to committed biliary progenitors (CBPs) indicated by staining for CK19 (green) and albumin (red). E and F expression of AFP (green) and albumin (red) indicates that erupting cells are hepatoblasts.

Fig 8. Transplantation of EpCAM+ Cells (or Colonies of Stem Cells in culture) results in Engrafted Liver Tissue in NOD/scid mice.

NOD/scid mice were transplanted with 10^6 cells of either freshly isolated and immunoselected EpCAM+ cells or colonies of hHpSCs from culture on plastic for 30-60 days (>~40 population doublings). Similar results were obtained with both populations. After transplantation, half the mice were treated with carbon tetrachloride (CCL4) (representative results shown in Fig. 8B, D, and F; representative results from transplanted mice not treated with CCL4 are shown in Fig. 8A, C, E and F). In Fig 8A, C, and E are shown sections of murine livers stained for human-specific proteins two days (Fig. A, C, and E), 8 days (Fig 8F) or 8 days after transplantation and 7 days after CCL4 treatment (Fig. B, D, G). Controls included sections of mice not transplanted (H) or sections stained with only the secondary antibody (I). All antibodies but that to albumin gave little no background; shown is the control for albumin

Online Supplemental Materials

I. Details on Materials and Methods

Optiprep Fractionation of liver cells from postnatal donors

OptiPrep (60% solution of Iodixanol, Accurate Chemicals, Westbury, NY) was diluted with RPMI-1640, without phenol red, to give a 25% solution of OptiPrep having a density of 1.12. After calculating the volume of cells based on weight, enough RPMI-1640 without phenol red was added to bring the final volume of cell suspension to 250 ml, with a total cell number not to exceed 10×10^9 (40×10^6 cells/ml). 250 ml of 25% OptiPrep will then was added to the cell suspension and mixed gently. The resulting OptiPrep/cell solution was then gravity fed into a COBE 2991 cell washer-processing bag. 100 ml of RPMI-1640 without phenol red will be

layered on top of the OptiPrep/cell solution using a peristaltic pump at a rate of 20 ml/min while the bag is spinning.

Purging of Contaminant Cells (e.g. Erythrocytes) Requires Gentle Procedures to Avoid Damaging the Hepatic Stem Cells. Cell suspensions from fetal livers are replete with erthryoid cells and other hemopoietic cells such that the parenchymal cells constitute only 8-9% of the cells by flow cytometric analyses of cells expressing albumin and *a*- fetoprotein (see supplemental data). The standard lysing buffer used for elimination of red blood cells from hemopoietic cell suspensions was found to damage the hepatic progenitors and could not be used (data not shown). Therefore, alternative methods for purging the cell suspensions of such hemopoietic cells were identified. One method found effective is a modification of that of Lilja and associates [386, 387] in which red blood cells are eliminated from pellets of parenchymal cells by slow speed centrifugation. The adaptation introduced in these studies was to use the slow speed centrifugation steps on partially enzymatically digested liver containing clumped parenchymal cells enabling ready separation from erythrocytes and other hemopoietic cells that are present as single cells. After debulking of the erythrocytes and other hemopoietic cells, the clumps of parenchymal cells are prepared as single cell suspensions by an additional collagenase step yielding cell suspensions that are more than 80% parenchymal cells as evidenced by percentage of cells expressing albumin and *a*- fetoprotein, approximately a ten fold enrichment. An alternative method, complement-mediated

cytotoxicity to erythrocytes (or to other hemopoietic cell populations) also proved successful.

Ficoll fractionation was tried initially and found to be ideal for isolating hepatoblasts that constituted >95% of the cells in the Ficoll pellets. The hepatic stem cells were found as a minor constitutent (~0.1%-0.5%) of the cells of the Ficoll interface (Supplement:Table 2). They were isolated far more efficiently by immunoselection technologies (Fig. 4).

Histology. Human or mouse liver specimens were fixed in 4% buffered paraformaldehyde for 12 hours and subjected to immunohistochemical staining by the methods noted in supplemental data.

Flow Cytometry. For cell surface markers 1 x 10^6 cells were labeled, following standard procedures, with 1 μg of each monoclonal antibody directly conjugated with fluorescein (FITC) or phycoerythrin (PE). For intracellular markers, cells first were fixed with 2% paraformaldehyde in PBS for 10 min at room temperature and then incubated in permeabilization/blocking buffer (2% Triton X-100, 10% goat serum, 2% teleostean fish gel in PBS) for an additional 30 to 60 min, prior to incubation with a monoclonal antibody, washing, and incubation for 30 min with a fluorescent-labeled secondary antibody. Analysis was performed using a FACSCalibur flow cytometer (BD Biosciences, San Jose, CA) and FlowJo software (Tree Star, Inc., Palo Alto, CA). Nonspecific binding with isotype-matched control antibodies (BD Pharmingen, San Jose, CA) was used to establish gating. Monoclonal

antibodies, labeled with fluorescein (F) or R-phycoerythrin (PE), were: EpCAM-F (clone Ber-EP4, DakoCytomation); CD133/1-PE (clone AC133, Miltenyi Biotec); CD34-PE (BD Pharmingen); CD45-PE (BD Pharmingen); CD14-PE (BD Pharmingen); CD38-PE (BD Pharmingen); CD4-PE (BD Pharmingen). For detection of intracellular antigens, primary mouse monoclonal antibodies of IgG_{2a} isotype to human serum albumin (clone HAS-11, Sigma Aldrich), *a*- fetoprotein (clone 4A3, Biodesign), or cytokeratin 19 (CK19, clone A53B/A2, Zymed) were utilized and detected using secondary Alexa Fluor® 647-goat anti-mouse IgG_{2a} (InVitrogen, Carlsbad, CA), which does not react with the IgG_1 EpCAM-F monoclonal antibody.

Fluorescent Staining of Cultured Cells. Cells were fixed with acetone/methanol (1:1) for 2 hrs at ambient temperature, rinsed with Hank's Balanced Salt Solution (HBSS), incubated with 20% goat serum in HBSS for 4 – 6 hours, and rinsed. Fixed cells were incubated with monoclonal antibodies to albumin and CK19 for 6 – 12 hrs, washed, incubated for 4 – 6 hrs with labeled isotype-specific secondary antibodies, and washed, always at 4° C. Stained cells were preserved with 2% formaldehyde in HBSS and viewed using an inverted fluorescence microscope.

Immunhistochemistry —Fetal livers (16 – 20 weeks of gestation) were fixed in 4% para-formaldehyde over night and stored in 70% ethanol. Tissues were embedded in paraffin and cut into 5 μm sections. Sections were de-paraffinized with xylene and re-hydrated with decreasing alcohol series. Antigens were retrieved by boiling sections for 25 min in a pressure cooker in Retrieval Buffer (Dako,

Carpinteria, CA). Endogeneous peroxidases were blocked by incubation for 30 min in 0.3% H_2O_2 solution. Sections were blocked in Serum Block (Dako); primary antibody was applied in Diluent (Dako), using rabbit anti-human telomerase reverse transcriptase (Calbiochem/EMD Biosciences, San Diego, CA). Secondary antibody and ABC-staining were performed using the RTU Vectastain Kit (Vector Laboratories, Burlingame, CA). DAB (Dako) was used as substrate and sections were counterstained with hematoxylin QS for nuclei staining (Vector Laboratories). Sections were de-hydrated with increasing alcohol series, fixed in xylene and embedded in Eukitt Mounting Media (Electron Microscopy Sciences, Hatfield, PA). Sections were analyzed using a Leica DMIRB inverted microscope and pictures were taken with a MicroPublisher camera (Q-Imaging, Burnaby, BC, Canada) controlled by SimplePCI (Compix Imaging Systems) software.

Antibodies used for Liver Sections, for freshly isolated cells and for cultures

Markers	Markers (sources)
Hemopoietic Markers	Glycophorin A (Caltag #MHGLA04); CD14-FITC (Pharmingen #555397), CD34-FITC (Caltag #CD3458101); CD38-PE (Pharmingen #M030098); CD45-FITC (BD #347463)
Mesenchymal Cell Markers	CD146, CD31 (PECAM), alpha-smooth muscle actin, VEGFr, (KDR), desmin
Cell Surface Proteins	EpCAM, 1:800 (Neomarkers; # MS-144-P1ABX); N-CAM (CD56), 1:100 (Novocastra, #NCL-CD56-1B6; also NCAM 16.2 –PE (BD# 340363); I-CAM-1 (CD54), 1:200 (Pharmingen; # 664970 or Bender MedSystems;#BMS108); c-kit or CD117 (Dako #R7145); CD133/1 (Myltenyi Biotec # 130-080-801); Epithelial Antigen (Dako # F0860); CD54 or I-CAM 1 (BD #347977).
Intracellular Proteins	Albumin, 1:800 (Sigma, # A6684); α- fetoprotein (*a*- fetoprotein), 1:500 (Sigma, # 8452); CK19, 1:200 (NovaCastra; #NCL-CK19), CK8 and CK18

Goat anti-mouse Isotype-specific antibodies	Alexa Fluor 568 conjugated goat anti-mouse IgG2a ,1:200 (Molecular probe, A21124), Cy5 conjugated goat anti-mouse IgG1, 1:200 (Southern Biotec;#1070-15)
Conjugated Isotype Controls	Mouse IgG FITC and PE (BD #'s 349041 and 349043).

Livers samples were fixed in buffered paraformaldehyde 4% over night at 4° C, followed by incubation with 30% sucrose at 4° C for 18-24 hours, washed with PBS and placed in optimal cutting temperature (O.C.T) compound (Sakura finetek , CA, USA), frozen in cold 2-Mythelbutane (Fisher scientific), and stored at -80° C. The tissue was sectioned at 5-10 μm thick frozen sections, in serial sections of 50 sections for each liver. Routine examinations were made in four sections stained with hematoxylin-eosin (H&E) and with the others for immunohistochemistry staining.

Confocal Microscopy. Immunofluorescence was observed using a Zeiss 510 Meta Laser Scanning Confocal Microscope (Zeiss; Jena, Germany) or Leica SP2 Laser Scanning Confocal Microscope (Leica; Wetzlar, Germany).

Cell Culture. The culture medium, "Kubota's Medium" (KM), is serum-free and its preparations are described in detail in prior publications [43].

Stromal feeders. Murine embryonic stromal feeder cells, STO cells, were prepared as described previously [43].

Gene	Gene Bank Acc. No.	Forward Primer (5' → 3')	Reverse Primer (5' → 3')	Tm Forward/ Reverse Primer (°C)	Product length (bp)
AFP	NM_001134	accatgaag tgggtggaatc	Tggtagccaggtca gctaaa	59.64/58.53	148
ALB	NM_000477	gtgggcagc aaatgttgtaa	tcatcgacttccaga gctga	59.59/59.66	188
C3A4	NM_017460	gcctggtgc tcctctatcta	ggctgttgaccatca taaaagc	57.11/60.86	187
CK19	NM_002276	ccgcgacta cagccactact	gagcctgttccgtctc aaac	60.47/59.85	152
c-kit	NM_000222	gatgacgagttggccct aga	caggtagtcgagcgt ttcct	60.22/59.50	233
EpCAM	NM_002354	ctggccgtaaactgcttt gt	agcccatcattgttct ggag	60.30/60.07	182
GAPD	NM_002046	atgttcgtcatgggtgtg aa	gtcttctgggtggca gtgat	59.81/60.12	173

Quantitative RT-PCR: The assays were done as described previously [46]. Gene specific primers used included the following:

Telomerase Activity Measurement —Measurement of telomerase activity was done using a modified, real-time PCR Telomeric Repeat Amplification

Protocol (TRAP) adapted for the use in the Roche LightCycler and Roche SYBR Green DNA kits (Roche). Collected cell pellets were resuspended in 20 µl ice cold CHAPS buffer (Chemicon, Temecula, CA) containing 20 U RNase out (Invitrogen), tissue was homogenized in 150 µl ice cold buffer using glass potter and pestle. Extracts were incubated for 30 min on ice. After centrifugation (20 min, 4°C, 20,000 g) supernatants were frozen on dry ice immediately and kept at -80°C. Total protein measurement was done using the DC-protein assay (Bio-Rad Laboratories, Hercules, CA). Extracts from cultured HeLa cells (American Type Culture Collection, Manassas, VA) were used as positive controls, CHAPS buffer with RNase out served as negative control, and heart tissue was used as reference. HeLa extracts were used to create standard curves in quantitative real time PCR, using the LightCycler (Roche) and SYBR Green Fast Start Master DNA kit (Roche). Extracts containing 0.2 µg total protein were incubated with SYBR green mix and oligonucleotide sequences (primer TS: 5' AAT CCG TCG AGC AGA GTT 3'; ACX: 5' GCG CGG CTT ACC CTT ACC CTT ACC CTA ACC-3') and incubated for 20 min at 25°C in the dark. Two step PCR was performed with 10 min denaturation at 95°C, and 35 cycles at 95°C for 20s and at 60°C for 90s. Standard curves were linear applying extracts from 1, 10, 100, 1,000 and 10,000 HeLa cells.

Mice. C57Bl/6 SCID/nod mice were purchased from Jackson Laboratories (Bar Harbor, Maine) and were housed in a barrier facility on the campus of the University of North Carolina-Chapel Hill (UNC-CH), NC . Animals received care

according to the Division of Laboratory Animal Medicine, UNC-CH guidelines, ones approved by AALAC.

***In vivo* Engraftment.** C57Bl/6 NOD/*scid* mice were purchased from Jackson Laboratories (Bar Harbor, Maine) and used at 5 weeks of age. Mice were anesthetized with Ketamine-HCl (Vedco Inc, St. Joseph, Mo) and Xylazine-HCl (ProLab LTD., St. Joseph, Mo) and injected intrasplenically with 8 x 10^5 cells. The spleen was exteriorized through a small left flank incision (5 – 10 mm), and 70 µl of cell suspension was injected slowly into it using a 26-gauge needle on a Hamilton syringe. The spleen was returned to the abdominal cavity and the incision site was closed. Seven days following transplantation animals were euthanized under sedation and the livers were recovered. In parallel, half the animals were treated with carbon tetrachloride at 0.6 ul/gm body weight. In some experiments the cells were injected after CCL4 treatment, and in others were injected prior to CCL4 treatment. A portion of tissue was frozen in liquid N_2 and stored at -80° C for isolation of RNA. The remainder was fixed for histological analysis.

II. Tables

Table 1. Antigenic Profiles of Human Hepatic Stem Cell (hHpSC) and Hepatoblasts

Markers	hHpSC on Plastic and in KM[1]	hHpSC on STO feeders and in KM[1]	Hepatoblasts
α- fetoprotein[2]	Negative		+++ in those from fetal liver; ± in those from postnatal livers

Albumin[2]	Negative or ±	++
P450-3A4[2]	Negative	
P450-A7[2]	Negative	Positive
CK 8/18, CD29, CAM 5.2	+++	
CK19[2]	+++	+ found as particular staining in cytoplasm
EpCAM[2]	+++ cytoplasmically and at membrane	++ at membrane surface but not cytoplasm
NCAM[2]	Strongly positive especially at edge of colonies	Negative
Indian and Sonic Hedgehog and Patch[3]	+++; Sonic is at periphery and Indian in center of cells	++
ICAM-1[2]	Negative	Positive (see **Figure 6**)
Claudin 3[2]	+++	Negative
CD44H [4]	+++	
CD133/1[2]	+++	
Telomerase[5]	+++	
CD117[2]	Debatable**	Negative
Mesenchymal[6] Cell Markers	Negative	
Endothelial Cell Markers[7]	Negative	
Hemopoietic Markers[8]	Negative	

**It is not detected on freshly isolated EpCAM+ cells from fetal or postnatal livers; RNA for it is enriched in EpCAM+ cells [356]; it is variably found in HpSC colonies from fetal but not adult livers and when found, is always near or overlapping with the companion cells; immunoselection for it does not yield hHpSCs . We suspect it is on angioblasts but not the hHpSCs (and for certain is not on hepatoblasts).

[1]Kubota's Medium. See reference for original description of it's development [117]and a review for its details of its preparation. [43]

[2]Phenotypic characterization of more than 20 genes by RT-PCR and Western blot analyses was done on hHpSCs, hepatoblasts and hepatocytes from livers from varying donor ages [356].

[3]More extensive studies on hedgehog signaling are presented elsewhere

[4]More extensive studies on hyaluronan receptors and their relevance to use of[362] hyaluronan hydrogels for ex vivo maintenance of hHpSCs are given elsewhere [45]

[5]Telomerase activity has been measured in hHpSCs, hepatoblasts versus in mature liver cells

[6]Mesenchymal markers: CD146, desmin, α-smooth muscle actin

[7]Endothelial cell markers: VEGFr (also called KDR), Von Willebrand factor, CD31

[8]Hemopoietic cell markers: CD45, CD34, CD14, CD38, Thy 1 (CD90), Glycophorin A

Table 2. Evidence for Self-Renewal

	hHpSCs	**Hepatoblasts**
Minimum Conditions for survival	KM[1] + Culture plastic	KM[1] + STO Feeders
Life-span of cells	Culture plastic:>6 months STO Feeders: indefinite	Plastic: No survival after ~5-8 days STO Feeders: ~2 months
Doubling Time on Plastic or feeders[2]	Plastic : 1.5-2 days STO Feeders: 12-24 days (<24 hours on certain matrix substrata[4])	Plastic: No survival STO Feeders: essentially no growth
[2]Cell number/colony after 2 weeks ("clonogenic" expansion)	Plastic: $1.4X10^3 \pm 5.2 X 10^2$ (derived from a single hHpSC partnered with a single companion cell—see movies)	Plastic: No survival
Phenotype of hHpSCs after > 150 divisions (>6 months in culture)	Identical to that of cells after initial plating; characterization summarized in Table 1	Within the ~ 2 months of survival time on STO feeders, cells retained expression of albumin, *a*- fetoprotein and CK19
Ability to form liver tissue after transplantation [3]	Capable after 1-2 months in culture on plastic and in KM[1]	Only if transplanted within ~7 days of culture on plastic (not tested with cells on STO feeders)

[1]KM =Kubota's Medium, serum-free RPMI 1640 with no copper, low calcium (0.3 mM) and supplemented with zinc, selenium, insulin, transferrin, HDL and lipids[388].

[2]See movies (**Supplement**) of day 1-day 8 colonies of hHpSCs. Clonogenic expansion occurs but requires each hHpSC to be partnered with at least one companion cell; the companion cells proved to be angioblasts or hepatic stellate cell precursors (see **Fig 5**; see also the movies in supplemental data for colony formation at low seeding densities and on days 1-8).

[3]In **Fig 8** are shown images from liver sections from animals transplanted with human hepatic stem cells.

[4]Elsewhere we report that plating the stem cells onto specific forms of extracellular matrix, found in abundance in embryonic or fetal tissues enables them to go for months through rapid divisions with doubling times of <24 hours for months (McClelland R,et al. submitted).

Supplement Table 1. Antigenic profile of freshly isolated cells in the Ficoll interface fraction versus Ficoll pellet fraction derived from suspensions of human fetal liver cells

Marker*	**Interface cell fraction**	**Pellet cell fraction**
α- fetoprotein	26.0 + 7.6	72.3 + 3.9
Albumin	33.7 + 5.4	79.8 + 9.2
CD117 (c-kit)	5.4 + 3.0	2.2 + 1.7
E-Cadherin	57.9 + 6.2	70.8 + 1.5
NCAM	5.7 + 1.8	2.0 + 0.9
EpCAM	63.9 + 9.4	61.2 + 9.5
CD146	7.5 + 1.5	0.6 + 0.2
CD133	4.9 + 1.3	3.0 + 1.9
CD31	11.0 + 1.9	3.7 + 2.0
ICAM-1	33.2 ± 15.3	22.6 ± 7.5
N-Cadherin	0.9 + 0.4	1.0+0.3
CD45	10.5 + 1.8	2.2 + 1.2
CD14	3.0 + 2.6	0.3 + 0.2
CD34	12.2 + 0.8	2.6 + 0.8
HLA	28.4 + 8.1	6.4 + 3.9

Mean + SEM. N=3

*All data are calculated for the glycophorin A-negative population (gated out by flow cytometric analyses). Glycophorin A was present at 57.5 + 7.6% in the interface fraction and at 39.5 + 7.0% in the pellet. The pellet fraction was found to be predominantly hepatoblasts.

Donor Age (yr)	Samples Analyzed	EpCAM+ Cells (%)	Hepatoblast Colonies	hHpSC Colonies
0.75	[1]Unfractionated	1.8	1209	2
	[2]EpCAM+	84.7	18	199
	[3]Flow-Through	< 0.05	1293	0
3	Unfractionated	0.5	339	0.5
	EpCAM+	75.0	237	76.2
	Flow-Through	< 0.05	308	0
9	Unfractionated	0.73	169	1.3
	EpCAM+	80.9	1.3	52.3
	Flow-Through	< 0.05	101	0.3
36	Unfractionated	3.9	> 500	11
	EpCAM+	93.2	1.7	27.7
	Flow-Through	< 0.05	> 500	3.3

Supplement Table 2. Colony forming Cells in Postnatal Human Livers

[1] Unfractionated: starting cell suspension after cell isolation

[2] EpCAM+ cells: positive fraction from immunoselection

[3] Flow-Through: cells not retained during magnetic selection for EpCAM

Data are means of triplicate wells seeded with 20,000 live cells.

Supplement Figures

Supplement-Figs 1 and 2. Hepatoblasts cultured on tissue culture plastic and in Kubota's Medium. The cells form cords and intensely co- express alpha-fetoprotein, albumin and cytokeratin 19. The cells survive only for 7-10 days. Hepatoblasts colonies do not survive on culture plastic but only on embryonic stromal feeders (see Suppl. Fig. 2). Cultures in Figs A-H are plated onto tissue culture plastic and those on I-N are on feeders of murine embryonic stromal cells, STO cells.

Figs A, C. E and G are cells after 1 day in culture; those in B, D.F and H are after 5 days; all Figs on STO cells are after 14 days in culture. A, B, J, and N are phase micrographs. Those in C, D and I are stained for albumin; those in E, F and K are stained for *a*- fetoprotein; those in G, H, and M are stained for CK 19. On day 1 the cells are tightly aggregated and show strong immunofluorescent staining for ALB, *a*-fetoprotein and CK19. By day 5 the cells have disaggregated and died. Immunostaining for albumin and *a*- fetoprotein is reduced to background levels; however residual cells still stain strongly for CK19. Scale bar = 20 μm.

Hepatoblasts plated directly onto a STO feeder layer, fixed, immunostained and imaged at day 14. Upper panels Phase contrast images of three groups of hepatoblasts. Lower panels: Immunofluorescent staining of ALB, *a*- fetoprotein, and CK19. Note how morphology and immunogenic profile is sustained on STO feeders, unlike the cultures on plastic. The cells survived for more than 2 months and grew very slowly when on STO feeder cells. Table 3 in Supplement-Fig. 1. Survey of markers on the cells on culture plastic; Table 4 in Suppl. Fig. 2. Survey of the markers on the hepatoblasts on STO feeders.

Supplement Fig.1: Hepatoblasts from Fetal Livers on Culture Plastic

Markers	Expression
Albumin	+++ (rapid decline within a week)
AFP	
CK 8/18, CK19, CD29, Ep-CAM	+++
N-CAM	Negative
I-CAM	+++
CAM 5.2	+
CD133/1	Negative
CD146	Negative
CD117	Negative
KDR	Negative
CD45, CD38, CD34, CD14	Negative

CD29= β1-integrin

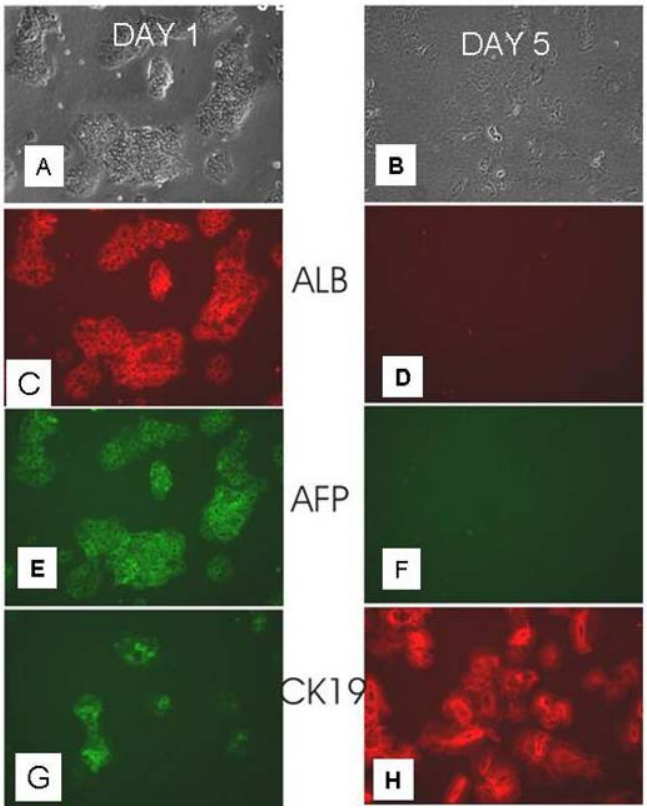

Figure 2-9 Details on Materials and Methods, Optiprep Fractionation of liver cells from postnatal donors

Supplement Fig. 2
Hepatoblasts from Fetal Livers on STO Feeder Cells

Markers	Expression
Albumin	+++ for more than 2 months
AFP	
CK 8/18, CK19, CD29, Ep-CAM	+++
N-CAM	Negative
I-CAM	+++
CAM 5.2	+
CD133/1	Negative
CD146	Negative
CD117	Negative
KDR	Negative
CD45, CD38, CD34, CD14	Negative

CD29= β1-integrin

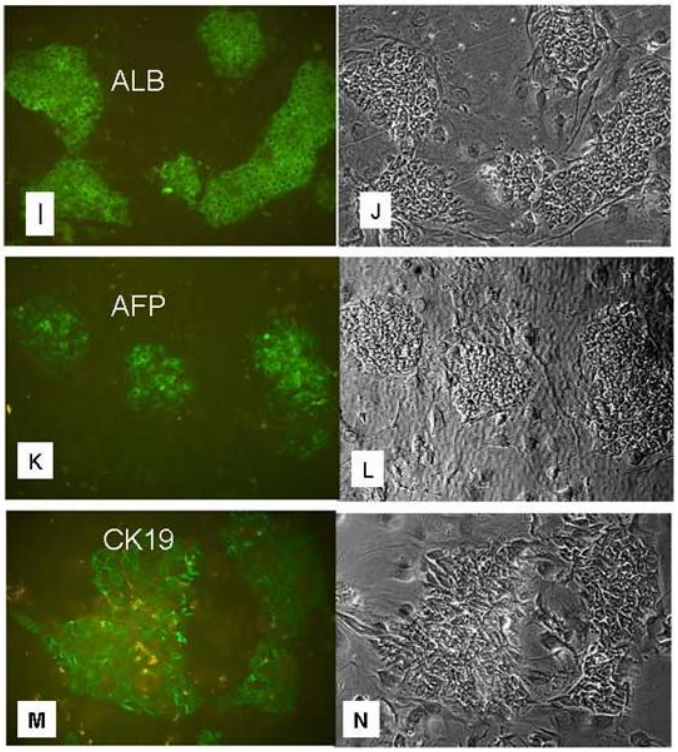

Figure 2-10 Purging of Contaminant Cells (e.g. Erythrocytes) Requires Gentle Procedures to Avoid Damaging the Hepatic Stem Cells.

Supplement-Fig 3. Phase microscopy shows the colonies of hepatic progenitors from postnatal livers that include hepatoblasts (A) and hHpSCs (B, C). Immunochemistry studies show expression in hHpSC colony of albumin (D), CK19 (E), and merged image (F).

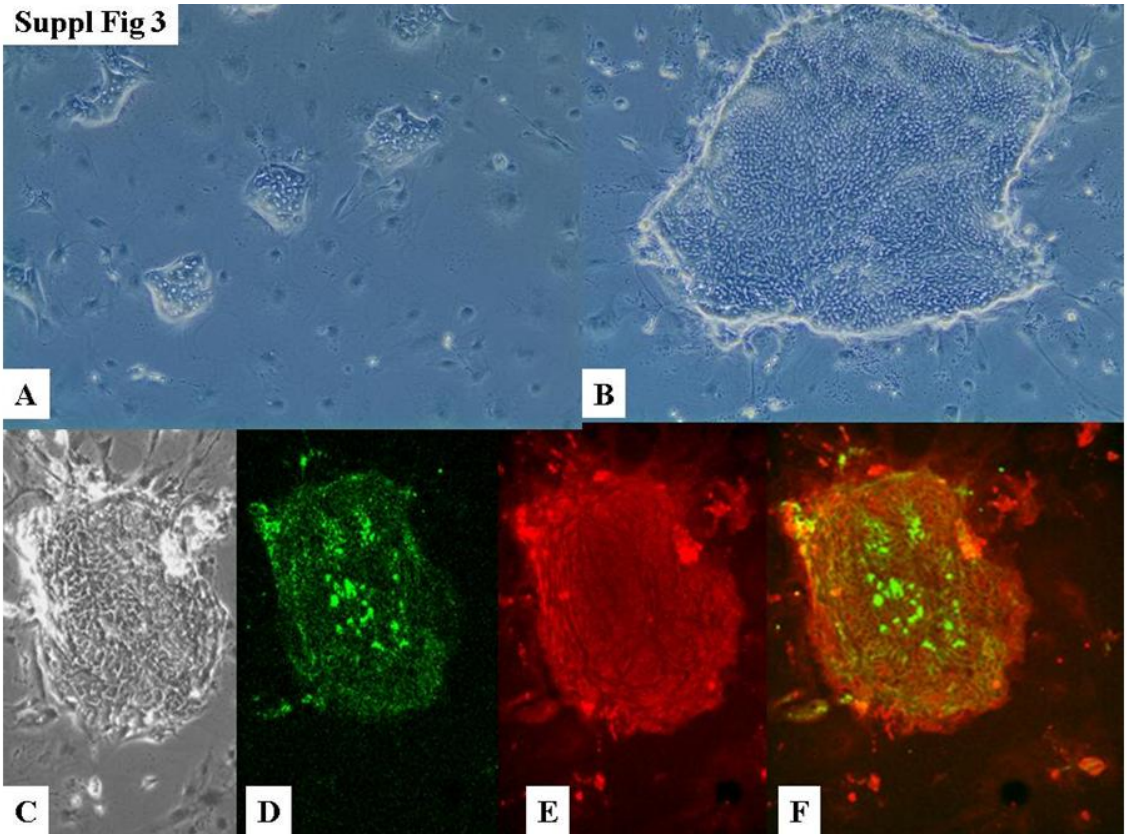

Figure 2-11 Hepatic Stem Cell Colonies

Supplement-Fig. 4. Hepatoblasts (A-F), sectored colonies (G, H, K, L) and unipotent progenitor colony (I, J) shown in phase microscopy (A, E, G, I, K) or for immunochemistry for albumin (green) and CK19 (red). Note that CK19 in hepatoblasts are filamentous and in hHpSCs (Suppl. Fig. 3) are particulate; in parallel, albumin expression is also distinct in hHpSCs and hepatoblasts. implicating distinctions in processing of these proteins in these two lineage stages.

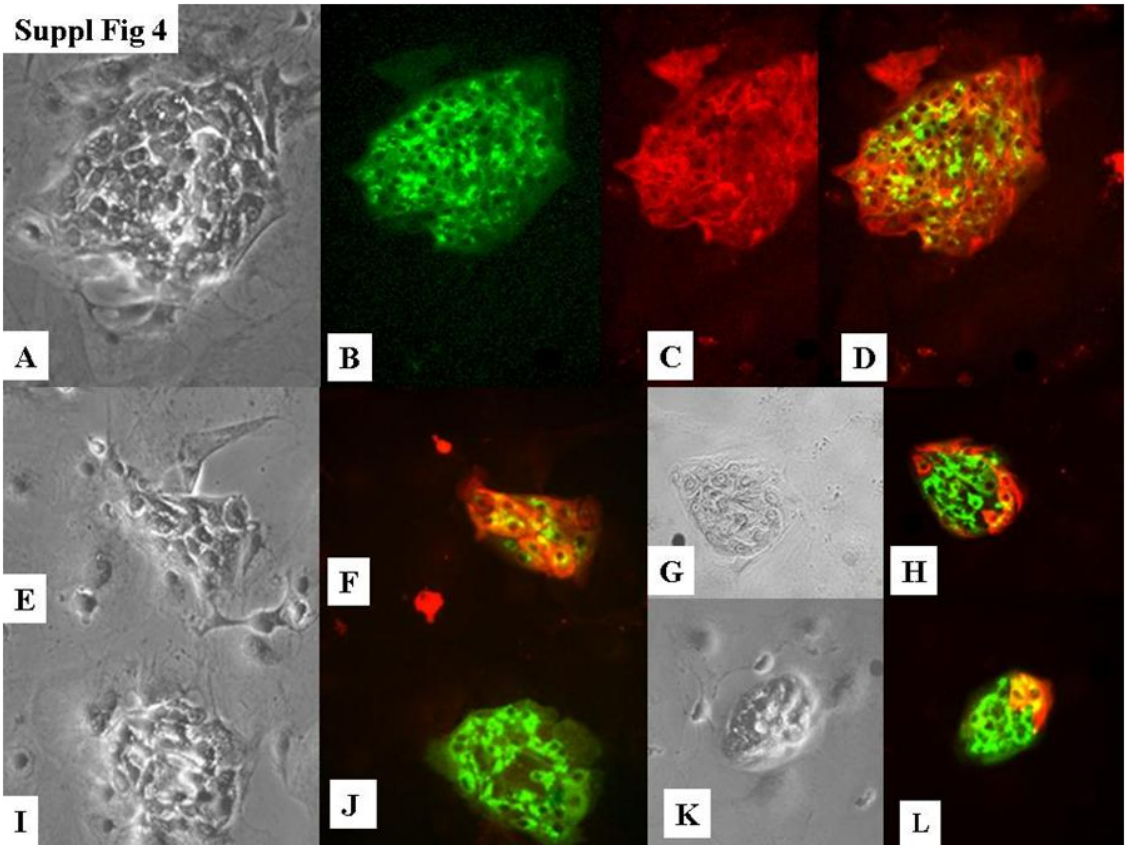

Figure 2-12 Characterization of Hepatic Stem Cell Colonies

Supplement: Movie 1. Day 1 after plating of hepatic stem cells on culture plastic and in Kubota's medium. Note the clonogenic expansion at cells at extremely low seeding densities. (On line not submitted)

Supplement: Movie 2. Day 3 after plating of hepatic stem cells on culture plastic and in Kubota's Medium. Colony formation has continued over that observed on day 1. (On line not submitted)

Supplement: Movie 3. Day 8 after plating of hepatic stem cells on culture plastic and in Kubota's Medium. The stem cell colony is expanding at the rate of ~ a division every 24-36 hours. Note the "companion cells" that surround the colony and that were determined to contain subpopulations of hepatic stellate cells and angioblasts (see **Fig 5** in the paper).

3 Chapter III. Initial Explorations with Hyaluronan Hydrogels for Cultures of Hepatic Stem Cells and Hepatoblasts: Hyaluronan Hydrogels with Aldehyde Linkages

3.1 Prelude:

Ex vivo maintenance of stem cell and progenitor populations from any tissue has been done almost always under monolayer conditions. Our studies, especially those expected in the near future, require that we utilize 3-dimensional cultures and wholly defined, serum-free medium and extracellular matrix components. We have already established the serum-free media needed for the hHpSCs, the hHpSTCss and are close to having one for the angioblasts (see Table 13), meaning that we are able to have the liver's trinity of cells found in the stem cell niche in co-culture. We now turned out attention to define the matrix components needed in scaffolds and that would allow the cells to grow, or distinct conditions that would allow them to differentiate. We have focused on extracellular matrix components found in the liver's stem cell niche: laminin, type III and IV collagen[25, 47] and in the studies here, hyaluronans, non-sulfated forms of glycosaminoglycans (GAGs). Early tests were done to see if the GAGs had any negative effect on the cultures by adding them to hepatoblasts and hHpSCs seeded onto plastic. The preliminary studies looked

promising. So we began the efforts with collaborators who had found ways to cross-link the HAs to increase their stability: Dr. Weillem Chen of SUNY at Stony Brook, New York. Dr. Chen made available an adipic dihydrazide-crosslinked sponge (Licensed through Clean Solutions Inc., Stony Brook, NY). The results of our studies are summarized in the following paper electronically published in December of 2006 and published in hard copy form in May, 2007. We show that the 3-D environment provided by the HA sponges facilitates cell survival and slow growth for weeks and keeps the cells in a lineage state intermediate between that of hHpSCs and hepatoblasts. The rate of growth of the cells was inhibited by the form of cross-linking (aldehyde bridges) that prevented the cells from turning over the scaffold.

Human Hepatoblast Phenotype Maintained by Hyaluronan Hydrogels

William S. Turner[1], Eva Schmelzer[2], Randall McClelland[2], Eliane Wauthier[2], Weiliam Chen[4], Lola M Reid[1, 2, 3]

Departments of Biomedical Engineering[1] and Cell and Molecular Physiology[2]

Program in Molecular Biology and Biotechnology[2], Lineberger Cancer Center[3]

UNC School of Medicine, Chapel Hill, NC 27599

And

Department of Biomedical Engineering[4]

State University of New York, Stony Brook, NY 11794-2580

3 Tables, 18 Figures

Keywords: Hyaluronan scaffolds, human hepatoblasts, hHpSCs, bioartificial livers, tissue engineering

Abbreviations: FBS = Fetal Bovine Serum; GAG = Glycosaminoglycan; HA= hyaluronans;

KM = Hiroshi Kubota's Hormonally Defined Media for Hepatic Progenitors; AFP= α-fetoprotein; PBS = phosphate buffered saline

Acknowledgements: Funding derived from NIH grants (DK52851, AA014243, IP30-DK065933, and DK068401), a Department of Energy Grant (DE-FG02-02ER-

63477), and by a Whitaker grant providing salary support. We wish to thank Lucendia English for technical and administrative support.

3.2 Abstract

Human hepatoblasts and hepatic stem cells, pluripotent hepatic progenitors that give rise to hepatocytes and biliary cells, were isolated from fetal livers and found to express hyaluronan receptors (CD44) in both the freshly isolated cells and after culture. This implicates an *in vivo* connection to hyaluronan (HA), an embryonic matrix component, as a candidate 3-dimensional scaffold for hepatic progenitor cell expansion and/or differentiation. To assess HAs as scaffolds, hepatoblasts and hepatic stem cells were seeded into HA hydrogels with a serum-free, hormonally defined medium tailored for expansion of hepatic progenitors. Cell aggregates formed within the HA hydrogels and remained viable, proliferative, and demonstrated a stable phenotype intermediate between that of hepatic stem cells and hepatoblasts throughout more than 4 weeks of culturing, with little evidence of lineage restriction towards either hepatocytic or biliary pathways. The phenotype consisted of stable co-expression of both hepatocytic and biliary markers such as biliary-specific cytokeratin, CK19, low levels of expression of albumin, and urea synthesis. HA hydrogels are ideal as 3-dimensional scaffolds for pluripotent hepatic progenitors and should be useful for generating cells to be used in bioartificial livers or tissue engineered liver grafts.

3.3 Introduction

In vivo, liver cells undergo interactions with both soluble signals (nutrients, gases, growth factors) and with insoluble ones found in the extracellular matrix [389]. All such interactions, especially cell-to-cell interactions, effects of soluble growth factors, and effects of extracellular matrix found in mature liver tissue, have been studied extensively [390-393]. However, less studied have been the effects of matrix chemistries found predominantly in embryonic and fetal tissues. Hyaluronans are glycosaminoglycans (GAGs) consisting of a disaccharide unit linked with β-1-4, β-1-3 bonds between N-acetyl-D-glucosamine and glucuronic acid moieties respectively [255]. HAs contribute to matrix structure stabilization and integrity, water and protein homeostasis, tissue protection, separation and lubrication, facilitation of cell movement/migration, transport regulation including steric exclusion, anchoring of hormones as a reservoir and integration of the immune inflammation response[249, 251, 252, 254, 255, 394, 395]. HA is evident in significant amounts in embryonic tissues[396] and in adult tissues undergoing cellular expansion and proliferation[249, 397-399], wound repair[252, 253] , and regeneration[253]. In the liver, HAs are present in the matrix of embryonic and fetal tissues and near the presumptive stem cell compartment, the Canals of Hering, located in zone 1 of adult livers[9], but are not in association with the mature parenchymal cells. Therefore, HAs are candidate matrix components as 3-D scaffolds for *ex vivo* cultures of hepatic progenitors.

Human livers are comprised of a mixture of hemopoietic, mesenchymal, and hepatic progenitor cells[46]. The hepatic progenitor subpopulations in human fetal livers consist of two pluripotent cell populations, hepatic stem cells and hepatoblasts, and two unipotent populations, hepatocytic and biliary committed progenitors. Hepatic stem cells constitute approximately 1.0-3.0% of liver parenchymal cells in livers of all donor ages and are 7-9 um diameter, whereas their immediate descendents, hepatoblasts are larger, 10-12 um in diameter, and constitute 80-85% of fetal livers but less than 0.1% of adult livers. The hepatic stem cells and hepatoblasts have extensive overlap in their phenotype; expressing albumin, epithelial-specific cytokeratins (CK) 8 and 18, a biliary-specific cytokeratin CK19, epithelial cell adhesion molecule EpCAM (CD326 or HEA125), CD133/1 (prominin), and being negative for hemopoietic (CD45, CD34) and mesenchymal (CD146, KDR) markers. They are distinguishable in that hepatic stem cells express NCAM and claudin 3, whereas hepatoblasts express ICAM-1 (CD54), alpha-fetoprotein (AFP), and fetal P450s (e.g. P450A7)[46] (see **Table 1**) *In vivo,* the pluripotent hepatic progenitor cells give rise to the hepatocytic and biliary lineages between the 11^{th} and 13^{th} weeks of gestation[400].

Hepatic progenitors from diverse mammalian species (murine, rat, porcine, human) have been cultured under classic culture conditions (plastic dishes and a serum-supplemented medium) under which the cells survived for less than 7 days. If serum is maintained, the stem cells and the hepatoblasts rapidly differentiate and lose their proliferative potential. However, if rodent hepatic progenitors are plated onto embryonic stromal feeders, and in a hormonally defined medium known as

"Kubota's Medium" (KM), which is a serum-free basal medium with no copper, low calcium (<0.5 mM), and supplemented with insulin, transferrin/fe, lipids (high density lipoprotein and free fatty acids), and certain trace elements (zinc, selenium)[43], they will undergo clonogenic expansion. On culture plastic, and in this same medium, hHpSCs, but not human hepatoblasts, will survive and expand for more than 6 months. If transferred to embryonic stromal feeders these stem cells will slow in expansion and give rise to eruptions of hepatoblasts and committed progenitors.[22] We report here that seeding hepatic progenitors from human fetal livers into hyaluronan hydrogels with KM medium elicits long-term (more than 4 weeks) survival and expansion of progenitors with maintenance of stable gene expression for a phenotype intermediate between that of stem cells and hepatoblasts.

3.4 Materials and Methods

3.4.1 Sourcing of Human Fetal Livers

Liver tissue from human fetuses between 18-20 weeks gestational age was obtained from an accredited agency (Advanced Biological Resources, San Francisco, CA). The research protocol was reviewed and approved by the Institutional Review Board for Human Research Studies at the University of North Carolina at Chapel Hill.

3.4.2 Cell Isolation

The methods for processing human fetal liver tissues have been previously reported.[40, 46] In brief, the livers were allowed to undergo partial digestion with an enzymatic buffer [60 mg collagenase (Sigma, catalog # C5138) plus 30 mg DNAse (Sigma, # DN-25) prepared in 100 ml of RPMI 1640 supplemented with 0.5 g of BSA (Sigma, # A8806-5G), selenium (10^{-8} M), antibiotics and antimycotics] to yield small clumps of tissue. The clumps were then centrifuged at low speed spins (20 revolutionary centrifugal force) to separate hemopoietic cells (largely red blood cells) from parenchymal cells. The parenchymal cell clumps were then subjected to further mechanical and chemical digestion to yield single cell and small aggregate suspensions. The majority of the parenchymal cells (hepatoblasts) were fully dispersed by filtration through a 75 μm nylon mesh (cat# 34-1800-02 PGC Scientific, Frederick Maryland). The process generated suspensions of single cell and small cell aggregates of 3 to 8 hepatoblasts per group. The viability of the cell suspension was greater than 95% on average and was assessed by Trypan Blue Exclusion assays.

Viability was assessed in cultures using one of several vital dyes: Lysotracker Green, Mitotracker Red, and Lysotracker Red (Molecular Probes, Eugene Oregon). The dye was chosen for contrast to other fluoroprobes used in co-staining process. Addition of the vital dyes was for a 30 minute incubation time period in KM media and at the following concentrations: 75nM Lysotracker Green, 75nM Lysotracker Red, 250nM Mitotracker Red.

3.4.3 Cell Culture Media

The suspensions of fetal human liver cells, highly enriched for hepatoblasts, were suspended into a serum-free medium tailored for hepatic progenitors[43] , referred to as "Kubota's Medium" (KM), and consisting of a serum-free basal medium (RPMI 1640, Gibco – Invitrogen, Carlesbad, CA) containing no copper, low calcium (< 0.5mM) and supplemented with insulin (5 ug/ml), transferrin/fe (5 ug/ml), high density lipoprotein (10 ug/ml), selenium (10^{-10} M), zinc (10^{-12} M) and 7.6uE of a mixture of free fatty acids bound to purified albumin; the detailed methods for its preparation have been published elsewhere[43, 212]. Following isolation, the hepatic progenitors were suspended in KM, and supplemented further with low levels of fetal bovine serum, typically 2.5%, in order to inactivate the enzymes used in the processing of the tissue. The plating medium was replaced after 16 hours with serum-free KM, and the cultures were maintained for greater than 4 weeks, with media changes every 2 to 3 days.

3.4.4 Culture Plastic

Suspensions of the human hepatic progenitors, enriched for hepatoblasts, were seeded onto plastic with a 2.5% Fetal Bovine Serum (FBS) addition to the KM medium. After 16 hours of incubation at 37°C with 5% CO_2, the media was replaced with serum free KM media for the remainder of the study. Cells on plastic were cultured with media changes every 3 days, until the end of the experiment. Cells that did not attach within the first 16 hrs of culture were aspirated at times of media

change. At the experiments end, the cells were fixed with 4% paraformaldehyde added to the plate after aspiration of the KM media.

3.4.5 Hyaluronan Hydrogels

Hyaluronan (average MW: 1,500,000) was obtained from Kraeber GMBH and Co. (Waldhofstr, Germany). Adipic dihydrazide (ADH) and Ethyl-3-[3-dimethyl amino] propyl carbodiimide (EDCI) was purchased from Sigma-Aldrich (St. Louis, MO). Hyaluronan matrices configured for cell culture were prepared using a method modified from previously published protocol.[401, 402] Briefly, a 1% aqueous Hyaluronan solution was prepared, aliquoted and deposited in aluminum molds of proper sizes, snap frozen on dry ice and lyophilized to form solid, spongy wafers. The wafers were incubated in a 0.1% ADH solution (90% isopropanol/10% water) for 30 minutes to enable the complete penetration of the ADH solution. EDCI (120 mg) was added to the ADH solution and quickly dissolved upon agitation. Cross-linking of the partially hydrated HA spongy wafers was initiated by adding 1N HCl to the reagent mixture to adjust the pH to ~4.5. The reaction was terminated by decanting the reagent mixture and replacing it with 100 ml of 90% isopropanol. The crosslinked HA matrices recovered were subsequently extracted with 100 ml of 90% isopropanol at least 5 times by incubating overnight. The HA matrices were transferred to pure isopropanol to remove all residual water and then air dried. The diameters of the cross-linked HA matrices were 0.7 or 3.5 cm, respectively. Upon re-hydration of the HA matrices, they readily absorbed water and formed highly porous HA spongy hydrogels.

3.4.5.1 Sterilization of the Hyaluronan Hydrogels

Sterilization of the HA hydrogels was performed by exposure to a Cesium source (JL Shepard Mark I Model 68 Cesium Irradiator - Department of Radiation Oncology, UNC) with a deliverable dosage of 40 Gray (40 Joule/kg), over a 10 minute period

3.4.5.2 Hepatoblast Cultures in Hyaluronan Hydrogels

HA hydrogels were placed into culture wells, either 6-well culture treated polystyrene (Falcon – Beckton-Dickinson, Franklin Lakes, NJ), or for the smaller sized hydrogel matrices, chambered coverglass culturing slides (Lab-Tek - Nunc, Napersville, IL). Smaller hydrogels required no manipulation (priming) prior to inoculation with freshly isolated cells other than a pre-soak with KM media. The larger hydrogels required slight manipulation to insure the removal of air bubbles from the sponges. In most cases, addition of 3mls of KM media onto the sponge would trap air bubbles; removal of air bubbles was mechanically accomplished by slight compression-relaxation of the sponge, forcing air from the lateral sides. After priming, suspensions of human hepatic progenitors, enriched for hepatoblasts, were seeded onto large HA hydrogels at 2 x 10^6 cells/hydrogel in KM medium with 2.5% FBS and at 2 x10^5 cells per small hydrogel. After 16 hours initial incubation at 37^{o}C in a CO_2 incubator (Forma Scientific, Baton Rouge, LA), the medium with FBS was

replaced with serum-free KM. The working volume for a 6 well plate was 3ml and for the 2-chambered wells was 2ml. Cells were cultured for 4 weeks under these same conditions, with changes of the media every 2-3 days.

3.4.6 Cultures on Collagen and In Collagen Sandwiches

Collagen gels are utilized in this study, and in all cases rat tail collagen type I (Cohesion Technologies, Palo Alto, CA) is the extra-cellular matrix (ECM) material. The Collagen ECM has a density concentration of 1.5 mg/ml, unless specified otherwise. For flat plate cultures of this investigation, 0.4ml of Collagen-I is plated over the 35mm diameter culture surface and incubated for 1 hour at 37°C and 95% O_2 - 5% CO_2 to allow gelation. Then 1E6 viable hepatocytes were seeded onto the gelled layer using media supplemented with 10% FBS. Following 8 hours of cell incubation, the medium was removed and 0.5 ml of serum free culture media is added to the top of the culture, and changed daily. Media samples were collected daily and stored at 4°C for later evaluation. For sandwich culture studies of this investigation, the culture incorporates a 35mm tissue culture dish. Briefly, 1 million viable cells were plated on a Flat Plate Collagen ECM and allowed to attach for 8 hours in media supplemented with 10% FBS at 37°C and 5% CO_2. The media is then removed and an additional 0.4ml of Collagen is applied to the top of the cells, followed by gelation for 1 hour at 37°C. Next 0.5ml of serum free culture media was added to the top of the culture, and changed daily. Media samples were collected daily and stored at 4°C for later evaluation.

3.4.7 Fixation and Sectioning of the Cells in the HA Hydrogels

KM medium was removed from the cultures by aspiration, followed by addition of 3mls of 4% paraformaldehyde to each well. After 1 hour incubation, the fixative was removed and replaced with serum-free RPMI 1640 and prepared for cryopreservation. Prior to freezing, the RPMI 1640 was removed and the matrix was lifted using a flat edge spatula. It was placed into Optimal Cutting Temperature Compound (OTC), (Tissue-Tek, Torrance, CA), in 2ml conical sample cups (Fischer Science, Pittsburgh, PA) and snap frozen using liquid nitrogen emersion. Preserved specimens were kept at -80^{o}C until sectioned. Slides were made with 10 micron sections through the HA hydrogels.

3.4.8 Cell Staining

Cells were stained for immunofluorescence using primary antibodies directly labeled with the relevant fluoroprobe or two-step staining with primary antibodies followed by secondary antibody coupled to the fluoroprobe (see **Table 2**). Prior to staining, approximately 1ml of Phosphate Buffer Solution (PBS) was placed on the site of interest to wash any debris away. Goat serum (10% in PBS solution) was added for 1 hour to block non-specific binding sites within the tissue. Blocking was removed and the site washed with 1x PBS. Monoclonal antibody was added and incubated overnight. After the overnight/18 hours incubation at 4^{o}C, the primary monoclonal antibody solution was removed, and the sample was washed three times

with 1x PBS for 10 minutes each time. Secondary antibody (Alexa 488 or Alexa 594, Molecular Probes – Invitrogen, Carlsbad, CA) was added at a dilution of 1:750 or 1:1000. The sample was covered from light exposure and left for 1 hour incubation at room temperature. Samples were washed 3 times with 1x PBS and prepared with cover slips using either DPX mounting media (Electron Microscopy Sciences, Fort Washington, PA) for microscopy or Vector Shield containing DAPI mounting media (Vector Laboratories, Burlingame, CA). The DAPI concentration was 1.5 ug/ml. Hepatic fetal stem cell colonies were fixed after 10 days in culture with 4% para-formaldehyde in PBS, and blocked for 1 hour at RT with 10% goat serum in PBS 0.1% Triton-X100 (Sigma , Saint Louis, MO). Primary antibodies rabbit IgG anti desmin (Abcam, Cambridge, MA) and mouse IgG1 anti EpCAM (Labvision, Fremont, CA) were applied in blocking buffer for 1 hour at RT; secondary antibodies anti-rabbit AlexaFluor 568, anti-mouse IgG1 AlexaFluor 488 conjugated (Molecular Probes/Invitrogen, San Diego, CA), and DAPI (Sigma) for nuclei staining were applied in blocking buffer for 1 hour at RT. Fluorescence was analyzed using a Leica SP2 laser scanning confocal microscope controlled by Leica SP2 TCS software (Leica Microsystems, Bannockburn, IL).

3.4.9 Confocal Microscopy

For analysis of cytoplasmic antigens (e.g. albumin, AFP) coupled to a fluorochrome label, cells were imaged with a LeicaSP2 AOBS Upright Laser Scanning Confocal, a Zeiss 510 Meta Inverted Laser Scanning Confocal Microscope,

and a Leica DMIRB Inverted Fluorescence/DIC Microscope - with B/W & Color digital cameras.

3.4.10 Measurement of Albumin and Urea Production

The media supernatant was collected from control (plastic) cultures and the HA smaller (0.7cm diameter) hydrogels once every day or every other day for the duration of a 4-week culture period. Media from the culture were frozen and stored at -20°C until analyzed. .

3.4.10.1 Albumin Production

Albumin production was measured by enzyme-linked immunosorbent assay (ELISA). Purified human albumin (Serologicals, Norcross, Georgia) was used as the standard, peroxidase-conjugated antibody (ICN Biomedicals/MP Biomedicals, Irvine, CA) was used as the fluoroprobe against albumin and measured with a Spectromax 250 multi-well plate reader (Molecular Devices, Sunnyvale, CA).

3.4.10.2 Urea Production

Urea Production was analyzed using the urea nitrogen sensitivity assays, based on direct interaction of urea with diacetyl monoxime (Sigma, St. Louis, MO). Urea concentration was measured spectrophotometrically at 515 - 540 nm with a cytofluor Spectromax 250 multi-well plate reader.

3.4.11 Isolation of RNA, DNA, and protein from cultured cells

Isolation of cultured cells in the HA hydrogels were accomplished using TRIzol isolation provided by Invitrogen (Carlsbad, CA). Hydrogels were removed from the culture plates and placed into 2ml Eppendorf tubes, and spun at 12000 rcf (11,953.34g) on a microfuge (Brinkman, Westbury, NY) at 4˚C. Supernatant was removed by aspiration and 1ml of TRIzol was added. In comparative plastic control cultures, where cells were adherent to the culture plates, TRIzol was added directly to the plate and then collected into tubes without spinning, but after aspiration of the media. Collection of RNA was done via phase separation with addition of 0.2ml chloroform (Cat # C-3422, Sigma). After aqueous phase collection, RNA was precipitated via isopropyl alcohol, followed by a 70% ethanol wash. Final preparations of RNA were air dried and resuspended in 100ul of RNase free water. Quantification was done with a DU7400 Spectrophotometer (Becker, Schaumberg, IL).

DNA isolation was performed by addition of 0.3ml of 100% ethanol to each tube of the remaining TRIzol. Tubes were incubated for 2 minutes at room temperature, and then centrifuged at 1000g, 4˚C, for 5 minutes. The phenol/ethanol aqueous phase was removed for further analysis of the protein. The DNA pellet was washed twice with sodium citrate solution, then with 75% ethanol, and centrifuged each time at 5000g at 4˚C. After a second ethanol spin, supernatant was removed by aspiration, and the sample was air dried for 15 minutes. The pellet was re-dissolved in 100ul of 8mM NaOH and buffered with 3.2ul 1M Hepes (Mediatech, Herndon, VA) for a final pH of 7.0. The samples were spun at 12000g for 10 minutes and the

supernatant was transferred to a new tube. DNA quantification was done with the Beckman Photospectrometer (Fullerton, CA).

Protein isolation from the extracted phenol/ethanol aqueous phase was performed by precipitation with 1.5ml isopropanol and centrifugation for 10 minutes at 12000g and at 4˚C. The protein extract was washed 3 times with 0.3M Guanidine HCl in 95% ethanol. After the final wash and centrifugation at 7500g for 5 minutes at 4˚C, the protein pellet was vacuum dried for 15 minutes. Resuspension of the protein was done in 1% SDS and incubation at 50˚C for 10 minutes.

3.4.12 Quantitative real time RT-PCR Analyses

Gene expression was analyzed by quantitative real time RT-PCR. Gene specific mRNAs were created as followed: total RNA from livers was extracted using the RNeasy kit (Qiagen, Valencia, CA) and reverse transcribed by Superscript II reverse transcriptase (Invitrogen) and oligo-$dT_{(12\text{-}18)}$ primer. cDNA was used as the template in conventional PCR with gene specific primers (for sequences see **Table 3**) from which the forward primer possessed an 5' overhang for T7-promotor sequence (5'gac tcg taa tac gac tca cta tag gg). This amplified gene specific DNA was used for *in vitro* transcription with T7-RNA polymerase (Promega, Madison, WI), generating gene specific RNA (with an additional 5'ggg included by T7-RNA polymerase) used as standards in quantitative RT-PCR using gene specific primers without 5' overhang; standard ranges were linear from 1 to 10^8 templates. Quantitative RT-PCR was done in the LightCycler instrument (Roche) using the

LightCycler RNA Master SYBR Green I kit. RNA from samples was extracted using RNeasy mini kit (Qiagen).

3.5 Results

3.5.1 HhHpSCs and hepatoblasts have receptors for hyaluronans

The hHpSCs and hepatoblasts are positive for hyaluronan receptors as evidenced by immunostaining of a tightly packed, 25 day-old colony of hHpSCs with fluorescent antibodies to CD44 as shown in **Figure 1a**. Freshly isolated hepatoblasts, which are AFP positive are also shown to be positive for the CD44 receptor in **Figure 1b-d**. CD44, a cell surface glycoprotein, is indicated in green, which highlights a receptor for the HA attachment. The receptors cover 100% of the cells in the stem cell colony in figure 1a, with individual cells containing varied amounts of the receptor seen as intense staining in some cells and lighter less intense staining of others. Individual cells are contrasted by use of DAPI staining (blue) of their nuclei. As shown, the stainings imply that each human hepatic progenitor cell has HA attachment capabilities. In **Figure 1e**, primary cultures of human hepatic progenitor cells, isolated from human fetal livers and cultured on plastic for 4 weeks, were imaged at 4x and are fluorescently stained for a HA-BODIPY conjugate. The hepatic progenitors express levels of receptors for HA at higher rates than other cells evident in the culture and that include stroma and endothelial cells. Hepatic progenitors, with heavy bodipy staining due to uptake of the conjugated HA are located in the lower left quadrant. Comparatively, fibroblasts

and non-parenchymal cells shown respectively in the lower right and upper quadrants are less active in their HA mediated binding and uptake. Immunohistochemical staining of the nonparenchymal cells has been done utilizing markers defined by others to identify specific subpopulations. The mesenchymal cells comprise multiple subpopulations that include angioblasts (KDR+/CD133-1+ /CD117+) ; mature endothelia, (CD31+); hepatic Stellate Cells (desmin+, alpha-smooth muscle actin+); hemopoietic cells (CD45+) including red blood cells (glycophorin A+). Representative of these cellular subpopulations are those shown in **Fig. 1f-i** (hepatic stellate cells positive for desmin expression located adjacent to EpCAM positive stem cells)

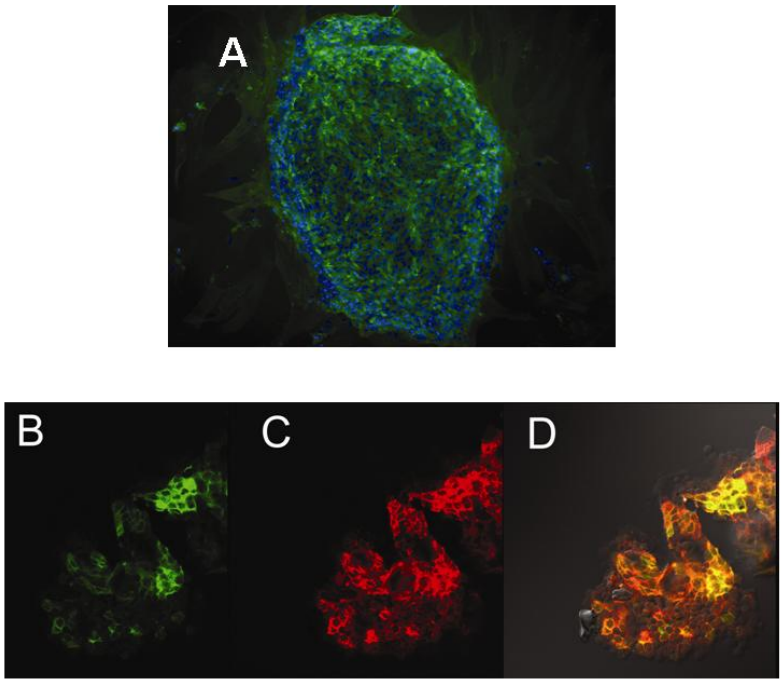

Figure 3-1: Evidence of Hyaluronan Receptors on Hepatic Progenitors

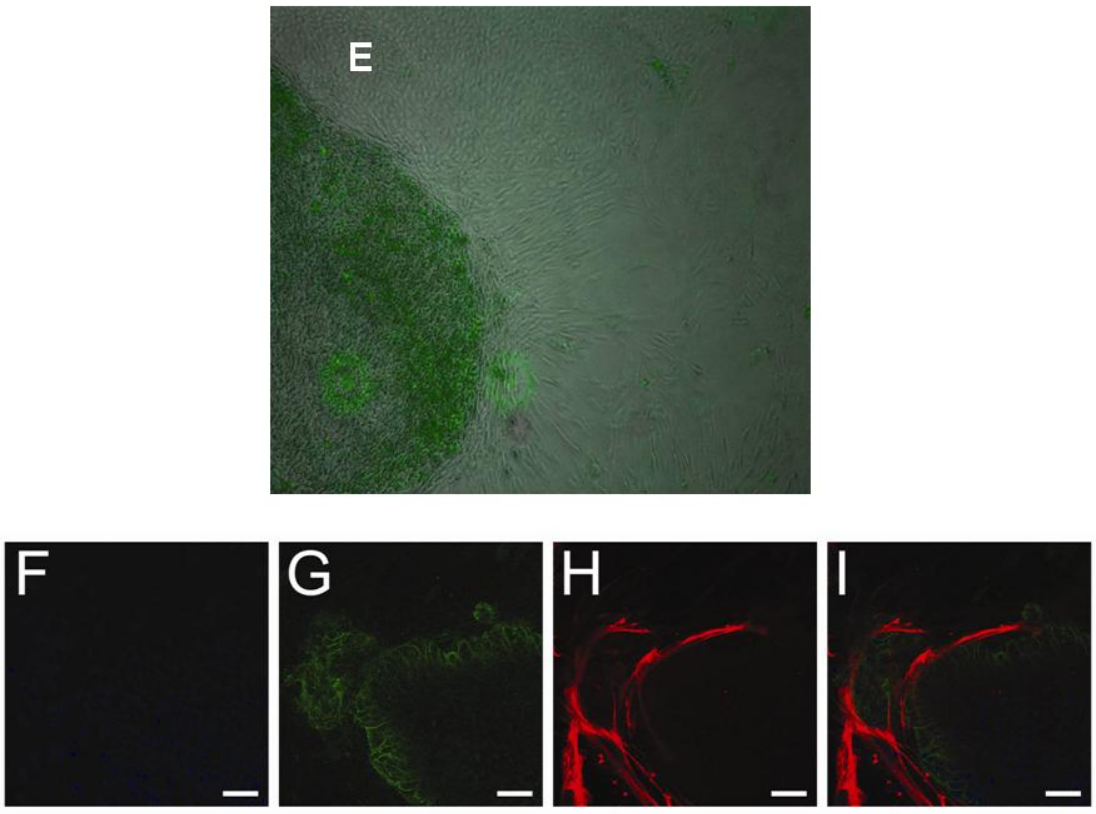

Figure 3-2 Evidence of Hyaluronan Receptors on Hepatic Progenitors (E thru I)

3.5.2 Human hepatic progenitors are viable and expand 3-dimensionally in the HA hydrogels

Cells isolated from freshly dissociated human fetal livers show an affinity for aggregation/expansion in the hydrogels. Single cells and aggregates with up to four cells/aggregate were initially seeded within the HA hydrogels. Cells aggregates, at the end of a 3 week culturing period, shown in **Figures 2a, 2b, 2c** and **2d** show much larger cell aggregates. Sampled aggregates of **Figure 2b** have cell counts

ranging between 63 and 2595 per aggregate. **Figures 2a & 2b** illustrate visible aggregate spheroids within the HA hydrogel. Furthermore those aggregates, **Figures 2c & 2d** display cell viability with fluorescence capture of Mitotracker and Lysotracker activity, where the fluoroprobe is cleaved into a visible component after active uptake. **Figure 2d** also represents a confocal plane that shows the aggregate spheroid is neither hollow nor necrotic within the interior (Mitotracker-red, stained) frames 2-5. DNA measurement shows a complete reversal of quantifiable cell DNA collected from the death of cells on plastic versus their expansion in the HA sponge with an average daily increase of 2.28% over a 14 day incubation period (Data not shown).

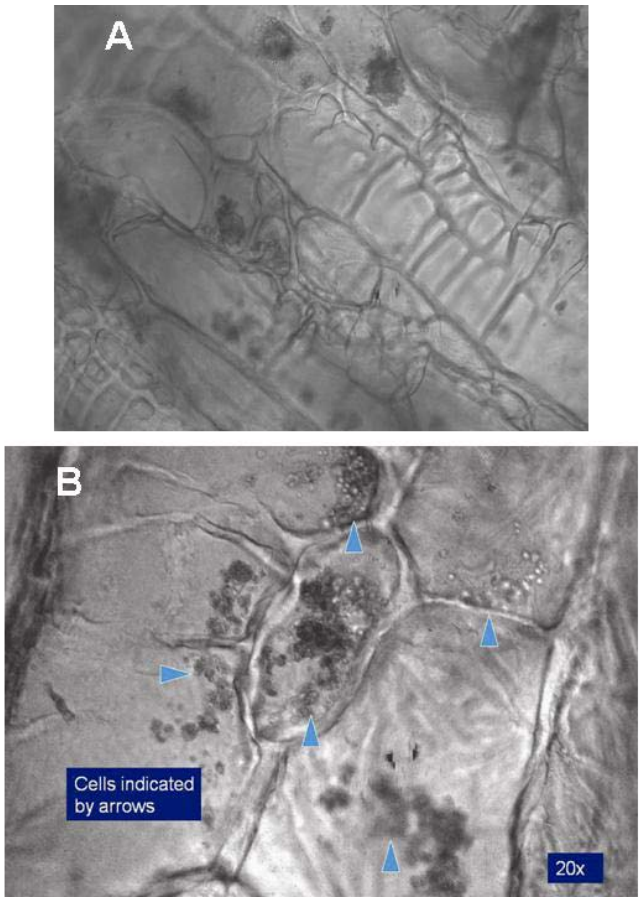

Figure 3-3 Viability of the Cells within Hyaluronan Hydrogels

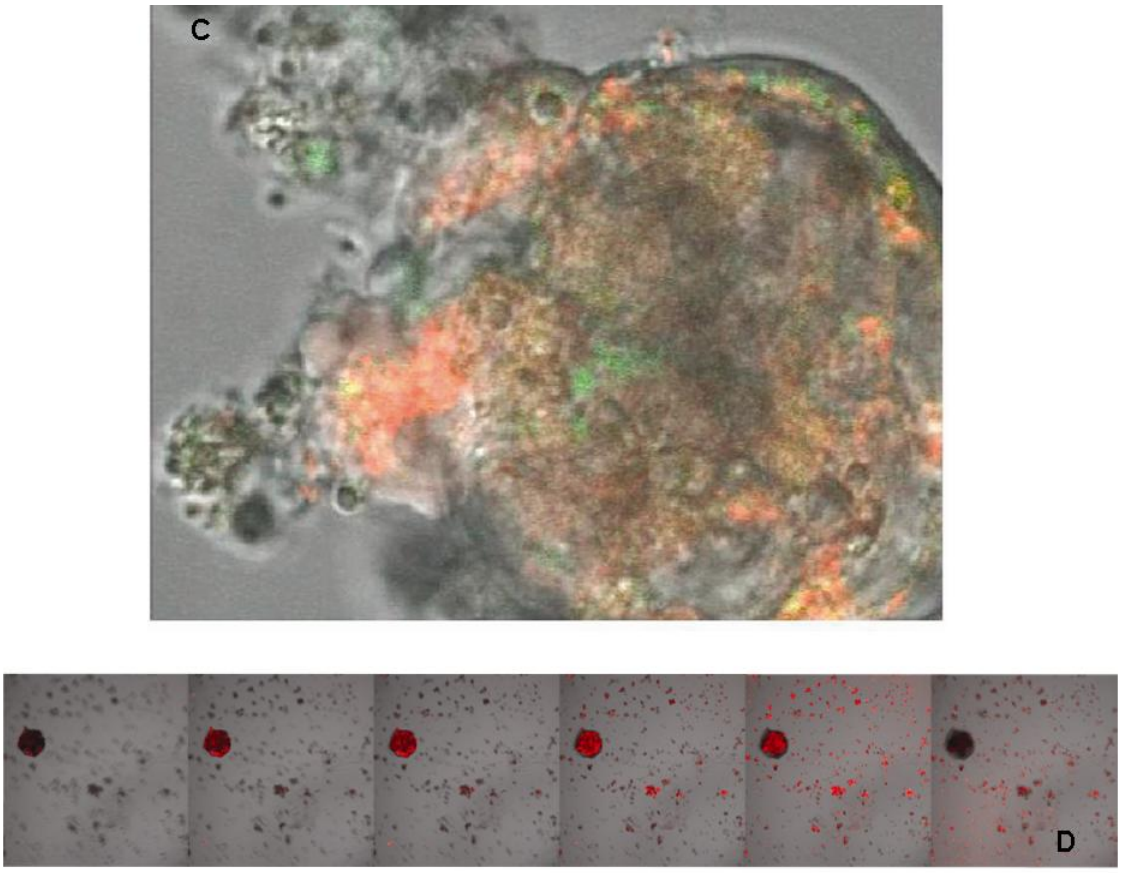

Figure 3-4 Viability of the Cells within Hyaluronan Hydrogels (C and D)

3.5.3 Hepatoblasts survive longer in hyaluronan hydrogels in comparison to those on culture plastic

Cells in the hydrogel sponges and in the KM medium maintained a stable phenotype intermediate between that for hepatic stem cells and hepatoblasts throughout more than 4 weeks of culture and did not lineage restrict towards either biliary or hepatocytic fates. Representative data are shown by immunohistochemistry staining given in **Figure 3**. The cells are hepatic parenchymal progenitors as evidenced by their co-expression of the biliary lineage

marker, CK19 with albumin (**Figure 3a-f)** and are epithelia as evidenced by their staining for CK8/18 (**Figure 3g**). The I-CAM staining (**Figure 3h**), found in the majority of the cells and the low levels of expression of alpha-fetoprotein, indicates they are held in a differentiated state close to that of hepatoblasts (fully differentiated hepatoblasts would be expected to have very high levels of alpha-fetoprotein), a conclusion corroborated by biochemical assays for functions (see below). Finally, hepatoblasts are marked by the co-expression of three markers: EpCAM, AFP, and Albumin (**Figure 3i-l**).

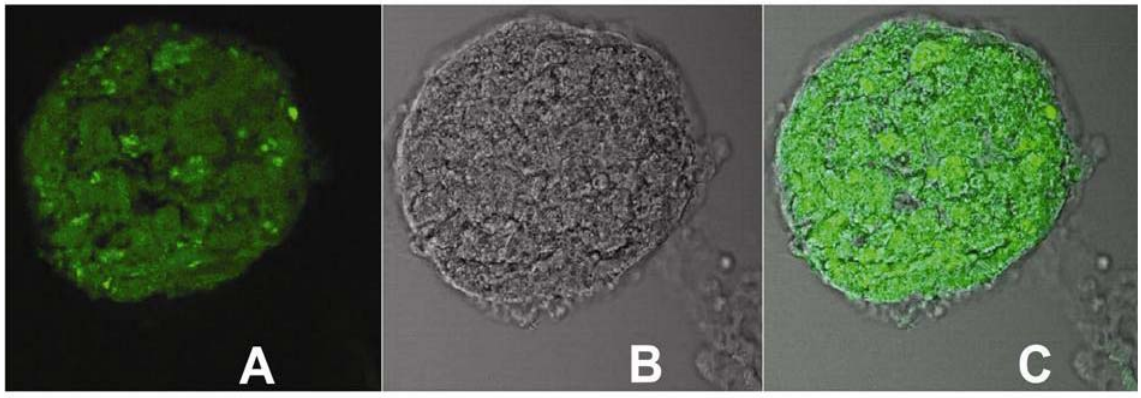

Figure 3-5 Antigenic Expression in Human Hepatoblasts Cultured in Hyaluronan Hydrogels

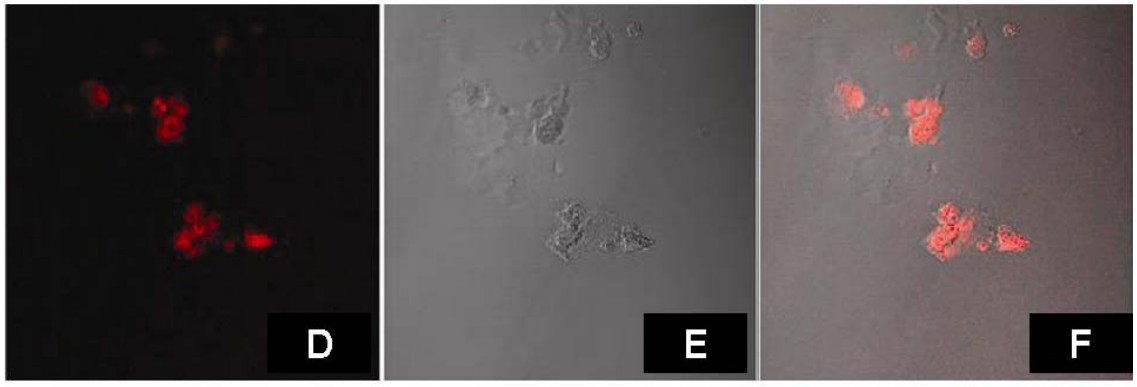

Figure 3-6 Antigenic Expression in Human Hepatoblasts Cultured in Hyaluronan Hydrogels (D through F)

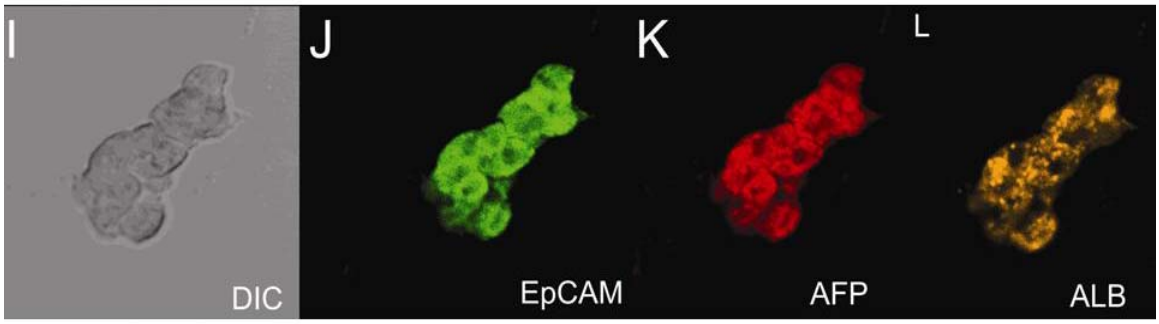

Figure 3-7 Antigenic Expression in Human Hepatoblasts Cultured in Hyaluronan Hydrogels (I through L)

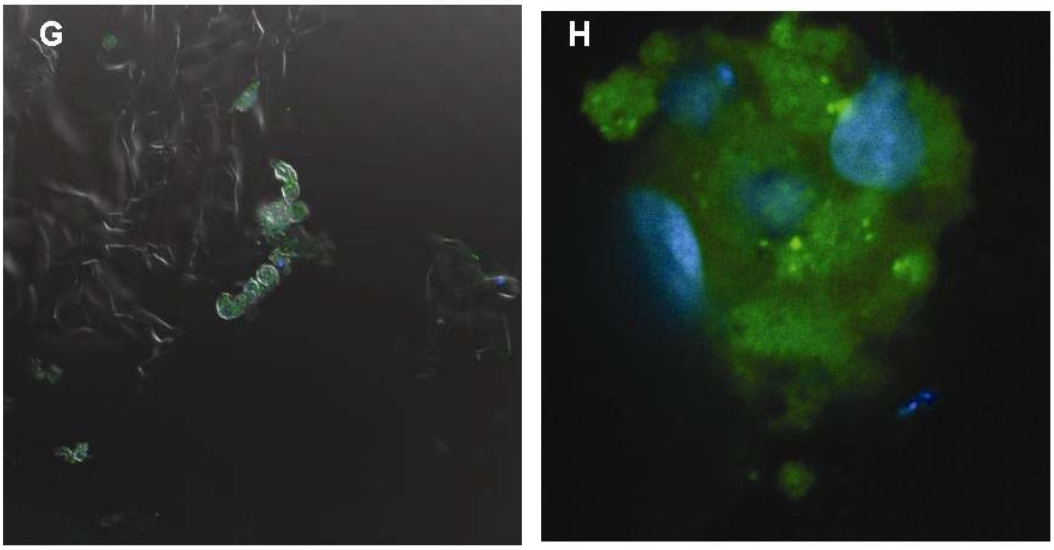

Figure 3-8 Antigenic Expression in Human Hepatoblasts Cultured in Hyaluronan Hydrogels (G and H)

3.5.4 Cells maintain phenotype of early stage hepatoblasts for longer than 4 weeks in HA hydrogels (Figures 4 and 5)

Albumin production of the hepatic progenitors cultured in HA hydrogels was compared to that of hepatic progenitors cultured on plastic over the course of 30

days of culture. The concentration of albumin (per volume) peaked between Days 7 and 10 for all cultures. Hepatoblasts lasted 7 to 10 days in cultures on plastic and reliably expressed significant levels of albumin. By contrast, the hepatic progenitors lasted for more than 4 weeks in the cultures in HA hydrogels.

Figure 4a is the normalized albumin production of hepatoblasts plated into HA sponges (Open Color Coded Circles). The albumin levels spike and fall between days 8 and 10, similar to that of cells plated onto culture plastic and on type I collagen substrata. The normalized amount of albumin is markedly higher modulating about a trend nearing 4.0 x 10^{-5} mg/ml, whereas hepatoblasts cultured on plastic are well below the 2.5 x 10^{-5} mg/ml baseline. When the albumin

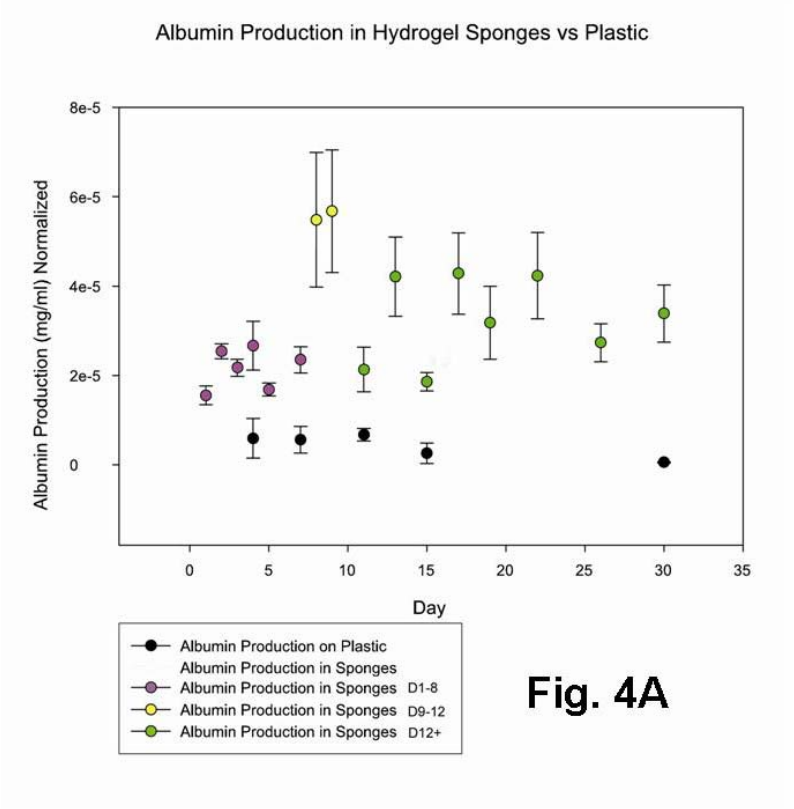

Figure 3-9 Synthesis of Albumin by Hepatoblasts Cultured in Hyaluronan (HA) Hydrogels.

data for the cells on plastic (Closed-Filled Circles) is plotted relative to that for cells in the hydrogels, the normalized data is consistently lower than the same cells cultured in the HA hydrogels.

Urea production, a common function for mature hepatocytes, is represented graphically in **Figure 4b**. The concentration of urea is given in mg/dl for this assay. Normalized mg/dl urea production by hepatoblasts in hyaluronan hydrogel sponges (upside down-open triangle) are compared to that from cells on plastic (Closed Circles), on monolayer collagen I cultures (Open Circle), and when cultured between two layers of type I collagen (Hash filled triangles). Again, there is a decrease in production in all cultures with the HA hydrogels performing slightly better than plastic, and forming a slower falling decay. [Exponential decay of the urea production in time without spiking the media with ammonia is an expected phenomenon, and low levels of urea would be expected for hepatoblasts as compared with mature parenchymal cells.]

Figures 5a, 5b, 5c are graphical comparisons of CK19, albumin and AFP RNA levels normalized to that for the GAPDH housekeeping gene in hepatic progenitors cultured in HA hydrogel sponges, in hepatic stem cells in culture on plastic and in hepatoblasts freshly isolated from fetal liver cell suspensions. For each 30ng of total RNA from freshly isolated hepatoblasts, there were high levels of AFP (130 strands), albumin (7000 strands), and relatively low levels of CK19 (1.2 strands). By contrast, the RNA isolated from hepatic stem cells demonstrated no AFP at all, low levels of albumin (2.6 strands) and high levels of CK19 (100 strands).

The hepatic progenitors seeded into the HA hydrogels showed low levels of CK19

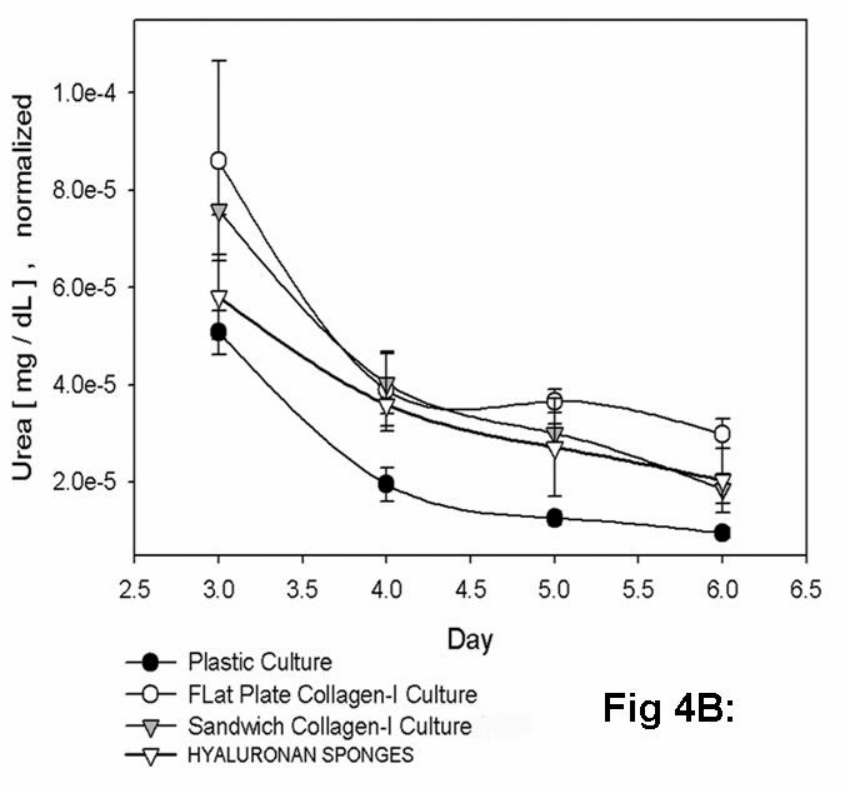

Figure 3-10 Synthesis of Urea by Hepatoblasts Cultured in Hyaluronan (HA) Hydrogels.

(1.66 strands), low but detectable levels of AFP (0.33 strands), and levels of albumin (5.77 strands) that are higher than that in the hepatic stem cells but dramatically lower than that observed in the freshly isolated hepatoblasts. Cyp3A4, a P450 cytochrome found in mature hepatocytes, could not be detected in either the hepatic stem cells or in the hepatic progenitors maintained in the HA hydrogels. Thus, the hepatic progenitors in the HA hydrogels are not stem cells, since they express AFP and ICAM-1, but the quantitative levels of their functions are closer to the stem cells than to the freshly isolated hepatoblasts. We conclude that they are early stage hepatoblasts.

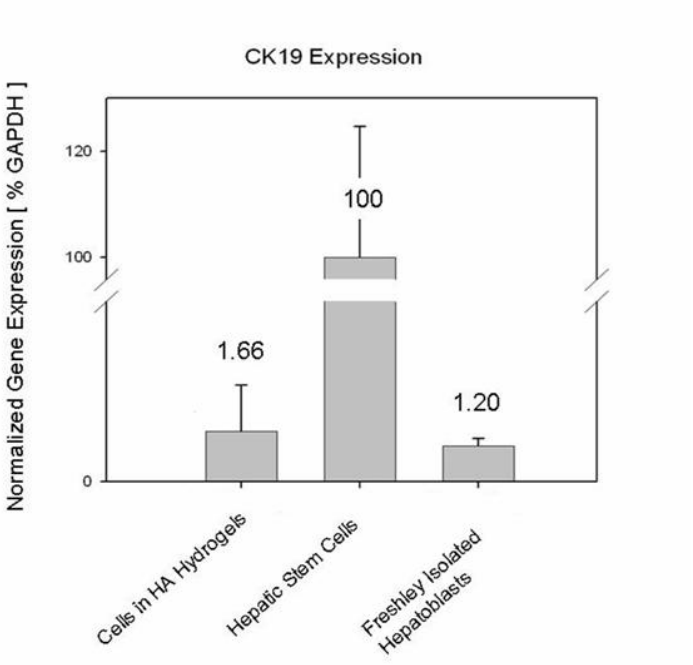

Figure 3-11 rt-PCR expression of CK19

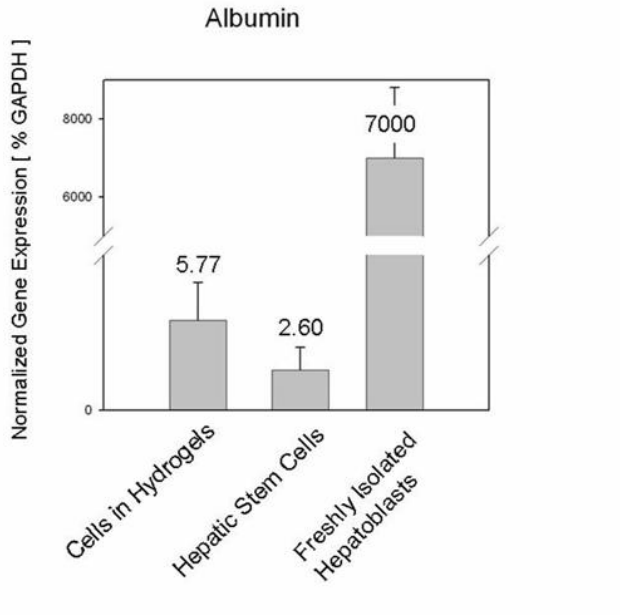

Figure 3-12 rt-PCR expression of Albumin

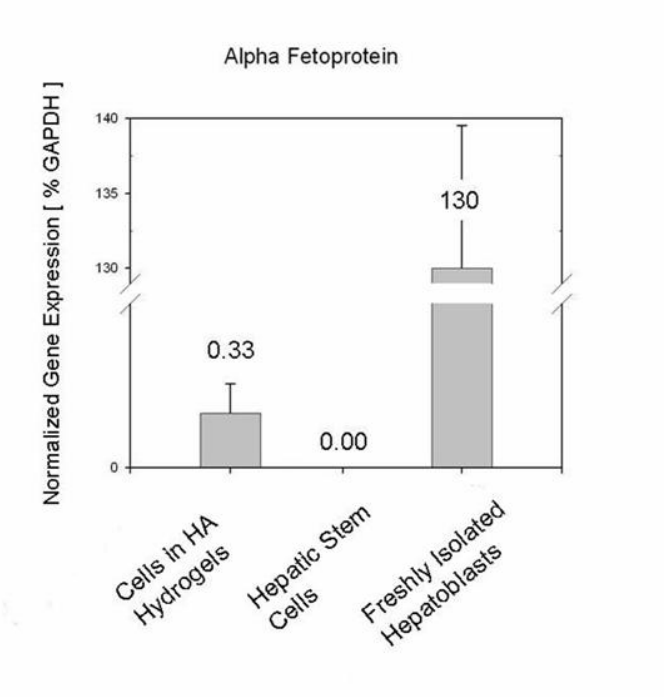

Figure 3-13 rt-PCR expression of Alpha-fetoprotein

3.6 Discussion

Hyaluronan hydrogels, in combination with a serum-free medium tailored for hepatic progenitors (KM medium), have proven suitable three-dimensional scaffoldings for human hepatic progenitors, particularly for hepatoblasts. They maintain the cells as early stage hepatoblasts in terms of viability, with proliferative capacity, with phenotypic stability through prolonged culture periods, and with minimal lineage restriction towards either biliary or hepatocytic fates.

Hyaluronans *in vivo* have high turnover rates[265] and possess unique mechanical/chemical properties that are ideal for embryonic tissues but yield scaffolds that are fragile and unstable, affecting their ability to be used in practical

ways needed for *ex vivo* cultures, for tissue engineering or in bioreactor systems[255, 273, 282, 292]. Therefore, it was desired to stabilize the HA scaffold sufficiently to make its use in cell cultures more practical. When in its natural molecular form, unbranched[403, 404] and unmodified, HA is hydrophilic[250, 405] and water soluble at room temperature.[295] The biophysical (mechanical strength and flexibility), and biochemical (polar group interactions) characteristics of the GAG underlie its functionality as a matrix component. Interactions between HA and other biological components are clearly controlled by the chemical structure of the GAG. The polar groups interact within the interior of the folded protein structure leaving limited availability for reactivity with other molecules.[405] As a result, fewer reactive groups offer a smaller quantity of points of attachment for multipoint functional adhesions, and thus the molecule experiences lower non-specific interactions with the environment. Many of the clinical applications using HA are not possible without modifications such as attachment of linking groups or modifications to the COOH or OH functional groups.[262, 295, 406, 407]

The random coiled structure of the HA GAG creates large areas for hydrogen bonding which can associate with up to 1000x the molecular weight in water[266, 396]. This hydration is due to the large negative charge carried by the molecule and the positioning of acidic groups, generating great water binding capacity[254]. NMR studies show that five hydrogen bonds can exist over as little space as four sugar units[247]. As a result of its water binding capacity, HA tends to become less flexible. The positive attribute of having a greater stiffness is the ability to resist compressive forces[253].

We tested the biological effects of hyaluronan chemically modified through cross-linking, which rendered the HA hydrogel scaffolds insoluble in water, and yet maintaining properties expected to be essential for their biological functions. Human hepatoblasts seeded into the HA hydrogels were found to retain their viability and their ability to divide for over 4 weeks, more than 3 times longer than those on plastic and the only 3-D scaffold found to sustain them for this length of time. As important was the surprising discovery that the cells remained stable as very early stage hepatoblasts throughout the culture period. Although other culture conditions are permissive for survival of hepatic stem cells (e.g. culture plastic or embryonic collagens or embryonic feeders)[16, 17,35], hyaluronans have been the only culture condition identified that facilitate survival, proliferation and maintenance of hepatoblasts; hepatoblasts do survive on ˌ STO embryonic stromal feeder cells but go essentially into growth arrest and undergo differentiation of the cells towards more mature fates.[46]

The expansion potential of the cells in the HA hydrogels was low with only a 2.28% increase/day of the cells. Growth rate of hepatic progenitors *in vivo* is regulated by Hedgehog signaling pathways involving rapid expansion of endothelia that, in turn, enzymatically digest the HA GAG facilitating turnover of the extracellular matrix, a process essential for cell division.[28] These particular HA hydrogels were extensively cross-linked via the carboxyl functionalities of HA and it is assumed were reduced in their ability to be digested by the endothelial progenitors typically found in association with the hepatic progenitors and evident in the HA cultures[46] The ability of the hydrogels to be dissolved was indicated by their

resistance to dissolution with hyaluronidase and harsh denaturants (data not shown). The turnover of the extracellular matrix, most typically accomplished *in vivo* by enzymatic digestion by cells, is an intrinsic process in the establishment of a tissue or organ.[408, 409] The stiffness of the HA scaffold could affect the maturation of the cells as could the large fluidic volume contained by the hydrogel capacity. Therefore, the physicochemical properties (such as flexibility and cross-linking density) of the HA spongy hydrogel have to be modulated to reduce the limitation on cell expansion. Other types of HA hydrogels, ones stabilized by alternative methods for crosslinking and complexed with other extracellular matrix components are now being tested for their efficacy as scaffolds for the hepatic progenitors.

Many HA-based medical devices are already approved for clinical applications including injection and grafting within the body. No matter what the source, the polysaccharide is conserved across all species and is biocompatible, eliciting no pyrogenic, inflammatory, immunologic or toxic responses[254]. HA hydrogels used to support human liver cells, including the several subpopulations of hepatic progenitors, will allow expansion of specific cell lineage states and provide a replenishing well for medical research and cell therapy.

Tables:

Table 1: Specific Markers of the Hepatic Cell Lineage:

	Hepatic Stem Cell	Hepatoblast	Adult Hepatocyte
EpCam	+++	++	---
AFP	---	+++	--
Albumin	+	++	+++
CK19	+++	++	--
I-CAM	---	+++	++
N-Cam	+++	---	---
C3A4 (rtPCR)	---	---	+++

Table 2: Antibodies and Fluoroprobes

Reagent	Dilution	Isotype	Source
Primary Antibodies			
Cytokeratin 19 (CK19)-biliary specific cytokeratin	1:500	IgG	Amersham
Cytokeratins 8/18 (CK 8/18)—epithelial-specific cytokeratins	1:800	IgG	Zymed
Hyaluronan receptor (CD44), a hyaladherins [410]	1:300	IgG	Molecular Probes (Invitrogen)
Albumin	1:800	IgG	Sigma
Alpha-fetoprotein	1:200	IgG	Zymed
ICAM-1 (CD54)	1:1000	IgG	PharMingen
Desmine	1:800	IgG	AbCam
EpCAM	1:800	IgG	Molecular Probes

			(Invitrogen)
Fluoroprobes			
Probe		Excitation/ Emission	
Alexa 647 (far red)	1:500		Sigma
Alexa 594 (red)	1:750	590/617	Sigma
Alexa 488 (Green)	1:1000	495/519	Molecular Probes
DAPI (blue)	1:1000	358/461	Molecular Probes
HA-Bodipy Conjugate	1:100	485/530	Invitrogen

Table 3. Primer Sequences used in the RT-PCR Assays

Gene	Gene Bank Acc. No.	Forward Primer (5' → 3')	Reverse Primer (5' → 3')	Tm Forward/Reverse Primer (°C)	Product length (bp)
ALB	NM_000477	gtgggcagca aatgttgtaa	tcatcgacttccag agctga	59.59/59.66	188
AFP**	NM_001134	accatgaagt gggtggaatc	tggtagccaggtca gctaaa	59.64/58.53	148
CK19	NM_002276	ccgcgactac agccactact	gagcctgttccgtc tcaaac	60.47/59.85	152
GAPD	NM_002046	atgttcgtcat gggtgtgaa	gtcttctgggtggc agtgat	59.81/60.12	173
C3A4	NM_017460	gcctggtgctc ctctatcta	ggctgttgaccatc ataaaagc	57.11/60.86	187

Alpha-fetoprotein (AFP). The AFP primers are ones to detect uniquely hepatic-specific AFP. As reported previously, hepatic progenitor cells make a unique AFP isoform that was cloned and sequenced in the Reid lab.

Figure Legends

Figure 1. Evidence of Hyaluronan Receptors on Hepatic Progenitors

A. Hyaluaronan receptors in hepatoblast cultures of human hepatic progenitors. Colony of hHpSCs in association with mesenchymal cells on culture plastic and stained for the hyaluronan receptors CD44 (Green) and Dapi (Blue). (10X)

B – D. Freshly isolated fetal hepatic hepatoblasts show receptors for CD44 (Green) and AFP (Red). (60x) Panels represented by B. CD44 C. AFP D. Overlay.

E. Contrast of hyaluronan receptor expression in hepatic stem cell colony versus the associated mesenchymal cells. Plate stained with Bodipy conjugated hyaluronan (4X)

F – I. Composite showing varied cell types present on cultured plastic. Colony of hHpSCs stained for DNA (Dapi-Blue), EpCAM (Green), and surrounded by hepatic stellate cells expressing Desmin (Red). (40x oil) Panels represented by A. DAPI B. EpCAM C. Desmin D. overlay.

Figure 2. Viability of the Cells within Hyaluronan Hydrogels.

A and B. Phase contrast of hyaluronan hydrogels seeded with human hepatoblasts and cultured for 20 days (20X)

C. Aggregate (spheroid) of human hepatic progenitors cultured in hyaluronan hydrogels, cultured for 11 days, and then dyed with Lysotracker (green; 488 nm) and Mitotracker (red; 543 nm) to indicate cell viability. Confocal section of the spheroid at 40x/1.3 Oil DIC; scaling .06 um x .06um.

D. Confocal sectioning through a spheroid showing viability of cells within the core of a spheroid within a hyaluronan sponge at day 11 of culture. Starting in frame 1 and ending in frame 6, the images slice through the spheroid showing live cells within the center. Stack Size 1024x1024x45 , 921.4um x 921.4um x 132.0um. Scaling .9um x .9um x 3.0 um. Objective Plan-Neofluar 10x/0.3 Wavelength: 543 nm. (Zeiss 510)

Figure 3. Antigenic Expression in Human Hepatoblasts Cultured in Hyaluronan Hydrogels

Aggregates of human hepatoblasts cultured in hyaluronan hydrogels were stained for various markers. All photographs were taken on a Zeiss 510, the Leica and Olympus FlowView confocal microscopes.

A. Cytokeratin 19 (CK19) expression. Wavelength 488nm. A 40X objective/1.3 Oil DIC Scaling 0.11 um x 0.11 um

B. Phase micrograph of the spheroid of hepatic progenitors in the hyaluronan hydrogel using a 40X objective/1.3 Oil DIC

C. Overlay image of A and B.

D. Albumin expression in the same culture of spheroids of cells as in B. Objective: Plan-Neofluar 40x/1.3 Oil DIC. Wavelength 543 nm. Stack size: 230.3um x 230.3um. Scaling 0.22um X 0.22um. Albumin expression (red) in human hepatoblasts within a hyaluronan hydrogel.

E. Phase micrograph of hepatoblasts within a hydrogel.

F. Overlay image of D and E.

G. Cytokeratin (CK) 8 and 18 expression (green; Alexa 488); nuclei stained with Dapi (Blue); the hyaluronan hydrogel does not stain and appears as wavy images in the background. 60x Oil Immersion (Leica).

H. Expression of I-CAM/1 (Alexa 488; green) in cells within the spheroid of cells within a hyaluronan hydrogel. The nuclei are stained with DAPI (Blue). 60x Oil Immersion (Leica).

I-L. Expression of EpCam, AFP, and Albumin in cells maintained in hydrogel cultures. 20x with 6x zoom. (Olympus FV500) Panel I. DIC (Black and White), Panel J. EpCam (Green), Panel K. AFP (Red), 20x with 6x zoom. Panel L. Albumin (Yellow). 20x with 6x zoom.

Figure 4. Synthesis of Albumin and Urea by Hepatoblasts Cultured in Hyaluronan (HA) Hydrogels.

A. Albumin Production in cells in HA gels as compared to cells on plastic substrata over the course of a 30 day culture. The Normalized Albumin production of hepatic progenitors cells plated into HA hydrogels (open color coded circles). modulate in the collected culture and can be seen with the

peak Albumin production falling post days 8 and 9 (yellow color coded). It is similar to that of the plastic. The Normalized amount of Albumin is much higher, and at minimal $2.5x10^{-5}$. It is a baseline as opposed to being a maximum peak. The albumin data for the plastic (closed-filled circles) is shown under the data for the hydrogel conditions with all points falling beneath the lowest concentration detected for the hydrogels. No data line is fit for Albumin production.

B. Urea production in cells in HA gels versus on other substrata. The normalized mg/dl urea produced by hepatic progenitors in the hyaluronan hydrogels (upside down-open triangle) as compared to plastic (closed circles), to cells plated on top of collagen I gels (open circles) or sandwiched in between collagen gels (filled triangles) cultures. Point to point curves are added to make day to day following of the graphed points easier. Fitted lines for the exponential decay of urea production over 6 days in HA hydrogels are not shown.

Figure 5. RNA expression of CK19, Albumin, Alpha-Fetoprotein (normalized to GAPDH)

RNA encoding CK 19 (A), albumin (B), and alpha-fetorpotein (C) isolated from cultures of freshly isolated hepatoblasts, hepatic stem cells and hepatic progenitors cultured in the HA hydrogels. All values are normalized to the housekeeping gene, GAPDH, and are expressed as the number of strands present per 30ng of total RNA for the sample.

4 CHAPTER IV. Human Hepatic Stem Cells and Hepatoblasts in Hyaluronan Hydrogels crosslinked with Disulfide Bridges

The studies with dihydrazide-crosslinked hyaluronan sponges indicated that the cells survive long-term in the hydrogels, but the form of cross-linking was too robust and slowed turnover of the gels by the cells, resulting in very slow cell growth, and obviated experimental evaluations (e.g. cell counts), since the hydrogels did not dissolve even in strong denaturants (e.g. 6 M Guanidine HCL!). Consequently, characterization of the cells in the dihydrazide-crosslinked hydrogels was done at great expense of time (e.g. manual counts of cells in sections of hydrogels). Subsequently, efforts were made to find hydrogels stabilized by other forms of cross-linking. An alternative cross-linking method has been developed by Dr. Glenn Prestwich and involves disulfide bridge crosslinking chemistry. The HA hydrogels with disulfide cross-linking were assessed for their utility with respect to the cultures of the cells and found to be ideal for the cells and for experimental needs.

Figure 1, contains images of cells in HA hydrogels with disulfide bonding to culture the hepatic stem cells and hepatoblasts. Cell populations of mostly hepatoblasts were seeded into the hydrogel and cultured for more than one week. A sample collected at week 1 was snap frozen and then treated with Dapi, that stains nuclei allowing for identification of cells within the hydrogel. Individual cells are

blue from DAPI staining (image on the left). The transmission image is given in the center of the trio of images, and then an overlay of the two is presented on the right. The hydrogel is clearly visable in the transmission and overlay images. Cells, within the HA hydrogel are presented as an H&E stain at 20x. These cells are located within a lacunae like area of the hydrogel. Furthermore, images taken on the Olympus Flowview Confocal microscope at 20x indicates how cells aggregate in colonies within the scaffolding. The FitC image was taken at the 488nm wavelength and is shows autofluorescencing hepatic cells in culture. Within monolayers cultures, the autoflourescence is not as bright as found here. Additional images of smaller spheroids are shown in the set of 4 images in the lower right hand corner. The spheroids of cells maintained antigenic expression of EpCAM, AFP, and Albumin, indicative of hepatoblasts. In cultures maintained on tissue culture plastic, the hepatoblasts disappear within a few days. By contrast, they persist for weeks in HA disulfide hydrogels.

Since there was definitive proof that the cells remained viable and phenotypically stable as progenitors, experiments were done to assess the effects of additional matrix molecules added to the hydrogels. Matrix components, known to be in the stem cell niche or found in association with more mature parenchymal cells. The additional matrix components were added to 100 percent pure hyaluronan hydrogel (Extracell). Colonies of hepatoblasts were collected manually from plastic

culture dishes and transferred to each test condition. Overall effects of numbers of

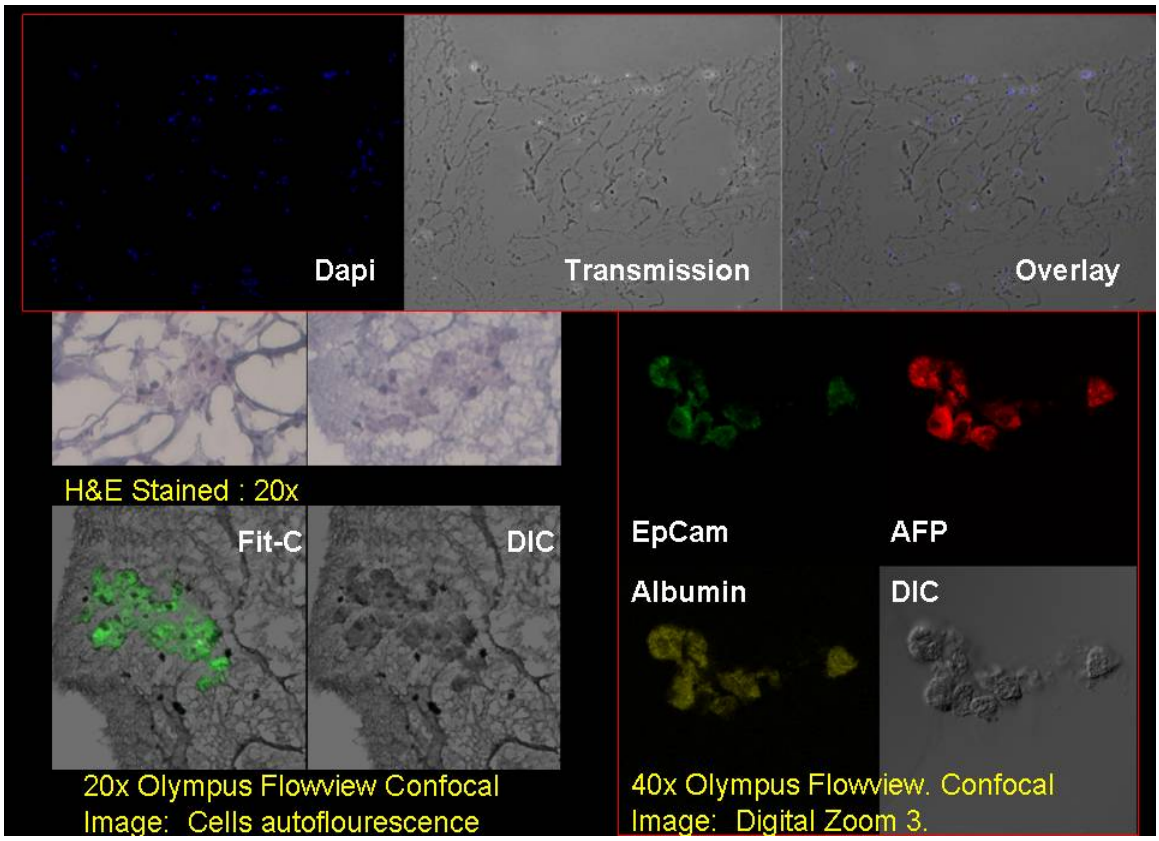

Figure 4-1 Characterization of Progenitors Populations in Disulfide Hydrogels

attachments and growth of colonies were measured. **Figure 2** is a representative panel of all the conditions tried. The bold red X marks where cells did not attach to the substrata used. The cells showed poor attachment to 100 percent HA, tissue culture plastic, and collagen IV. However, they showed better attachment to hydrogels mixed with fibronectin, Laminin, or Collagen III. From the numbers of colonies attached and the amount of visible spreading of the colonies across the substrata, laminin performed the best giving the highest number of attachments for colonies and the most area covered by those that attached. From this step, it was determined to carry on with the laminin into the next step which is inclusive of

metabolic profiling of the hepatic progenitor populations on various substrata. Furthermore, the addition of collagen I and laminin together caused a morphological change in the progenitors seeded. **Figure 3**, represents colonies grown on this combination of substrata in which there are visible morphological changes within the cultured system such as cords and 3-dimensional structures indicating differentiation of the cells. .The following article submitted to Nature Biotechnology relates the findings via implementation of metabolomics on the characterization on the progenitor population in varied 3-D hydrogels.

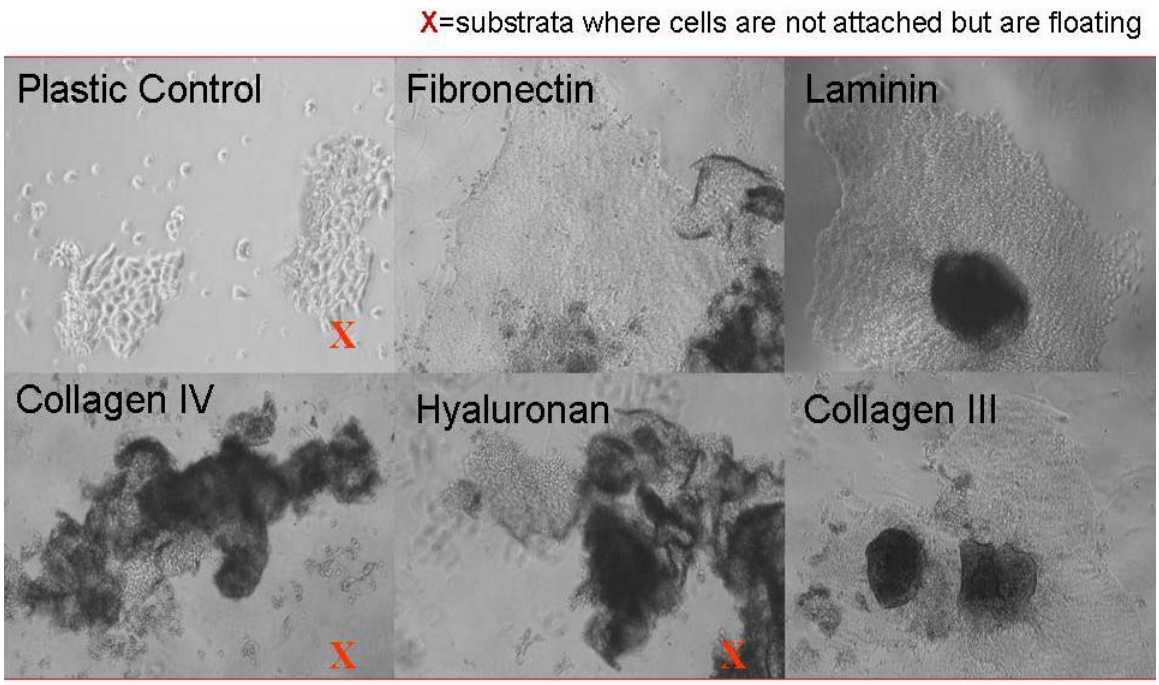

Figure 4-2 Matrix effects on hHpSCs attachment

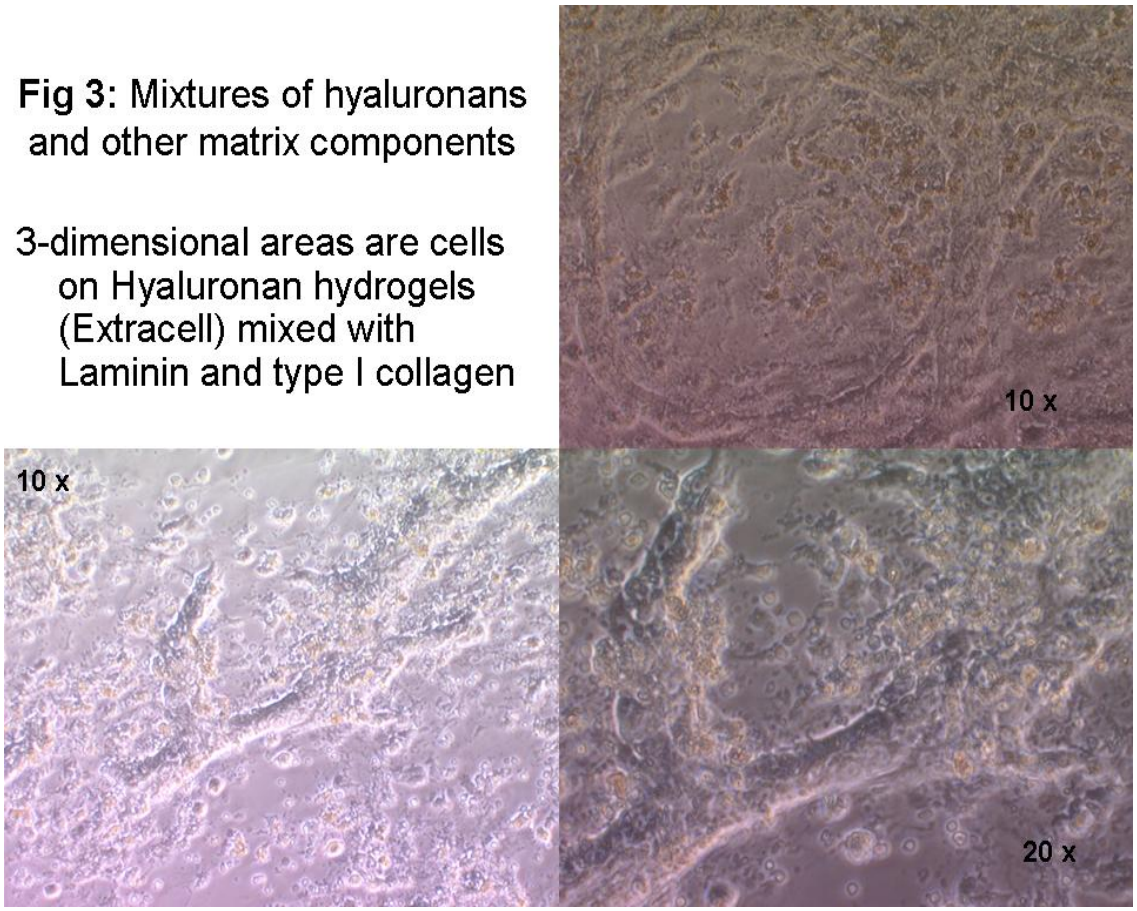

Figure 4-3 Morphology effects of Laminin, Collagen I and HA.

5 Nuclear Magnetic Resonance Metabolomic Footprinting of Human Hepatic Stem Cells and Hepatoblasts Cultured in Hyaluronan Hydrogels

W.S. Turner[1-4], C. Seagle[2], J. Galanko[4], O. Favorov[2], G.D. Prestwich[5], J.M. Macdonald[2], and L.M. Reid[1-4]

[1]Departments of Cell and Molecular Physiology and [2]Biomedical Engineering,

[3]Program in Molecular Biology and Biotechnology,

[4]Cancer Center and Center for Gastrointestinal and Biliary Disease Biology (CGIBD),

UNC School of Medicine, Chapel Hill, NC 27599

And

[4] Department of Medicinal Chemistry

Center for Therapeutic Biomaterials

419 Wakara Way, Suite 205

Salt Lake City, Utah 84108

Running Title: Metabolomic Footprinting of Human Hepatic Progenitors

Table: 1 **Figures**: 6 **Supplements**: 1

Word and Character Counts: Abstract: 189 Text: 4586

Corresponding Authors: WS Turner and LM Reid, UNC School of Medicine, Campus Box 7038, Glaxo Building Rms 32-35, Chapel Hill, NC 27599. Phone: 919-966-0347; FAX: 919-6112. Email: wsturner@email.unc.edu, lmreid@email.unc.edu

Keywords: Nuclear Magnetic Resonance (NMR), Metabolomics, Footprinting, Hepatic Stem Cells, Hepatoblasts, Progenitors, Human Liver, Extracellular Matrix, Hyaluronans, Tissue Engineering

5.1 Abstract

Metabolomic footprinting by nuclear magnetic resonance spectroscopy (NMR) has been used with cultures of human hepatic stem cells (hHpSCs) and hepatoblasts (hHBs) seeded into hyaluronan hydrogels mixed with other matrix components (specific collagens, laminin) and in a serum-free medium tailored for hepatic progenitors, "Kubota's Medium" (KM). NMR analyses were used to establish a metabolomic profile of the cells under each chemical version of the hydrogel scaffold. The assays did not require destruction of the cells and allowed daily monitoring for the duration of the experiments (more than 4 weeks). Metabolomic profiling was performed for numerous metabolites (glucose, lactate, glutamine, alanine, etc), and the data were utilized to assess cellular regulation of glycolysis, the Krebs cycle and other metabolic pathways. The cells were found to remain viable, expanding, and as stem cells. Small changes in the extracellular matrix chemistry were found to influence the metabolism of the hHpSCs indicating the ability of these assays to discern even subtle effects by factors that influence changes in viability, growth and differentiation. Such non-destructive analyses should be invaluable for projects in lineage restricting and differentiation of stem cells *ex vivo* to adult fates.

5.2 Introduction

Nuclear magnetic resonance (NMR) is used to analyze low molecular weight moieties, typically 10,000 Daltons or less, not detectable on large scale by standard biochemical assays[411],[412]. Based on detection of the absorption of electromagnetic radiation at specific frequency in a magnetic field, the chemical environment of a particular metabolite can be discerned[391]. In the past, it has been used as a tool for monitoring metabolic changes in biological systems including glycolysis, acetate production of hepatocytes, the Krebs cycle, urea synthesis and transamination. The power in experimental strategies using NMR is in its ability to detect diverse metabolites non-invasively without extensive sample preparation[412]. An additional strength is that instead of looking at one particular metabolite or one class of metabolites such as amines, amino acids, carbohydrates, organic acids and their derivatives, NMR can be used to survey in parallel the entire spectrum of metabolites. The subtleties of observing the metabolites to characterize a system may be overlooked as this system is potentially better than looking at the proteome to establish a defining phenotype based on amplification of next step reactions within the cell[413]. For example, the metabolome is the downstream result of the *in vivo* proteome, but ultimately, it is the small molecules acting on the proteome that act upstream on transcription.

The cellular model systems to be subjected to metabolomic analyses are human hepatic stem cells (hHpSCs) and hepatoblasts (hHBs) placed under serum-free, wholly defined culture conditions and with variations in the matrix substratum conditions. The long-term goals are to determine precise sets of factors that alone or

in combination will lineage restrict and differentiate the stem cells to their mature fates while *ex vivo*. The hHpSC, the first stage of the liver's parenchymal lineages, are small cells (7-9 μm in diameter), with a unique antigenic profile [EpCAM+, NCAM+, ICAM1-, Claudin 3+, cytokeratin (CK) 19+, albumin ±, α-fetoprotein (AFP)-, sonic and Indian hedgehog proteins+, telomerase+] and located *in vivo* in the ductal plates in fetal and neonatal livers[128] and in the canals of Hering in pediatric and adult livers near to the portal triads of the liver acini[118]. The hHpSCs give rise to the second lineage stage, the hHBs, that are larger (10-12 μm in diameter), with an overlapping but distinct profile [EpCAM+, NCAM-, ICAM1+, Claudin 3-, CK19+, albumin ++, AFP++, sonic and Indian hedgehog proteins+, telomerase+] and located throughout the parenchyma of fetal and neonatal livers but limited to a handful of cells tethered to the ends of the canals of Hering in pediatric and adult livers[128]. The hHBs give rise to an additional 5-7 maturational lineage stages that include unipotent, committed progenitors (biliary and hepatocytic), diploid adult parenchyma (hepatocytes or cholangiocytes), multiple stages of mature parenchymal cells identifiable by ploidy and/or by gene expression, and ending with the final stage, apoptotic cells located near the central veins.

The methods for identification, isolation and culture of the hHpSCs and hHBs under wholly defined culture conditions are also described in prior reports[22, 25, 27, 28, 46, 47, 128]. The cells are cultured in a serum-free medium tailored for hepatic progenitors, called "Kubota's Medium" (KM)[43] and on one or more purified extracellular matrix components. Thus far, we have shown that self-replication occurs with KM and purified type III collagen[47]; lineage restriction to

hHBs occurs with cells on type IV collagen or on laminin and in KM[25]; more extensive differentiation occurs with type I collagen and with certain proteoglycans [25, 47]. The hHpSCs can be maintained also in a 3-dimensional (3-D) format on hyaluronan hydrogels[45]. Current efforts are towards identifying the conditions for lineage restriction of the hHpSCs through all of its maturational lineage stages to yield cells with mature liver cell fates. We are using the studies reported here to begin to establish metabolomic data bases characteristic of the parenchymal cells at each lineage stage and that permit one to assess the effects of culture conditions on the progression of the cells through differentiation. This report defines the database for the cells maintained as stem cells for weeks in 3-D hyaluronan hydrogel culture systems.

5.3 Results

5.3.1 Cultures

Human hepatic stem cells and hepatoblasts have been shown to have receptors for hyaluronans (CD44) and to survive and grow in hydrogels prepared from hyaluronans cross-linked by aldehyde bridges[45]. The ability of the cells to be maintained in hyaluronan hydrogels prepared with disulfide bridge cross-linking is equal to or better than that found previously with hydrogels cross-linked by aldehyde bridges. Certainly, the ability to remove the cells from the hydrogels was enhanced dramatically given that one can dissolve the gels using reducing agents such as dithiothreitol along with hyaluronidase. Cell biological characterizations, such as

growth curves, morphology, and immunohistochemistry of markers in the cells in the matrix/hyaluronan hydrogels are given in a separate manuscript (Turner et al, in preparation). The focus for these studies has been the NMR analyses. Although data supports the conclusion that the amount of cross-linking does effect the cellular-hydrogel dynamic, this study focuses upon the use of NMR (a known technology) to develop a new method/technique.

5.3.2 Identification and Quantification of Metabolites in Cultured Human Hepatic Stem Cells (hHpSCs) and Hepatoblasts (hHBs)

Areas of the spectra, **Figure 1**, that are of little interest due to the vicinity of water, the controls, or are beyond the range of the signal were not considered for principal component analysis PCA analysis and hence are represented as "dark" regions of the spectra. These dark regions specifically fall into three distinct ranges. The first is 0.2 ppm or less; it conflicts with TSP and contains data out of range on the low end of the spectra. The second dark region falls between 4.06 and 5.02 ppm, a region that captures the water peak, which is the strongest carrier frequency detected within the sample. The last dark region falls between 8.24 and 8.48 and includes the known peak for formate, which is used as a standard to quantify the concentration [414]of metabolites present as a percentage of area under their respective spectral curve. Many of the PCA determined significant metabolites fall within the region of 0.84 and 4.46 ppm, and include a vast majority of the amino acids and derivatives. The box is expanded and metabolites assignments are shown in the upper left hand corner of the figure.

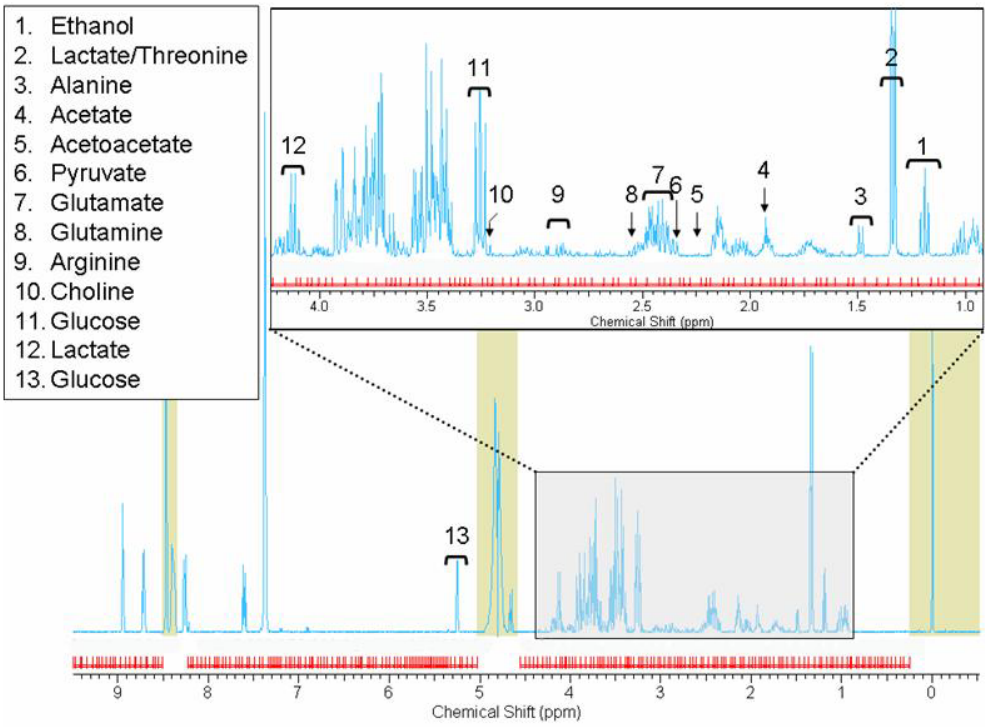

Figure 5-1 1H NMR spectra

The Principal Component Analysis was used to determine whether NMR spectra change systematically with time of incubation. This analysis revealed that, indeed, the time of incubation is one of the most significant sources of variability among the samples. The time-dependent variability was captured most prominently by the first two principal components, PC1 and PC2, which are shown in **Figure 2**. The score plot in Figure 2A was generated by plotting the value (score) of each sample along PC1 vs. its value along PC2. The samples are color-coded according to the day on which they were obtained, revealing substantial clustering of samples taken on different days in different regions of the plot. From day 2 to day 8 and then to day 12, samples tend to shift in the upper-leftward direction in the plot. Still, there is a major overlap among the three day-defined clusters. Some of this

overlap happens to be due to systematic differences between liver 3 and livers 1 and 2 used in this study. To show these differences and also to remove this source of spectral variability, samples obtained from livers 1 and 2 are plotted in Figure 2B, while samples obtained from liver 3 are plotted separately in Figure 2C. These two score plots clearly show that for each liver the day-2 samples are prominently displaced relative to the day-8 samples, which in turn are displaced – although to a lesser degree – relative to the day-12 samples.

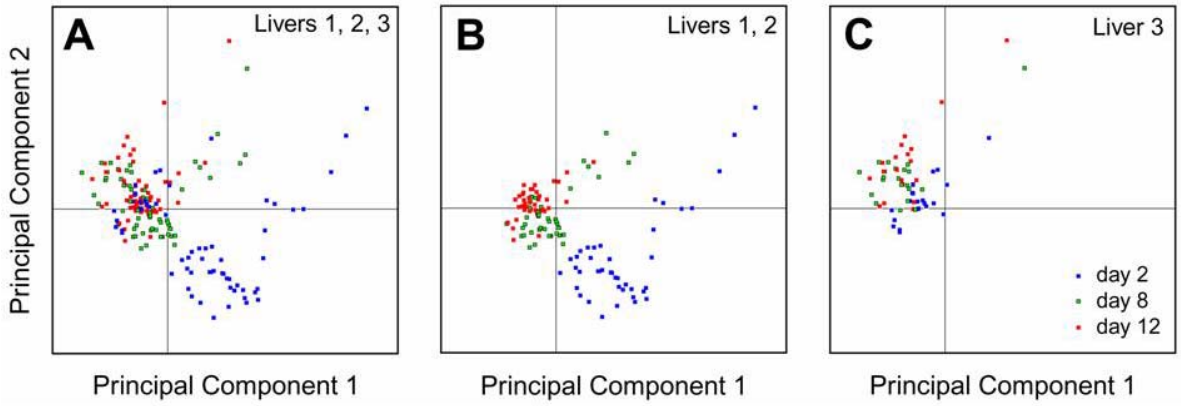

Figure 5-2 Scores plots from PCA

To determine whether different treatments of the cell cultures had different effects on their temporal development, **Figure 3** shows a score plot of group averages. In this plot, each point is an average of scores of all the samples of a given day and a given treatment. Different treatments are coded by different colors and different days of the same treatment are connected by lines, to make clear the paths traveled in the score plot by different treatments during the incubation period. This plot fails to show any clearly evident differences in temporal trajectories that might be due to different treatments.

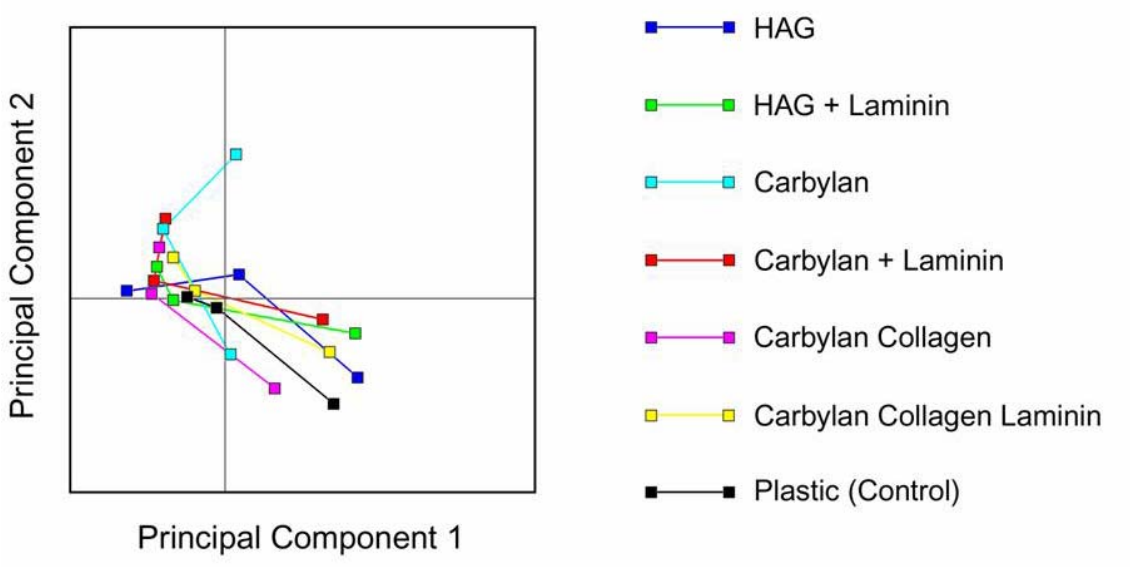

Figure 5-3 Average scores plot

To determine which metabolites were primarily responsible for the temporal changes in the NMR spectra, the contributions (loadings) of each spectral bin to PC1 and PC2 are plotted in **Figure 4**. In this loadings plot each bin is shown as a point. The bins that have little or no impact on PC1 and PC2 are placed at or near the plot origin. The more significant the contribution of a bin to one or both principal components, the farther away from the origin is its position in the plot. The bins responsible for the temporal shift of the spectra in the PC1 vs. PC2 score plots (i.e., the left-upward – or ~135° – shift of points in Figures 2 and 3) are the bins which in Figure 4 loadings plot are shifted in the same (~135°) or opposite (~215°) direction from the plot origin. In other words, the spectral bins sensitive to incubation time are located in the upper-left and bottom-right corners of the loadings plot. Among these bins we find, in particular, the bins containing the following metabolites: glucose, alanine, lactate, arginine, glutamine, and glutamate. These bins are labeled

accordingly in the Figure 4 plot. Thus, PCA suggests that concentrations of glucose, alanine, lactate, arginine, glutamine, and glutamate in the supernatant change systematically from day 2 to day 12.

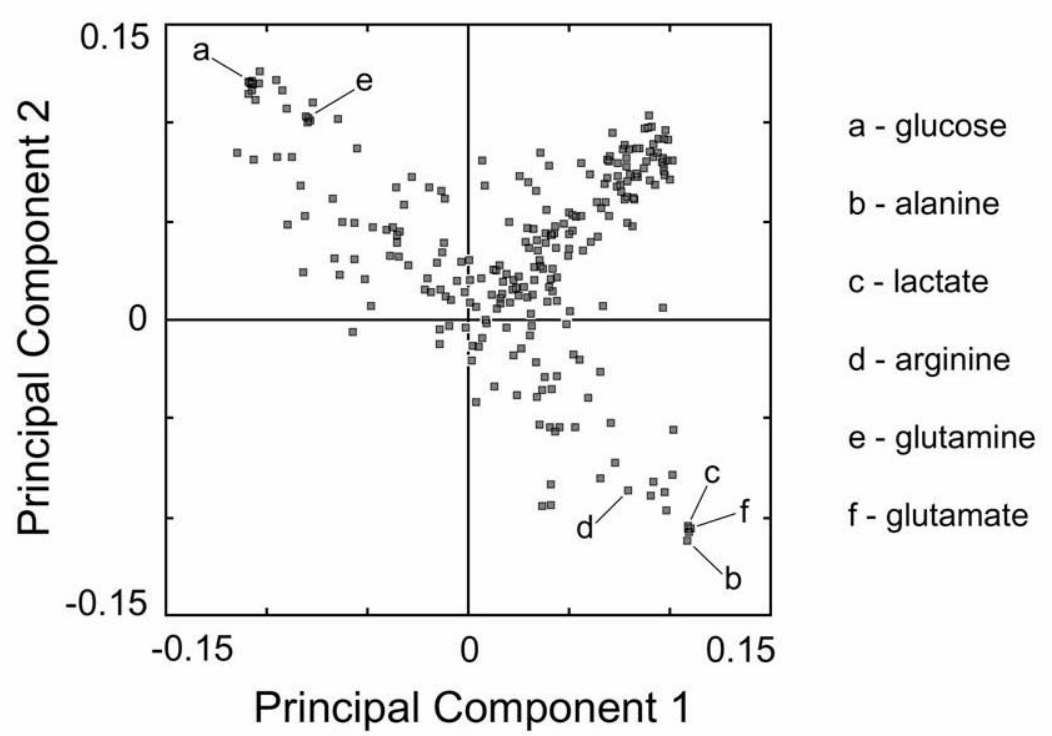

Figure 5-4 Principal component loadings plot

The concentrations derived from the spectral data are related as a percent area correlation to that of formate. Representative samples are of glucose, alanine, lactate, arginine, and glutamine and are exhibited in **Figure 5**. In each case the substrate is labeled as the X axis in the graph where the following seven different scaffolds for the cells are compared: Carbylan (C), Carbylan/Laminin (C+L), Carbylan/Gelatin (C+G), Carbylan/Gelatin/Laminin (C+G+L), Hyaluronan/Gelatin (H+G), Hyaluronan/Gelatin/Laminin (H+G+L), and Plastic (PL). The last single column represents the endogenous amount of the metabolite found within the KM

media, also just labeled Media. The sample days represented as 2, 8 and 12 are color coded and sequenced, thus giving a triplet of 2 (red), 8 (tan), 12 (blue) with day two on the left, and day 12 on the right for any given scaffold being assessed. The height of the histogram is demarked by the y axis representing the percent formate peak. By setting the area under the formate peak in all spectra to be 100% of the concentration, then comparisons can be made between the spectra in regard to concentration of metabolite present.

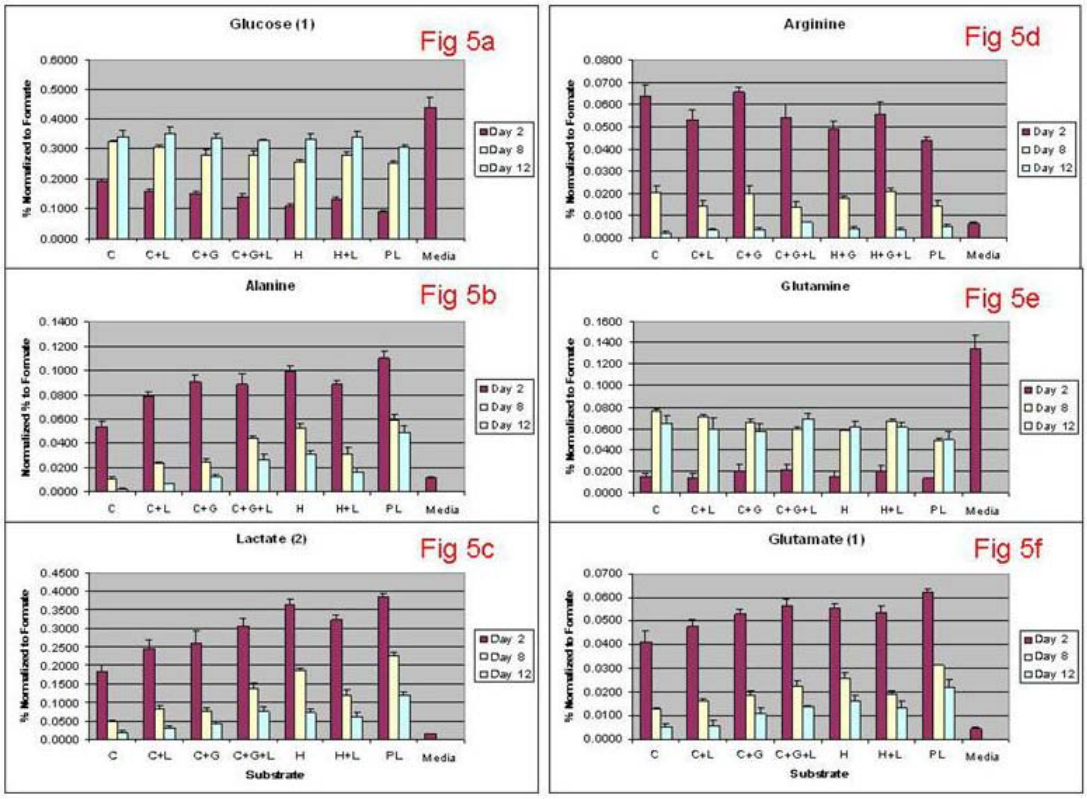

Figure 5-5 Formate Normalize Metabolites

Figure 5a representing glucose shows that all cultures on all forms of matrix-hydrogels are consumers of available glucose within the system. Of the bins recognized as important in the PCA, three of them are representative of glucose. When peaks plotted for the three different glucose representative areas are

compared, they each show the same histogram differences (Data not shown for all three graphs). The percentage then translates into a net amount for each known metabolite as is recorded as a net loss or production within the mass balance of the system. Media Glucose is highest in the KM solution (the controls-no cells), whereas on other scaffolds, the net use of the glucose decreases from day 2 to day 12. Therefore, the cells are consuming glucose, not generating it as would occur in more differentiated liver cells capable of gluconeogenesis.

Figure 5b is the histogram of alanine. Again the x-axis represents the substratum, that is the type of matrix-hyaluronan scaffold, and the y-axis is the percent formate region under the curve of the spectra. Alanine is produced in high quantity at day 2 of the culturing process and subsequently declines in production by day 12. There is a shift between the first two graphed matrix-hyaluronan hydrogel scaffolds, carbylan and carbylan-laminin, in which production falls and consumption begins by day 12.

Figure 5c represents the histogram for lactate. The level of lactate within the medium, KM, is at a low level [0.0157 % Formate Peak]. However, cells by day 2 of culture show a minimum of an 8-fold increase in lactate in the media. Tissue culture plastic is the substratum with the highest induction of lactate metabolites in the cells. Over the course of the experiment, lactate production subsequently falls to close to the amount found in KM. This suggests that the cells are recovering from the processing procedures that have injured them and have subsequently settled down to a more normal metabolism indicated by the restoration of lactate to low levels.

Figure 5d represents Arginine. The amino acid metabolite is present in KM at low levels compared to that found by day 2. Cells cultured on all forms of scaffolds or substrata demonstrate a high level of arginine which subsequently falls in concentration fairly quickly. By day 12, arginine levels almost reached a concentration at which it is equivalent with the starting amount introduced by changes of culture media or that being consumed in the culture.

Figure 5e represents Glutamine which has an overall consumption rate within the culture system on all substrates as recognized by the difference in height between the media and the cultures on days 2, 8 and 12. However, net consumption of the Glutamine goes down over the course of time and appears to stabilize within a narrow range by day 8. A common set of metabolites for this experiment are listed in **Supplemental Table 1** for the basis of reference for phenotyping the footprint of the human progenitor metabolites.

The statistical model employed (see methods), contains the predicted lines for each treatment over time with consideration of the substratum. The model is constructed by using the actual values to predict or give an idea of what occurs after all factors are taken into account. As with any of the metabolites, the model is considered individualized. The overall p-values for this model are significant for time, but not for substratum or the day/substratum interactions, which considers all the factors at once. The statistical model shows that the overall mean response of any metabolite is the combination of a fixed substratum effect, a fixed time effect, a random liver effect and the interaction of the substratum and time variables. These effects are documented in pair-wise comparisons for significance found in **Table 1**.

5.3.3 Metabolomic Profiles

The metabolites identified by the PCA anaylsis **Figure 1 (supplemental Table 1)** can be mapped into the cellular metabolism. **Figure 6 (insert)** illustrates the connection between many of the significantly identified metabolites including alanine, glucose, lactate, glutamine, and arginine. Those metabolites can further be used to describe the metabolic pathways in which the cells produce proteins identified through ELISA assays. During glycolysis, glucose is transformed through a chain of chemical modifications into Pyruvate and then Acetyl-CoA. The Acetyl-CoA is located within the mitochondria and enters the Krebs Cycle, also known as the citric acid cycle; the cycle is denoted in the figure as a green sphere.

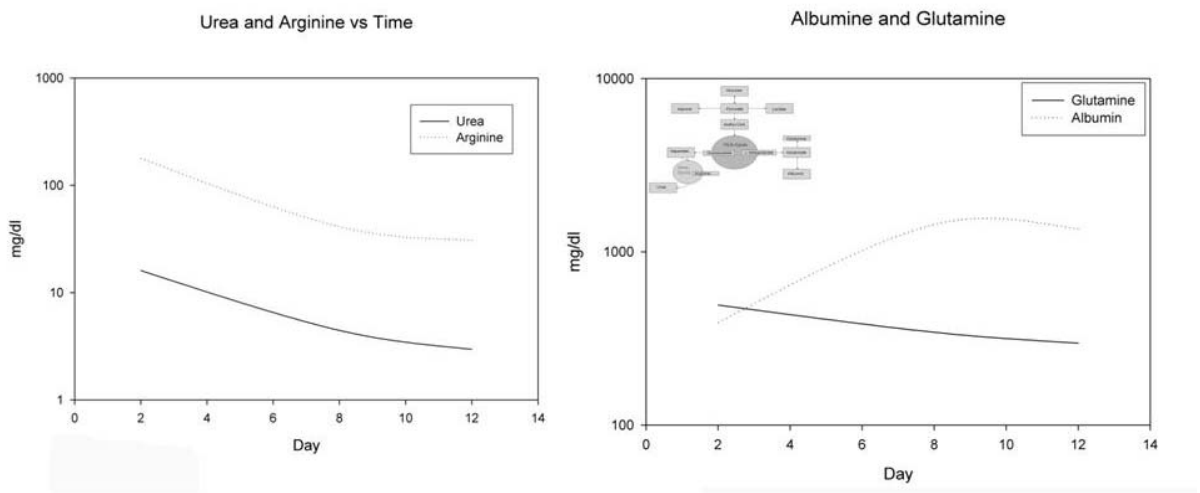

Figure 5-6 Metabolomic Pathways

Alpha-ketoglutarate in the Kreb cycle can be affected by aspartate to yield glutamate, which in turn is an intermediate towards the production of Glutamine

and/or Albumin. Oxaloacetate from the TCA cycle is the by-product of the interaction of the alpha-ketoglutamate with the aspartate, as well as the conversion from malate, and in similar fashion, the combination of oxaloacetate and glutamate forms aspartate and alpha-ketoglutarate. Aspartate is funneled into the urea cycle leading to the eventual production of arginine and eventually urea. Pyruvate can be metabolized into alanine or lactate, with reversal of the process being plausible.

Measured end products, urea and albumin, are indicative of the metabolism of the cells. As diagrammed in the previous figure, the relationship between arginine and urea production is indicated by the data in **Figure 6a.** The double x axis represents the normalized arginine concentration as compared to the net urea analysis, where the y-axis represents the day. Across all substrata tested, the trend from day 2 to day 12 is a decrease in production of both arginine and urea. The base amount of arginine in KM is 200 mg/L which correlates to the extracted value of 0.0066 concentration percentage of formate. From day 2 through day 12 the amount of arginine productions falls from an average percent of formate of 0.058988 to 0.010146, (178.7516 mg/dl to 30.7449 mg/dl arginine). The paths of the arginine (blue) and the urea (red) are similar, because they are directly tied to a couple reaction in which arginine is used to make urea. As the system slows and less arginine is produced, then less is available for the production of urea.

Similarly, albumin production in **Figure 6b** can be tied to metabolites detected in the phenotype through glutamate. Glutamate production like that of arginine is highest early in the culturing period (**Figure 5f**) on all substrata and decreases over the course of time. However, net production is shown over all

substrata when removing the amount introduced by the KM media. The net effect when paths are skewed according to culturing techniques shows that as time progresses throughout the experiment the amount of the cells, the conversion of glutamate to albumin or glutamine are opposite. The albumin production of the system decreases as the glutamine production increases.

5.4 Discussion

Metabolite profiling through NMR analysis has been done with hHpSCs and hHBs cultured in wholly defined medium and on specific forms of matrix-hyaluronan hydrogel scaffolds. It has proven to an ideal strategy for phenotyping the cells given that it is non-invasive and provides a global survey of all the metabolic pathways operating in the cells. To our knowledge, this is the first report of such a metabolic phenotyping of a stem cell population, the hHpSCs, via unbiased high through-put analytical methods utilizing computational mathematics to interpret the complex metabolic profiles. The novelty with respect to such an analysis being done on a stem cell population is furthered by the fact that there have been relatively few studies on metabolomics even of mature hepatocytes; most of the published reports are with respect to drug metabolism[312, 345, 412] or on a specific metabolic pathway, such as carbohydrates[415] or lipids[416]. These studies characterized transcription factors or signaling pathways but did not analyze the complement of small molecules produced by the cells. It is possible, that the metabolomics was ignored in those studies due to the need for certain methods development for metabolomics of cell culture. In this study, we carefully modified the extracellular

matrix composition of the hydrogels, insoluble components of the culture conditions, in order to identify their influence on metabolomic differences indicative of a stem cell versus differentiative phenotype.

The extracellular matrix contains critical signals that along with various soluble signals (autocrine, paracrine, endocrine) regulating the phenotype of all metazoan cells.[389][-3]. Moreover, the chemistry of the matrix and of the soluble signals change in parallel with the maturation of the parenchyma [10, 38, 156, 214]. The known matrix components in or near the liver's stem cell niche include hyaluronans and their receptors, CD44H, fetal laminins and certain integrins (α4β6, β1) that bind them, type III and IV collagen, and chondroitin sulfate proteoglycans (CS-PGs) [10, 25, 47, 128, 156]; (Bruce Caterson, personal communication). The matrix chemistry transitions from that niche environment to that associated with the fully mature parenchymal cells located near the central vein. The matrix components associated with the mature parenchyma are found in the Space of Disse and consist of collagen type I, some collagen type III, forms of heparan sulfate proteoglycans and heparin proteoglycans but not laminin, hyaluronans or type IV collagen[3-8] The matrix components more distant from the parenchyma include also perlecan and tenascin.[6, 9, 10, 156, 417] Due to matrix chemistry and positioning[25, 47], the hHpSCs are far less likely to come into contact with the shear stresses from blood flow or with the hormonal factors contained within the blood of the sinusoids than their hepatocyte progeny, which are adjacent to fenestrated endothelial cells of the sinusoids[418]. The fenestrated endothelia offer cellular boundaries in some regions of the Space of Disse and only matrix chemistry at the

sites of the fenestrae of the endothelia located near to the central vein. The Kupffer cells are attached to the endothelium.

Applying metabolomics analytical methods, extensive multi-variate statistical analyses was performed on the NMR data, and it further illustrates that the changes in the matrix materials can give rise to significant changes in the production of certain metabolites and the consumption of specific compounds. Implications of the changes in the matrix chemistry and comparison to what occurs to the control (plastic) cultures are indicative as to what is going on within the cells on matrix scaffolds, especially those in 3-D cultures. Table 1 is indicative of the comparison between plastic and Carbylan cultured hHpSCs. Of the 560 paired comparisons, that between the Carbylan and the plastic show as being the most significant in metabolic divergence. This is not to be confused as conclusions to the best culturing condition, because that is dependent upon the final desired result. However, using this method of analysis, Carbylan does exhibit properties which make it the preferred system, of those assayed, for the maintenance of hHpSCs as stem cells under a 3-D culture system, that is with minimal differentiation. Cells that are engaged primarily in anaerobic, not aerobic metabolism are highly indicative or stem cells in the adult human liver[334]. Niche studies of the liver acinus show that cells derived from the periportal region experience lower levels of oxygen than do those of pericentral local[336]. The matrix chemistry used as substrata for hHpSCs and hHBs has been established by the known chemistry in the stem cell niche *in vivo*.[128] and components of it, such as type III collagen shown to elicit self-replication of hHpSCs in culture[47]. Furthermore, isolated hepatocytes express

distinct gene expression, and thus metabolic phenotype, dependent on the matrix chemistry utilized [6, 146, 312, 419-421]. As the hHpSCs and hHBs have been characterized previously in serum-free KM and on plastic versus on matrix substrata in monolayer conditions[25, 27, 46, 47] this report offers studies on 3-dimensional cultures with evidence for significant changes in metabolic functionality with the pair-wise contrasts of each version of hydrogel (HA alone, HA with laminin, HA with collagen) versus plastic. As applied to this set of experiments, we have cultured the hHpSCs in KM and without the use of serum throughout the 4 weeks of the experiment. Serum is known to result in lineage restriction and differentiation of the hepatic progenitors and to overgrowth of mesenchymal cell populations such as fibroblasts. Others have reported that cultures that are serum free are least likely to have pronounced disparity in gene expression [312].

The establishment of the proper matrix chemistry was launched with studies assessing hyaluronan hydrogels utilizing aldehyde cross-linking, and found to be quite supportive for cultures of human hepatic progenitors albeit with very slow growth of the cells and with difficulties in retrieval of the cells[45]. Furthermore, methods of cell adaptation and mitochondrial energy supplementation implicate that levels of metabolites from aerobic metabolism of glucose are consuming available quantities rather than producing as seen in mature hepatocytes. Evidence has been presented in support of phenotyping via NMR of hepatic stem cell populations. Metabolites are indicative of the processes in these cells and the influence of special configuration (3-D) and chemical scaffolding. Metabolic functions related to reported metabolites (e.g. **Figure 5** and **Table 1**) have been

reported by others and are reflective of changes in diverse functions from cell viability to general homeostasis. Alanine and lactate are indicative of hypoxia[300], which can be due to cells being cultivated in 3-D as opposed to monolayer conditions. Others have reported that low oxygen concentrations in mammalian embryonic tissues are natural, and if true, is a plausible strategy for maintenance of the hHpSCs in 3-D culturing conditions and under low oxygen tensions[336, 422, 423] . Indeed, corroborative data in support of the strategy has been found in that hHpSCs have proven very tolerant of ischemia enabling their isolation from livers from asystolic donors for some hours following cardiac arrest[27, 86]; thus, low oxygen tension is a selective culture condition for the hHpSCs.

Mammalian cells in general act in response to a hypoxic environment by increasing their carbohydrate consumption and switching to anaerobic respiration[336, 424]. Properties such as metabolic activity change with passage, and even mitochondrial placement and have been linked to differentiation[334] For example, metabolic conversion from anaerobic pathways to aerobic mediates a change in condition recognized to indicate “stemness.” Glycolytic enzymes are presnt in the cytosol, and do not require mitochondria, and is associated with dedifferentiated cancer cells. Therefore, lactate is an end product of anaerobic glycolysis, and indicative of low oxygen availability or a relatively undifferentiated state[300] or consumption by specific cell types. Anaerobic utilization of glucose with low production of lactate has been reported within the hepatic culturing system. Gluconeogenic amino acids are alanine, threonine, tyrosine and phenylalanine[412]. Profiles for these can be constructed using the NMR phenotyping method.

Reduction of these could be indicative of that metabolic pathway. Specific stem cell populations such as those related to the hemopoetic system are able to survive in this state by using glycolytic pathways[336, 425]. Grayson etal. report that human mesenchymal stem cells have increased glucose consumption and lactate production under such conditions. Dependent on the type of cell, it may have the ability to survive under hypoxic conditions over extended periods of time, and stem cells may especially be able to do this as it is a reflection of there native microenvironment,[336] tolerance for ischemia,[86] and relatively undifferentiated state. Within the analyses of the data presented here, glucose consumption is high, and lactate production is high (**Figure 4**). Each of these metabolites are reduced over time, which can be explained also as a shift from one lineage stage (cellular subpopulation) to another during the culturing period. Transamination of pyruvate, which leads to increased amounts of alanine, occurs to help decrease systems of lactate. .

In addition, the pathways activated during the production of both, albumin and urea, are equally important in evaluating how the system is working. Liver is primary in the metabolism for the urea cycle producing biomarkers of arginine, glutamine, and urea[301]. Arginine is taken up from the system in order to produce urea[412]. As a direct player in production (**Figure 5 insert**), the log-log graph of arginine as compared to production of urea follows the same path. Furthermore, the impact of this pathway and the albumin production pathway is complicated where the production of glutamine from glutamate is concerned. Glutamate can be shuttled towards one pathway or another, and in the production of glutamine, it is

used as a cationic scavenger[412]. This is plausible for the graphic illustrated in **Figure 5b** in which glutamine and albumin follow opposing trends in production and consumption.

The work further lends itself to applications[426] and modification to bioreactors. The advancement of functional bioreactors allows tissue engineers to better mimic the multifaceted complexity of *in vivo* situations[47, 412, 427]. However, the short-comings of matching engineered constructs that are favorable for many applications call for either one of two design approaches. Many groups are working to create bioreactors with particularly useful features, i.e. dissolvable boundaries, see-through portals, etc. Other groups seek to create a unique platform of analysis in which the tools for studying the device overcome the limitations of the device. Here we have offered one such tool, which is a plausible alternative to years of bioreactor modifications. In addition we have offered new information on the human hepatic cell progenitors.

The vision of this work was to set forth a means of declaring if a particular set of cells, namely hHpSCs or any maturational lineage stage within the tissue, can be identified by metabolomic analyses alone. This application will be developed further for use in the fields of 3-Dimensional culture systems, especially the fields of bioartificial organs. The data base being established permits non-invasive assessment of a system by metabolomic analyses of the conditioned medium from the cultures, a data base that should prove ideal for rapid assessment of stem cells being lineage restricted to specific adult fates.

5.5 Methods

5.5.1 Sourcing of Human Fetal Livers

Liver tissue from human fetuses between 16-18 weeks gestational age was obtained from an accredited agency (Advanced Biological Resources, San Francisco, CA). The research protocol was reviewed and approved by the Institutional Review Board for Human Research Studies at the University of North Carolina at Chapel Hill.

5.5.2 Cell Isolation

Methods for processing human fetal liver tissues have been previously reported.[46, 212] In brief, the livers undergo partial digestion with an enzymatic buffer; [60 mg collagense (Sigma, catalog # C5138) plus 30 mg DNAse (Sigma, # DN-25) prepared in 100 ml of RPMI 1640 supplemented with 0.5 g of BSA (Sigma, # A8806-5G), selenium (10^{-8} M), antibiotics and antimycotics] to yield small clumps of tissue. The small cellular aggregates were then centrifuged at low speed spins (20 revolutionary centrifugal force) to separate hemopoietic cells (largely red blood cells) from parenchymal cells. The parenchymal cell clumps were then subjected to further mechanical and chemical digestion to yield single cell and small aggregate suspensions of one to four cells in most cases. The parenchymal cells were fully dispersed by filtration through a 75 μm nylon mesh (cat# 34-1800-02 PGC Scientific, Frederick Maryland). The process generated suspensions of single cell and small cell aggregates. The viability, determined by trypan blue exclusion assay, was greater

than 95% . In prior studies[27] we showed that freshly prepared suspensions of fetal liver cells are ~ 12% cells that are positive for epithelial cell adhesion molecule, EpCAM, a marker identifying hepatic stem cells, hepatoblasts, and unipotent parenchymal progenitors. The isolation protocol above strongly enriched for EpCAM+ parenchymal cells such that the suspensions were >80% hepatoblasts [EpCAM+, ICAM+, CK19+, albumin+, alpha-fetoprotein +) and ~ 10% hepatic stem cells [EpCAM+, NCAM+, CK19+, albumin ±, alpha-fetoprotein -). The remainder of the cell types in the suspension included small percentages (2-5%) angioblasts (VEGFr+, CD117+, CD133/1+], hepatic stellate cells [CD146, desmin, alpha-smooth muscle actin], and hemopoietic cells [CD45+, CD34+].

5.5.3 Cell Culture Medium

The suspensions of hHpSCs and hepatoblasts were suspended in a serum-free medium tailored for hepatic progenitors[43] , called “Kubota’s Medium” (KM), consisting of a serum-free basal medium (RPMI 1640, Gibco – Invitrogen, Carlesbad, CA) containing no copper, low calcium (< 0.5mM) and supplemented with insulin (5 μg/ml), transferrin/fe (5 μg/ml), high density lipoprotein (10 μg/ml), selenium (10^{-10} M), zinc (10^{-12} M) and 7.6uE of a mixture of free fatty acids bound to purified albumin; the detailed methods for its preparation have been published elsewhere[43, 428]. Following isolation, the hepatic progenitors were suspended in freshly prepared, serum-free KM. There was no use of fetal bovine serum (FBS), used at any point in culturing or processing of the tissue. The plating medium was

replaced every 24 hours with serum-free KM, and the cultures were maintained for greater than 4 weeks, with media changes every day.

5.5.4 Culture Plastic

Suspensions of human hepatic progenitors, enriched for hHpSCs and hepatoblasts, were seeded onto traditional polystyrene culture plastic with a 2.5% Fetal Bovine Serum (FBS) addition to KM medium. After 16 hours of incubation at 37°C with 5% CO_2, the medium was replaced with serum-free KM medium for the remainder of the study. Cells on plastic were cultured with media changes every day, the same as the rest of the cultures, until the end of the experiment. At the experiments end, the cells were lysed and collected for analyses with Trizol extraction buffer (Invitrogen, Carlsbad, CA).

5.5.5 Hyaluronan Hydrogels/Extracellular Matrix Complexes

The major components of the complexes were two forms of chemically-modified hyaluronan (HA)[429]. First, HA-DTPH is a chemically modified HA possessing multiple thiols for cross-linking with disulfide bridges[255] or with a bivalent electrophile[430] Second, Carbylan-S (or, CMHA-S) is a carboxymethlated HA derivative that has been further modified with multiple thiols for crosslinking.[431] The cross-linking was triggered by a PEGDA crosslinker, enabling the hydrogels to be formed in desired containers, to a variable but controllable level of cross-linking (affecting stiffness of the hydrogel), and permitting at the end of the

experiments for the hydrogels to be dissolved easily by reducing agents (e.g. dithiothreitol) together with hyaluronidase. The *in situ* crosslinkable hydrogel technology[432],[431],[433] has been extensively validated *in vivo* for tissue engineering and repair[434],[435],[436] and all materials are commercially available as Extracel™ from Glycosan Biosciences (Salt Lake City, Utah). We prepared complexes of HA-DTPG or of Carbylan-S with a collagen , type I collagen (Sigma, St. Louis, MO) and/or a basal adhesion molecule, laminin (Sigma, St. Louis, MO). There were 7 variations on the matrix substrata tested: 1) culture plastic (PL)—the controls, 2) Hyaluronan+collagen in a gelatin form (H + G), 3) Hyaluronan-Gelatin-Laminin (H+G+L), 4) Carbylan (C), 5) Carbylan+Laminin (C+L), 6) Carbylan+Gelatin (C+G), and 7) Carbylan+Gelatin+Laminin (C+G+L).

The hydrogel scaffolds or substrata were constructed as follows: dry reagents were dissolved in serum-free KM to give a 2.0% solution (weight/volume) for the HA and the Carbylan-S gels. The dry gelatin reagent was dissolved in the KM to yield a 3.0% (weight/volume) solution. The crosslinker (PEGDA) was dissolved in KM to give a 4.0% weight/volume solution. Re-suspension of the gel based components in solution was accomplished more readily by allowing them to incubate in a 37° C water bath for 15-60 minutes depending on the final volume of solution desired. All solutions used in preparing hydrogels were adjusted to a pH of 7.4 with 0.1N NaOH, after which they were ready to be mixed; they were stable as individual components for a few hours at room temperature. Exposure to air increases the crosslinking of any individual component. Therefore the solutions were kept under ceiled conditions avoiding air contact until ready for mixing with other matrix components.

The base ratios of crosslinker, medium (KM) and hyaluronan was based on a 1:1:3 ratio. Blending of hyaluronans with other matrix components could be achieved by varying the ratios of hyaluronans to matrix components. The hydrogels containing 90% HA and 10% Collagen/Gelatin were mixed at a ratio of 1:3:1 respectively to gelatin, Hyaluronan/Carbylan, and crosslinker, and the cell suspension was made in the pH adjusted mixtures. Addition of laminin was made prior to the addition of the crosslinker allowing it to diffuse throughout the hyaluronan/collagen complex. It was added at a concentration of 1.5 mg/ml (1.5 $\mu g/cm^2$). The final volume for each loading was 30 $\mu g/0.2\ cm^3$.

Sterilization of the Matrix/Hyaluronan Hydrogels

The starting materials from Glycosan are steriled at the time of production with a 2 micron filter and tested for bioburden. The use of special care for routine sterile procedures during set-up and seeding of cells was found to minimize the need for sterilization procedures. This simple strategy proved very successful such that no infectious organisms found in any culture. However, if sterilization is deemed necessary, then sterilization of the hydrogels can be done either in solution phase or in solid phase. If done while in solution (that is prior to cross-linking), it was filtered through a 0.45 mm syringe filter. Once cross-linked, the complex was sterilized by exposure to UV light. Theoretically it can be sterilized by40 Grey of radiation from a Cesium source.

Substrata of Matrix/Hyaluronan Hydrogels

The solutions of the hydrogel/matrix mixtures were placed into 6-well polystyrene culture dishes (Falcon – Beckton-Dickinson, Franklin Lakes, NJ) just after addition of the cross-linker and prior to gelation. After 16 hours initial incubation at 37°C in a CO_2 incubator (Forma Scientific, Baton Rouge, LA) to allow the gel to solidify, 1ml of serum-free KM was added to the top of each hydrogel. The hHpSCs and hepatoblasts were prepared as described above and were suspended in KM. The cells were placed onto or into the hydrogels at seeding densities of 1 million/hydrogel (volume 0.5 ml). If placed into the hydrogel/matrix complexes, cells are seeded prior to cross-linking; if cells are suspended within the hydrogel/matrix complex, the cells remain as small aggregates of cells throughout the hydrogel. Cells were cultured for 4 weeks under these same conditions, with changes of the medium every day.

5.5.6 Measurement of Albumin and Urea Production

The medium was collected from control (plastic) cultures and from the hydrogels every day for the duration of the culture period. Samples were labeled, frozen, and stored at -20°C until analyzed.

5.5.6.1 Albumin Production

Albumin production was measured by enzyme-linked immunosorbent assay (ELISA). Purified human albumin (Serologicals, Norcross, Georgia) was used as the standard, peroxidase-conjugated antibody (ICN Biomedicals/MP Biomedicals,

Irvine, CA) was used as the fluoroprobe against albumin and measured with a Spectromax 250 multi-well plate reader (Molecular Devices, Sunnyvale, CA).

5.5.6.2 Urea Production

Urea Production was analyzed using the urea nitrogen sensitivity assays, based on direct interaction of urea with diacetyl monoxime (Sigma, St. Louis, MO). Urea concentration was measured spectrophotometrically at 515 - 540 nm with a cytofluor Spectromax 250 multi-well plate reader.

5.5.7 Nuclear Magnetic Resonance Spectroscopy (NMR)

Sample Collection. Samples were taken in triplicate from each study condition and control on days 2, 8, and 12. Samples were stored at -80°C immediately following collection.

Sample Preparation. After thawing at room temperature, an aliquot of 540 µL of each sample was added to 5 mm MR tubes (Wilmad Lab-Glass Inc. Buena, NJ) along with 60 µL of a D_2O (Cambridge Isotope Laboratories, Andover, MA) solution containing 81.84 mM formate (Alfa Aesar, Ward Hill, MA) for ratiometric peak quantitization, 8.94 mM 3-(trimethylsily)propionic-2,2,3,3-d_4 acid sodium salt (TSP) (Aldrich, St. Louis, MO) for a chemical shift reference, and 0.2% NaN_3 (Sigma, St. Louis, MO) to inhibit bacterial growth.

^{1}H NMR Spectroscopy: All ^{1}H NMR spectra were obtained using a Varian INOVA 400 MHz NMR spectrometer (Varian Inc., Palo Alto, CA). A standard one pulse sequence with a 1.5 s H_2O presaturation was used with a interpulse delay of 4 s, acquisition time of 2.558 sec, a sweep width of 4650.08 Hz and the transmitter offset centered on the H_2O signal. The spectra were digitized with 24K points.

Spectral Processing. Processing of all NMR spectra was done in ACD/1D NMR Manager version 8.0 (Advanced Chemistry Development, Inc., Toronto). Exponential line broadening of 0.1Hz and zero filling to 32K points were applied to each spectrum. After Fourier transformation spectra were auto-phased and baseline corrected using uniform settings applied to all spectra. All spectra were referenced to the TSP peak at 0.00 ppm. Regions of the spectra associated with TSP (0.25 ppm and upfield), formate (8.23 – 8.51 ppm), and water (4.55 – 5.03 ppm) were excluded from the spectra for the purposes of spectral binning. The spectra were integrated using the Intelligent Bucketing method in the ACD software with bin sizes of 0.02 – 0.06 ppm. This resulted in 250 bins. Bin area values for each bin were then used as inputs into PCA.

Principal Component Analysis: Principal Component Analysis (PCA) was used to identify the effects of various substrates and times of incubation on the ^{1}H NMR spectra of the media. PCA was performed using standard procedures (Jolliffe, 2002). Each spectral bin was mean-centered and auto-scaled by subtracting its

mean and dividing by its standard deviation. The covariance matrix was computed using all spectrum samples from all three livers, seven substrates, and three days. The 250 eigenvectors of this covariance matrix were sorted in the descending order by their eigenvalues. These eigenvectors define the new dimensions, or *principal components*, of the 250-dimensional data space originally defined by the 250 spectral bins. Unlike the coordinate system defined by the values of individual bins, the new coordinate system – defined by the principal components – maximizes the data variance along the first principal components. For analysis, the data samples (represented in the data space by single points) are projected onto a two-dimensional plane defined by two among the first several principal components so as to reveal any groupings of samples with respect to substrate of incubation time.

Post PCA Spectral Binning Modifications: Full batch manual integrations were applied to the PCA identified regions of interest to allow for sufficient bin broadening to fully capture integral values that may have been diminished due to the upper bin limit of 0.06 ppm. Care was taken to ensure that resonances adjacent to bins of interest were not captured in this process.

Spectral Assignments: Spectral assignments were made by reference to literature values of chemical shifts in various media and biological fluids.

5.5.8 Statistical Analyses

For each metabolite, a mixed model was fit with metabolite as the response. Time (2, 8 and 12 days) and scaffold: plastic (PL), Carbylan (C), Carbylan/Laminin (C+L), Carbylan/Gelatin (C+G), Carbylan/Gelatin/Laminin (C+G+L), Hyaluronan/Gelatin (H), and Hyaluronan/Gelatin/Laminin (H+L). Fixed time points were used for assessing substrata effects, so that data for different matrices were compared at the same time point. Major variables that were impossible to control in the samples were the distinctions in the human livers from one donor to another. Those variations were managed in the statistical analyses as a random effect. Five hundred and sixty pairwise comparisons were made between scaffolds all falling in the classes of (C v CL; C v GC; C v Plastic; CL v GCL; GC v H; GCL v HL; GCL v Pla; H v HL; H v Plastic; HL v Plastic) for each of the samples for three times as well as for overall comparisons for all times combined. Since ten comparisons were being made for each time point, a Bonferroni correction was done to account for multiple comparisons and consequently only those p-values less than 0.05 / 10 = 0.005 were considered statistically significant.

Model

The Statistical Model [$Y_{ijkl} = \dot{\alpha} + \beta_i + \gamma_j + \lambda_k + \Delta_{i \cdot j} + \varepsilon_{ijkl}$] can be expressed as the equation shown where alpha ($\dot{\alpha}$) is the overall mean response of the metabolite. Beta (β) is a fixed substrate effect and the subscript (i) indicates the seven substrates numbered from 1 to 7. Gamma (γ) is a fixed effect of time and is denoted by the subscript j which is numbered from 1 to 3, and indicates the day

where 1 is day 2, j = 2 is day 8, and j = 3 is day 12. Lambda (λ) is the random effect of liver, which is interpreted by recognition that all livers in the study are considered to be random samples of all possible livers. The subscript k, which is labeled from 1 to 3 indicates which of the three livers in the study is being used. Delta (Δ) is the interaction effect of substrate and day and consequently has the subscripts i and j. Epsilon (ε) is the random error associated with the l^{th} repetition of any set of substrate, day, and liver. The subscript l also registers from 1 to 3 to indicate the repetition.

Acknowledgements: We'd like to thank Dr. Justyna Wolak for discussion and construction of the metabolic pathway diagram in this paper. Funding for the studies was by a Sponsored Research Agreement (SRA) from Vesta Therapeutics, by NIH grants (DK52851, AA014243, IP30-DK065933, P30-DK034987, GM075941-01, CA114365-01A1), by a DOE Grant (DE-FG02-02ER-63477) and by a Centers of Excellence Award (Utah). Glycosan BioSystems provided the CMHA.

Abbreviations:

KM = Hiroshi Kubota's Medium, a serum-free, hormonally defined medium for progenitors

NMR = Nuclear Magnetic Resonance

1H = Proton

CMHA = Chemically-Modified Hyaluronan

TSP = 3-(trimethylsily)propionic-2,2,3,3-d_4 acid sodium salt

PCA = Principle Component Analysis

PC1 = Principle Component 1

PC2 = Principle Component 2

TCA = Tricarboxylic acid cycle (aka citric acid cycle)

GAG = Glycosaminoglycan

HA = Hyaluronan

FBS = Fetal Bovine Serum

PBS = Phosphate Buffered Solution

RT = Room Temperature

ECM = Extracellular Matrix

5.5.9 Figure Legends

Figure 1. 1H NMR spectra

Spectra and peak identification of culture media obtained at 9.4T. Metabolite assignments are shown in the upper left corner and correspond to the numbered spectra peaks. Chemical Shift (ppm) is shown at the bottom from 0 to 9 from left to right. Sized bins are immediately above and parallel to the horizontal Chemical Shift axis except in dark regions. Dark regions fall in ppm regions of less than 0.02, 4.06 to 5.02, and 8.24 to 8.48 eliminating peaks for TSP, water and formate respectively. Many of the significant metabolites fall within the boxed region from 0.84 to 4.46, and this area is expanded for better visualization.

Figure 2. Scores plots from PCA of all 187 samples of ^{1}H NMR spectra. Each point represents an individual supernatant sample, color-coded according to its incubation age. **A:** shown are all 187 samples. **B:** shown are 124 samples originated from livers 1 and 2. **C:** shown are 63 samples originated from liver 3. Note that samples in C are less dispersed than in B and they are also shifted overall relative to samples in B. Despite these differences, B and C show the same trend of day 12 samples being partially shifted relative to day 8 samples, which in turn are shifted relative to day 2 samples.

Figure 3. An average scores plot. Each point represents the average position of all samples of a given day and a given treatment. Points representing successive days of the same treatment are connected by lines. Note similar upward-left paths taken by all the differently treated groups of samples.

Figure 4. Principal component loadings plot. Loadings are shown for the same principal components PC1 and PC2 used to construct scores plots in Figures 2 and 3. Each point represents one of the 250 spectral bins. Note that the bins most responsible for the upward-left shift of samples in the scores plots are located in the upper-left and bottom-right corners of the loadings plot. Some of those bins are identified by the metabolites they represent.

Figure 5a-f. Formate Normalize Metabolites of glucose, alanine, lactate, arginine glutamine, and glutamate are shown as they vary with time with respect to each substratum. The substrata are listed along the horizontal axis: Carbylan (C), Carbylan/Laminin (C+L), Carbylan/Gelatin (C+G), Carbylan/Gelatin/Laminin (C+G+L), Hyaluronan/Gelatin (H), Hyaluronan/Gelatin/ Laminin (H+G+L), Plastic (PL). Normal amounts of metabolites found within fresh KM media are reported as baseline (Controls). Days are demarcated as individual colors with every 3 bar sets forming the pattern of Day 2 on the left, Day 8 in the middle and Day 12 on the right. Y axis is representative of the percent of metabolite normalized to the formate control.

Figure 6 (Insert)

Metabolomic Pathways represented schematically within a normal cell. The block diagram denotes principle component identified metabolites. Glucose consumption produces pyruvate which in turn produces Alanine and Lactate as well as Acetyl-CoA. Acetyl-CoA is shunted into the TCA cycle which is tied to key metabolites of alpha-ketogluterate and oxaloacetate. Alpha-ketogluterate is tied to production of glutamine and albumin through the common pathway divergent at glutamate. Metabolites of the TCA cycle act on aspartate and affect the urea cycle, tying Arginine consumption to urea production.

Figure 6a. Urea production as compared to arginine. The normalized data to formate for the concentration of arginine in the system has been averaged over the substrates. KM media contains a base amount of Arginine of 200mg/L which correlates to an extracted value of .0066 concentration. From Day 2 (.058988 percent Formate / 178.7516 mg/dl concentration) through Day 12 (.010146 percent Formate / 30.74449 mg/dl concentration) there is production of arginine in the system however the net time effect in the system is a loss of production of arginine

Figure 6b. Albumin production is represented graphically with the graph representation of glutamine and glutamate. As diagrammed in figure 6, both

of these can effect the production of the albumin. Glutamine is consumed by the culture system, where the cells on day 2 consume almost all of the glutamine in the KM media. By days 8 and 12 the consumption has subsided to just over half of the available glutamine in the media. Glutamate, production still occurs throughout the longevity of the culture, but decreases as the cultures age. Albumin production drops also with time.

Table 1. Model Derived Significant Data for Metabolites based on Substratum. This table is the summation of the significance of effects for Carbylan versus Plastic in each metabolite as a factor or overall effect, day 2 effect, day 8 effect and day 12 effect. A single 'X' represents a significant value where the p-value is 0.05 or less, and the double 'XX' represents a significant value where the p-value is less that 0.01. Because multiple peaks of the same metabolite can be discerned, there are multiples of some metabolites, which include Lactate, Glutamate, and Glucose. It should be noted that not all metabolites are included. In the Supplement Table 1 are NMR data on other metabolites not presented here. Their data are part of the total summation analysis.

Supplement Table 1. Metabolites Footprint for the different substrata as compared to formate. The metabolites as identified by the PCA data are labeled across the top of the table (in three repeated sections) and are made up of lactate, alanine, acetoacetate, glutamine, choline, glucose, arginine and glutamate. The vertical axis of the table is labeled as Treatments and consists of the 7 substrata

(Hyaluronan/Collagen I; Hyalurnona/Collagen I/Laminin; Carbylan; Carbylan/Collagen I; Carbylan/Laminin; Carbylan/Collagen I/Laminin, Plastic, and KM Media). With the exception of the data KM, each block is represented by three values +/- a standard error. The value is the mean percentage formate of that metabolite as identified by NMR. The sequence of values is given in order by day, corresponding to the measurements at days 2, 8, and 12. Values for pyruvate, glycine, and valine were not calculated as to the end relationship of other metabolites in the pathways described by **Figure 6.**

Tables:

Table 1:

Carbylan (HA – disulfide cross-linkage) vs Plastic Culturning Conditions				
Metabolite	Overall Effect	Day 2	Day 8	Day 12
Arginine		XX		
Choline	XX			XX
Ethanol				XX
Lactate/Threonine	XX	XX	XX	
Alanine	XX	XX	XX	X
Lactate	XX	XX	XX	
Glucose-alpha	X			XX
Glutamate-2				X
Gluatmate-3				XX
Glucose-2	X			XX
Gluatmine				X
P values	X < .05		XX < .01	

Table 2: Supplemental (On line, not submitted)

6 CHAPTER VI. Summary Discussion

Establishment of normal human liver tissue *ex vivo* from hepatic stem cells (hHpSCs) and their progeny is the strategy being pursued by the Reid lab and a strategy in which I have been a participant. The several years of work have enabled the identification and isolation of purified hHpSCS and their expansion *ex vivo*. The goals now are to convert to differentiation studies in which the purified hHpSCs are lineage restricted and differentiated into fully mature parenchymal cells. Towards these goals, three-dimensional (3-D) culture systems are requisite. Hyaluronans, a natural component of stem cell niches throughout the body, have been explored as a base scaffold for *ex vivo* maintenance of human hepatic stem cells and hepatoblasts in a 3-D format.

The hyaluronan hydrogel from Glycosan Biosciences, based upon technologies established by Glenn Prestwich and associates[255, 429-436] proved the best form of hyaluronans tested to date, offering many attributes that include non-immunogenicity, incorporation of other matrix molecules of relevance to liver tissue engineering such as collagen I or heparins and, most importantly, the stabilization by disulfide cross-linking enabling one to disperse the hydrogel readily and safely. The hydrogel chemistry established by Prestwich and associates is well defined and involves only purified components. Hyaluronan hydrogels offer distinct advantages over other 3-D matrices such as tissue extracts with many contaminants, such as

Matrigel [437]; the tissue extracts may work for experimental purposes but cannot be envisaged as a scaffold for clinical programs. The same issue applies to synthetic 3-D scaffolds such as microspun fibers[438] and hydroxyapetite[439] that can be used only for *ex vivo* experimental applications. They are even an advantage over the popular polylactide scaffolds[440], since they can be tailored in their chemistry for precise responses known for specific maturational lineage stages of cells by making mixtures of matrix molecules and soluble signals found *in vivo* in association with the specific lineage stage.

The use of the hyaluronan hydrogels was successful in combination with serum-free media meaning that defined mixtures of soluble signals can be used together with the defined hyaluronan hydrogel scaffold to yield a 3-D culture system in which all components are known. This may prove one of the most important outcomes of the dissertation work, given that serum, a biological fluid found only in wounds, and one that can drive cells towards undesired fates (e.g. fibrotic responses). By having a serum-free system, there is elimination of concerns that residual serum components might affect andy enzymatic or chemical digestion of the hydrogels. The methods for recovery of the cells from the hyaluronan hydrogel stabilized by dithiol chemistry were developed in my studies and complement those found previously by others.

Characterization of the hepatic progenitors was accomplished by means of immunochemistry for protein expression, rt-PCR for messenger RNAs, and metabolomics. Expression under all means of analyses led to the same conclusions

that the cells embedded in the hydrogel were proliferating and maintaining a state that was closely related to that of hHpSCs or their immediate progeny, hepatoblasts.

The use of metabolomics to evaluate stem cell lineage systems is essentially in its infancy. The application of NMR to the hepatic lineage system to evaluate the effects of matrix chemistry perturbations is the first known to have been done. Finally, the specific aim of application of hydrogels as a scaffold to a bioreactor were accomplished in pilot studies. This being a long range goal for the expansion of many cells types intended to be used in cell therapies. It is the logical first step for application of the findings from my studies.

Future directions

The use of the hydrogels will be expanded in future studies and include exploration of many different combinations of matrix components and soluble signals. Studies in which different combinations of matrix and soluble signals should lead to knowledge of how to design the 3-D scaffolds in order to elicit desired behaviors and responses by the cells. For example, will combinations of type III collagen and the hydrogel along with Kubota's Medium enable the cells to expand 3-dimensionally with the speed found when they are plated onto monolayers of type III collagen.

Usage of the hydrogels in more sophisticated bioartificial devices are logical next steps for the tissue engineering programs. Those devices are designed to support solid tissue by using perfusion for mass transport of nutrients and oxygen.

Thus, the microenvironment is being designed to combine the requisite extracellular matrix components, hormones and paracrine signals with highly regulated supply of nutrients and gases, all essential variables needed for tissue engineering. The ease of recovery of cells from the hydrogels, allows investigators to do the customary cellular and molecular analyses on the cells at any stage of the experiment.

Exploration of the cell-hydrogel interactions needs to be further explored. The responses of the cells in hydrogels with different forms of crosslinking used in stabilizing the gels showed that there is a significant difference between those gels that possess one site for linkage per disaccharide unit (Extracell) as opposed to those that have two sites per unit (Carbylan). Possible methods for analyzing this include the use of Atomic Force Microscopy analysis of cells cultured on or in hydrogels versus other surfaces. From an engineering perspective, the AFM can define the stiffness of a specific substrate.

Metabolomics should provide a wealth of information especially with such a novel and unexplored model system as maturational lineage stages of human liver. My initial foray into such a project has proven that it is a feasible approach for explorations of stem cells and their progeny. Such applications of known analytical technologies to biological systems are some of the advantages of using NMR. Alternate technologies (e.g. gas chromatography-mass spectrometry, liquid chromatography-mass spectrometry) can complement the findings reported here

and offer results that will help to fully characterize the stem cells and each lineage stage of their descendents.

7 Chapter VII: References

1. Lemaigre, F. and K.S. Zaret, *Liver development update: new embryo models, cell lineage control, and morphogenesis.* Curr Opin Genet Dev, 2004. **14**(5): p. 582-90.

2. Gittes, G.K., et al., *Lineage-specific morphogenesis in the developing pancreas: role of mesenchymal factors.* Development, 1996. **122**(2): p. 439-47.

3. Reid, L.M. and D.M. Jefferson, *Culturing hepatocytes and other differentiated cells.* Hepatology, 1984. **4**(3): p. 548-59.

4. Young, H.E., et al., *Mesenchymal stem cells reside within the connective tissues of many organs.* Developmental Dynamics, 1995. **202**(2): p. 137-44.

5. Reid, L.M., et al., *Extracellular matrix gradients in the space of Disse: relevance to liver biology.* Hepatology, 1992. **15**(6): p. 1198-203.

6. Brill, S., et al., *Extracellular matrix regulation of growth and gene expression in liver cell lineages and hepatomas*, in *Liver Biology and Pathobiology*, I.M. Arias, et al., Editors. 1994, Raven Press: New York. p. 869-897.

7. Furthmayr, H., *Basement membrane collagen: structure, assembly, and biosynthesis*, in *Extracellular Matrix: Chemistry, Biology, and Pathobiology with Emphasis on the Liver*, M. Zern and L.M. Reid, Editors. 1993, Marcel Dekker: New York. p. 149-185.

8. Nimni, M.E., *Fibrillar collagens: their biosynthesis, molecular structure, and mode of assembly*, in *Extracellular Matrix: Chemistry, Biology, and Pathobiology with Emphasis on the Liver*, M. Zern and L.M. Reid, Editors. 1993, Marcel Dekker: New York. p. 121-148.

9. Martinez-Hernandez, A. and P.S. Amenta, *The extracellular matrix in hepatic regeneration.* FASEB Journal, 1995. **9**(14): p. 1401-10.

10. Martinez-Hernandez, A. and P.S. Amenta, *The hepatic extracellular matrix. I. Components and distribution in normal liver [editorial].* Virchows Archiv - A, Pathological Anatomy & Histopathology, 1993. **423**(1): p. 1-11.

11. Terada, T., et al., *Expression of epithelial-cadherin, alpha-catenin and beta-catenin during human intrahepatic bile duct development: a possible role in bile duct morphogenesis.* J Hepatol, 1998. **28**(2): p. 263-9.

12. Stamatoglou, S.C. and R.C. Hughes, *Cell adhesion molecules in liver function and pattern formation.* FASEB Journal, 1994. **8**(6): p. 420-7.

13. Kallunki, P. and K. Tryggvason, *Human basement membrane heparan sulfate proteoglycan core protein: a 467-kD protein containing multiple domains resembling elements of the low density lipoprotein receptor, laminin, neural cell adhesion molecules, and epidermal growth factor.* Journal of Cell Biology, 1992. **116**(2): p. 559-71.

14. Bernfield, M., et al., *Biology of the syndecans: a family of transmembrane heparan sulfate proteoglycans.* Annual Review of Cell Biology, 1992. **8**: p. 365-93.

15. LeCluyse, E.L., P.L. Bullock, and A. Parkinson, *Strategies for restoration and maintenance of normal hepatic structure and function in long-term cultures of rat hepatocytes. Adv. Drug. Del. Rev*, 1996. **22**: p. 133-186.

16. Bhatia, S., M. Yarmush, and M. Toner, *Controlling cell interactions by micropatterning in co-cultures: Hepatocytes and 3T3 fibroblasts.* Journal of Biomedical Materials Research, 1996. **32**: p. 1-11.

17. Liu, Z. and T.M. Chang, *Effects of bone marrow cells on hepatocytes: when co-cultured or co-encapsulated together.* Artif Cells Blood Substit Immobil Biotechnol, 2000. **28**(4): p. 365-74.

18. Jefferson, D.M., et al., *Posttranscriptional modulation of gene expression in cultured rat hepatocytes.* Molecular & Cellular Biology, 1984. **4**(9): p. 1929-34.

19. Tillotson, L.G., et al., *Isolation, maintenance, and characterization of human pancreatic islet tumor cells expressing vasoactive intestinal peptide.* Pancreas, 2001. **22**(1): p. 91-98.

20. Xu, A., et al., *Liver stem cells and lineage biology*, in *Principles of Tissue Engineering*, R. Lanza, R. Langer, and J. Vacanti, Editors. 2000, Academic Press: San Diego.

21. Sigal, S., et al., *The liver as a stem cell and lineage system*, in *Extracellular Matrix: Chemistry, Biology, and Pathobiology with Emphasis on the Liver*, M.A. Zern and L.M. Reid, Editors. 1993, Marcel Dekker, Inc.: New York. p. 507-538.

22. Schmelzer, E., et al., *Hepatic Stem Cells*, in *Tissue Stem Cells*, C.S. Potten, et al., Editors. 2006, Taylor and Rancis Group: New York. p. 161-214.

23. Cheng, N., H. Yao, and L. Reid, *Pluripotent Hepatic Stem cells and Maturational lineage biology*in *Principles in Tissue Engineering and Regenerative Medicine*, A. Attala, Editor. 2007, Elsevier: San Diego, California. p. In Press.

24. Jung, J., et al., *Initiation of mammalian liver development from endoderm by fibroblast growth factors.* Science, 1999. **284**: p. 1998-2003.

25. Yao, H., et al., *Matrix paracrine signaling defining self-replication, lineage restriction and differentiation of human hepatic stem cells.* Journal of Biological Chemistry, 2007. **Submitted**.

26. Kubota, H., H. Yao, and L.M. Reid, *Identification and characterization of vitamin A-storing cells in fetal liver.* Stem Cells, 2007: p. In press.

27. Schmelzer, E., et al., *Human hepatc stem cells from fetal and postnatal donors.* Journal of Experimental Medicine, 2007. **(in press)**.

28. Sicklick, J.K., et al., *Hedgehog signaling maintains resident hepatic progenitors throughout life.* Am J Physiol Gastrointest Liver Physiol., 2006. **290**(5): p. G859-70. Epub 2005 Dec 1.

29. McClelland, R., et al., *Tissue Engineering*, in *Biomedical Engineering*, Editor. 2004: New York.

30. Yang, L., R.A. Faris, and D.C. Hixson, *Phenotypic heterogeneity within clonogenic ductal cell populations isolated from normal adult rat liver.* Proceedings of the Societyof Experimental Biological Medicine, 1993. **204**(3): p. 280-288.

31. Stamp, L., et al., *A novel cell-surface marker found on human embryonic hepatoblasts and a subpopulation of hepatic biliary epithelial cells.* Stem Cells, 2005. **23**(1): p. 103-12.

32. Zhou, H., et al., *Identification of hepatocytic anad bile ductular cell lineages and candidate stem cells in bipolar ductualr reactions in cirrhotic human liver.* Hepatology, 2007. **45**: p. 716-724.

33. Dutton, J.R., et al., *Beta cells occur naturally in extrahepatic bile ducts of mice.* Journal of Cell Science, 2007. **120**: p. 239-245.

34. Temple, S. and A. Alvarez-Buylla, *Stem cells in the adult mammalian central nervous system.* Current Opinion in Neurobiology, 1999. **9**(1): p. 135-41.

35. Fuchs, E. and S. Raghavan, *Getting under the skin of epidermal morphogenesis.* Nature Reviews/Genetics, 2002. **3**: p. 199-209.

36. Fuchs, E. and C. Byrne, *The epidermis: rising to the surface.* Current Opinion in Genetics & Development, 1994. **4**(5): p. 725-36.

37. Reid, L.M., *Stem cell biology, hormone/matrix synergies and liver differentiation.* Current Opinion in Cell Biology, 1990. **2**(1): p. 121-30.

38. Sigal, S.H., et al., *The liver as a stem cell and lineage system.* Am J Physiol, 1992. **263**(2 Pt 1): p. G139-48.

39. Sigal, S.H., et al., *Evidence for a terminal differentiation process in the rat liver.* Differentiation, 1995. **59**(1): p. 35-42.

40. Macdonald, J.M., et al., *Liver cell culture and lineage biology*, in *Methods of Tissue Engineering*, A. Atala and R.P. Lanza, Editors. 2002, Academic Press: London. p. 151-202.

41. Sigal, S.H., et al., *Characterization and enrichment of fetal rat hepatoblasts by immunoadsorption ("panning") and fluorescence-activated cell sorting.* Hepatology, 1994. **19**(4): p. 999-1006.

42. Sigal, S.H., et al., *Partial hepatectomy-induced polyploidy attenuates hepatocyte replication and activates cell aging events.* American Journal of Physiology, 1999. **276**(39): p. G1260-G1272.

43. Kubota, H. and L.M. Reid, *Clonogenic Hepatoblasts, Common Precursors for Hepatocytic and Biliary Lineages, Are Lacking Classical Major Histocompatibility Complex Class I Antigen.* Proceedings of the National Acadmey of Sciences of the United States of America, 2000. **97**(22): p. 12132-12137.

44. LaGasse, E., *Isolation of human hepatic progenitors*. 2007, Stem Cells, Inc.: U.S.A.

45. Turner, W.S., et al., *Human hepatoblast phenotype maintained by hyaluronan hydrogels.* J Biomed Mater Res B Appl Biomater, 2006. **82B**(1): p. 156-168.

46. Schmelzer, E., E. Wauthier, and L.M. Reid, *The Phenotypes of Pluripotent Human Hepatic Progenitors.* Stem Cells, 2006. **20**: p. 20.

47. McClelland, R.E., et al., *Type III collagen substratum permissive for self-replication ex vivo of Human Hepatic Stem Cells.* Cell-Stem Cell, 2007. **Submitted**.

48. Potten, C.S., et al., eds. *Tissue Stem Cells*. 2006, Taylor and Francis: New York.

49. Chen, U., *Careful maintenance of undifferentiated mouse embryonic stem cells is necessary for their capacity to differentiate to hematopoietic lineages in vitro.* Current Topics in Microbiology & Immunology, 1992. **177**: p. 3-12.

50. Westgren, M., et al., *Establishment of a tissue bank for fetal stem cell transplantation.* Acta Obstetricia et Gynecologica Scandinavica, 1994. **73**(5): p. 385-8.

51. Ek, S., et al., *Cryopreservation of fetal stem cells.* Bone Marrow Transplantation, 1993. **11**(Suppl 1): p. 123.

52. Deans, R.J. and A.B. Moseley, *Mesenchymal stem cells: biology and potential uses.* Experimental Hematology, 2000. **28**(8): p. 875-884.

53. Gage, F.H., *Neuronal stem cells: their characterization and utilization.* Neurobiology of Aging, 1994. **15 (supplement 2)**: p. S191.

54. Maltsev, V.A., et al., *Embryonic stem cells differentiate in vitro into cardiomyocytes representing sinusnodal, atrial and ventricular cell types.* Mechanisms of Development, 1993. **44**(1): p. 41-50.

55. Resnick, J.L., et al., *Long-term proliferation of mouse primordial germ cells in culture [see comments].* Nature, 1992. **359**(6395): p. 550-1.

56. Cowan, C.A., et al., *Derivation of embryonic stem-cell lines from human blastocysts.* N Engl J Med, 2004. **350**(13): p. 1353-6.

57. Levenberg, S., A. Khademhosseini, and R. Langer, *Embryonic Stem Cells in Tissue Engineering*, in *Handbook of Stem Cells*, R. Lanza, et al., Editors. 2004, Elsevier: New York. p. 737-746.

58. Guyomard, C., et al., *Influence of alginate gel entrapment and cryopreservation on survival and xenobiotic metabolism capacity of rat hepatocytes.* Toxicology & Applied Pharmacology, 1996. **141**(2): p. 349-56.

59. Koebe, H.G., et al., *Cryopreservation of porcine hepatocyte cultures.* Cryobiology, 1996. **33**(1): p. 127-41.

60. Koebe, H.G., et al., *A new approach to the cryopreservation of hepatocytes in a sandwich culture configuration.* Cryobiology, 1990. **27**(5): p. 576-84.

61. Watts, P. and M.H. Grant, *Cryopreservation of rat hepatocyte monolayer cultures.* Human and Experimental Toxicology, 1996. **15**: p. 30-37.

62. Mitaka, T., et al., *Growth and maturation of small hepatocytes. [Review] [44 refs].* Journal of Gastroenterology & Hepatology, 1998. **13**(7): p. S70-7.

63. Mitaka, T., et al., *Small cell colonies appear in the primary culture of adult rat hepatocytes in the presence of nicotinamide and epidermal growth factor.* Hepatology, 1992. **16**(2): p. 440-7.

64. Ogawa, K., et al., *The generation of functionally differentiated, three-dimensional hepatic tissue from two-dimensional sheets of progenitor small hepatocytes and nonparenchymal cells.* Transplantation, 2004. **77**(12): p. 1783-9.

65. Hamilton, G.A., et al., *Regulation of cell morphology and cytochrome P450 Expression in human hepatocytes by ext4racellular matrix and cell-cell interactions.* Cell and Tissue Research, 2001. **306**: p. 85-99.

66. Beardsley, T., *Stem cells come of age [news].* Scientific American, 1999. **281**(1): p. 30-1.

67. Brinster, R.L., *The effect of cells transferred into the mouse blastocyst on subsequent development.* J Exp Med, 1974. **140**(4): p. 1049-56.

68. Schuldiner, M., et al., *Effects of eight growth factors on the differentiation of cells derived from human embryonic stem cells.* Proceedings of the National Academy of Science, U.S.A., 2000. **97**(21): p. 11307-11312.

69. Martin, G.R., *Isolation of a pluripotent cell line from early mouse embryos cultured in medium conditioned by teratocarcinoma stem cells.* Proc Natl Acad Sci U S A, 1981. **78**(12): p. 7634-8.

70. Mendiola, M.M., et al., *Research with human embryonic stem cells: ethical considerations.* Hastings Center Report, 1999. **29**(2): p. 31-36.

71. Nozaki, T., et al., *Syncytiotrophoblastic giant cells in teratocarcinoma-like tumors derived from Parp-disrupted mouse embryonic stem cells.*

Proceedings of the National Academy of Sciences of the United States of America, 1999. **96**(23): p. 13345-50.

72. Pedersen, R.A., *Embryonic stem cells for medicine.* Scientific American, 1999. **280**(4): p. 68-73.

73. Susick, R., et al., *Hepatic progenitors and strategies for liver cell therapies.* Ann N Y Acad Sci, 2001. **944**: p. 398-419.

74. Gluckman, E., et al., *Hematopoietic reconstitution in a patient with Fanconi's anemia by means of umbilical cord blood from an HLA-identical sibling.* New England Journal of Medicine, 1989. **321**(17): p. 1174-1178.

75. Rubinstein, P., et al., *Stored placental blood for unrelated bone marrow reconstitution.* Blood, 1993. **81**(7): p. 1679-1690.

76. Bruder, S.P., D.J. Fink, and A.I. Caplan, *Mesenchymal stem cells in bone development, bone repair, and skeletal regeneration therapy.* Journal of Cellular Biochemistry, 1994. **56**(3): p. 283-94.

77. Caplan, A.I., *The mesengenic process.* Clinics in Plastic Surgery, 1994. **21**(3): p. 429-35.

78. Cattaneo, E. and R. McKay, *Identifying and manipulating neuronal stem cells.* Trends in Neurosciences, 1991. **14**(8): p. 338-340.

79. Reinholt, F.P., et al., *Survival of fetal porcine pancreatic islet tissue transplanted to a diabetic patient.* Xenotransplantation, 1998. **5**(3): p. 222-225.

80. Shumakov, V.I., et al., *Transplantation of cultures of human fetal pancreatic islet cells to diabetes mellitus patients.* Klinicheskaia Meditsina, 1983. **61**(2): p. 46-51.

81. Xu, R.H., et al., *BMP4 initiates human embryonic stem cell differentiation to trophoblast.* Nat Biotechnol, 2002. **20**(12): p. 1261-4.

82. Smith, A.G., et al., *Inhibition of pluripotential embryonic stem cell differentiation by purified polypeptides.* Nature, 1988. **336**(6200): p. 688-90.

83. O'Shea, K.S., *Embryonic stem cell models of development.* Anat Rec, 1999. **257**(1): p. 32-41.

84. Mitaka, T., et al., *Growth and maturation of small hepatocytes isolated from adult rat liver.* Biochemical & Biophysical Research Communications, 1995. **214**(2): p. 310-7.

85. Mitaka, T., et al., *Effects of mitogens and co-mitogens on the formation of small-cell colonies in primary cultures of rat hepatocytes.* Journal of Cellular Physiology, 1993. **157**(3): p. 461-8.

86. Reid, L.M., E. LeCluyse, and H. Kubota, *Liver tissue source (patent).* U.S. Patent, 2000. **Application # 113918**(Date of Application: January 23, 2000).

87. Gerlyng, P., et al., *Binucleation and polyploidization patterns in developmental an regenerative rat liver growth.* Cell Proliferation, 1993. **26**(6): p. 557-65.

88. Mossin, L., et al., *Ploidy-dependent growth and binucleation in cultured rat hepatocytes.* Experimental Cell Research, 1994. **214**(2): p. 551-60.

89. Saeter, G., et al., *Changes in ploidy distributions in human liver carcinogenesis.* Journal of the National Cancer Institute, 1988. **80**(18): p. 1480-5.

90. Seglen, P.O., P.E. Schwarze, and G. Saeter, *Changes in cellular ploidy and autophagic responsiveness during rat liver carcinogenesis.* Toxicologic Pathology, 1986. **14**(3): p. 342-8.

91. Liu, H., et al., *Citron kinase is a cell cycle-dependent, nuclear protein required for G2/M transition of hepatocytes.* J Biol Chem, 2003. **278**(4): p. 2541-8.

92. Higgins, P.J., et al., *Characterization and cell cycle kinetics of hepatocyte populations isolated from adult liver tissue by a nonenzymatic procedure.* Journal of Histochemistry & Cytochemistry, 1985. **33**(7): p. 672-6.

93. Severin, E., E.M. Meier, and R. Willers, *Flow cytometric analysis of mouse hepatocyte ploidy. I. Preparative and mathematical protocol.* Cell & Tissue Research, 1984. **238**(3): p. 643-7.

94. Anatskaya, O.V., A.E. Vinogradov, and B.N. Kudryavtsev, *Hepatocyte polyploidy and metabolism/life-history traits: hypotheses testing.* Journal of Theoretical Biology, 1994. **168**(2): p. 191-9.

95. Brodsky, W.Y., A.M. Arefyeva, and I.V. Uryvaeva, *Mitotic polyploidization of mouse heart myocytes during the first postnatal week.* Cell & Tissue Research, 1980. **210**(1): p. 133-44.

96. Carriere, R., *Polyploid cell reproduction in normal adult rat liver.* Exp Cell Res, 1967. **46**(3): p. 533-40.

97. Anti, M., et al., *DNA ploidy pattern in human chronic liver diseases and hepatic nodular lesions. Flow cytometric analysis on echo-guided needle liver biopsy.* Cancer, 1994. **73**(2): p. 281-8.

98. Kudryavtsev, B.N., et al., *Human hepatocyte polyploidization kinetics in the course of life cycle.* Virchows Archiv. B, Cell Pathology Including Molecular Pathology, 1993. **64**(6): p. 387-93.

99. Watanabe, T. and Y. Tanaka, *Age-related alterations in the size of human hepatocytes. A study of mononuclear and binucleate cells.* Virchows Archiv. B, Cell Pathology Including Molecular Pathology, 1982. **39**(1): p. 9-20.

100. Gumucio, J.J., ed. *Hepatocyte heterogeneity and liver function*. Vol. 19. 1989, Springer International: Madrid.

101. Traber, P.G., J. Chianale, and J.J. Gumucio, *Physiologic significance and regulation of hepatocellular heterogeneity [see comments].* Gastroenterology, 1988. **95**(4): p. 1130-43.

102. Gaasbeek Janzen, J.W., et al., *Heterogeneous distribution of glutamine synthetase during rat liver development.* J Histochem Cytochem, 1987. **35**(1): p. 49-54.

103. Burger, H.J., et al., *Different capacities for amino acid transport in periportal and perivenous hepatocytes isolated by digitonin/collagenase perfusion.* Hepatology, 1989. **9**(1): p. 22-8.

104. Stein, G.I. and B.N. Kudryavtsev, *A method for investigating hepatocyte polyploidization kinetics during postnatal development in mammals.* Journal of Theoretical Biology, 1992. **156**(3): p. 349-63.

105. Tateno, C. and K. Yoshizato, *Growth potential and differentiation capacity of adult rat hepatocytes in vitro.* Wound Repair Regeneration, 1999. **7**(1): p. 36-44.

106. Gebhardt, R., *Different proliferative activity in vitro of periportal and perivenous hepatocytes.* Scandinavian Journal of Gastroenterology - Supplement, 1988. **151**: p. 8-18.

107. Overturf K, A.-D.M., Finegold M, Grompe M, *The repopulation potential of hepatocyte populations differing in size and prior mitotic expansion.* American Journal of Pathology, 1999. **155**(6): p. 2135-2143.

108. LeCluyse, E.L., et al., *Induction of cytochrome P450 enzymes in primary cultures of human hepatocytes. J. Biochem. Molec. Toxicol*, 2000: p. (in press).

109. Brodsky, W.Y. and I.V. Uryvaeva, *Cell polyploidy: its relation to tissue growth and function. [Review] [247 refs].* International Review of Cytology, 1977. **50**: p. 275-332.

110. Epstein, C.J. and E.A. Gatens, *Nuclear ploidy in mammalian parenchymal liver cells.* Nature, 1967. **214**(92): p. 1050-1.

111. Matturri, L., et al., *Cell kinetics and DNA content (ploidy) of human skin under expansion.* European Journal of Basic & Applied Histochemistry, 1991. **35**(1): p. 73-9.

112. Brodskii, V., et al., *[Measurement of the absolute cell count in the heart and liver. The quantitative preservation of proteins and DNA in isolated cells].* Tsitologiia, 1983. **25**(3): p. 260-5.

113. Baumann, U., et al., *Expression of the stem cell factor receptor c-kit in normal and diseased pediatric liver: identification of a human hepatic progenitor cell?* Hepatology, 1999. **30**(1): p. 112-117.

114. Zaret, K.S., *Regulatory phases of early liver development: paradigms of organogenesis.* Nat Rev Genet, 2002. **3**(7): p. 499-512.

115. Zaret, K., *Developmental competence of the gut endoderm: genetic potentiation by GATA and HNF3/fork head proteins.* Developmental Biology (Orlando), 1999. **209**(1): p. 1-10.

116. Kubota, H., R.W. Storms, and L.M. Reid, *Variant forms of alpha-fetoprotein transcripts expressed in human hematopoietic progenitors. Implications for their developmental potential towards endoderm.* J Biol Chem, 2002. **277**(31): p. 27629-35.

117. Tanimizu, N., et al., *Isolation of hepatoblasts based on the expression of Dlk/Pref-1.* J Cell Sci, 2003. **116**(Pt 9): p. 1775-86.

118. Theise, N., *The Canals of Hering and Hepatic Stem cells in Humans.* Hepatology, 1999. **30**: p. 1425-1433.

119. Crosby, H.A., D.A. Kelly, and A.J. Strain, *Human hepatic stem-like cells isolated using c-kit or CD34 can differentiate into biliary epithelium.* Gastroenterology, 2001. **120**(2): p. 534-44.

120. Shiojiri, N., *Transient expression of bile-duct-specific cytokeratin in fetal mouse hepatocytes.* Cell & Tissue Research, 1994. **278**(1): p. 117-23.

121. Van Eyken, P., et al., *The development of the intrahepatic bile ducts in man: a keratin-immunohistochemical study.* Hepatology, 1988. **8**(6): p. 1586-95.

122. Corbeil, D., et al., *Selective location of the polytopic membrane protein prominin in microvilli of epithelial cells-a combination of apical sorting and*

retention in plasma membrane protrusion. Journal of Cell Science, 1999. **112**(pt. 7): p. 1023-1033.

123. Weigmann, A., et al., *Prominin, a novel microvilli-specific polytopic membrane protein of the apical surface of epithelial cells, is targeted to plasmalemmal protrusions of non-epithelial cells.* Proceedings of the National Academy of Science, U.S.A., 1997. **94**: p. 12425-12430.

124. Dhillon, A., et al., *Liver Cell Progenitor and Use for Treatment of Liver Diseases*, U.L. College, Editor. 2001: United Kingdom.

125. Schmelzer, E. and L.M. Reid, *EpCAM Expression in Normal, Non-Pathological Tissues.* Frontiers in Biosciences, 2007: p. In Press.

126. Ros, J.E., et al., *High expression of MDR1, MRP1, and MRP3 in the hepatic progenitor cell compartment and hepatocytes in severe human liver disease.* J Pathol, 2003. **200**(5): p. 553-60.

127. Joseph, B., et al., *Sestamibi is a Substrate for MDR1 and MDR2 P-glycoprotein Genes.* European Journal of Nuclear Medicine and Molecular Imaging, 2003. **30**: p. 1024-1031.

128. Zhang, L., N. Theise, and L.M. Reid, *Stem Cell Niche in Human Livers: Symmetries between Regeneration and Development.* Cell-Stem Cell, 2007. **Submitted**.

129. Tanimizu, N., et al., *Long-term culture of hepatic progenitors derived from mouse Dlk+ hepatoblasts.* J Cell Sci, 2004. **117**(Pt 26): p. 6425-34.

130. Jensen, C.H., et al., *Transit-amplifying ductular (oval) cells and their hepatocytic progeny are characterized by a novel and distinctive expression of delta-like protein/preadipocyte factor 1/fetal antigen 1.* Am J Pathol, 2004. **164**(4): p. 1347-59.

131. Li, A.P., et al., *Isolation and culturing of hepatoyctes from human livers.* Journal of Tissue Culture Methods, 1992. **14**: p. 139-146.

132. Strom, S.C., et al., *Use of human hepatocytes to study CYP450 gene induction.* Methods in Enzymology, 1996. **272**: p. 388-401.

133. LeCluyse, E.L., *Human hepatocyte culture systems for the in vitro evaluation of cytochrome P450 expression and regulation.* Eur J Pharm Sci, 2001. **13**(4): p. 343-68.

134. Seglen, P.O., *Preparation of isolated rat liver cells*, in *Methods in Cell Biology*. 1976, Academic Press: New York. p. 29-83.

135. Bruce, A., et al., *Novel processing procedure for human livers that facilitates isolation of hepatic progenitors.* submitted, 2007.

136. Freshney, R.I., *Culture of Animal Cells*. 2000, New York: A. John Wiley and Sons, Inc. 577.

137. Sato, G.H., *Hormonally defined media and long-term marrow culture: general principles.* Kroc Foundation Series, 1984. **18**: p. 133-7.

138. McKeehan, W.L., et al., *Frontiers in mammalian cell culture.* In Vitro Cellular & Developmental Biology, 1990. **26**(1): p. 9-23.

139. Taub, M. and G. Sato, *Growth of functional primary cultures of kidney epithelial cells in defined medium*. Journal of Cellular Physiology, 1980. **105**(2): p. 369-78.

140. Eckl, P.M., et al., *Effects of EGF and calcium on adult parenchymal hepatocyte proliferation.* Journal of Cellular Physiology, 1987. **132**(2): p. 363-366.

141. Santella, L., *The role of calcium in the cell cycle: facts and hypotheses.* Biochem Biophys Res Commun, 1998. **244**(2): p. 317-24.

142. Chessebeuf, M. and P. Padieu, *Rat liver epithelial cell cultures in a serum-free medium: primary cultures and derived cell lines expressing differentiated functions.* In Vitro, 1984. **20**(10): p. 780-95.

143. Reid, L.M. and T.L. Luntz, *Ex vivo maintenance of differentiated mammalian cells.* Methods in Molecular Biology, 1997. **75**: p. 31-57.

144. Rosenberg, E., D.C. Spray, and L.M. Reid, *Transcriptional and posttranscriptional control of connexin mRNAs in periportal and pericentral rat hepatocytes.* European Journal of Cell Biology, 1992. **59**(1): p. 21-6.

145. Fujita, M., et al., *Extracellular matrix regulation of cell-cell communication and tissue- specific gene expression in primary liver cultures.* Prog Clin Biol Res, 1986. **226**: p. 333-60.

146. Spray, D.C., et al., *Proteoglycans and glycosaminoglycans induce gap junction synthesis and function in primary liver cultures.* J Cell Biol, 1987. **105**(1): p. 541-51.

147. Lin, Y., et al., *Origins of circulating endothelial cells and endothelial outgrowth from blood.* J Clin Invest, 2000. **105**(1): p. 71-7.

148. Muschel, R., G. Khoury, and L.M. Reid, *Regulation of insulin mRNA abundance and adenylation: dependence on hormones and matrix substrata.* Molecular & Cellular Biology, 1986. **6**(1): p. 337-41.

149. Enat, R., et al., *Hepatocyte proliferation in vitro: its dependence on the use of serum- free hormonally defined medium and substrata of extracellular matrix.* Proc Natl Acad Sci U S A, 1984. **81**(5): p. 1411-5.

150. Zvibel, I., E. Halay, and L.M. Reid, *Heparin and hormonal regulation of mRNA synthesis and abundance of autocrine growth factors: relevance to clonal growth of tumors.* Mol Cell Biol, 1991. **11**(1): p. 108-16.

151. Zvibel, I., S. Brill, and L.M. Reid, *Insulin-like growth factor II regulation of gene expression in rat and human hepatomas.* Journal of Cellular Physiology, 1995. **162**(1): p. 36-43.

152. Brill, S., et al., *Hepatic progenitor populations in embryonic, neonatal, and adult liver.* Proc Soc Exp Biol Med, 1993. **204**(3): p. 261-9.

153. Maher, J.J. and D.M. Bissell, *Cell-matrix interactions in liver.* Seminars in Cell Biology, 1993. **4**(3): p. 189-201.

154. Suzuki, A., et al., *Role for growth factors and extracellular matrix in controlling differentiation of prospectively isolated hepatic stem cells.* Development, 2003. **130**(11): p. 2513-24.

155. Runge, D., et al., *Matrix induced re-differentiation of cultured rat hepatocytes and changes of CCAAT/enhancer binding proteins.* Biological Chemistry, 1997. **378**(8): p. 873-81.

156. Martinez-Hernandez, A. and P.S. Amenta, *The hepatic extracellular matrix. II. Ontogenesis, regeneration and cirrhosis.* Virchows Archiv - A, Pathological Anatomy & Histopathology, 1993. **423**(2): p. 77-84.

157. Martinez-Hernandez, A. and P.S. Amenta, *Morphology, Localization, and Origin of the Hepatic Extracellular Matrix*. Extracellular Matrix; Chemistry, Biology, and Pathobiology with Emphasis on the Liver, ed. M.A. Zern and L.M. Reid. 1993, New York: Marcel Dekker. 255-327.

158. Maher, J.J. and R.F. McGuire, *Extracellular matrix gene expression increases preferentially in rat lipocytes and sinusoidal endothelial cells during hepatic fibrosis in vivo.* Journal of Clinical Investigations, 1990. **86**: p. 1641-.

159. Reid, M.Z.a.L., *Extracellular Matrix Chemistry and Biology*. 1993, New York: Academic Press.

160. Reid, L.M., *Stem cell/lineage biology and lineage-dependent extracellular matrix chemistry: keys to tissue engineering of quiescent tissues such as liver*, in *Principles of Tissue Engineering*, R.P. Lanza, R. Langer, and W.L. Chick, Editors. 1997, R.G. Landes Co. and Academic Press: Austin. p. 481-514.

161. Ingber, D.E., et al., *Cell shape, cytoskeletal mechanics, and cell cycle control in angiogenesis.* Journal of Biomechanics, 1995. **28**(12): p. 1471-84.

162. Mooney, D., et al., *Switching from differentiation to growth in hepatocytes: control by extracellular matrix.* Journal of Cellular Physiology, 1992. **151**(3): p. 497-505.

163. Singhvi, R., G. , Stephanopoulos, and D.I.C. Wang, *Effects of substratum morphology on cell physiology.* Biotech. Bioeng., 1993. **43**: p. 764-771.

164. MacDonald JM, W.S., Roy-Chowdhury I, Kubota H, Reid LM., *Effect of Flow Configuration and Membrane Characteristics on Membrane Fouling in a Novel Multicoaxial Hollow-Fiber Bioartificial Liver.* Ann NY Acad Sci, 2001. **944**(1): p. 334-343.

165. Griffith, L.G. and S. Lopina, *Microdistribution of substratum-bound ligands affects cell function: hepatocyte spreading on PEO-tethered galactose.* Biomaterials, 1998. **19**(11-12): p. 979-86.

166. Fujimoto, I., J.L. Bruses, and U. Rutishauser, *Regulation of cell adhesion by polysialic acid. Effects on cadherin, immunoglobulin cell adhesion molecule, and integrin function and independence from neural cell adhesion molecule binding or signaling activity.* J Biol Chem., 2001. **276**(34): p. 31745-51. Epub 2001 Jun 25.

167. Vongchan, P., et al., *Structural characterization of human liver heparan sulfate.* Biochim Biophys Acta, 2005. **1721**(1-3): p. 1-8.

168. Ruoslahti, E. and Y. Yamaguchi, *Proteoglycans as modulators of growth factor activities.* Cell, 1991. **64**(5): p. 867-9.

169. Stow, J.L., et al., *Heparan sulfate proteoglycans are concentrated on the sinusoidal plasmalemmal domain and in intracellular organelles of hepatocytes.* J Cell Biol, 1985. **100**(3): p. 975-80.

170. Geerts, A., et al., *Collagen type I and III occur together in hybrid fibrils in the space of Disse of normal rat liver.* Hepatology, 1990. **12**(2): p. 233-41.

171. Schuppan, D., et al., *Collagens in the liver extracellular matrix bind hepatocyte growth factor.* Gastroenterology, 1998. **114**(1): p. 139-52.

172. Seyer, J.M., E.T. Hutcheson, and A.H. Kang, *Collagen polymorphism in normal and cirrhotic human liver.* J Clin Invest, 1977. **59**(2): p. 241-8.

173. Seyer, J., D. Brickley, and M. Glimcher, *The identification of two types of collagen in the articular cartilage of postnatal chickens.* CALCIFIED TISSUE RESEARCH, 1974. **17**: p. 43-55.

174. Liu, X., et al., *Type III collagen is crucial for collagen I fibrillogenesis and for normal cardiovascular development.* Proc Natl Acad Sci U S A, 1997. **94**(5): p. 1852-6.

175. Hudson, B.G., S.T. Reeders, and K. Tryggvason, *Type IV collagen: structure, gene organization, and role in human diseases. Molecular basis of Goodpasture and Alport syndromes and diffuse leiomyomatosis.* Journal of Biological Chemistry, 1993. **268**(35): p. 26033-26036.

176. Hahn, E., et al., *Distribution of basement membrane proteins in normal and fibrotic human liver: collagen type IV, laminin, and fibronectin.* Gut, 1980. **21**(1): p. 63-71.

177. Quondamatteo, F., et al., *Immunohistochemical localization of laminin, nidogen, and type IV collagen during the early development of human liver.* Histochem Cell Biol, 1999. **111**(1): p. 39-47.

178. Bissell, D.M., et al., *Interactions of rat hepatocytes with type IV collagen, fibronectin and laminin matrices. Distinct matrix-controlled modes of attachment and spreading.* European Journal of Cell Biology, 1986. **40**(1): p. 72-8.

179. Kuo, H.J., et al., *Type VI collagen anchors endothelial basement membranes by interacting with type IV collagen.* J Biol Chem, 1997. **272**(42): p. 26522-9.

180. Kielty, C., et al., *Type VI collagen microfibrils: evidence for a structural association with hyaluronan.* JOURNAL OF CELL BIOLOGY, 1992. **118**(Aug): p. 979-90.

181. Timpl, R. and J.C. Brown, *The laminins.* Matrix Biology, 1994. **14**(4): p. 275-81.

182. Carlsson, R., et al., *Laminin and Fibronectinin Cell Adhesion: Enhanced Adhesion of Cells from Regenerating Liver to Laminin.* Proceedings of the National Acadmey of Sciences of the United states of America, 1981. **78**(4): p. 2403-2406.

183. Li, S., et al., *Matrix assembly, regulation, and survival functions of laminin and its receptors in embryonic stem cell differentiation.* J Cell Biol, 2002. **157**(7): p. 1279-90.

184. Yurchenco, P.D., Y.S. Cheng, and H. Colognato, *Laminin forms an independent network in basement membranes.* J Cell Biol, 1992. **117**(5): p. 1119-33.

185. Timpl, R. and M. Dziadek, *Structure, development, and molecular pathology of basement membranes.* Int Rev Exp Pathol, 1986. **29**: p. 1-112.

186. Milani, S., et al., *Cellular localization of laminin gene transcripts in normal and fibrotic human liver.* Am J Pathol, 1989. **134**(6): p. 1175-82.

187. Timpl, R. and J.C. Brown, *Supramolecular assembly of basement membranes.* Bioessays, 1996. **18**(2): p. 123-32.

188. Yurchenco, P.D. and J.J. O'Rear, *Basement membrane assembly.* Methods Enzymol, 1994. **245**: p. 489-518.

189. Galliano, M.F., et al., *Cloning and complete primary structure of the mouse laminin alpha 3 chain. Distinct expression pattern of the laminin alpha 3A and alpha 3B chain isoforms.* J Biol Chem, 1995. **270**(37): p. 21820-6.

190. Kallunki, P., et al., *A truncated laminin chain homologous to the B2 chain: structure, spatial expression, and chromosomal assignment.* J Cell Biol, 1992. **119**(3): p. 679-93.

191. Talts, J.F. and R. Timpl, *Mutation of a basic sequence in the laminin alpha2LG3 module leads to a lack of proteolytic processing and has different effects on beta1 integrin-mediated cell adhesion and alpha-dystroglycan binding.* FEBS Lett, 1999. **458**(3): p. 319-23.

192. Colognato, H. and P.D. Yurchenco, *Form and function: the laminin family of heterotrimers.* Dev Dyn, 2000. **218**(2): p. 213-34.

193. Bissell, D.M., et al., *Support of cultured hepatocytes by a laminin-rich gel. Evidence for a functionally significant subendothelial matrix in normal rat liver.* Journal of Clinical Investigation, 1987. **79**(3): p. 801-12.

194. Boudreau, N. and M.J. Bissell, *Extracellular matrix signaling: integration of form and function in normal and malignant cells.* Current Opinion in Cell Biology, 1998. **10**(5): p. 640-6.

195. Schulz, R., D. Schuppan, and E. Hahn, *Mesenchymal-Epithelial interactions in neural development*. NATO ASI, Series H, ed. J. Wolff, J. Sievers, and M. Berry. 1987.

196. Clement, B., et al., *Identification of a cell surface-binding protein for the core protein of the basement membrane proteoglycan*. Journal of Biological Chemistry, 1989. **264**(21): p. 12467-71.

197. Rescan, P.Y., et al., *Distribution and origin of the basement membrane component perlecan in rat liver and primary hepatocyte culture.* American Journal of Pathology, 1993. **142**(1): p. 199-208.

198. Wewer, U.M., et al., *Laminin A, B1, B2, S and M subunits in the postnatal rat liver development and after partial hepatectomy.* Laboratory Investigation, 1992. **66**(3): p. 378-89.

199. von der Mark, K., P. Osdoby, and A.I. Caplan, *Effect of 4-methylumbelliferyl-beta-d-xyloside on collagen synthesis in chick limb bud mesenchymal cell cultures.* Developmental Biology, 1982. **90**(1): p. 24-30.

200. Mardon, H.J., et al., *Development of osteogenic tissue in diffusion chambers from early precursor cells in bone marrow of adult rats.* Cell & Tissue Research, 1987. **250**(1): p. 157-65.

201. Nissinen, M., et al., *Primary structure of the human laminin A chain. Limited expression in human tissues.* Biochem J, 1991. **276 (Pt 2)**: p. 369-79.

202. Salmivirta, K., L.M. Sorokin, and P. Ekblom, *Differential expression of laminin alpha chains during murine tooth development.* Dev Dyn, 1997. **210**(3): p. 206-15.

203. Schuger, L., *Laminins in lung development.* Exp Lung Res, 1997. **23**(2): p. 119-29.

204. Sorokin, L.M., et al., *Developmental regulation of the laminin alpha5 chain suggests a role in epithelial and endothelial cell maturation.* Dev Biol, 1997. **189**(2): p. 285-300.

205. Dziadek, M. and R. Timpl, *Expression of nidogen and laminin in basement membranes during mouse embryogenesis and in teratocarcinoma cells.* Dev Biol, 1985. **111**(2): p. 372-82.

206. Shim, C., H.B. Kwon, and K. Kim, *Differential expression of laminin chain-specific mRNA transcripts during mouse preimplantation embryo development.* Mol Reprod Dev, 1996. **44**(1): p. 44-55.

207. Smyth, N., et al., *Absence of basement membranes after targeting the LAMC1 gene results in embryonic lethality due to failure of endoderm differentiation.* J Cell Biol, 1999. **144**(1): p. 151-60.

208. Timpl, R., et al., *Characterization of protease-resistant fragments of laminin mediating attachment and spreading of rat hepatocytes.* J Biol Chem, 1983. **258**(14): p. 8922-7.

209. Lyon, M., et al., *Elucidation of the structural features of heparan sulfate important for interaction with the Hep-2 domain of fibronectin.* J Biol Chem, 2000. **275**(7): p. 4599-606.

210. Han, S., F.R. Khuri, and J. Roman, *Fibronectin stimulates non-small cell lung carcinoma cell growth through activation of Akt/mammalian target of rapamycin/S6 kinase and inactivation of LKB1/AMP-activated protein kinase signal pathways.* Cancer Res, 2006. **66**(1): p. 315-23.

211. Xu, A. and L. Reid, *Soft, porous poly (D,L-lactide,-co-glycotide) microcarriers designed for ex vivo studies and for transplantatin of adherent cell types including progenitors.* Annals of the New York Academy of Science, 2002.

212. Macdonald, J.M., et al., *Ex Vivo Maintenance of Cells from the Liver Lineage*, in *Methods of Tissue Engineering*, W.L. Lanza, R. Langer, and J. Vacanti, Editors. 2002, Academic Press: San Diego. p. 151-201.

213. Wauthier, E., et al., *Hepatic Stem Cells and Hepatoblasts: Identification, Isolation and Ex Vivo Maintenance*, in *Methods for Stem Cells*, J. Mather, Editor. 2007, Academic Press.

214. Fiegel, H.C., et al., *Influence of flow conditions and matrix coatings on growth and differentiation of three-dimensionally cultured rat hepatocytes.* Tissue Eng, 2004. **10**(1-2): p. 165-74.

215. Berthiaume, F., et al., *Effect of extracellular matrix topology on cell structure, function, and physiological responsiveness: hepatocytes cultured in a sandwich configuration.* Faseb J, 1996. **10**(13): p. 1471-84.

216. Ben-Ze'ev, A., et al., *Cell-cell and cell-matrix interactions differentially regulate the expression of hepatic and cytoskeletal genes in primary cultures of rat hepatocytes.* Proc Natl Acad Sci U S A, 1988. **85**(7): p. 2161-5.

217. Brill, S., et al., *Extracellular Matrix Regulation of Growth and Gene Expression in Liver Cell Lineages and Hepatomas*, in *The Liver: Biology adn Pathobiology*, I.M. Arias, et al., Editors. 1994, Raven Press, Ltd.: New York. p. 869-897.

218. Allen, J.W., T. Hassanein, and S.N. Bhatia, *Advances in bioartificial liver devices.* Hepatology, 2001. **34**(3): p. 447-55.

219. Kleinman, H.K., et al., *Biological activities of laminin.* J Cell Biochem, 1985. **27**(4): p. 317-25.

220. Maher, J.J., *Primary hepatocyte culture: is it home away from home?. [Review] [56 refs].* Hepatology, 1988. **8**(5): p. 1162-6.

221. Chalazonitis, A., et al., *The alpha1 subunit of laminin-1 promotes the development of neurons by interacting with LBP110 expressed by neural crest-derived cells immunoselected from the fetal mouse gut.* J Neurobiol, 1997. **33**(2): p. 118-38.

222. Desban, N. and J.L. Duband, *Avian neural crest cell migration on laminin: interaction of the alpha1beta1 integrin with distinct laminin-1 domains mediates different adhesive responses.* J Cell Sci, 1997. **110 (Pt 21)**: p. 2729-44.

223. Matter, M.L. and G.W. Laurie, *A novel laminin E8 cell adhesion site required for lung alveolar formation in vitro.* J Cell Biol, 1994. **124**(6): p. 1083-90.

224. Sorokin, L., et al., *Recognition of the laminin E8 cell-binding site by an integrin possessing the alpha 6 subunit is essential for epithelial polarization in developing kidney tubules.* J Cell Biol, 1990. **111**(3): p. 1265-73.

225. Yurchenco, P.D., *Assembly of basement membranes.* Ann N Y Acad Sci, 1990. **580**: p. 195-213.

226. Jedrzejas, M.J., et al., *Mechanism of hyaluronan degradation by Streptococcus pneumoniae hyaluronate lyase. Structures of complexes with the substrate.* J Biol Chem, 2002. **277**(31): p. 28287-97.

227. Terada, T. and Y. Nakanuma, *Expression of tenascin, type IV collagen and laminin during human intrahepatic bile duct development and in intrahepatic cholangiocarcinoma.* Histopathology, 1994. **25**(2): p. 143-50.

228. Couvelard, A., et al., *Expression of integrins during liver organogenesis in humans.* Hepatology, 1998. **27**(3): p. 839-847.

229. Wilting, J., et al., *The proepicardium delivers hemangioblasts but not lymphangioblasts to the developing heart.* Dev Biol, 2007. **305**(2): p. 451-9.

230. Kojima, T., et al., *Changes in cellular distribution of connexins 32 and 26 during formation of gap junctions in primary cultures of rat hepatocytes.* Experimental Cell Research, 1996. **223**(2): p. 314-26.

231. Berthoud, V.M., et al., *Connexins and glucagon receptors during development of rat hepatic acinus.* American Journal of Physiology, 1992. **263**(5 Pt 1): p. G650-8.

232. Rosenberg, E., et al., *Correlation of expression of connexin mRNA isoforms with degree of cellular differentiation.* Cell Adhesion and Communication, 1996. **4**(4-5): p. 223-235.

233. Gebhardt, R., *Primary cultures of rat hepatocytes as a model system of canalicular development, biliary secretion, and intrahepatic cholestasis. III. Properties of the biliary transport of immunoglobulin A revealed by immunofluorescence.* Gastroenterology, 1983. **84**(6): p. 1462-70.

234. Gebhardt, R. and D. Mecke, *Glutamate uptake by cultured rat hepatocytes is mediated by hormonally inducible, sodium-dependent transport systems.* FEBS Lett, 1983. **161**(2): p. 275-8.

235. Linhardt, R.J., et al., *Structural features of dermatan sulfates and their relationship to anticoagulant and antithrombotic activities.* Biochem Pharmacol, 1991. **42**(8): p. 1609-19.

236. Linhardt, R.J., et al., *Isolation and characterization of human heparin.* Biochemistry, 1992. **31**(49): p. 12441-5.

237. Gallagher, J.T. and J.E. Turnbull, *Heparan sulphate in the binding and activation of basic fibroblast growth factor.* Glycobiology, 1992. **2**(6): p. 523-8.

238. Gressner, A.M. and A. Vasel, *Proteochondroitin sulfate is the main proteoglycan synthesized in fetal hepatocytes.* Proc Soc Exp Biol Med, 1985. **180**(2): p. 334-9.

239. Couvelard, A., et al., *Structural and functional differentiation of sinusoidal endothelial cells during liver organogenesis in humans.* Blood, 1996. **87**(11): p. 4568-80.

240. Terada, N., et al., *Bone marrow cells adopt the phenotype of other cells by spontaneous cell fusion.* Nature, 2002. **416**(6880): p. 542-5.

241. Caterson, B., et al., *Modulation of native chondroitin sulphate structure in tissue development and in disease.* JOURNAL OF CELL SCIENCE, 1990. **97 (Pt 3)**(Nov): p. 411-7.

242. Martinez-Hernandez, A., F.M. Delgado, and P.S. Amenta, *The extracellular matrix in hepatic regeneration. Localization of collagen types I, III, IV, laminin, and fibronectin [published erratum appears in Lab Invest 1991 Aug;65(2):257].* Laboratory Investigation, 1991. **64**(2): p. 157-66.

243. Martinez-Hernandez, A., *The hepatic extracellular matrix. I. Electron immunohistochemical studies in normal rat liver.* Lab Invest, 1984. **51**(1): p. 57-74.

244. Maher, J.J., *Yet another role for the "good" matrix protein: laminin in regenerating liver.* Hepatology, 1992. **15**(1): p. 164-6.

245. Mouta Carreira, C., et al., *LYVE-1 is not restricted to the lymph vessels: expression in normal liver blood sinusoids and down-regulation in human liver cancer and cirrhosis.* Cancer Res, 2001. **61**(22): p. 8079-84.

246. Roskams, T., *Different types of liver progenitor cells and their niches.* J Hepatol, 2006. **45**(1): p. 1-4.

247. Scott, J. and F. Heatley. *Hyaluronan forms specific stable tertiary structures in aqueous solution: A 13C NMR Study*. in *Biochemistry*. 1999.

248. Tammi, M.I., A.J. Day, and E.A. Turley, *Hyaluronan and homeostasis: a balancing act.* J Biol Chem, 2002. **277**(7): p. 4581-4.

249. Vrochides, D., et al., *Biosynthesis and Degradation of Hyaluronan by Nonparenchymal Liver Cells During Liver Regeneration.* Journal of Hepatology, 1996. **23**(6): p. 1650-1655.

250. McCarthy, J. and M. Simpson. *Hyaluronan in Prostate Cancer Progression*. 2007 [cited; Available from: http://www.glycoforum.gr.jp/science/hyaluronan/HA26/HA26E.html

251. Luo, Y., K. Kirker, and G. Prestwich, *Cross-linked hyaluronic acid hydrogel films: new biomaterials for drug delivery*. Journal of Controlled Release, 2000. **69**(169-184).

252. Pouyani, T. and G. Prestwich, *Functioanized Derivatives of Hyaluronic Acid Oligosaccharides: Drug Carriers and Novel Biomaterials.* Bioconjugate Chemistry, 1994. **5**: p. 339-347.

253. Shepard, S., H. Becker, and J. Hartman, *Using Hyaluronic Acid to Create a Fetal-like Environment in vitro.* Annals of Plastic Surgery., 1996. **36**(1): p. 65-69.

254. Shah, C. and S. Barnett, *Hyaluronic Acid Gels. Chapter 7*, in *ACS Symposium Series 480. Polyelectrolyte gels: properties, preparation, and applications.*, H. RS and R. Prud'homme, Editors. 1992, American Chemical Society: Washington, DC. p. 116-130.

255. Shu, X., et al., *Disulfide Cross-linked Hyaluronan Hydrogels.* Biomacromolecules, 2002. **3**: p. 1304-1311.

256. Banerji, S., et al., *LYVE-1, a new homologue of the CD44 glycoprotein, is a lymph-specific receptor for hyaluronan.* J Cell Biol, 1999. **144**(4): p. 789-801.

257. McCourt, P.A., *How does the hyaluronan scrap-yard operate?* Matrix Biol, 1999. **18**(5): p. 427-32.

258. Kikuchi, S., et al., *Role of CD44 in epithelial wound repair: Migration of rat hepatic stellate cells utilizes hyaluronic acid and CD44v6.* Journal of Biological Chemistry, 2005. **280**(15): p. 15398-15404.

259. Laurent, T.C., *Biochemistry of Hyaluronan.* Acta Oto-laryngologica, 1987. **442**: p. 7-25.

260. Hoekstra, D. *Hyaluronan-Modified Surfaces for Medical Devices.* 1999 cited; Available from: http://www.devicelink.com/mddi/archive/99/02/005.html.

261. Laurent, T. and J. Fraser, *Chapter 16 Catabolism of Hyaluroans.*, in *Degradation of bioactive substances: Physiiology and pathophysiology.*, H. Henriksen, Editor. 1991, CRC Press: Boca Raton.

262. Prestwich, G.D., et al., *Controlled Chemical Modification of Hyaluronic Acid: Synthesis, Applications, and Biodegradation of Hydrazide Derivatives.* Journal of Controlled Release, 1998. **53**: p. 93-103.

263. Mahoney, D.J., et al., *Novel Methods for the Preparation and Characterization of Hyaluronan Oligosaccharides of Defined Length.* Glycobiology, 2001. **11**(12): p. 1025-1033.

264. Itano, N., et al., *Abnormal accumulation of hyaluronan matrix diminishes contact inhibition of cell growth and promotes cell migration.* PNAS, 2002. **99**(6): p. 3609-3614.

265. Laurent, T.C. and J.R.E. Fraser, *Catabolism of Hyaluronan*, in *Degradation of Bioactive Substances: Physiology and Pathophysiology*, H. Henriksen, Editor. 1991, CRC Press: Boca Raton. p. 249-265.

266. Luo, Y., K. Kirker, and G. Prestwich, *Hyaluronic Acid. Chapter 45.*, in *Modification of Ntural Polymers:*. 2002, Academic Press.

267. Scott, J.E., *Secondary Structures in Hyaluronan Solutions: Chemical and Biological Implications*, in *The Biology of Hyaluronan*. 1989, Wiley, Chichester. p. 6-20.

268. Day, A.J. and G.D. Prestwich, *Hyaluronan-binding proteins: tying up the giant.* J Biol Chem, 2002. **277**(7): p. 4585-8.

269. Turley, E.A., P.W. Noble, and L.Y. Bourguignon, *Signaling properties of hyaluronan receptors.* J Biol Chem, 2002. **277**(7): p. 4589-92.

270. Toole, B.P., T.N. Wight, and M.I. Tammi, *Hyaluronan-cell interactions in cancer and vascular disease.* J Biol Chem, 2002. **277**(7): p. 4593-6.

271. Laurent, U. and R. Reed, *Turnover of hyaluronan in the tissues.* Advanced Drug Delivery Reviews, 1991. **7**: p. 237-256.

272. Guss, J., et al., *Hyaluronic Acid: Molecular Conformations and Interactions in Two Sodium Salts.* Journal of Molecular Biology, 1975. **95**: p. 359-384.

273. Laurent, T. and J. Fraser. *The Properties and Turnover of Hyaluronan.* in *Ciba Foundation Symposium 124*. 1986: Wiley, Chichester.

274. Ogata, T., et al., *Serum hyaluronan as a predictor of hepatic regeneration after hepatectomy in humans.* European Journal of Clinical Investigation. **29**: p. 780-785.

275. Roden, L., et al., *Enzymic Pathways of Hyaluronan Catabolism*, in *The Biology of Hyaluronan*. 1989, Wiley, Chichester. p. 60-86.

276. Karvinen, S., et al., *Keratinocyte Growth Factor Stimulates Migration and Hyaluronan Synthesis in the Epidermis by Activation of Keratinocyte Hyaluronan Synthases 2 and 3.* The Journal of Biological Chemistry., 2003. **278**(49): p. 49495-49504.

277. Aruffo, A., et al., *CD44 Is the Principal Cell Surface Receptor for Hyaluronate.* Cell, 1990. **61**: p. 1303-1313.

278. Lesley, J., et al., *Variant cell lines selected for alterations in the function of the hyaluronan receptor CD44 show differences in glycosylation.* J Exp Med, 1995. **182**(2): p. 431-7.

279. Hu, M., et al., *Polypeptide resurfacing methods improves fibroblast's adhesion to hyaluronan strands.* 1999: John Wiley & Sons, Inc.

280. DeGrendele, H.C., et al., *CD44 and its ligand hyaluronate mediate rolling under physiologic flow: a novel lymphocyte-endothelial cell primary adhesion pathway.* J Exp Med, 1996. **183**(3): p. 1119-30.

281. Tzaicos, C., et al., *Inhibition of hyaluronan uptake in lymphatic tissue by chondroitin sulphate proteoglycan.* Biochem J, 1989. **264**(3): p. 823-8.

282. Laurent, T.C. and J.R.E. Fraser, *The Properties and Turnover of Hyaluronan*, in *Functions of Proteoglycans*. 1986, Wiley, Chichester. p. 9-29.

283. McCarthy, J. and M. Simpson, *Hyaluronan in Prostate Cancer Progression.*

284. Prehm, P., *Identification and Regulation of the Eukaryotic Hyaluronate Synthase*, in *The Biology of Hyaluronan*. 1989, Wiley, Chichester. p. 21-40.

285. Fujii, K., et al., *Effects of the Addition of Hyaluronate Segmetns with Different Chain Lengths on the Viscoelasticity of Hyaluronic Acid Soultions.* Biopolymers, 1996. **38**: p. 583-591.

286. Prehm, P. *The Biology of Hyaluronan. Identification and regulation of the Eukarytic hyaluronate synthase.* in *Ciba Foundation Symposium 143*: Wiley, Chichester.

287. Gamini, A., et al., *Structural Investigations of Cross-Linked Hyaluronan.* Biomaterials, 2002. **23**: p. 1161-1167.

288. Potter, V.R., *Phenotypic diversity in experimental hepatomas: the concept of partially blocked ontogeny. The 10th Walter Hubert Lecture.* Br J Cancer, 1978. **38**(1): p. 1-23.

289. Sell, S., *Cellular origin of hepatocellular carcinomas.* Semin Cell Dev Biol, 2002. **13**(6): p. 419-24.

290. Aterman, K., *The stem cells of the liver--a selective review*. J Cancer Res Clin Oncol, 1992. **118**(2): p. 87-115.

291. Zvibel, I., et al., *Phenotypic characterization of rat hepatoma cell lines and lineage-specific regulation of gene expression by differentiation agents.* Differentiation, 1998. **63**(4): p. 215-23.

292. Laurent, T.C., et al., *The Catabolic Fate of Hyaluronic Acid.* Connective Tissue Research, 1986. **15**: p. 33-41.

293. Kikuchi, A. and T. Okano, *Nanostructured designs of biomedical materials: applications of cell sheet engineering to functional regenerative tissues and organs.* J Control Release, 2005. **101**(1-3): p. 69-84.

294. Balazs, E.A. and D.A. Gibbs, *The Rheological Properties and Biological Function of Hyaluronic Acid*, in *CHemistry and Molecular Biology of the*

Intracellular Matrix, E.A. Balazs, Editor. 1970, Academic Press: London. p. 1241-53.

295. Tomihata, K. and Y. Ikada, *Crosslinking of Hyaluronic Acid with Water-Soluble Carbodiimide.* Journal of Biomedical Materials Reserach, 1997. **37**: p. 243-251.

296. Mo, Y., et al., *Effects of Sodium Chloride, Guanidine Hydrocloride, and Surcose on the Viscoelastic Properties of Sodium Hyaluronate Soultions.* Biopolymers, 1999. **50**: p. 23-34.

297. Bligny, R. and R. Douce, *NMR and plant metabolism*. Curr Opin Plant Biol, 2001. **4**(3): p. 191-6.

298. Claridge, T., *High-Resolution NMR Techniques in Organic Chemistry*. 1999: Oxford.

299. Nicholson, J.K., et al., *Metabonomics: a platform for studying drug toxicity and gene function.* Nat Rev Drug Discov, 2002. **1**(2): p. 153-61.

300. Griffin, J.L. and J.P. Shockcor, *Metabolic profiles of cancer cells.* Nat Rev Cancer, 2004. **4**(7): p. 551-61.

301. Wishart, D.S., *Metabolomics: The Principles and Potential Applications to Transplantation.* American Journal of Transplantation, 2005. **5**(12): p. 2814-2820.

302. Nicholson, J.K. and I.D. Wilson, *Opinion: understanding 'global' systems biology: metabonomics and the continuum of metabolism*. Nat Rev Drug Discov, 2003. **2**(8): p. 668-76.

303. Fiehn, O., *Metabolomics--the link between genotypes and phenotypes.* Plant Mol Biol, 2002. **48**(1-2): p. 155-71.

304. Kell, D., et al., *Metabolic footprinting and systems biology: the medium is the message.* Nat Rev Micro, 2005. **3**(7): p. 557-565.

305. Villas-Boas, S.G., et al., *Extracellular metabolomics: a metabolic footprinting approach to assess fiber degradation in complex media*. Anal Biochem, 2006. **349**(2): p. 297-305.

306. Sumner, L.W., P. Mendes, and R.A. Dixon, *Plant metabolomics: large-scale phytochemistry in the functional genomics era.* Phytochemistry, 2003. **62**(6): p. 817-836.

307. Goodacre, R., *Metabolic profiling: pathways in discovery*. Drug Discov Today, 2004. **9**(6): p. 260-1.

308. Robertson, D.G., *Metabonomics in toxicology: a review*. Toxicol Sci, 2005. **85**(2): p. 809-22.

309. Teusink, B., et al., *Intracellular glucose concentration in derepressed yeast cells consuming glucose is high enough to reduce the glucose transport rate by 50%.* J Bacteriol, 1998. **180**(3): p. 556-62.

310. Kell, D.B., *Metabolomics and systems biology: making sense of the soup.* Current Opinion in Microbiology, 2004. **7**(3): p. 296-307.

311. Nicholson, J.K., et al., *The challenges of modeling mammalian biocomplexity*. Nat Biotechnol, 2004. **22**(10): p. 1268-74.

312. Hewitt, N.J., et al., *Primary hepatocytes: current understanding of the regulation of metabolic enzymes and transporter proteins, and pharmaceutical practice for the use of hepatocytes in metabolism, enzyme induction, transporter, clearance, and hepatotoxicity studies.* Drug Metab Rev, 2007. **39**(1): p. 159-234.

313. Allen, J., Davey, HM, Broadhurst, D, Heald, JK, Rowland, JJ, Oliver, SG, Kell, DB, *High-throughput classification of yeast mutants for functional genomics using metabolic footprinting.* Nat. Biotechnol., 2003. **21**(6): p. 692.6.

314. Bales, J.R., et al., *Use of high-resolution proton nuclear magnetic resonance spectroscopy for rapid multi-component analysis of urine.* Clin Chem, 1984. **30**(3): p. 426-32.

315. Bales, J.R., et al., *Metabolic profiling of body fluids by proton NMR: self-poisoning episodes with paracetamol (acetaminophen).* Magn Reson Med, 1988. **6**(3): p. 300-6.

316. Urenjak, J., et al., *Proton nuclear magnetic resonance spectroscopy unambiguously identifies different neural cell types.* J Neurosci, 1993. **13**(3): p. 981-9.

317. Holmes, E., J.K. Nicholson, and G. Tranter, *Metabonomic Characterization of Genetic Variations in Toxicological and Metabolic Responses Using Probabilistic Neural Networks.* Chem. Res. Toxicol., 2001. **14**(2): p. 182-191.

318. Dabos, K.J., et al., *1H NMR spectroscopy as a tool to evaluate key metabolic functions of primary porcine hepatocytes after cryopreservation.* NMR Biomed, 2002. **15**(3): p. 241-50.

319. Foxall, P.J., et al., *High resolution proton magnetic resonance spectroscopy of cyst fluids from patients with polycystic kidney disease.* Biochim Biophys Acta, 1992. **1138**(4): p. 305-14.

320. Viant, M.R., E.S. Rosenblum, and R.S. Tieerdema, *NMR-based metabolomics: a powerful approach for characterizing the effects of environmental stressors on organism health.* Environ Sci Technol, 2003. **37**(21): p. 4982-9.

321. Reo, N.V., *NMR-based metabolomics.* Drug Chem Toxicol, 2002. **25**(4): p. 375-82.

322. Nicholas, P.C., et al., *Proton nuclear magnetic resonance spectroscopic determination of ethanol-induced formation of ethyl glucuronide in liver.* Anal Biochem, 2006. **358**(2): p. 185-91.

323. Nicholson, J.K., J.C. Lindon, and E. Holmes, *'Metabonomics': understanding the metabolic responses of living systems to pathophysiological stimuli via multivariate statistical analysis of biological NMR spectroscopic data.* Xenobiotica, 1999. **29**(11): p. 1181-9.

324. Abel, C.B., et al., *Characterization of metabolites in intact Streptomyces citricolor culture supernatants using high-resolution nuclear magnetic*

resonance and directly coupled high-pressure liquid chromatography-nuclear magnetic resonance spectroscopy. Anal Biochem, 1999. **270**(2): p. 220-30.

325. Bubb, W., Wright, LC, Cagney, M, Santangelo, RT, Sorrell, TC, Kuchel, PW, *Heteronuclear NMR studies of metabolites produced by Cryptococcus neoformans in culture media: Identification of possible virulence factors.* Magnetic Resonance in Medicine, 1999. **42**(3): p. 442-453.

326. Holmes, E., et al., *Chemometric Models for Toxicity Classification Based on NMR Spectra of Biofluids.* Chem. Res. Toxicol., 2000. **13**(6): p. 471-478.

327. Nicholson JK and W. ID., *High resolution proton magnetic resonance spectroscopy of biological fluids.* Prog. NMR Spectrosc., 1989. **21**: p. 449-501.

328. Anthony, M.L., et al., Biomarkers, 1996(1): p. 35.

329. Florian, C.L., et al., *Cell type-specific fingerprinting of meningioma and meningeal cells by proton nuclear magnetic resonance spectroscopy*. Cancer Res, 1995. **55**(2): p. 420-7.

330. Dell, K. and J. Frost, *Identification and Removal of Impediments to Biocatalytic Synthesis of Aromatics from D-Glucose: Rate-Limiting Enzymes in the Common Pathway of Aromatic Amino Acid Biosynthesis.* J. Am. Chem. SOC., 1993. **115**: p. 11581-11589.

331. Ramos, A., et al., *Enzyme Basis for pH Regulation of Citrate and Pyruvate Metabolism by Leuconostoc oenos.* Appl Environ Microbiol, 1995. **61**(4): p. 1303-1310.

332. Lohmeier-Vogel, E.M., B. Hahn-Hagerdal, and H.J. Vogel, *Phosphorus-31 and carbon-13 nuclear magnetic resonance studies of glucose and xylose metabolism in Candida tropicalis cell suspensions.* Appl Environ Microbiol, 1995. **61**(4): p. 1414-9.

333. Gavaghan, C.L., et al., *An NMR-based metabonomic approach to investigate the biochemical consequences of genetic strain differences: application to the C57BL10J and Alpk:ApfCD mouse.* FEBS Lett, 2000. **484**(3): p. 169-74.

334. Nesti, C., et al., *The Role of Mitochondria in Stem Cell Biology*. Biosci Rep, 2007.

335. Jansen, J.F., et al., *Stem cell profiling by nuclear magnetic resonance spectroscopy*. Magn Reson Med, 2006. **56**(3): p. 666-70.

336. Grayson, W.L., et al., *Effects of hypoxia on human mesenchymal stem cell expansion and plasticity in 3D constructs.* J Cell Physiol, 2006. **207**(2): p. 331-9.

337. Griffin, J.L., et al., *Spectral profiles of cultured neuronal and glial cells derived from HRMAS (1)H NMR spectroscopy*. NMR Biomed, 2002. **15**(6): p. 375-84.

338. Holmes, E., et al., *Automatic data reduction and pattern recognition methods for analysis of 1H nuclear magnetic resonance spectra of human urine from normal and pathological states.* Anal Biochem, 1994. **220**(2): p. 284-96.

339. Nicholson, J.K., et al., *750 MHz 1H and 1H-13C NMR spectroscopy of human blood plasma.* Anal Chem, 1995. **67**(5): p. 793-811.

340. Beckwith-Hall, B.M., et al., *Nuclear magnetic resonance spectroscopic and principal components analysis investigations into biochemical effects of three model hepatotoxins.* Chem Res Toxicol, 1998. **11**(4): p. 260-72.

341. el-Deredy, W., *Pattern recognition approaches in biomedical and clinical magnetic resonance spectroscopy: a review*. NMR Biomed, 1997. **10**(3): p. 99-124.

342. Somorjai, R.L., et al., *Computerized consensus diagnosis: a classification strategy for the robust analysis of MR spectra. I. Application to 1H spectra of thyroid neoplasms.* Magn Reson Med, 1995. **33**(2): p. 257-63.

343. Derome, A., *Modern NMR Techniques for Chemistry Research*. Vol. 6. 1987, Oxford: Pergamon Press.

344. Hotellin, H., *Analysis of a complex of statiscal variables into principal components.* Journal of Educational Psychology., 1933. **24**: p. 417-441.

345. Soars, M.G., et al., *The pivotal role of hepatocytes in drug discovery.* Chem Biol Interact, 2007. **168**(1): p. 2-15.

346. Allen, J.W., S.R. Khetani, and S.N. Bhatia, *In vitro zonation and toxicity in a hepatocyte bioreactor.* Toxicol Sci, 2005. **84**(1): p. 110-9.

347. Gebhardt, R., *Metabolic zonation of the liver: regulation and implications for liver function.* Pharmacology & Therapeutics, 1992. **53**(3): p. 275-354.

348. Michalopoulos, G.K. and M.C. DeFrances, *Liver regeneration.* Science, 1997. **276**(5309): p. 60-6.

349. Thorgeirsson, S.S., Factor, Valentina M., and Grisham, Joe W. , *Stem Cells.* 1 ed. Adult and Fetal Stem Cells, ed. R. Lanza. Vol. 2. 2004, London: Elsevier. 497-512.

350. Alison, M.R., et al., *Hepatic stem cells: from inside and outside the liver?* Cell Prolif, 2004. **37**(1): p. 1-21.

351. Oh, S.H., H.M. Hatch, and B.E. Petersen, *Hepatic oval 'stem' cell in liver regeneration.* Semin Cell Dev Biol, 2002. **13**(6): p. 405-9.

352. Matsumoto, K., et al., *Liver organogenesis promoted by endothelial cells prior to vascular function.* Sciencexpress, 2001(10.1126/science.1063889).

353. Haruna, Y., et al., *Identification of bipotential progenitor cells in human liver development.* Hepatology, 1996. **23**(3): p. 476-81.

354. Saxena, R. and N. Theise, *Canals of Hering: recent insights and current knowledge.* Semin Liver Dis, 2004. **24**(1): p. 43-8.

355. Abelev, G.I., *Alpha-fetoprotein in ontogenesis and its association with malignant tumors.* Adv Cancer Res, 1971. **14**: p. 295-358.

356. Balzar, M., et al., *The biology of the 17-1A antigen (Ep-CAM).* Journal of Molecular Medicine, 1999. **77**: p. 6999-6712.

357. Balzar, M., et al., *Cytoplasmic tail regulates the intercellular adhesion function of the epithelial cell adhesion molecule.* Mol Cell Biol., 1998. **18**(8): p. 4833-43.

358. Theise, N.D., et al., *The Canals of Hering and Hepatic Stem cells in Humans.* Hepatology, 1999. **30**: p. 1425-1433.

359. Roskams, T.A., et al., *Nomenclature of the Finer Branches of the biliary Tree: Canals, Ductules, and Ductular Reactions in Human Livers.* Hepatology, 2004. **39**: p. 1739-1745.

360. Libbrecht, L., et al., *Expression of neural cell adhesion molecule in human liver development and in congenital and acquired liver diseases.* Histochem Cell Biol, 2001. **116**: p. 233-239.

361. Roskams, T., et al., *Hepatic OV-6 expression in human liver disease and rat experiments: evidence for hepatic progenitor cells in man.* J Hepatol, 1998. **29**(3): p. 455-63.

362. Van Den Heuvel, M., et al., *Expression of anti-OV6 antibody and anti-N-CAM antibody along the biliary line of normal and diseased human livers.* Hepatology, 2001. **33**(6): p. 1387-1393.

363. Potgens, A.J., et al., *Monoclonal antibody CD133-2 (AC141) against hematopoietic stem cell antigen CD133 shows crossreactivity with cytokeratin 18.* Journal of Histochemistry & Cytochemistry, 2002. **50**: p. 1131-1134.

364. Wells, M.J., et al., *Cytokeratin 18 is expressed on the hepatocyte plasma membrane surface and interacts with thrombin-antithrombin complexes.* Journal of BIological Chemistry, 1997. **272**: p. 28574-28581.

365. Goridis, C. and J.F. Brunet, *Neural Cell Adhesion Molecule (NCAM): structural diversity, function and regulation of expression.* Seminars in Cell Biology, 1992. **3**: p. 189-197.

366. Fausto, N., J.M. Lemire, and N. Shiojiri, *Cell lineages in hepatic development and the identification of progenitor cells in normal and injured liver.* Proc Soc Exp Biol Med, 1993. **204**(3): p. 237-41.

367. Crawford, J.M., *Development of the intrahepatic biliary tree.* Seminars in Liver Disease, 2002. **22**: p. 213-226.

368. Forbes, S., et al., *Hepatic stem cells.* J Pathol, 2002. **197**(4): p. 510-8.

369. Grisham, J.W. and S.S. Thorgeirsson, *Liver stem cells*, in *Stem Cells*, C.S. Potter, Editor. 1997, Academic Press: London. p. 233-282.

370. Thorgeirsson, S.S. and J.W. Grisham, *Overview of recent experimental studies on liver stem cells.* Semin Liver Dis, 2003. **23**(4): p. 303-12.

371. Alison, M.R., et al., *Liver damage in the rat induces hepatocyte stem cells from biliary epithelial cells [see comments].* Gastroenterology, 1996. **110**(4): p. 1182-90.

372. Cunningham, B.A., et al., *Neural cell adhesion molecule:structure, immunoglobulin-like domains, cell surface modulation, and alternative RNA splicing.* Science, 1987. **236**: p. 799-806.

373. Fabris, L., et al., *Characterization and isolation of ductular cells coexpressing neural cell adhesion molecule and Bcl-2 from primary cholangiopathies and ductal plate malformations.* American Journal of Pathology, 2000. **156**(5): p. 1599-612.

374. Neubauer, K., et al., *Glial fibrillary acidic protein--a cell type specific marker for Ito cells in vivo and in vitro.* J Hepatol., 1996. **24**(6): p. 719-30.

375. Jiang, Y., et al., *Pluripotency of mesenchymal stem cells derived from adult marrow.* Nature, 2002. **418**: p. 41-49.

376. Bhatia, M., *AC133 expression in human stem cells.* Leukemia, 2001. **15**(11): p. 1685-8.

377. Yu, Y., et al., *AC133-2, a novel isoform of human AC133 stem cell antigen.* J Biol Chem, 2002. **277**(23): p. 20711-6.

378. Bardin, N., et al., *Identification of CD146 as a component of the endothelial junction involved in the control of cell-cell cohesion.* Blood., 2001. **98**(13): p. 3677-84.

379. Gronthos, S., et al., *Surface protein characterization of human adipose tissue-derived stromal cells.* J Cell Physiol., 2001. **189**(1): p. 54-63.

380. Seftalioglu, A. and L. Karakoc, *Expression of CD146 adhesion molecules (MUC18 or MCAM) in the thymic microenvironment.* Acta Histochem., 2000. **102**(1): p. 69-83.

381. Johnson, J.P., *Cell adhesion molecules in the development and progression of malignant melanoma.* Cancer Metastasis Rev., 1999. **18**(3): p. 345-57.

382. Benveniste, H., et al., *Detection of neuritic plaques in Alzheimer's disease by magnetic resonance microscopy.* Proc. Natl. Acad. Sci. USA, 1999. **96**: p. 14079.

383. Dan, Y.Y., et al., *Isolation of multipotent progenitor cells from human fetal liver capable of differentiating into liver and mesenchymal lineages.* Proceedings of the National Academy of Science, USA, 2006. **103**: p. 9912-9917.

384. Crosby, H.A., et al., *Progenitor cells of the biliary epithelial cell lineage.* Semin Cell Dev Biol, 2002. **13**(6): p. 397-403.

385. Craig, C.E., et al., *The histopathology of regeneration in massive hepatic necrosis.* Semin Liver Dis, 2004. **24**(1): p. 49-64.

386. Lilja, H., et al., *Fetal rat hepatocytes: isolation, characterization, and transplantation in the Nagase analbuminemic rats.* Transplantation, 1997. **64**(9): p. 1240-8.

387. Lilja, H., et al., *Response of cultured fetal and adult rat hepatocytes to growth factors and cyclosporine.* Cell Transplantation, 1998. **7**(3): p. 257-66.

388. Kubota, H. and L.M. Reid, *Clonogenic hepatoblasts, common precursors for hepatocytic and biliary lineages, are lacking classical major histocompatibility complex class I antigen.* Proc Natl Acad Sci U S A, 2000. **97**(22): p. 12132-7.

389. Lauffenburger, D. and L. Griffith, *Who's got pull around here? Cell organization in development and tissue engineering.* Proc Natl Acad Sci USA, 2001. **98**: p. 4282-4284.

390. Bhatia, S., et al., *Effect of cell-cell interactions in preservation of cellular phenotype: cocultivation of hepatocytes and nonparenchymal cells.* FASAB J, 1999. **13**: p. 1883-1900.

391. Alberts, B., et al., *Molecular Biology of the Cell.* 3 ed. 1995, New York: Garland Publishing.

392. Zandstra, P.W., et al., *Leukemia inhibitory factor (LIF) concentration modulates embryonic stem cell self-renewal and differentiation independently of proliferation.* Biotechnol Bioeng, 2000. **69**(6): p. 607-17.

393. Heldin, P., *Importance of hyaluronan biosynthesis and degradation in cell differentiation and tumor formation.* Brazilian Journal of Medical and Biological Research, 2003. **36**: p. 967-973.

394. Pouyani, T., G. Harbison, and G. Prestwich, *Novel Hydrogels of Hyaluronic Acid: Synthesis, Surface Morphology, and Solid-State NMR.* Journal of American Chemistry Society., 1994. **116**: p. 7515-7522.

395. Pouyani, T. and G. Prestwich, *Biotinylated Hyaluronic Acid: A new Tool for Probing Hyaluronate-Receptor Interactions.* Bioconjugate Chemistry, Technical Notes., 1994. **5**: p. 370-372.

396. Luo, Y., K.R. Kirker, and G.D. Prestwich, *Cross-Linked Hyaluronic Acid Hydrogel Films: New Biomaterials for Drug Delivery.* Journal of Controlled Release, 2000. **69**: p. 169-184.

397. Toole, B.P., *Hyaluronan in Morphogenesis and Tissue Remodeling.* 1998.

398. Toole, B.P., *Developmental role of hyaluronate.* Connective Tissue Research, 1982. **10**: p. 93-100.

399. Toole, B.P., et al., *Hyaluronate-Cell Interactions*, in *The Role of Extracellular Matrix in Development*. 1984, Alan R. Liss, Inc.: New York. p. 43-66.

400. Mahieu-Caputo, D., et al., *Repopulation of athymic mouse liver by cryopreserved early human fetal hepatoblasts.* Human Gene Therapy., 2004. **15**(12): p. 1219-1228.

401. Vercruysse, K.P., et al., *Synthesis and In Vitro Degradation of New Polyvalent Hydrazide Cross-Linked Hydrogels of Hyaluronic Acid.* Bioconjugate Chemistry, 1997. **8**: p. 686-694.

402. Kim, A., et al., *Characterization of DNA-hyaluronan matrix for sustained gene transfer.* Journal of Controlled Release, 2003. **90**: p. 81-95.

403. Laurent, T., *Chemistry and molecular biology of the intercellular matrix.* Structure of Hyaluronic Acid., ed. E. Balazs. Vol. 2. 1970, London: London Academic Press. 703-732.

404. Laurent, T.C., *Structure of Hyaluronic Acid*, in *Chemistry and Molecular Biology of the Intracellular Matrix*, E.A. Balazs, Editor. 1970, Academic Press: London. p. 703-732.

405. Scott, J. *Secondary structures in Hyaluronan solutions: Chemical and biological implications.* in *Ciba Foundation Symposium*. 1989: Wiley, Chichester.

406. Tomihata, K. and Y. Ikada, *Preparation of Cross-Linked Hyaluronic Acid Films of Low Water Content.* Biomaterials, 1997. **18**(3): p. 189-195.

407. Balazs, E.A., et al., *Hyaluronan Biomaterials: Medical Applications*, in *Encyclopedic Handbook of Biomaterials and Bioengineering. Part A: Materials*, D.L. Wise, Editor. 1995, Marcel Dekker, Inc.: New York. p. 1693-1715.

408. Keely, P., et al., *R-Ras signals through specific integrin alpha cytoplasmic domains to promote migration and invasion of breast epithelial cells.* Journal of Cell Biology, 1999. **145**(5): p. 1077-1088.

409. Awad, H., et al., *In vitro characterization of mesenchymal stem cell-seeded collagen scaffolds for tendon repair: Effects of initial seeding density on contraction kinetics.* Journal of Biomedical Materials Research, 2000. **51**(2): p. 233-240.

410. Day, A. and G. Prestwich, *Hyaluronan-binding Proteins: Tying up the Giant.* The Journal of Biological Chemistry, 2002. **277**(7): p. 4585-4288.

411. Bell, J.D., et al., *Nuclear magnetic resonance studies of blood plasma and urine from subjects with chronic renal failure: identification of trimethylamine-N-oxide.* Biochim Biophys Acta, 1991. **1096**(2): p. 101-7.

412. Dabos, K., et al., *1H NMR spectroscopy as a tool to evaluate key metabolic functions of primary porcine hepatocytes after cryopreservation.* NMR Biomedicine, 2002. **15**(3): p. 241-250.

413. Kell, D.B., *Systems biology, metabolic modelling and metabolomics in drug discovery and development.* Drug Discov Today, 2006. **11**(23-24): p. 1085-92.

414. Kriat, M., Confort-Gouny, S., Vion-Dury, J., Sciaky, M., Viout, P., Cozzone, P., *Quantitation of metabolites in human blood serum by proton magnetic resonance spectroscopy. A comparative study of the use of formate and TSP as concentration standards.* NMR Biomed., 1992. **5**(4): p. 179-94.

415. Raddatz, D. and G. Ramadori, *Carbohydrate metabolism and the liver: actual aspects from physiology and disease.* Z Gastroenterol, 2007. **45**(1): p. 51-62.

416. Canbay, A., L. Bechmann, and G. Gerken, *Lipid metabolism in the liver.* Z Gastroenterol, 2007. **45**(1): p. 35-41.

417. Zvibel, I., et al., *Phenotypic characterization of hepatoma cell lines and lineage- specific regulation of gene expression by differentiation agents.* Differentiation, 1998. **63**(4): p. 215-23.

418. Braet, F., et al., *Liver sinusoidal endothelial cell modulation upon resection and shear stress in vitro.* Comp Hepatol, 2004. **3**(1): p. 7.

419. LeCluyse, E.L., P.L. Bullock, A. Madan, K. Carroll, and A. Parkinson, *Influence of extracellular matrix composition and medium formulation on the induction of cytochrome P450 2B enzymes in primary cultures of rat hepatocytes. Drug Metab. Dispos*, 1999. **27**: p. 909-915.

420. LeCluyse, E.L., D.J. Coon, B. Barros, S.L. Jolley, and G. A. Hamilton, *Regulation of cell morphology and gene expression in human hepatocytes by extracellular matrix and cell-cell interactions. Cell Tissue Res..*,, 2000: p. (in press).

421. Tuschl, G. and S.O. Mueller, *Effects of cell culture conditions on primary rat hepatocytes-cell morphology and differential gene expression.* Toxicology, 2006. **218**(2-3): p. 205-15.

422. Fischer, B. and B.D. Bavister, *Oxygen tension in the oviduct and uterus of rhesus monkeys, hamsters and rabbits.* J Reprod Fertil, 1993. **99**(2): p. 673-9.

423. Faller, D.V., *Endothelial cell responses to hypoxic stress.* Clin Exp Pharmacol Physiol, 1999. **26**(1): p. 74-84.

424. Guillemin, K. and M.A. Krasnow, *The hypoxic response: huffing and HIFing.* Cell, 1997. **89**(1): p. 9-12.

425. Cipolleschi, M.G., P. Dello Sbarba, and M. Olivotto, *The role of hypoxia in the maintenance of hematopoietic stem cells.* Blood, 1993. **82**(7): p. 2031-7.

426. Allen, J. and S. Bhatia, *Engineering Liver Therapies for the Future.* Tissue Eng., 2002. **8**(5): p. 725-737.

427. Macdonald, J.M. and S.P. Wolfe, *Bioreactor design and process for engineering tissue from cells. (Patent).* Patent (US #113918.200), 1999. **Filed June 3, 1999**.

428. MacDonald, J., O. Schmidlin, and T. James, *In Vivo Monitoring of Hepatic Glutathione in Anesthetized Rats by 13C NMR*. Magnetic Resonance Medicine, 2002. **48**(3): p. 430-439.

429. Shu, X.Z. and G.D. Prestwich, *Therapeutic biomaterials from chemically modified hyaluronan*, in *Chemistry and Biology of Hyaluronan*, H. Garg and C. Hales, Editors. 2004, Elsevier Press: Amsterdam. p. 475-504.

430. Shu, X.Z., et al., *In situ crosslinkable glycosaminoglycan hydrogels for tissue engineering*. Biomaterials, 2004. **25**: p. 1339-1348.

431. Prestwich, G.D., et al., *Injectable synthetic extracellular matrices for tissue engineering and repair*. Adv Exp Med Biol, 2006. **585**: p. 125-33.

432. Shu, X.Z., et al., *Synthesis and evaluation of injectable, in situ crosslinkable synthetic extracellular matrices for tissue engineering*. J Biomed Mater Res A, 2006. **29**: p. 29.

433. Prestwich, G.D., et al., *3-D culture in synthetic extracellular matrices: New tissue models for drug toxicology and cancer drug discovery*. Adv Enzyme Regul, 2007.

434. Liu, Y., et al., *Accelerated repair of cortical bone defects using a synthetic extracellular matrix to deliver human demineralized bone matrix*. J Orthop Res., 2006. **24**(7): p. 1454-62.

435. Liu, Y., et al., *Release of basic fibroblast growth factor from a crosslinked glycosaminoglycan hydrogel promotes wound healing*. Wound Repair Regen, 2007. **15**(2): p. 245-51.

436. Liu, Y., X.Z. Shu, and G.D. Prestwich, *Osteochondral defect repair with autologous bone marrow-derived mesenchymal stem cells in an injectable, in situ, cross-linked synthetic extracellular matrix*. Tissue Eng, 2006. **12**(12): p. 3405-16.

437. LaGier, A.J., et al., *Inhibition of human corneal epithelial production of fibrotic mediator TGF-beta2 by basement membrane-like extracellular matrix*. Invest Ophthalmol Vis Sci, 2007. **48**(3): p. 1061-71.

438. Tuzlakoglu, K., et al., *Nano- and micro-fiber combined scaffolds: a new architecture for bone tissue engineering.* J Mater Sci Mater Med, 2005. **16**(12): p. 1099-104.

439. Ang, T., et al., *Fabrication of 3D chitosan-hydroxyapatite scaffolds using a robotic dispensing system.* Materials Science and Engineering C, 2002. **20**: p. 35-42.

440. Park, T.G., *Perfusion culture of hepatocytes within galactose-derivatized biodegradable poly(lactide-co-glycolide) scaffolds prepared by gas foaming of effervescent salts.* J Biomed Mater Res, 2002. **59**(1): p. 127-35.